DREAM
Danish Research institute for
Economic Analysis and Modelling

GREEN REFORM

Modelling the Energy Sector in GreenREFORM

Rasmus Kehlet Berg, Janek Bligaard Eskildsen, and Jens Sand Kirk

Economic memo
11 June 2020

www.dreamgruppen.dk

Modelling the Energy Sector in GreenREFORM*

Rasmus K. Berg† Janek B. Eskildsen‡ Jens S. Kirk§

June 11, 2020

Abstract

This paper provides documentation of the modelling of the energy sector in the GreenREFORM model of the Danish economy at its current state of development. A paper describing a base run simulation towards 2040 supplementing the documentation is expected by the end of January 2020. Apart from minor updates the text is identical to the master thesis of the authors of July 31 2019.

The energy model is the first of several sector specific models currently being developed, and even if fully functional already, still needs further development itself. The energy model will be fully integrated with the CGE-model in a modular fashion. In the CGE-model energy transformation and distribution is divided into three sectors based on national account statistics, namely district heating, electricity and natural gas. The energy model provides a very detailed model of production of heat and electricity, and thus it does not encompass the entire energy system. It is based on bottom data, but will be calibrated to match national account statistics to ensure seamless integration with the CGE-model. During simulations, the CGE-model provides information to the energy model on input prices of intermediary input in production wage rates etc. and yearly demand for heat and electricity. Simultaneously, the energy model will provide information to the CGE-model on intermediary demand, labour demand and the yearly average price of heat and electricity.

At the current stage, the documentation outlines a model that draws on plant-level information from detailed bottom-up dispatch models. It further outlines a modelling approach that nests the traditional linear programming approach conventionally applied in bottom-up models while being compatible with conventional CGE models, thus facilitating a straightforward and efficient integration link. The approach fully accounts for the costs of intermittency of energy production by building on intra-year equilibria. The model further covers instruments aimed at mitigating the costs of intermittency as flexible short run demand, storage technologies, dispatchable back-up capacity, and transmission lines facilitating trade in electricity between neighboring countries.

Development of the energy model is currently focused on endogenous investments. Other areas on the board are individual solutions for production and storage of heat and electricity, Power-to-X technologies, dependence on its usage (electric vehicles etc.) of the intertemporal pattern and price dependency of electricity demand.

*The documentation consists primarily of material developed in Berg and Eskildsen (2019). A shortened version is also available for download here.

†University of Copenhagen. Oster Farimagsgade 5, 1353 Copenhagen K, Denmark. E-mail: rasmus.kehlet.berg@econ.ku.dk.

‡University of Copenhagen. Oster Farimagsgade 5, 1353 Copenhagen K, Denmark. E-mail: jbe@econ.ku.dk

§DREAM modelling group. E-mail: jsk@dreammodel.dk

0 Updates:

0.1 Storage technologies and the aggregation of hours to clusters

In part III the documentation outlines how to reduce the dimensionality of the model. To capture the intra-year variation in production from intermittent technologies (wind, solar) and short-run demand (habits), the model is initially set up for all 8760 hours of the year. With chronological hours it is straightforward (in the model framework developed here) to include storage technologies that intertemporally maximize expected profits with constraints on how much they can store at any given hour. However, solving for 8760 equilibria for each electricity (up to 15) and heating area (up to 34) comes at a substantial computational cost. To cope with this, part III outlines a machine learning approach that group hours into representative clusters from variation in key variables (intermittent production capacity variation, demand habits, inflow of water to hydro plants etc..). However, this clustering breaks the chronology of the intra-year variation, thus posing an issue when it comes to the modelling of storage technologies. We propose to tackle this issue by using finite Markov-chains, with a one-cluster perfect foresight (see section 9.3.3 for how this works).

In section 14 the documentation details an issue with regards to how this approach performs, when it comes to representing the capacity on the storage technologies reservoir constraints (how much potential energy they can store in a given hour). The documentation points to the fact that the Markov-chain representation makes it much less likely for the reservoir constraints to bind. In particular, the issue of large seasonal build-ups was not captured by the original formulation. This issue has since been dealt with.

In the latest version of the model the year is initially split into chronological seasons using conditional inference trees. For each seasonal split the states are then clustered non-chronologically using the K-means algorithm.[1] The end-result of this machine-learning-based clustering is still a finite Markov-chain representation of the state space, and thus the storage representation is identical to the one outlined in section 9.3.3. Figure 0.1 illustrates that even with a very low cluster value ($k = 25$), the seasonal variation in both power generation and reservoir levels is very similar to the full model (8760 hours) simulation.

0.1.1 A small guide when comparing reservoir levels for full and clustered models

At a first sight the illustration of the reservoir level in a model with $k = 25$ clusters and the full model in figure 0.1b might give the impression of a poor fit. However, in all the way that matters for the model outcome (power generation and prices), the 25-cluster represents the variation quite well.

First, note that by construction the 25-cluster does not have 8760 unique values to feature, but rather **at most** 25^2.[2] So how do we compare the path for the reservoirs in figure 0.1b? Consider the winter/spring season in hours 1 to approximately 3000. The full model shows that the reservoirs are gradually being emptied from a level of roughly 1.75GWh to around 0.5GWh. For the clustered model,

[1] Technically we add another step to the process, where the number of clusters in each season is chosen by minimizing the sum of total within cluster variation across all seasons.

[2] Let p be the $(k \times k)$ Markov process. For each $p_{i,j} > 0$ there is a unique level of the reservoir, measuring the stored energy in clusters i that transitions to state j.

Figure 0.1: Performance of the state-contingent aggregation scheme.

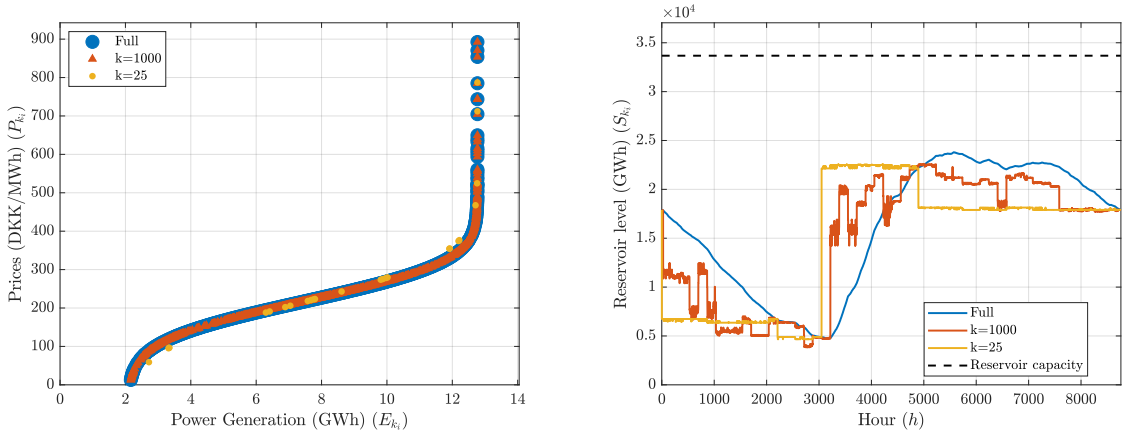

(a) Power generation (GWh). (b) Reservoir level (GWh).

the values are generally in the region of 0.5-0.7GWh. For the economic decision of the storage plants however, the only thing that matters is whether the reservoir level **at the lowest point** reaches the lower bound (0). The technical reason is that the shadow-cost of the reservoir constraints are always zero, as long as the reservoir constraint does not reach the capacity constraints. In other words: The forward looking plant-manager's economic decision is only influenced by the reservoir constraints, if the reservoir level at its lowest point is near the constraint. For the clustered model to be affected by the incentives of a binding storage constraint, we should then in general see the following:

- Assume that the full model exhibits a downward trend in the reservoir levels within a cluster k_i. For the clustered model to capture identical effects of a binding reservoir constraint, the level of reservoir in k_i should coincide with the minimum level observed in the full model.
- Assume that the full model exhibits an upward trend in the reservoir levels within a cluster k_i. For the clustered model to capture identical effects of a binding reservoir constraint, the level of reservoir in k_i should coincide with the maximum level observed in the full model.

These patterns are generally confirmed by figure 0.1b. For more on the effects of reservoir constraints on the economic decision of storage plants, we refer to section 4.3.

0.2 Fitting the residual load curve in clustered model

As briefly outlined in the update section 0.1, part III aggregates intra-yearly variation using K-means and conditional inference trees. In the baseline version outlined in the documentation, the representative intra-yearly states were simply computed by averaging over relevant hours identified by the K-means algorithm. In particular when the number of states (K) is small, this approach naturally averages out some variation. One way to assess this, is to simply plot the pre- and post-clustered variation for the residual demand curves:

When K is relatively small, the tails of the distribution is not sufficiently captured by the K-means aggregation. To account for this, we add the option to fit the residual load curves after the K-means

Figure 0.2: Residual-to-average hourly demand

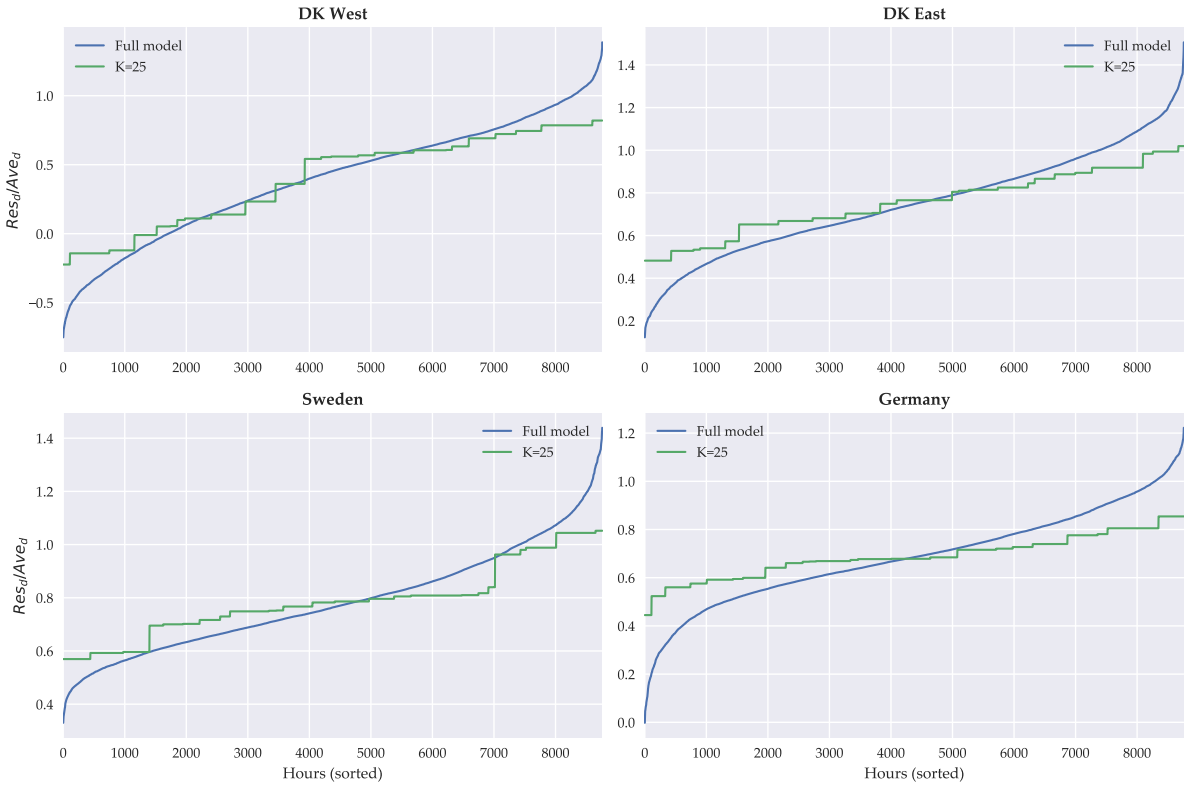

Note: The residual demand (Res_d) is defined as the hourly demand after production of intermittent technologies (wind, solar and run-off-river hydro).

aggregation procedure.

Contents

Part I

Introduction

1 Introduction

Throughout recent years the scientific community has gradually increased its warnings concerning emissions of anthropogenic greenhouse gasses (GHG). In its latest assessment report IPCC (2014) concludes with a 95% probability that humans are the main cause of current global warming and according to the prominent professor of economics Nicolas Stern (2008) emissions of GHGs constitute the largest market failure the world has ever experienced. Faced with the threat of global warming and driven by the desire to lead the international community by example, the Nordic countries have set ambitious goals for their climate policies aimed at phasing out the use of fossil fuels over the coming decades (Calmfors et al., 2019). As a milestone towards this goal, the Danish government recently announced a target of reducing Danish GHG emissions with 70% in 2030 compared to the 1990-level.

Compared to the pace of reductions undertaken so far, the new ambitious target for reductions requires a massive expansion of renewable energy supply from intermittent sources such as wind and solar energy. In its yearly status report, Klimarådet (2018b) estimates that reductions are anticipated to reach only 42-43% in 2030, when including the effects of the recent Energy Agreement (*Energiaftalen*). There are currently no agreements on which specific policies to enact in order to achieve the 70% reduction and considering the expansion of intermittent energy, several fundamental concerns are raised: How can society safeguard energy supply if most of it has to come from intermittent sources? Given our current state of knowledge, what technologies can provide the necessary back-up capacity for energy production, when the wind is not blowing and the sun not shining? How large are the social costs of integrating a much higher share of intermittent renewable energy in the energy system likely to be?

The purpose of the present paper is to start the development of an evaluation tool for environmental policies and provide answers to the above mentioned concerns. As part of a larger research project aimed at modelling the transition of the Danish economy to a fossil-free energy system and a carbon-neutral society (SUSY Project, 2019), the paper focuses on modelling the production of electricity and district heating (the transformation sector) and the associated emissions. In 2017 these forms of energy accounted for roughly one third of total energy consumption in Denmark, and are expected to account for a significantly larger share in a fossil-free economy, where renewable-based electricity is a main carrier of energy (Klimarådet, 2017; Energinet, 2019). Although primarily clean electricity is expected to be a main carrier of energy due to the expected electrification of other sectors, the inclusion of district heat in the analysis is necessary due the tight coupling between the markets through the widespread use of combined heat and power (CHP) plants in Denmark.

The paper presents a framework for a detailed modelling of production of electricity and district heating, relying on plant level data embodied in large-scale partial equilibrium models of the energy

system. In this context, the model relates to the general class of models termed *bottom-up* (BU) models. Given that the ultimate goal of the larger research project is to evaluate the social costs of transitioning to a fossil-free economy, it is necessary to combine a realistic model of the energy system with a detailed Computable General Equilibrium (CGE) model of the rest of the economy. The framework presented in this paper therefore emphasises the BU model's compatibility with a general equilibrium framework. 41 Unfortunately, conventional BU energy system models are traditionally specified as so-called linear programming problems that are hard to combine with standard large-scale CGE models, which are usually cast as non-linear, differentiable systems of equations. Integrating BU models with CGE models (or top-down (TD) models) has been a long-standing methodological issue in energy economics. This paper contributes to this literature by developing a non-linear BU framework for the energy system that allows for the *simultaneous* computation of the general equilibrium of a standard economic CGE model. Our approach has two important technical features: First, the BU framework includes a set of *smoothing* parameters. These parameters essentially smooth out potential discontinuities occurring in the BU model. When the smoothing parameters approach zero, the non-linear framework nests the conventional linear programming problem. Second, by increasing the smoothing parameters the BU model essentially becomes linear; this ensures that the developed approach has *global numerical convergence properties* under very mild conditions.[3]

To illustrate the usefulness of the non-linear BU framework, a number of exogenous policy-induced shocks, are simulated in a model of the transformation sector; all policy shocks that are expected to be instrumental in the transition to a carbon-neutral society. The four policy shocks are: (1) A significant increase in the supply of energy from intermittent renewable sources, (2) an increase in the flexibility of energy demand, (3) an increase in the capacity for energy storage, and (4) an increase in (network) capacity for international trade in electricity. For each of the four experiments, the paper provides contributions to the way production of and trade with energy goods can be modelled in a general equilibrium framework. First, to account for intermittency of energy supply the model solves for equilibria in the electricity and district heating markets on an hourly basis. To increase tractability and reduce the dimensionality of the model, the 8760 hours are aggregated into 40 representative, short run states. Second, we propose an analytically convenient way of modelling an increase in the flexibility of energy demand. Third, we propose a tractable new method for modelling energy storage that facilitates the integration of energy storage technologies in large-scale CGE models. Fourth and finally, to realistically capture trade patterns in the electricity sector in a general equilibrium framework, we offer a number of new solution algorithms that allow the identification of an equilibrium when electricity is a homogeneous good and international trade is subject to constraints on transmission lines' capacity.

The framework developed in the paper is applicable to any country but for the purposes of model validation and simulation of policy shocks, the model is calibrated to a data set for Denmark and neighbouring partners of trade in electricity.[4] The scope of the paper is limited to simulating the short run

[3]Global numerical convergence refers to the property that the algorithm, solving for equilibria in electricity and heat markets, will reach a solution, even with a poor initial guess of the solution.

[4]A standard criticism against national efforts by individual EU member states to expand the use of renewable energy

equilibria in the energy markets , treating production capacities as given. The policy experiments should therefore be seen as exercises in comparative statics, illustrating the effects of different initial conditions. However, given the importance of time dynamics in a green transition, a theoretical foundation for investment decisions in a dynamic version of the BU model is presented.

The paper is organized as follows: Part I proceeds to review the related literature on the cost of intermittency and the coupling of energy system and CGE models. It then provides an overview of the Danish energy sector and the relevant data used in this paper. Part II outlines the supply of electricity and heating in our technical BU model. In the most disaggregated version this covers individual firms' supply decisions in various electricity areas and heating districts on an hourly basis. Part III deals with what, in the literature of computational economics, is generally referred to as *the curse of dimensionality*. This is done by aggregating the hourly decisions into a number of aggregated representative states. Furthermore, the model is calibrated to fit a number of facts for the Danish energy sector in 2017. Finally, III carries out four simulation experiments in the calibrated model. Part IV deals with avenues for future work. Given that our agenda for future research is to incorporate endogenous investment in new capacity and embed the BU module in a dynamic CGE model of the Danish economy, a framework for endogenizing investments in the BU module is presented, along with a clear set of guidelines for how to calibrate the investment behavior in a CGE model. Finally, part V concludes.

2 Literature Review

The paper builds on a large body of existing literature in energy economics. Below we outline the two main areas of research that our paper relates to: 1) intermittency in energy production and the instruments that mitigate the related problem, and 2) integration of BU models of the energy system and CGE models.

2.1 Intermittency in electricity production and mitigating instruments

The research on intermittency in electricity generation has increased significantly, as the associated cost of intermittency rise with higher market penetration rates of technologies using intermittent renewable energy (such as wind and solar power). The costs and complications of electricity generation being intermittent can be described in both technical and economic terms. Delarue and Morris (2015) outline the primary technical complications: Firstly, increasing the share of intermittent electricity generation makes it difficult to safeguard electricity supply. Power transmission grids operate at a certain frequency (typically 50 Hertz) and for the grid to stable, supply and demand has to balanced. With an increasing share of fluctuating supply, however, it is more difficult to balance load and supply at all times. Secondly, the authors stress that intermittency lowers the average load factor, creating a need for costly back-up

within the sector covered by the European Emissions Trading System (ETS) has been that such efforts do not reduce total European emissions, due to the cap on total emissions within the ETS. Some readers might therefore argue that it is not very interesting to analyze national climate policy measures targeted at the electricity and district heating sectors, which are typically covered by the ETS. However, because of the huge surplus of emission allowances and the recent ETS reform, which effectively endogenizes the supply of allowances, national policies to promote renewable energy in the ETS sector can in fact secFure a permanent reduction in global emissions, as shown by Silbye and Sørensen (2019).

dispatchable capacity. The load factor is defined as the ratio of production to generation capacity and therefore measures the degree of utilization of the existing capital. Even with a large capacity installment of intermittent technologies there is a need for back-up capacity when the wind is not blowing sufficiently. Without an adequate mitigation of intermittency this necessary back-up capacity requires quite large investments. For our purposes the relevance of the technical complications is essentially how it translates into economic considerations. The economic implication is the need for a sufficient back-up generation from conventional dispatchable technologies. Investment in these are based on the profits covered in peak hours of demand or when the productivity of intermittent technologies is low. The value of intermittent technologies in turn depends not only on the cost of producing electricity but also largely on which hours the productivity is large (Joskow, 2011). Thirdly, intermittent technologies such as wind and solar power have the general feature that marginal costs of production are near zero. This creates a *downlift* in the producer price that intermittent technologies' receive compared to the average producer price.[5] Thus, in the absence of subsidies or mandated feed-in tariffs there is less incentive to undertake further investments in intermittent renewable-based technologies. Interestingly, Hirth et al. (2015) argues that the cost of intermittency can be summed up by the size of the downlift. Even though we generally agree that the downlift is a key aspect of intermittency, the social cost of intermittency will in a future CGE model be measured in utility terms. In the BU framework presented in this paper, however, the focus is primarily on the size of the downlift for assessing intermittency cost similar to Hirth et al. (2015). Fourth and finally, Delarue and Morris (2015) argue that there are network costs associated with the installation of new intermittent capacity. These occur in the form of e.g. connecting off-shore wind turbines to the electricity grid and developing the grid to absorb a larger intermittent electricity production. We take all of these considerations into account in the BU module.

In assessing the costs related to intermittency, the existing economic literature has focused primarily on key instruments for mitigating the costs: Feed-in tariffs, renewable portfolio standards, energy storage technologies, increased demand flexibility, and increased capacity for trade in electricity. The importance of the various instruments as well as the overall assessment of the costs of intermittency varies significantly across studies. Here, we focus on the literature concerning energy storage, demand flexibility, and trade because considerable effort in the paper is spent on modelling and including these three avenues for mitigating the costs of intermittency.

Energy storage has been examined in a large body of economic literature. Sinn (2017) argues that it is prohibitively costly to sustain large penetration rates of intermittent technologies in Germany due to the required investments in storage capacity. His analysis is based on a BU simulation model of the energy system. Zerrahn et al. (2018), however, shows that by relaxing some of the assumptions in Sinn (2017), e.g. allowing for demand curtailment, required investments in storage capacity is unlikely to be a barrier for a transition to intermittent renewable-based energy. In an dynamic extension of the theoretical model in Ambec and Crampes (2012), Ambec and Crampes (2017) model intermittency in a two-state structure where one is characterised by high intermittent production and the other low intermittent production.

[5]The downlift cost of intermittent energy production is defined as the difference in yearly average prices and average price intermittent technologies receive.

In this analytically tractable framework, the authors find that the value of energy storage is the ability to move supply from low-value (low price) to high-value (high price) states. Thus, the value can be measured by differences in prices on the wholesale market. We follow this insight in the interpretation of the counterfactual scenarios in section 11.

Ambec and Crampes (2017) also examine the effects of increased demand responsiveness. They assume that consumers are equipped with smart-meters and load-switching devices when wholesale electricity prices are passed down to consumers.[6] They find that such instruments are substitutes to energy storage technologies, given their implementation has similar effects. We come to an equivalent empirical conclusion in our paper. Similar to Ambec and Crampes (2017) this paper also captures intermittency by including states with high and low intermittent productivity. However, the focus here is aimed more directly at applying it to real data. In this respect, the BU module in the paper shares more with applied energy system models.

With regard to trade in electricity with neighbouring areas, there are in general two different modelling approaches in the literature. The first is to assume that domestic and foreign electricity are heterogeneous. An example hereof is Gowrisankaran et al. (2016), who estimate the costs of intermittency for Southeastern Arizona. They conclude that at current market shares the costs of intermittency in solar generation accounts for roughly one-third of total social costs of providing solar power. The authors account for trade in electricity with neighbouring areas by modelling net-imports as a linear iso-elastic demand specification. Their method is the standard approach (in the general trade literature) for modelling international trade and is based on the Armington specification (Armington, 1969). The Armington approach assumes that domestic and foreign goods are heterogeneous and consequently imperfect substitutes. Trade flows can then be determined by means of a trade elasticity below infinity. While Gowrisankaran et al. (2016) find that trade have small impacts in terms of changing the social costs of large-scale solar implementation, we come to an opposite conclusion in this paper and find that in the short run (one-year horizon) - where other elements are fixed - trade is the primary valuable instrument for mitigating the cost of intermittency. One explanation for the differences in results is that we assume electricity is homogeneous, implying domestically and foreignly produced electricity are perfect substitutes.

The framework based on the assumption of homogeneity is the standard approach applied in large-scale BU models of the electricity sector (Balyk et al., 2019; EA, 2018; Danish Energy Agency, 2018a). Using data on transmissions lines' capacity, BU models of the energy system are able to simulate trade in electricity.[7] This approach is also applied here. In general, we rely heavily on existing large-scale BU models of the transformation sector for describing the technical workings of the currently available technologies and energy system. In particular, we draw on the three BU models for the Danish energy system: TIMES-DK (Balyk et al., 2019), Balmorel (EA, 2018), and Ramses (Danish Energy Agency, 2018a). Compared to these conventional BU models, the approach applied in this paper is in some ways

[6] Smart-meters measure real-time consumption of energy and load switching-devices are intelligent technologies that use electricity when prices are low. An example could for instance be setting a dryer to run on a certain time of day where prices are low.

[7] Under the assumption of a homogeneous good, one is left with explaining why the law of one price does not hold in electricity markets and why a single electricity area does not capture the entire market. The key constraint here is transmission capacities. We comment on this in section 3.2.1.

not as detailed. Given the purpose of this paper is to develop a model that can be integrated with a large-scale CGE model of the Danish economy, simplification is necessary. For example the BU model presented here does not include any explicit formulation on how the electricity grid is managed. In other contexts, however, the paper provides innovations on how to model the transformation sector. This is the case for the supply of a number of technologies such as CHP plants and storage technologies and the way trade in electricity is modelled. Specifically, foreign electricity prices are assumed exogenous in TIMES-DK.[8] The approach developed in this paper is more general, as it in handles foreign countries' electricity markets equivalently to the domestic ones. While the application of interest is the Danish energy sector, the framework is sufficiently general to be applied to electricity regions including several countries (e.g. the European market). In this paper, trade in electricity is modelled by a novel trade mechanism that emulates the trade algorithm on the day-ahead market on the nordic electricity exchange, Nord Pool spot market.

2.2 Energy system modelling and coupling of Bottom-Up and Top-Down CGE models

Because the simulation model presented here is a BU model for the transformation sector that is meant to be compatible with a CGE model, our paper also relates to the growing literature on the integration of BU and Top-Down (TD) models. Below we review the BU/TD nexus and the integration methodology applied in this paper compared to previous studies.

Integrating BU energy models with TD models has been a longstanding issue in energy economics. BU models are typically *engineering* models, describing physical flows and stocks in the energy system. Their main advantage consists of being highly disaggregated and rich on technological detail. The main disadvantage is that they are typically partial equilibrium models that lack feedback effects between the energy system and the macro economy. TD models on the other hand are general equilibrium models, describing monetary flows and stocks and are therefore rich on economic dynamics. They are appropriate for capturing economy wide effects but often oversimplify physical and technological constraints on the economy.

The distinction between TD and BU models is not only in application but also in technical terms. TD models typically represent economic sectors by smooth, differentiable production functions, where transformation possibilities are captured by means of elasticities of substitution (Böhringer and Rutherford, 2009).[9] The substitution elasticities are structural parameters that amongst other things attempt to capture, if the sector includes more than one available production technology. The model is then solved by using non-linear optimization algorithms, typically based on (some variant of) Newton's method.[10] Consequently, TD models are not suitable for analyzing discrete choices such as the choice of a discrete

[8] Prices on import/export of electricity does however vary (exogenously) over transmission lines and time, in a way that is based on data and projections from other models.

[9] The most prominent production function used in the CGE literature is the constant elasticity of substitution (CES) function.

[10] In this paper we use GAMS' Newton-based solver, CONOPT4, which is documented in Drud (2019). This is also the solver used in the Danish models REFORM (Stephensen et al., 2019) and MAKRO (The MAKRO modelling Group, 2018).

set of production technologies that produces an identical good. In contrast to TD models, BU models are usually formulated as *linear programming* problems to analyze energy production, using precisely a set of discrete energy technologies (Böhringer and Rutherford, 2009).

The literature has generally distinguished between different degrees of integration of BU and TD models. Wene (1996) and subsequently Helgesen et al. (2018) categorise the degree of integration into soft-linking, hard-linking and full integration.[11] The distinction is illustrated in figure 2.1.

Figure 2.1: Integration methodologies

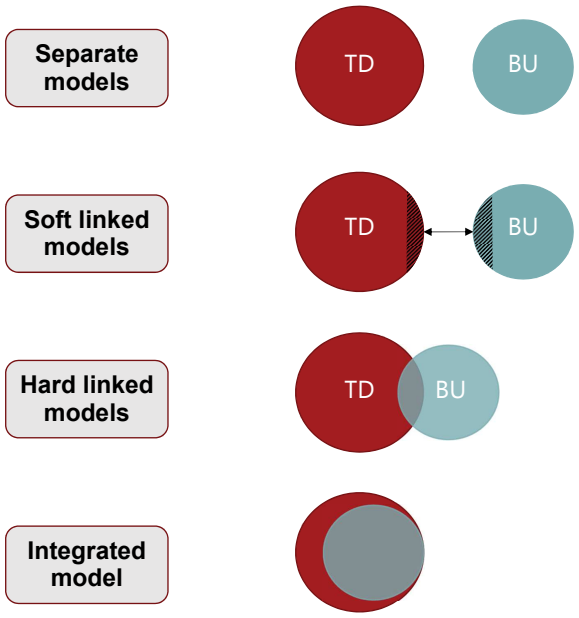

Note: TD is top-down model and BU i bottom-up model. Size of circles does not represent dimensionality of models.
Source: Helgesen et al. (2018, p. 197).

Soft-linked models are the interaction between two separate models. Here, the information flow (e.g. demand and supply) between the BU and TD model is *manually* controlled by the user and there are rarely consistent feed-back effects between the models. This generally challenges the consistency of the interaction (Helgesen et al., 2018). Hard-linked models are still considered as separate models but the information flow is more formally stated and automated without the interference of the user. Most often, hard linked models are solved by means of an iterating convergence algorithm. Roughly speaking the algorithm alternates between solving each of the two models, until the information flow between the models has converged. Finally, fully integrated models are modelled in one unified framework. Consequently, there is no exchange of information or separate model runs (Helgesen et al., 2018). The methodology applied in this paper belongs to the category of fully integrated models.

[11] Böhringer and Rutherford (2009) group the different methods into (i) coupling of existing large-scale models, (ii) having one main model completed with a reduced form representation of the other, and (iii) directly combining models as mixed complementarity models. Although these different categories should be viewed as overlapping and complementary we adopt the terminology of Helgesen et al. (2018) because we view the authors' distinction as more general.

Böhringer (1998) and Böhringer and Rutherford (2008) have been the main advocates for and pioneers of fully integrated models, with Böhringer (1998) being one of the first to apply a TD model recasted as mixed complementary problems (MCP). Here 'mixed' refers to the property that the model is comprised of both equalities and weak inequalities. 'Complementarity' reflects that each equation with equality or weak inequality is associated with an endogenous variable, such that the system of equations is square and can be solved (Andersen et al., 2019). For instance, each weak inequality is associated with a Karush-Kuhn-Tucker (KKT) slackness variable (or shadow variable in economic terms).

The primary motivation for the MCP formulation is to capture both discrete energy producing technologies and economic richness in a single mathematical format (Böhringer and Rutherford, 2009). Solving an integrated model as a MCP, however, suffers in particular from the curse of dimensionality. As the MCP approach adds weak inequalities to the model, it often doubles the number of equations (dimensions) of the model, slowing down computational speed and in some instances making the model intractable (Böhringer and Rutherford, 2009; Andersen et al., 2019). If the BU model is very disaggregated (in terms of both technologies and time steps) or the integrated model consists of multiple sectors, the number of weak inequalities explodes, making the MCP format an impracticable approach to apply.

An alternative to the fully integrated MCP framework is to iterate between hard linked models, which is the approach taken in the IntERACT model of the Danish economy. The focus of IntERACT is to link energy service supply and demand within industrial and residential sectors (e.g. high temperature process heat in industry and residential space heating). IntERACT hard links the energy system model TIMES-DK (Balyk et al., 2019) formulated as a linear programming problem to a CGE model formulated in the MCP format. Andersen et al. (2019) outline the linking methodology using a stylised example of the production of heat, and so show that all information (demand, supply, and prices) are fully consistent across the BU and TD model, similar to the fully integrated MCP framework.

However, when the dimensionality of linked models increases, such hard links face substantial problems in achieving convergence of the iterative solution algorithm, because the models are run and solved separately (Böhringer and Rutherford, 2008) - a point also raised by Andersen et al. (2019). To mitigate this issue, and to overcome conceptual differences of the BU and TD models, Andersen et al. (2019) applies a partial information linking-approach that relies on average cost pricing for some energy services; an approach that proves superior when linking a TD model formulated as a MCP and a BU model formulated as a LP. Furthermore, the aforementioned curse of dimensionality of the MCP format is ameliorated by coupling the BU model to a static CGE with calibrated exogenous investments.

The approach applied in GreenREFORM is motivated by the fact that most large scale CGE models are developed as constrained nonlinear systems (CNS), including the body of dynamic models developed by DREAM. In this case, the linking approach developed for the IntERACT model no longer appears appropriate. To this end, we develop a BU module of the production of electricity and district heat in the CNS format. We show that our formulation nests the solution to the traditional linear programming problems used in BU models in the limit. Furthermore, as the BU model is formulated in the same format as standard CGE models, the BU model can be fully integrated with a CGE model in the typical nonlinear programming format. In section 12 we further present formulations on how endogenous capital

investment in capacity can be integrated in a dynamic CGE model.

3 Institutional framework and data

3.1 The Danish transformation sector and the scope of our model

The BU module in this paper is a model of the Danish transformation sector, which is a subset of the entire energy sector. The transformation sector includes only the production and distribution of electricity and district heating, which are separate from e.g. the extraction and refinement of primary energy. While GHG emissions from the Danish transformation sector have decreased by 45% since 1990, it remains an essential sector both in terms of its emissions today (19% of all emissions from the public and private sector), but also due to its expected role in the electrification of other key sectors (Klimarådet, 2017; Energinet, 2019). Moreover, electricity and heating are key energy goods in Danish consumption. The Danish Energy Agency (2017a) provides an overview of the final consumption of all energy goods categorised into eight groups. The development in final energy consumption from 1990-2017 is plotted in figure 3.1. Part (b) of figure 3.1 shows that oil products are by far the most consumed energy good, but electricity and district heat are second and third, respectively. Out of all final energy consumption, they made up more than one third in 2017. Part (a) of figure 3.1 illustrates the development in the

Figure 3.1: The transformation sector and the total energy sector

(a) Consumption of renewable energy

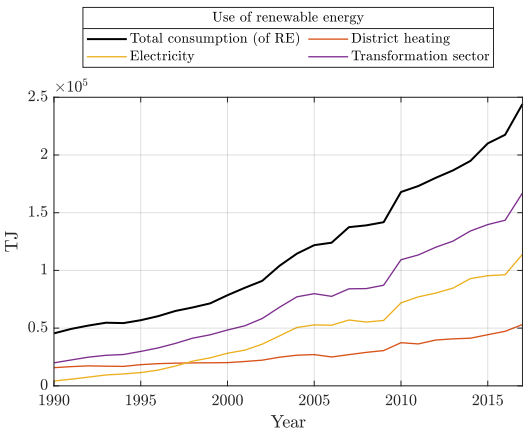

(b) Consumption of energy

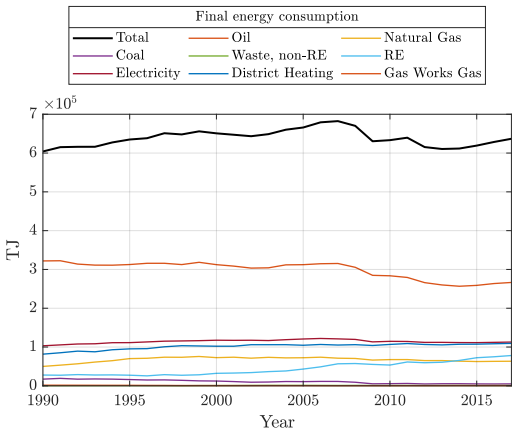

Source: Danish Energy Agency (2017a)

consumption of renewable energy for the electricity and district heating sector. The electricity sector has been the main driver of an increasing consumption of renewable energy (using mainly wind power, PV, and biomass). In short, the transformation sector supplies around one-third of the final energy consumption, but it uses more than two-thirds of all the renewable energy in Denmark (Danish Energy Agency, 2017a). This emphasizes that in a green transition of the energy sector the transformation sector is instrumental.

A general overview of the scope of the BU module can be illustrated from the supply chain for electricity production (see figure 3.2). In the first step of the supply chain, primary energy such as oil and natural

gas are extracted. These are used as fuel inputs in the second step where power and heat are produced. The BU model developed in this paper will focus heavily on this section, exploiting data supplied by the Danish Energy Agency. In the third step electricity is sold on the wholesale market (Nord Pool spot market) and distributed to electricity areas via transmission lines. This step will similarly be modeled quite detailed, using information on neighboring countries' electricity markets as well as ENTSO-E data on trade capacities. In the fourth step electricity reaches the distribution network within a given electricity area, which is then supplied to the end-consumer in the final step. In the BU module developed here the distribution part will be latent, and only included as a wedge between production and consumption, reflecting an exogenous grid-loss rate.

Figure 3.2: The supply chain of electricity

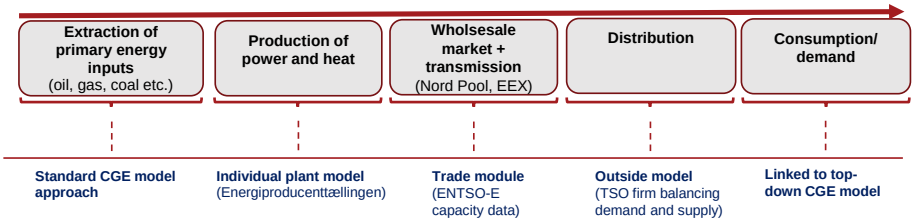

Note: The supply chain for district heat is similar but given that heat is not traded, there is no wholesale market for district heating.

We take the production and trade of primary energy inputs as given in the BU module. Consequently, prices on primary fuel inputs are exogenously given. Once the model is coupled to a CGE model, this sector will work similarly to other sectors using a standard nested CES production technology methodology. The primary reason for not including this part of the energy sector in the detailed bottom up module, is that these sectors are not influenced by the same short run characteristics of the electricity and heat market. In other words, while the modelling of extraction of primary inputs is important in a final CGE model of the Danish economy, the most important features can - in our view - be captured by the standard nested CES approach.[12]

The supply of electricity and heating can, however, not be modelled using the standard approach in CGE models. The electricity market is a complex market where demand and supply has to be continuously balanced for the electricity grid to be stable; a challenging task when facing more intermittent energy production *within a year*. Thus, we need to account for dynamics within a given year. Furthermore, electricity is a homogeneous good and the only market imperfections preventing prices from equalizing across countries, are the capacity constraints from transmission lines. Modelling electricity trade using the Armington approach (Armington, 1969) is therefore not appropriate. We return to this issue and provide suitable alternatives in section 6. Further, to accurately capture marginal changes in emissions, we need a realistic modelling of the discrete set of competing technologies producing power and heat.

[12]One difference is in the case of PtX technologies, where electricity is used in the production of a range of fuels. See e.g. Energinet (2019). These technologies do not play an important role today but can be invested in and thus penetrate the market at a later time. However, the framework presented in this paper does allow for interactions between production of electricity and bio fuels.

These features make the CES structure unsuitable to describe the production from the transformation sector.

Besides detailed information on production plants in the transformation sector, we include a rich description of trade of electricity in our model. In particular we model neighbouring countries in a similar way as the Danish supply of electricity and connect the areas with transmission lines that facilitate trade. Section 6 outlines the trade module in detail. Since heating are not traded across districts, there is no trade module for the district heating sector. Furthermore, this version of the BU module only covers a detailed description of the district heating part of the sector and does not include a description of individual heating, due to the coverage of the applied data. As the framework developed in this paper is inspired by the technology data published by Danish Energy Agency (2016), it makes the introduction of new technologies straightforward in future work.[13] Section 4 and appendix B describe the transformation sector in more detail.

Finally, the model does not explicitly include an agent that handles the distribution from plants to end-consumers. It is implicitly accounted for by including a wedge between supply and demand, representing an exogenous loss-rate in distribution; this is similar to the Balmorel model (EA, 2018). Furthermore, the cost of connecting a plant to the grid is included in the investment cost of constructing a new plant. To the best of our knowledge this is not a critical simplification of the model. The demand for both electricity and heating are modelled in two steps. First, the yearly level of demand is determined from a standard price-sensitive function. Second, this level is mapped onto hourly components. This novel modelling strategy contains structural parameters that represent both habits in demand as well as short run price responsiveness. The approach allows us to simulate the effects of varying the flexibility of short run demand and evaluate the effects of e.g. the introduction of smart meters in households.[14] Furthermore, the approach provides a straightforward link when integrating it in a CGE model. As the BU module is solved given the yearly demand, it leaves room for a different module or CGE model to specify how yearly demand depends on equilibrium prices. An equivalent linking approach is found in the Danish IntERACT model (Andersen et al., 2019). Section 5 outlines the demand for final energy consumption in more detail.

3.2 The Danish transformation sector: An overview

Below we describe in more detail the structure of the electricity market and the district heating sector. We give an introduction to the current market structure and supply composition. The sections outline the challenges facing the sectors in a future transition to a fossil-free society and motivates important features of the markets that we aim at capturing in the BU module.

[13] The framework presented in this paper needs information on the following to include it in the model: (1) Short run marginal costs, (2) investment costs, and to realistically model future penetration of the technology (3) expert information on economy-wide potential.

[14] This is seen as part of the essential solutions in a Danish context (Danish Energy Agency, 2013).

3.2.1 The electricity market

The market structure:

The Danish electricity system is comprised of two interconnected areas, Western Denmark (DK-West) and Eastern Denmark (DK-East). The two areas are separated by the Great Belt. DK-West is interconnected with Germany and DK-East is connected with Sweden and Norway via direct current (DC) connections. This is illustrated in Figure 3.3. Thus, Denmark currently only trades electricity with Germany, Sweden and Norway. Before 2010 DK-West and DK-East were completely separated and operated as two independent markets. There was no need for a pairing of the two electricity markets since the cost structure of the two areas were very similar. However, with the expansion of wind energy and decentralized joint production of heat and electricity (decentralised CPH plants) during the 1990s a need for a connected transmission grid emerged. Consequently, the Danish transmissions system operator (TSO) established a (DC) connection across the Great Belt in 2010 to facilitate trade between the two domestic areas (Energinet.dk, 2016). This highlights the need for better integrated electricity networks when a larger share of electricity is based on intermittent energy sources and motivates an explicit modelling of trade in electricity.

Figure 3.3: Development of the Danish electricity production and transmission grid

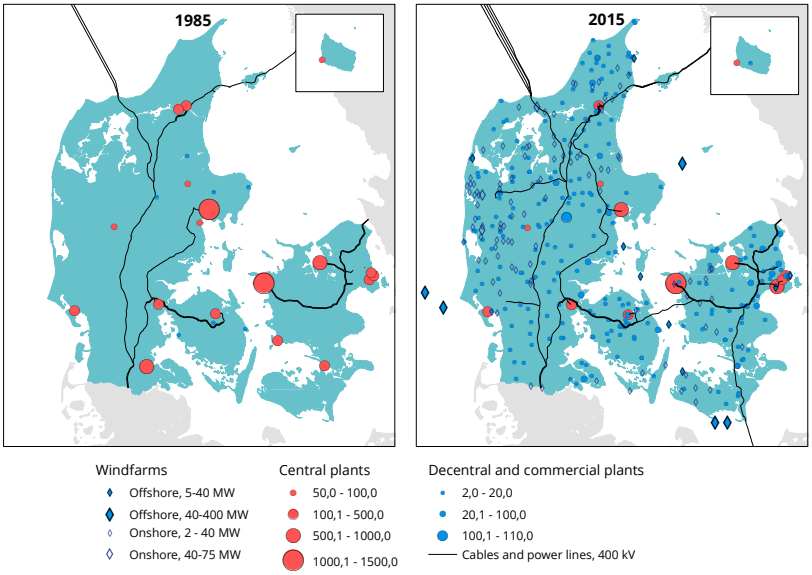

Source: Danish Energy Agency (2017b)

It is important to note that while the electricity distribution network is a natural monopoly, production of electricity as well as trade with electricity in the wholesale and retail market is subject to competition. Initially, electricity is traded in the wholesale market consisting of several markets. The primary wholesale market in Denmark is the Nordic electricity exchange Nord Pool for trading with Norway and Sweden. As of 2016 more than 90% of the Danish electricity consumption is traded on Nord Pool (Energy Commission, 2016). However, it also possible to trade on the European Electricity eXchange EEX for trading with Germany, as well as trading within a single geographical area via bilateral contracts between sellers

and buyers. Furthermore, in the wholesale markets electricity can be traded both one day ahead of consumption (also known as the day-ahead market) and on the day of planned consumption (the intraday market). In our model the equilibrium on the electricity market resembles that of the day-ahead market.[15] In the last steps of the value chain domestic, imported, and exported electricity is directed to the retail market for final consumption via the transmissions grid and local distribution networks. The only way this last step appears in our model is via an exogenous distribution loss rate.

The current state of supply: Production

The supply of electricity in the wholesale market comes from a range of technologies using different fuels. In figure 3.4 we plot the gross supply of Danish electricity split onto production types and fuel shares. A number of trends are evident from the data: Firstly, the production of electricity comes either from CHP plants, intermittent technologies as wind turbines, or from imports. Dispatchable plants that only produce electricity (and not heat) only provide around 2% of the domestic supply.[16] Secondly, with the increased use of wind turbines in domestic production, import becomes more important. Net imports have in recent years covered around 15% of Danish supply with imports providing 45% of Danish supply. Thirdly, the increased use of wind turbines and import has primarily led to less use of coal, oil and natural gas. The only fuel type that is used in dispatchable domestic plants, which has had an increasing share of supply, is biomass. In section 3.4 we outline how the tax scheme in recent years has favoured the use of biomass in production, which is directly modelled in the BU module.

Figure 3.4: The Danish supply of electricity

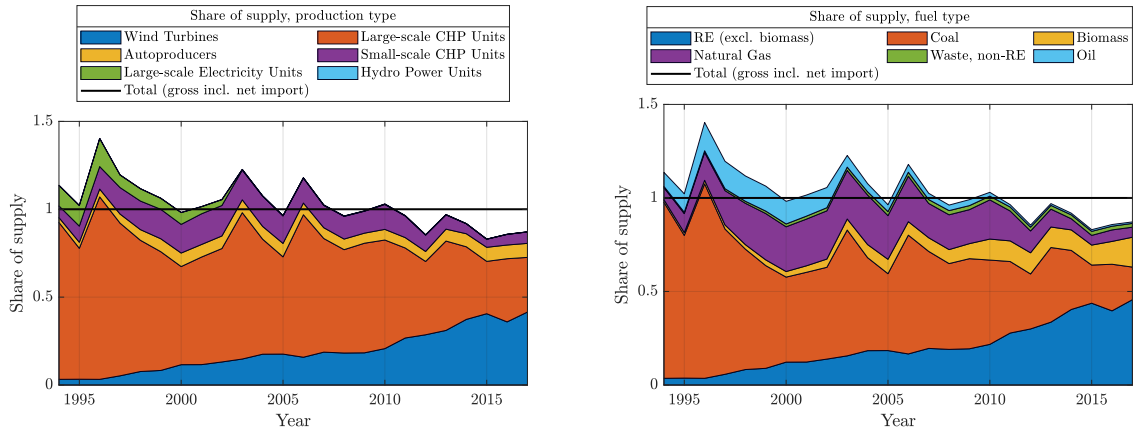

(a) (b)

Source: Danish Energy Agency (2017a).

We observe another interesting trend when we compare the supply from domestic dispatchable plants to their capacity. From 1994-2017 the domestic production of electricity excluding intermittent sources

[15] While we have variation in productivity and demand in our model, we do not have uncertainty. This means that we cannot model e.g. the importance of being able to ramp up production fast to ensure the balancing of supply and demand. We believe it is a natural next step to model an intraday market, where only peak power plants and reserve technologies can operate. This is, however, well beyond the scope of this paper.

[16] The term *autoproducers* refers to firms that to some degree produce themselves the electricity and/or heat used in their production of some other good. Autoproducers can further be split into CHP units and electricity producing units: Within this category around 25% is electricity producing units.

(wind, solar, hydro) has decreased by around 60%. At the same time the capacity has "only" decreased by around 22%.[17] The much smaller adjustments in capacity than production is expected with the increase of intermittent technologies. In part, back-up capacity is still needed for the hours of the year, where wind power is not sufficient to cover demand. The implication is that for a lot of plants the short run profits of operating in peak demand hours still exceeds the value of the outside option of re-purposing the capital tied to the plants.

The current state of supply: Trade

As already noted, the importance of trade has been growing in recent years. At the moment Denmark can trade with Norway, Sweden and Germany. As a part of the plans to increase the share of renewable energy in the EU, significant investments have already been undertaken to integrate the electricity market. From a Danish perspective this means that new transmission lines are already being build to the Netherlands and The United Kingdom (ENTSO-E, 2018).[18] A model for the Danish electricity sector therefore needs to incorporate the trend that European electricity markets become more integrated over time.

To illustrate the current state of trade, we have collected data on hourly electricity prices, consumption, production, and transmission capacities for Denmark and its neighbouring countries (Energy Data Service, 2018b,a). As electricity is a homogeneous good, prices should be largely equalized across geographical areas unless there are capacity restrictions in trade preventing this. Figure 3.5 tests this assertion by plotting how often prices are equalized across the relevant geographical areas. The data covers the entire period from 1st of January 2011 to 30th of August 2018 on an hourly basis, providing 67.912 hours in total. The trade data indicates that most of the time the electricity price in Denmark is equalized with at least one of our trade partners (mostly Sweden or Norway), cf. part (b) of figure 3.5. But almost 100% of the time prices will not be equalized in *all* neighbouring countries, cf. part (a) of figure 3.5.[19] The trade algorithm implemented on Nord Pool's trade platform is based on the fundamental assumption that electricity is a homogeneous good such that electricity flows from high-price areas to low-price areas until prices are equalised. The only constraint preventing prices from equalising is the binding of transmission capacities. Note that within a single hour, electricity only moves in *one* direction but when we examine yearly data, there are both positive import and export flows due to the hourly variation.

The key take away from the descriptive evidence is that trade of electricity is not suitable to model with a standard CGE approach based on the Armington assumption (Armington, 1969). Within capacity constraints, foreign and domestic electricity are perfect substitutes, which means that around certain thresholds the model needs to switch from an *open* to a *closed economy* methodology. In the model

[17] See Danish Energy Agency (2017a) pages 11 and 14.

[18] See here for information on the Viking DKW-GB cable and here for the COBRA cable.

[19] Trade with Sweden and Norway occurs almost absent frictions within the available capacity of the existing transmission cables. Historically, however, the trade patterns we observe with Germany does not indicate a frictionless line. In fact, the Danish TSO filed a complaint against the largest German TSO (TenneT) for systematically limiting the southward capacity on the interconnector between DK-West and Germany. In December 2018, the European Commission imposed a binding obligation on the German TSO to increase transmission capacity between Denmark and Germany data from European Commission (2018). In the BU module, we only deal with this issue by adjusting the transmission capacity to the average available capacity in 2017 using (Energy Data Service, 2018a).

Figure 3.5: Market allocations in the day-ahead market

(a) Frequency of unique hourly prices

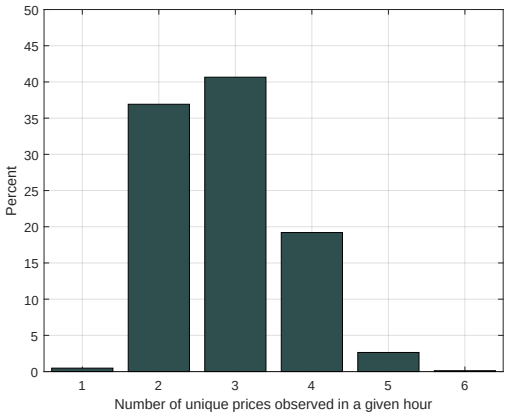

Note: The figure illustrates the frequency of unique prices observed in DK and all its trading partners (DE, NO2, SE3, and SE4). Rarely, prices are the same in all electricity areas due to binding transmission capacities. Note that maximum number of electricity areas is six.

(b) Most frequent market couplings

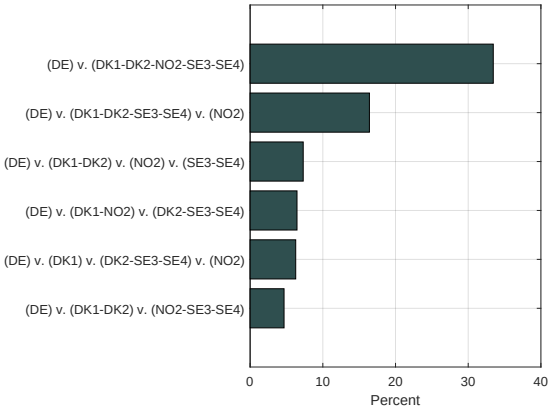

Note: The figure illustrates electricity areas where prices are equalised. For instance, the most often allocation (34.5%) is when DK prices are equalised with all Nordic trading partners (areas NO2, SE3, and SE4) with the German price being different. Note that DK1=DK-West and DK2=DK-East.

Source: Own calculations based on Energy Data Service (2018a,b).

for the Danish transformation sector presented here, the supply from neighboring countries' plants are modelled similarly to Danish plants. Furthermore, we use data on existing transmission line capacity as well as planned connections, to account for how future integration of European electricity markets will affect the Danish economy. The model approach for trade is outlined in more detail in section 6.

3.2.2 The provision of heating

The market structure:

The Danish heat supply sector is comprised of two supply systems: district heat and individual heat. Individual heat supply is typically produced using oil or natural gas boilers but also include technologies based on renewable energy such as individual heat pumps and biomass boilers. Currently, there is a Danish ambition to phase out the use of oil and natural gas boilers in the individual heat supply (Energy Commission, 2016). Furthermore, due to expansion of the district heating system, especially in the 1980s, individual heat supply is now mainly dominant in rural areas and small towns and account for 37% of Danish households' consumption of heating (Energy Commission, 2016).[20] These 37% are not accounted for in the BU module. Figure 3.6 illustrates the Danish supply of heating. As this illustrates the individual heat supply is a significant component of the total supply of heat in Denmark. In the current version of the model the individual heat supply is not included. The reason for this is purely due to the data set applied at this moment. The proposed methods for modeling competition between heat technologies and investments therein, can be applied to both individual and district heating technologies.

[20]This figure varies somewhat across sources. In Danish Energy Agency (2014b) the share of district heating coverage is 50% for 2014, but with the estimated coverage of 69% for 2020. When it comes to the heating of houses (*boliger*) the figure for district heating coverage is even higher at 80%, see `https://ens.dk/ansvarsomraader/varme/information-om-varme`. Other sources cite a 50% share of district heating (Dansk Energi, 2018) as of 2016.

Figure 3.6: Denmark's heat supply in 2014

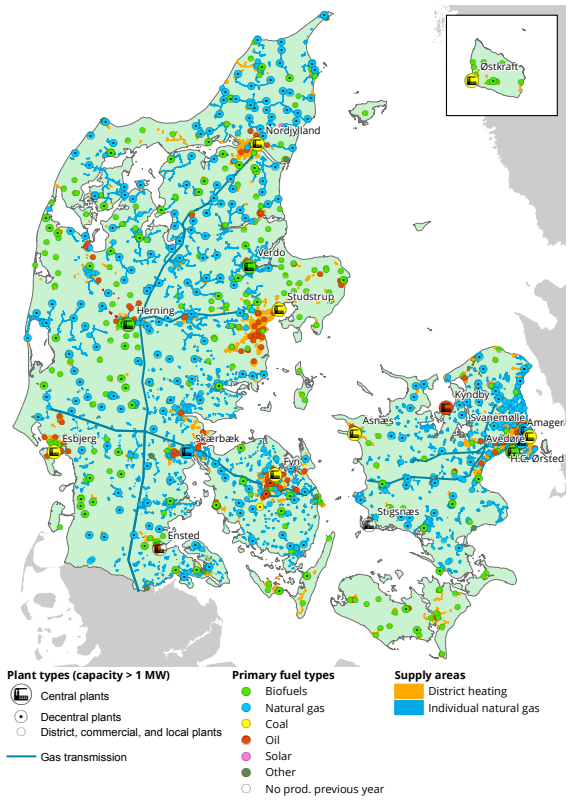

Source: Danish Energy Agency (2014a)

Compared to the electricity market (where Denmark consists of two zones), heating are not traded across geographical areas and the geographical areas are far smaller (34 zones in Denmark). The heating supply is highly regulated in Denmark, to the point where some geographical areas have *tilslutningspligt* to the district heating system. This entails that households in some areas have to use the local district heat supply. Furthermore, given there is no spot market for heating, district heating prices are fixed according to a *hvile-i-sig-selv* principle (cost-plus pricing), i.e. where prices are determined on the basis of the costs of the plant.[21]

The current state of supply:

Figure 3.7 illustrates how the composition of district heat supply has evolved since 1994. First, in contrast to the electricity sector, the share of heating coming from CHP plants has slightly decreased, cf. part (a) of figure 3.7.[22] But more importantly, part (b) of figure 3.7 indicates that the district heat supply has been less affected by the ongoing green transition compared to the electricity supply. Whereas wind turbines and import of cheap clean energy (hydro) play a larger role in the supply of electricity today, renewable-based heat production (excluding biomass, i.e. solar heating and heat pumps) accounts for a much smaller share of the district heat supply. Biomass is by far the most important fuel today. While

[21] For an overview of the regulation (in Danish) see Danish Energy Agency (2018b).

[22] We note that the *level* of heat production from CHP plants has increased slightly though. The decreasing share is due to the an increased production from plants producing only heat.

renewable energy including biomass makes up almost 50% of total supply, the renewable production without biomass is only slightly below 4%. The increasing use of biomass has primarily displaced the use of oil and coal, which has decreased significantly, similar to the electricity sector. We also note that the use of natural gas has decreased slightly.

Heat pumps are also used in district heating supply, which partly falls under the renewable energy category in part (b) of figure 3.7. Although investments to increase the capacity of more (and more efficient) heat pumps have already been undertaken, the current penetration of renewable energy provided by heat pumps is only at 1 per-mille (1.4% for all electrical heaters including heat pumps). In this context, the district heating sector faces many of the same obstacles as other sectors such as transportation in further reducing GHG emissions: The road to GHG reductions primarily relies on a combination of using renewable electricity and bio fuels.

Figure 3.7: The Danish supply of district heating

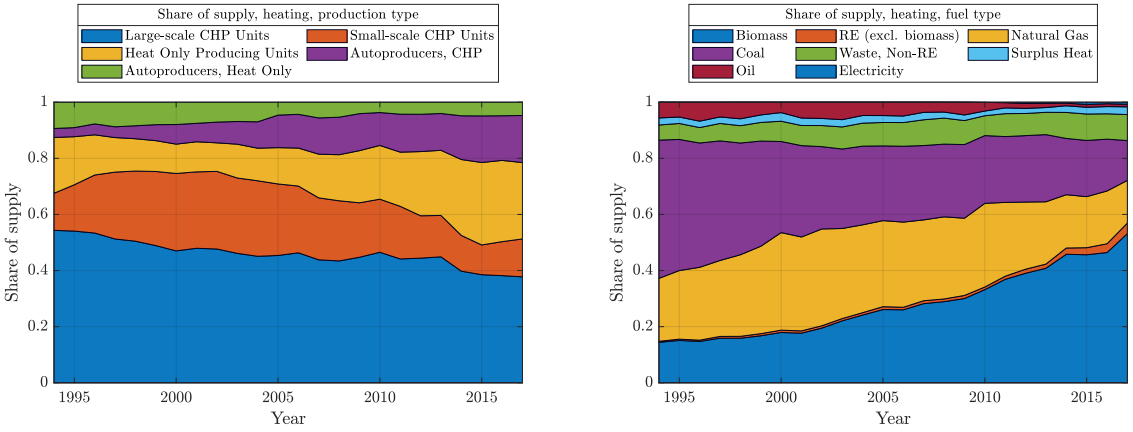

Source: Danish Energy Agency (2017a).

Note: Fuel type categories are aggregated. Compared to the convention used in Danish Energy Agency (2017a), the category *RE (excl. biomass)* includes solar heating, geothermal heating and the share of production from heat pumps included under renewable energy. The category *electricity* is defined as non-renewable heating produced using electricity, (see Danish Energy Agency (2017a) page 17).

3.3 Data

Below we describe the data used in this paper for developing the BU module of the energy system described in the previous sections. The most import data sources are:

i. The Danish Energy Agency's yearly energy statistics (Danish Energy Agency, 2017a) for calibrating fuel- and production type composition of Danish electricity and heat production as well as net-exports and consumption.

ii. The Danish Energy Agency's technology catalogue for information on investment costs and production potential of various technologies.

iii. Information on the hourly transmission line capacity and hourly spot prices are collected from (Energy Data Service, 2018a,b).

iv. For technical information on individual plants in the transformation sector we use a national inventory of domestic plants (*Energiprocenttællingen*).

Finally information on fuel prices, taxes, subsidies, and hourly variation in productivity and demand have been collected by the Danish Energy Agency for the energy system model Ramses (Danish Energy Agency, 2018a). We use this data as exogenous parameters in the BU module. Most of the data is open-source and readily available with the exception of individual plant data from *Energiproducenttællingen*. Due to its central role in the coming sections, we give a brief overview of the plant data collected and organized by the Danish Energy Agency for Ramses.

The Ramses data covers information on all electricity and district heating producing plants coupled to the public grid in Denmark. For heating this covers around 63% of the total heat supply as noted in section 3.2.2. The data furthermore includes data on a number of foreign aggregate plants, representing a specific plant type for the relevant geographical area. The data used in modelling the supply from plants can be split into categorical and numerical data. The categorical data is defined as integer/categorical sets (or indices), for which all plants can be placed in a given subset of a set. A list of the relevant sets in the bottom-up information is provided in table 1. Every plant is characterized by all of the sets, each one informing how to calculate the supply and costs of the given plant. As an example, consider a plant that can only use one fuel mix ($\mathcal{M}$). This fuel mix can consist of 90% coal and 10% fuel oil ($\mathscr{F}_F$). Thus the marginal costs of the plant depends largely on emission taxes and the fuel price of coal. Both fuel prices, taxes, and the plants' capacity varies with the relevant year (t). Which emission taxes the plant is subject to and what output prices it receives, depends on which electricity and heating area the plant is located in ($\mathcal{G}_E, \mathcal{G}_H$). The way marginal costs are computed and the ultimate dispatch decision of a plant further depends on the plant type ($\mathcal{T}$). For instance, a condensation plant only produces electricity, whereas an extraction plant type also produces heat: The optimal dispatch decision for an extraction plant involves not only the equilibrium price on electricity but also the price on heating in the given region. The capacity of the plant not only depends on the relevant year but may also depend on the relevant hour (h). For *dispatchable* plants, such as the condensation and extraction plants mentioned above, the hourly capacity is constant across the year; however, for *intermittent* plants as wind turbines the capacity fluctuates throughout the year. This yearly variation pattern ($\mathcal{V}$) can be more geographically detailed than the relevant electricity and district heating area. For instance, off-shore wind farms in West Denmark have disaggregated locations within West Denmark (e.g. *Hornsrev*). Finally, some plants, such as the *Hornsrev* wind farms, receives feed-in tariffs (subsidy type, $\mathcal{S}$) that ensures a constant price, essentially decoupling the plant's dispatch decision from the electricity price. The plant supplies electricity in a *prioritized* way ($\mathcal{B}$) and not according to its *marginal* costs.

A comprehensive list of the different set values is left for appendix A. Part II and appendix B details how the bottom up module uses the information listed here, e.g. in the form of computation of marginal costs and deriving equilibrium prices on electricity and heating.

Table 2 lists some of the relevant bottom-up variables that are coupled to individual plants. Most of these variables are only used in intermediate computations, e.g. in a plant's marginal costs, yearly

Table 1: Sets defined by bottom up information

Sets:	Notation	Example of set values
Basic fuel type	$\mathscr{F}_B$	{ Coal, fueloil, natural gas, straw, ... }
Full fuel type	$\mathscr{F}_F$	{ Coal, Avedøreværket, NoFuel, ... }
Number of available fuel mixes	$\mathcal{M}$	{ 1, 2 }
Time (year)	t	{ 2014, 2015, 2016, 2017, ... }
Hour of the year	h	{ 1, 2, ..., 8760 }
Electricity area	$\mathcal{G}_E$	{ DK-West, DK-East, Norway , ... }
Heating area	$\mathcal{G}_H$	{ Copenhagen, Aarhus, NatGas DK-west, ... }
Plant type	$\mathcal{T}$	{ Condensation plant, Electrical Heater, ... }
Hourly variation	$\mathcal{V}$	{ Hornsrev2, Demand-DK1-2014, ... }
Bid type	$\mathcal{B}$	{ Marginal, prioritized }
Subsidy type	$\mathcal{S}$	{ Elpatron, Hornsrev2, BiogasD, ... }

Note: Most of these sets characterise individual plants. A plant is characterised by a full fuel type (97 types). Each full fuel type is a linear combination of the basic fuel types (13 types). A plant is characterised by the year variable, by being either active or not active. The bid type indicates whether or not the plant supplies electricity at its marginal costs or if it is prioritised electricity (produces no matter the equilibrium price).

profits, or a corrected capacity. Section 4 and appendix B deals with this in more detail.

Table 2: Plant specific variables from data

Variable:	Notation	
Year of commission	$Comm$	
Year of decommision	$DeComm$	
Capacity, electricity production	q_E	
Capacity, heating production	q_H	
Inflow,	$\tilde{q}$	(used if yearly production is known)
Storage capacity	S	
Fuel efficiency	Eff	
Electricity-to heat ratio	C_b	(the exact use depends on plant type)
Transformation rate (E to H)	C_v	(used for CHP plants)
Probability of outage	$POutage$	
Tax efficiency	$TaxEff$	(used in taxation scheme)
Yearly maintenance costs	FOM	
Variable maintenance costs	VOM	
Included in CO2 quota sector	$CO2Cap$	(value between 0 and 1)
Desulphurization	$Desulp$	
NO2 emission per GJ input	$NO2$	
CH4 emission per GJ input	CH_4	
N2O emission per GJ input	$N2O$	

Note: The *inflow* variable is used typically for plants of an intermittent nature, where the total production over a year is more or less certain. However, it is also used for hydro power plants that have an inflow of water from adjacent rivers. The variable *CO2Cap* can in principle be strictly between 0 and 1, indicating that a plant is only partly included in the quota sector.

Table 1-2 illustrates the level of detail used in the BU model in computing equilibrium prices and production. In particular, the various sets illustrate that it is possible to run the model with a quite granular spatial resolution with e.g. up to 34 heating areas. Furthermore, it is possible to assess the

impact of very specific regulation of the sector. For instance, it is possible to include regulation/taxation across technology and fuel mix types. This aspect brings us to the next part, which describes the current tax scheme in the transformation sector.

3.4 Taxation of production of electricity and heating in Denmark

Both the consumption and production of electricity and heating are subject to taxation. Given, however, that this paper focus on modelling the production of power and heat, we only describe taxation of production.[23]

The taxation of the production of electricity and heating is quite detailed. It includes emission taxes, various subsidy schemes (feed in tariffs, premiums, fixed price), transmission and distribution tariffs (user fees), the PSO tariff (Public Service Obligation), taxation of electricity used in the production of heating as well as fuel taxes levied only on fuels in production of district heating. The tax function therefore includes plant-specific characteristics, among others the specific fuel mix used, plant type, subsidy type etc.. Appendix B outlines in more detail how taxes affect the different types of plants. Here we give a brief introduction along with a few examples of how we deal with the tax schemes in the BU model. It builds entirely on the taxation scheme implemented in Ramses (Danish Energy Agency, 2018a).

Taxation of fuels and emissions:

This section deals with the relevant taxes facing electricity and heat producing plants. The current tax system can be divided into taxes on emissions and energy taxes on fuel consumption. Furthermore, the tax scheme is differentiated for the production of electricity and the production of district heating.

GHG emissions are taxed either through the EU ETS system or the national CO_2 tax (*CO2-afgiften*). In the production of electricity GHG emissions are covered by the ETS system. In the current version of the BU module the price for a CO_2 quota is exogenously given by 44.1 DKK/ton CO_2-equivalents in 2017.[24] The district heating sector is generally subject to the national CO_2 tax. For CHP plants the GHG emissions from fuels used in production of heating are also subject to the CO_2 quota price in the EU ETS in addition to the national CO_2 tax. Furthermore, all plants that produce either electricity or heat are subject to national taxes on NO_x and SO_2 emissions (i.e. polluting emissions). For 2017 the tax rates are set at 5.5 DKK per kilo NO_x and 24 DKK per kilo SO_2 emitted.

For the plants producing electricity taxation is almost entirely limited to emission taxes. In order to keep competition more fair in markets where foreign plants operate as well, some taxes as the national energy tax (*energiafgiften*) are not placed on the producers, but rather on end-consumers of electricity, so as to not favor foreignly produced electricity. For the heat producing plants there are not the same concerns over international competition; thus the energy tax is levied on a number of fuels as coal, oil products and natural gas. In 2017 this energy tax is by far the most prominent one in the computation of marginal costs, at a value of roughly 200 DKK per MWh of fuel input (55.5 DKK/GJ), (Klimarådet,

[23] The taxation of consumption is left for future work in developing the CGE model where yearly energy demand is determined.

[24] As the model computes the total *demand* for CO_2 quotas given the price level, there is nothing that prohibits the implementation of an endogenous CO_2 tax reflecting the EU Emissions Trading System (ETS).

Table 3: A non-exhaustive list of tax rates applied in the BU model, 2017

Tax		
Electricity-to-heat	392.5	(DKK/MWh)
National energy tax	199.8	(DKK/MWh)
Transmission, electricity (tariff)	82.9	(DKK/MWh)
Distribution, electricity (tariff)	111.6	(DKK/MWh)
Distribution (heat pumps, tariff)	21.1	(DKK/MWh)
PSO (tariff)	155.0	(DKK/MWh)
CO_2 (ETS)	44.1	(DKK/ton)
Danish national CO_2 tax	170	(DKK/ton)
Danish national NO_x tax	5.5	(DKK/kg)
Danish national SO_2 tax	23.7	(DKK/kg)

Note: The table here lists the tax rates applied in the model. It does not cover all regulations included in the model, e.g. a number of subsidy schemes. The list covers the most important energy taxes faced by electricity and/or heat producing plants. Transmission, distribution, and PSO tariffs are paid per MWh of electricity.

2018a). Figure 3.8 illustrates the importance of these taxes in the production of heat. Here the *fuel-tax* category illustrates the sum of the energy tax and the CO_2 tax.[25] Similar to emission taxes biomass is generally exempt from energy taxes. This is an essential explanation for the observed transition in part (b) of figure 3.7, where fossil fuels are gradually replaced by biomass.

The difference in taxation between electricity and heat producing plants warrants a further explanation of the taxation of CHP plants. As the use of fuels are only taxed in the production of heat, the taxation of CHP plants' depends on how large a fraction of fuel-inputs goes to the production heat, and how much goes into the production of electricity. In practice the split can be done in one of two ways: The V-formula or the E-formula.[26] For simplicity, we assume that plants use the V-formula. The V-formula states that the fuel used in production of heating is given by the production of heat divided by 1.2. As will be demonstrated further in our calibrated BU module (section 10), the difference in fuel taxation on electricity and heat production leads to interesting incentives for a certain type of CHP plant. Specifically, CHP plants, that can (i) adjust its relative production of electricity and heating and (ii) use more than one type of fuel mix, have incentives to use biomass when electricity prices are low to medium but switch to coal or natural gas when electricity prices are high. This has the implication that the demand for biomass fuels after a certain threshold, is *decreasing* in the equilibrium price on electricity output.

Taxation of electricity to heat and heat pumps:

In section 3.2 we briefly highlighted the low penetration rate of electrical heaters and heat pumps in the district heating system (1.4% in 2017). One of the main reasons for this is that electrical heaters in 2017 paid around 750 DKK per MWh of electricity they used in production of district heat. This fee is the sum of a number of tariffs/taxes including (i) electricity-to-heat tax (*elvarmeafgiften*), (ii) transmission, (iii) distribution, and (iv) the PSO tariff. Of these taxes the electricity-to-heat tax accounts for over

[25] Taxes on emissions of NO_x and SO_2 are not included in this category, as it depends on plant specific characteristics as well as the fuel input type in our model.

[26] For more (in Danish only, unfortunately) see here: `https://tax.dk/jv/ea/E_A_4_4_10_2.htm`.

Figure 3.8: Fuel price and taxes in heat production, 2017

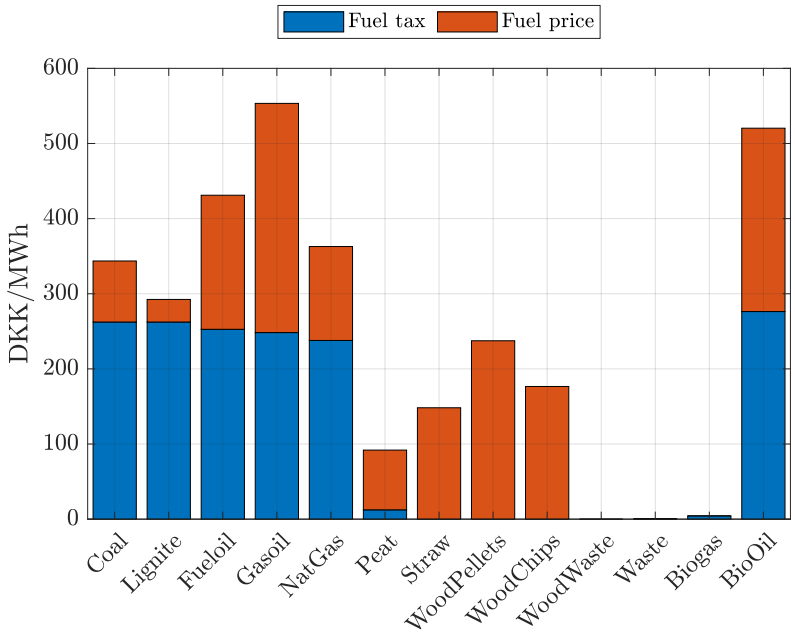

Note: The 'fuel tax' is defined as the sum of the energy tax (around 200 DKK/MWh) and the national CO_2 tax. Heat producing plants are furthermore subject to SO_2 and NO_x taxes. Compared to particularly the energy tax, the effect of the emission taxes are only secondary.

half of this at roughly 400 DKK/MWh in 2017. It should be noted that significant reforms of these policies have already been planned. Firstly the PSO tariff is out-phased gradually towards 2022 from the level of 155 DKK/MWh in 2017. Secondly the electricity-to-heat tax was temporarily lowered by 150 DKK/MWh in May 2018. In 2020 the reduction is increased to 200 DKK/MWh. From 2021 the reduction is permanently set at 100 DKK/MWh (Klimarådet, 2018a).

Heat pumps are regulated separately from other plants using electricity to produce heat under *Elpatronordningen*. Under this regulation they are exempt from the electricity-to-heat tax. Furthermore, heat pumps are only subject to transmission and distribution tariffs. Moreover, the distribution tariff paid by heat pumps is significantly lower for heat pumps than other electrical heaters. As such the effective tax included in our model is at 104.6 DKK/MWh in 2017 for heat pumps. While the penetration of heat pumps in the district heating system is currently limited, the installed capacity is already quite significant (and increasing in recent years). The idea of the lower taxation of heat pumps is that cheap electricity e.g. from wind power in peak production hours, can be used to produce renewable heat.

Different types of subsidy schemes:

We generally distinguish between two types of subsidy schemes: Constant feed-in premiums and a variable feed-in premium that ensures a fixed marginal revenue. While the constant feed-in premiums are offered to e.g. plants using biomass, offshore wind is generally eligible for the variable feed-in premium.[27] The simple constant feed-in premium is illustrated in part (a) of figure 3.9. The variable feed-in premium

[27]See IEA's data sheet for feed in tariffs in Denmark here: `https://www.iea.org/policiesandmeasures/pams/denmark/name-24650-en.php`.

is illustrated in part (b) of figure 3.9. For subsidies of this type the plant sells electricity to a constant agreed upon price. In figure 3.9 this is denoted the *subsidy price*. The variable feed-in premium is given by the difference between the subsidy price and the spot price. As part (c) of figure 3.9 illustrates, this completely decouples the production decision of the plant from the equilibrium spot price on electricity: As long as the subsidy price is larger than its marginal costs, it is optimal to dispatch electricity for the plant. There is one exception to this decoupling of spot market equilibrium price and the plants dispatch decision: When equilibrium prices approach a minimum price. In these cases the supply from plants that receive the variable feed-in premium gradually decreases around this threshold as illustrated in part (d) of figure 3.9. Technically this approach ensures that an equilibrium is always feasible in the bottom up module, as supply decreases to around zero around this price level. Besides being technically advantageous this assumption is still grounded in reality. The Nord Pool spot market operates with a minimum price on electricity. In scenarios where this minimum price is reached, a part of the supply is cut off, to ensure the balancing of demand and supply.

Figure 3.9: Feed-in premium types

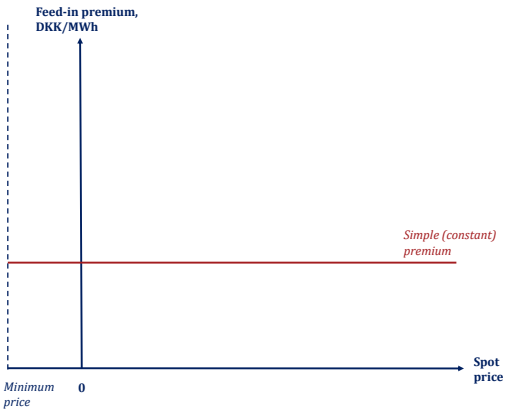

(a) Constant feed-in premium

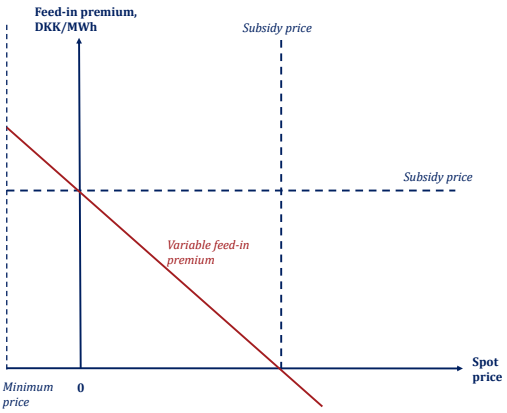

(b) Variable feed-in premium

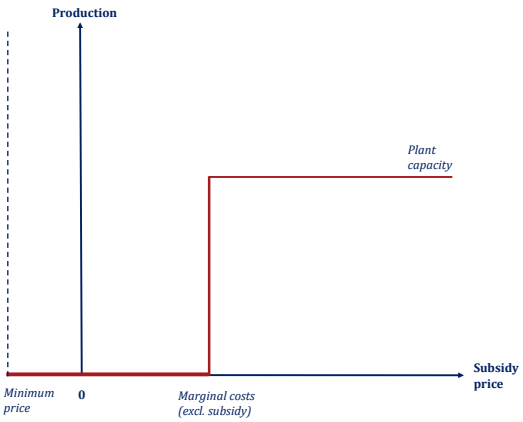

(c) Supply with variable feed-in premium, fixed spot price > minimum price.

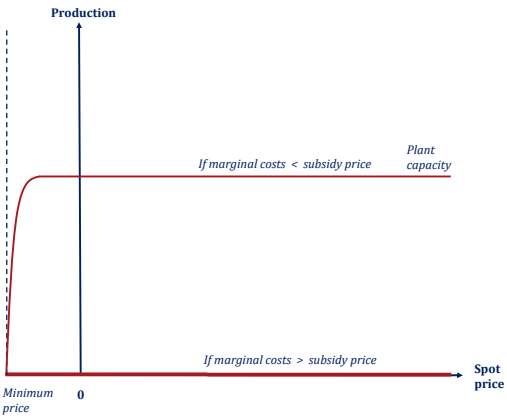

(d) Supply with variable feed-in premium, spot price on x-axis

Note: Part (d) in the figure represents how the model deals with spot prices approaching the *minimum price*; thus the jump in supply around the price floor has been smoothed out.

Part II

The Bottom-Up Module for the Transformation Sector

We generally distinguish between two time horizons in the model: The long run and the short run. When discussing *long run* perspectives of the model, we think of decisions that change over a number of *years*. For a power and/or heat producing firm this is the relevant time horizon, when choosing investment in new capacity and whether to keep or scrap existing plants. When discussing the *short run*, investment decisions are taken as given. Thus the short run is concerned with intra-year decisions, such as optimally utilizing the existing capacity. The short run time-increments are loosely referred to as *hours*, as this is the most detailed level the BU model can describe. The BU module developed here concerns itself with this time horizon.

In the following, we proceed to describe the modelling of the bottom-up derived supply function for electricity and heat in section 4. This includes our approach for approximating the standard linear programming problem in conventional BU models as a typical non-linear programming problem, as well as an approximate but computationally efficient formulation of energy storage technologies' linear *dynamic* programming problem. We also describe the modeling of intermittent versus dispatchable technologies. In section 5 we describe the specification of demand on the hourly basis and how we model increased demand flexibility. This section also includes an empirical part, which determines the structural parameters of the short run demand function. In section 6 we outline how trade in the electricity market is defined on the hourly basis. In section 7 we present a small-scale toy model that is used in section 8, where the solution method applied to compute an equilibrium in the energy market is described. The toy model builds intuition for how our trade algorithm emulates the trade algorithm on Nord Pool spot market.

4 Short run bottom-up supply

In this section we focus on establishing how individual plants supply electricity and district heat in the short run. From the Ramses data presented in section 3 we can distinguish plants in a number of different ways. The information that is available on plants matters for the way marginal costs are computed. This includes technical parameters determining the dispatching of one additional unit of MWh electricity (E) or heat (H). The computation of marginal costs is of course essential for the workings of the model, however, as we do not offer any innovations in this area, the technical section outlining these computations is left for appendix B. In the following sections we therefore take the computation of a marginal cost component (c) as given and instead focus on, how to map this into a choice of supply for an individual plant i.

As briefly mentioned earlier in section 3, the plants are characterized by a number of sets and parameters. For notational convenience we will not refer to each plant using all ten subscripts, but rather

include the few that are essential to the relevant section. Most notably this notation includes:

- Each individual plant uses a particular technology type (τ) belonging to the set of technologies $\mathcal{T}$. The full set is listed in table 4.
- Each individual plant is characterized by a geographical electricity area (g_E) belonging to the set of areas $\mathcal{G}_E$.
- A plant is further characterized by being located in a heating area (g_H), belonging to the set of areas $\mathcal{G}_H$. Area sets are defined such that each electricity area is partitioned into subsets of heating areas.[28] This implies that all plants that supply both heat and power in one heating area g_H, also faces the same price of electricity.
- When relevant, we will use (t) for yearly index and (h) for hourly index (variation within a given year).

Table 4: Technology Sets in bottom up module:

Technology set $\mathcal{T}$:	
Condensation plant	(standard)
Extraction plant	(CHP)
Backpressure plant with bypass	(CHP)
Backpressure plant	(CHP)
Electric heater	(standard)
Wind	(intermittent)
Photo Voltaics (PV)	(intermittent)
Hydro (Run-off-river)	(intermittent)
Boiler heating plant	(standard)
Solar heating plant	(intermittent)
Heat storage	(storage)
Industry surplus	(intermittent)
Electricity storage	(storage)
Hydro with storage	(storage)
Electricity deficit plant	(EDF)
Heating deficit plant	(EDF)

'Standard' technology types are modeled using the same supply function approach, but differ in the way marginal costs of production are calculated. The hydro plant that is categorized as 'intermittent' only includes Run-Off-River plants (ROR).

Given the computed level of marginal costs for plant i (c_i), we distinguish between five different type of plants: (1) Standard plants, (2) combined heat and power plants (CHP), (3) plants with storage capacity, (4) plants with intermittent production, and (5) energy deficit plants (EDF). We deal with each of these in the following sections. Note that hydro plants with storage capacity are also affected by hourly variation in water inflow. When referring to intermittent technologies, we do not include hydro plants with storage capacity in this category. Only Run-off-River (ROR) hydro power plants are characterized as an intermittent technology.

[28] The geographical sets are defined in appendix A.

4.1 *Standard* technology types

In the current version of the model there are three *standard* technologies: Condensation plants (CD), boiler heaters (BH) and electrical heaters (EH). The condensing plant produces electricity (E) using various fuel-mixes; in Denmark these are primarily fossil fuels such as coal or oil. A condensing plant can use a range technologies for example steam or gas turbines, to produce electricity. There is no co-production of heat in this process. For both the CD and the BH plants, a standard bottom-up model approach is to assume a roughly constant fuel efficiency (Danish Energy Agency, 2018a). Thus, the ratio of fuel input to output measured in GJ or MWh is constant for a given plant. This implies a constant unit cost of production. The electrical heater transforms electricity into heat. The assumption is similar to the other two standard plants that the efficiency of electricity-to-heat is roughly constant. The individual EH plant takes the electricity price as given. For a given price on electricity, the unit cost of the EH plant is constant as well. In deriving the short run equilibrium, this is however obviously not the case: The unit cost c_i of the EH plant depends largely on the short run price on electricity. However, for the presentation of the EH plant's optimal dispatch decision, the model approach is standard.

Consider a standard power plant i that only produces electricity (E). From bottom-up data on the plant we can identify: (1) The marginal cost of production without taxation (c_i), (2) the capacity at any point in time (q_i), (3) taxes, subsidies, and other regulation, affecting the profitability of the plant, and (4) its emissions.[29] Formally, the relevant information on plant i can be summed up in the triplet

$$\left\{c_i, q_i, F^i(\mathbf{t})\right\},$$

where $F^i(\mathbf{t})$ is a tax function. The superscript i is included to indicate that this function depends on plant-specific characteristics such as the fuel efficiency of the plant. The notation $\mathbf{t}$ is used as a short-hand for all the relevant tax rates. For the decision of optimal supply from plant i the relevant metric is the after-tax unit costs defined simply as

$$\mathbf{c}_i \equiv c_i + F^i(\mathbf{t}).$$

The computation of the cost and tax terms differs across technology and fuel types. To compute these terms, we rely on data from *Energiproducenttællingen* as outlined in section 3. We leave the technical details of this for appendix B. With a constant marginal cost function and no storage capacity, the short run profit maximizing behavior is straightforward to characterize: If the equilibrium price p^E exceeds the unit cost of production ($\mathbf{c}_i$), the plant produce at capacity (q_i) and otherwise produce nothing:

$$E_i \begin{cases} = q_i, & \text{if } p^E > \mathbf{c}_i \\ \in [0, q_i], & \text{if } p^E = \mathbf{c}_i \\ = 0, & \text{if } p^E < \mathbf{c}_i \end{cases} \tag{1}$$

[29] The assumption of constant marginal costs of production is relatively standard in bottom-up literature. It should, however, only be seen as an approximation.

In the short run, the individual plant takes installed capacity q_i as given and can, in general, not substitute between inputs to alter the unit cost measure $\mathbf{c}_i$. This is in part due to the short time horizon and partly due to the level of granularity.[30] There are a few exceptions to this rule. Firstly, there are certain plants that can substitute between fuel inputs in production. Secondly, the technology catalogue published by the Danish Energy Agency includes estimates for the investment costs of rebuilding a plant that uses coal to a biomass-fired plant. In section 12 we outline, how this information can be applied to endogenize investment decisions for existing plants. The implication of modelling a plant's supply this way is a step-wise supply function as demonstrated in figure 4.1.

Figure 4.1: The bottom-up step-wise supply function

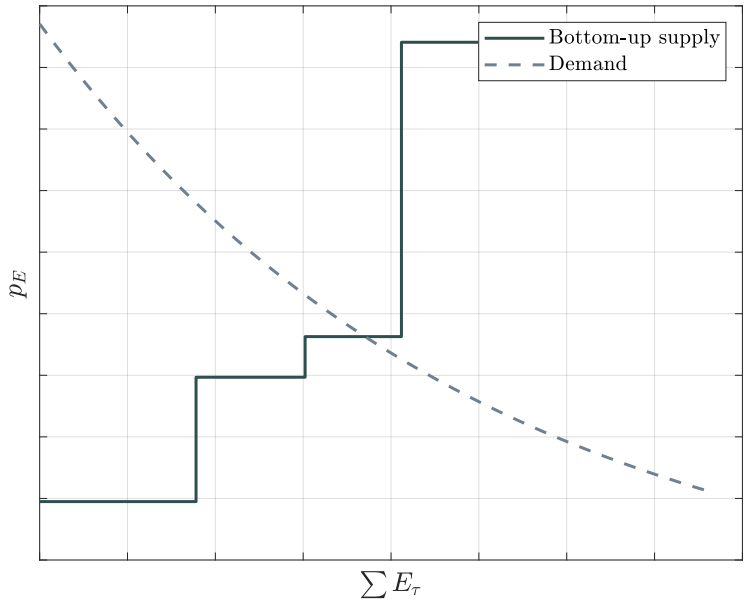

The step-wise supply function is not differentiable in the kinks. In technical energy system models this is not an issue because the conventional approach in the traditional approach is to write the model as a linear programming problem.[31] Given that the long run goal of the BU model, we develop in this paper, is a direct integration in a standard CGE model, we modify this setup in order to obtain a differentiable supply function. To this end, the constant unit costs ($\mathbf{c}_i$) are replaced with the assumption that costs are distributed according to some function $f(\cdot)$. In doing so, equation (1) is replaced with

$$E = q \int^{p^E} f(c^j) dj,$$

[30] In the macroeconomic literature the idea of having perfect complementarity between capital and energy inputs is well-known. See for instance the *putty-putty*/Pindyck-Rotemberg model in Pindyck and Rotemberg (1983).

[31] Andreas Bloess and Zerrahn (2018) provide and overview of the different solution methods used in research and technical models used for examining the potential for flexibility technologies. Of the approximate 45 models they research, 29 of these used either a linear program or a mixed-integer linear program and 14 was not stated/not applicable.

and a total cost function of the form

$$C = q \int^{p^E} c^j f(c^j) dj.$$

To choose the functional form of $f(\cdot)$, we want a specification that allows us to flexibly weigh the need for computational speed, against obtaining a model close to the traditional bottom-up solution. Using the normal- or log-normal distribution allows us to do just that, with the only difference that the first allows for negative prices and the latter does not. The two smoothed supply functions are given by

$$E^N = q\Phi\left(\frac{p^E - c}{\sigma}\right), \tag{2}$$

$$E^{LN} = q\Phi\left(\frac{log(p^E) - log(c) + \sigma^2/2}{\sigma}\right), \tag{3}$$

and corresponding cost functions

$$C^N = E^N\left[c - \frac{\phi\left(\frac{p^E - c}{\sigma}\right)}{\Phi\left(\frac{p^E - c}{\sigma}\right)}\right].$$

$$C^{LN} = E^{LN} c \frac{\Phi\left(\frac{log(p^E) - log(c) - \sigma^2/2}{\sigma}\right)}{\Phi\left(\frac{log(p^E) - log(c) + \sigma^2/2}{\sigma}\right)}.$$

Here $\Phi(\cdot)$ is the cumulative density function of the standard normal distribution, $\phi(\cdot)$ is the corresponding probability density function, and σ governs the degree of smoothing. One interpretation of $\Phi(\cdot) \in [0, 1]$ is that it measures the utilisation of the existing capital. Note that both assumptions nest the step-wise bottom-up supply function by letting σ approach zero. The importance of the normal smoothing parameter (σ) (along with several other parameters that will be defined throughout the following sections) for solving the model will be further explained in section 10.1.

4.2 Combined Heat and Power production

The model includes three different types of CHP plants: Extraction, back-pressure and back-pressure with bypass. The simplest CHP plants is the back-pressure type. A back-pressure plant, using a steam turbine in its production, operates as a condensation plant only at a higher pressure/temperature. At these high temperatures the back-pressure plant produces electricity and heat at a roughly constant ratio. Compared to the back-pressure plant, an extraction plant can flexibly adjust its relative production of electricity-to-heat ratio between a pure condensation plant (only E) to a back-pressure plant. Finally, the back-pressure plant with bypass essentially works as a back-pressure plant with an attached electrical boiler: If it is profitable, the plant can use the electricity produced in back-pressure mode to produce heat.

Here we deal briefly with the *extraction plant* type as it involves the endogenous choice of the electricity-to-heat ratio in production. The other two CHP types are dealt with in appendix B. For a characterization of a more general joint production framework, we refer to appendix C.

Recall from section 3.4 that taxation of a CHP plant is different, depending on how much electricity and heat it produces. Compared to the standard case discussed above, this implies that the unit costs have to be split into more components. Let $F^i(\mathbf{t})$ denote the tax function on plant i that does not depend on whether the plant produces electricity or heat, $F^i_E(\mathbf{t})$ is the additional marginal tax from production of electricity, and $F^i_H(\mathbf{t})$ is the additional marginal tax from production of heat. Furthermore, as the output from CHP plants can be both electricity (E) and heat (H), let *total output* be a measure of MWh produced by the plant, being purposed either as E or H.[32] Let d^i_E be the marginal change in E when *total output* is increased and d^i_H the analogue term for heat production. We then define the unit cost of production as

$$\mathbf{c}_i = c_i + F^i(\mathbf{t}) + d^i_E F^i_E(\mathbf{t}) + d^i_H F^i_H(\mathbf{t}).$$

Furthermore, define the tax-corrected output prices

$$\tilde{p}^E \equiv p^E - d^i_E F^i_E(\mathbf{t}), \qquad \tilde{p}^H \equiv p^H - d^i_H F^i_H(\mathbf{t}).$$

To model the optimal joint production of a CHP plant a standard approach is to split the problem into two steps. This is done by assuming that the plant produces an aggregate good (EH, read: total output), which can then be split into electricity and heat, following some transformation function. Following the description in the technology catalog (Danish Energy Agency, 2016), we assume that the plant has approximate constant unit costs ($\mathbf{c}_i$) in production of EH.[33] The plant produces electricity and heat following a linear transformation function of this aggregate output good. For the extraction plant there is an additional minimum co-production constraint on electricity. This minimum co-production constraint comes from the fact that when it maximizes its heat production, it operates as a back-pressure plant, in which case the electricity production is not zero.

In the case of the extraction plant, the Ramses data offers us information on the unit cost of a plant operating as a condensation plant (thus no co-production of heat), a linear transformation rate of electricity-to-heat denoted C_v, a minimum co-production constraint C_b, and a capacity constraint on electricity q in condensation mode. With the linear transformation rate and constant unit costs, we can maximize the extraction plants' profits in two steps: (1) Given the scale of production, what is the optimal production split d^i_E, d^i_H between electricity and heating? And (2) given the optimal split of production, what is the optimal scale ($\mathcal{Q}$)? Figure 4.2 illustrates the production possibility set where we have expressed the scale variable $\mathcal{Q} \in [0, 1]$ as proportional to the capacity q.

Similar to standard plant types (see section 4.1), the conventional approach implies a corner solution; in this case two types, even. Similar to the standard plant types, the extraction plant should either

[32] The phrasing *purposed* is important here: The *total output* is a measure of total energy produced, but not necessarily the sum of E and H. The reason is - as is explained in the following - that one can assume different technology functions splitting this *total output* onto E and H. Total output only equals the sum of E and H if the technology function features constant returns to scale. This is, however, always the case in out setting but does not need to be.

[33] In the general case the unit cost of production may not be constant, either due to share functions d_E, d_H that may vary when the production of EH is adjusted, or due to non-linear tax functions $F_E(\mathbf{t}), F_H(\mathbf{t})$. As will be verified in the following, the assumptions made here ensure that d_E, d_H are indeed constant given the relative prices of $\tilde{p}^E/\tilde{p}^H$.

Figure 4.2: A sketch of the production possibility set of an extraction plant

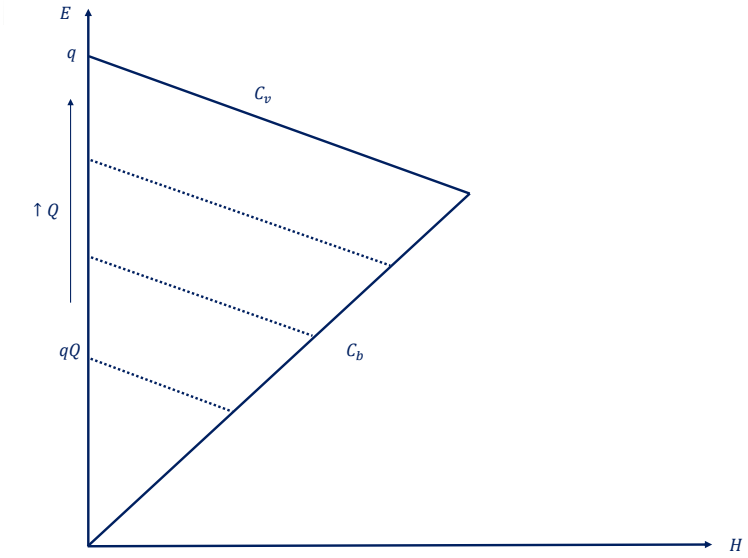

produce at capacity ($\mathcal{Q} = 1$) or not at all ($\mathcal{Q} = 0$). In this case it depends on the threshold:

$$\mathcal{Q}^* = \begin{cases} 1, & \text{if } p^{EH} \geq \mathbf{c}_i \\ 0, & \text{if } p^{EH} < \mathbf{c}_i \end{cases}, \qquad p^{EH} \equiv p^E d_E^i + p^H d_H^i.$$

This states that when producing an additional unit of the aggregate good (EH), a profit maximising firm chooses to split this into d_E units of electricity and d_H units of heat. Given that the unit costs of producing (EH) are constant across scale, the plant should simply choose $\mathcal{Q} = 1$ if the revenue from selling d_E units of electricity and d_H units of heating exceeds the unit cost $\mathbf{c}_i$. Secondly, with a linear transformation rate the optimal shares (d_E and d_H) similarly follow corner solutions:

$$(d_E^i)^* = \begin{cases} 1, & \text{if } \tilde{p}^E C_v > \tilde{p}^H \\ \dfrac{C_b}{C_b + C_v}, & \text{else} \end{cases}$$

$$(d_H^i)^* = \begin{cases} 0, & \text{if } \tilde{p}^E C_v > \tilde{p}^H \\ \dfrac{1}{C_b + C_v}, & \text{else} \end{cases}$$

With a constant transformation rate the plant has the choice of producing one unit of heating to obtain the revenue $\tilde{p}^H$ or C_v units of electricity, thereby receiving the revenue $\tilde{p}^E C_v$. In other words, the plant should either work in full condensation or full back-pressure mode. Combining the constant unit costs with a linear transformation rate, therefore implies that a profit maximising plant chooses one of the three corners of the production possibility set in figure 4.2.

To smooth out the discontinuities of this supply function, we start by replacing the assumptions of a linear transformation and minimum co-production constraint with a *normalized constant elasticity of*

transformation (NCET) assumption. The plant now solves

$$\max_{E,H} \tilde{p}^E E + \tilde{p}^H H - q_i \left(c_i + F^i(\mathbf{t})\right),$$

$$\text{s.t. } q_i = \frac{C_v + C_b}{C_v} \left[\left(E - \frac{q_i C_b}{C_v + C_b} \right)^{\frac{\sigma_{chp}-1}{\sigma_{chp}}} + C_v^{\frac{\sigma_{chp}-1}{\sigma_{chp}}} H^{\frac{\sigma_{chp}-1}{\sigma_{chp}}} \right]^{\frac{\sigma_{chp}}{\sigma_{chp}-1}}, \qquad \sigma_{chp} < 0,$$

where the constraint represents the NCET assumption. figure 4.3 illustrates how the NCET adds curvature to the production possibility frontier, in a way that respects the minimum co-production constraint.

Figure 4.3: Illustration of the NCET smoothing of the production possibility frontier

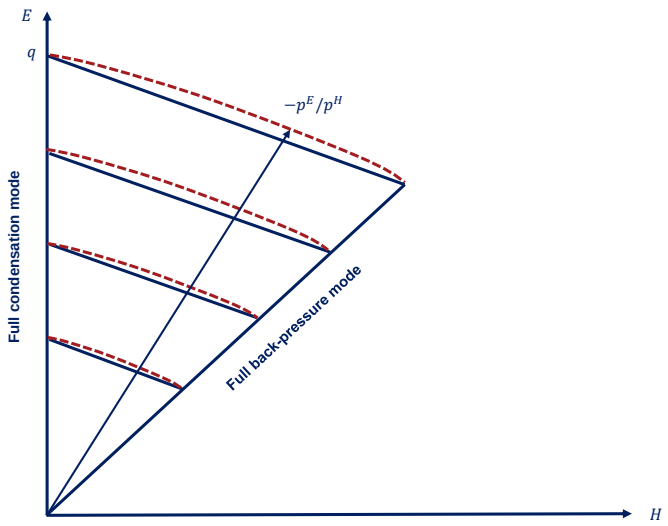

In this case the resulting optimal behavior is determined by optimal production split functions d_E^i, d_H^i:

$$\begin{pmatrix} E_i \\ H_i \end{pmatrix} = \mathcal{Q}^* q_i \begin{pmatrix} d_E\left(\frac{\tilde{p}^E}{\tilde{p}^H}\right) \\ d_H\left(\frac{\tilde{p}^E}{\tilde{p}^H}\right) \end{pmatrix}, \tag{4}$$

$$d_E\left(\frac{\tilde{p}_E}{\tilde{p}_H}\right) = \frac{1}{C_v + C_b} \frac{C_v + C_b \left[1 + C_v^{\sigma_{chp}-1} \left(\frac{\tilde{p}^E}{\tilde{p}^H}\right)^{\sigma_{chp}-1}\right]^{\frac{\sigma_{chp}}{\sigma_{chp}-1}}}{\left[1 + C_v^{\sigma_{chp}-1} \left(\frac{\tilde{p}^E}{\tilde{p}^H}\right)^{\sigma_{chp}-1}\right]^{\frac{\sigma_{chp}}{\sigma_{chp}-1}}}$$

$$d_H\left(\frac{\tilde{p}^E}{\tilde{p}^H}\right) = \frac{1}{C_v + C_b} \frac{C_v^{\sigma_{chp}} \left(\frac{\tilde{p}^E}{\tilde{p}^H}\right)^{\sigma_{chp}}}{\left[1 + C_v^{\sigma_{chp}-1} \left(\frac{\tilde{p}^E}{\tilde{p}^H}\right)^{\sigma_{chp}-1}\right]^{\frac{\sigma_{chp}}{\sigma_{chp}-1}}}$$

The share functions d_E and d_H are now continuously differentiable and nest the solution to the conventional bottom-up solution, by adjusting the smoothing parameter σ_{chp} appropriately.[34] The profit function is still, however, linear in scale ($\mathcal{Q}$) with the NCET assumption. We smooth this discontinuity

[34] In the limiting case where $\sigma_{chp} \to -\infty$ we are back in the corner solution of the bottom-up approach.

exactly as with the standard plant types by assuming that unit costs $\mathbf{c}_i$ are not constant, but rather distributed according to a standard normal distribution:

$$\mathcal{Q}^* \approx \Phi\left(\frac{p^{EH} - \mathbf{c}_i}{\sigma}\right),$$

where $\Phi(\cdot)$ denotes the standard normal distribution and σ our normal smoothing parameter.

4.3 Plants with storage capacity

The BU model also includes various types of plants with storage capabilities. At the moment these consist of heat storage (HS) technologies, electricity storage (ES) technologies, and hydro-electric plants with reservoirs and water inflow (HY). Currently, ES only covers pure-pumped hydro-electric plants with reservoirs, but our modelling framework allows for other potential storage technologies for electricity such as batteries. HS technologies include both technologies that can store energy on a long-term basis (such as storing heat in the underground and in rocks), as well as technologies that store heat on a short-term basis (such as hot water tanks). Currently, the Ramses data does not distinguish between the different HS technologies.

As opposed to the other technology types presented above, the profit maximization problem of these plants is inherently dynamic; if prices build up gradually, stored energy should be dispatched when the stored energy is most profitable - at peak prices. The objective of these plants is to maximize the net present value of profits subject to a law of motion for the storage level and technological constraints. In the conventional bottom-up literature the store/dispatch decision is usually modeled with two control variables: One for storage and one for dispatch.[35] We deviate from this by only including one control variable and let it be either positive (dispatch) or negative (store). As noted in Zerrahn et al. (2018), it is commonly assumed that the efficiency of storing energy is around 81%, while the efficiency of dispatching is around 92%. Initially, this is dealt with by including an explicit kink in the law of motion for the level of stored energy. This represents that by both storing and dispatching energy, there is an energy loss. The different types of storage plants face slightly different setups. For instance, ES plants have reservoirs but no water inflow. When prices are low they pump water into upper reservoirs and release water, when prices are high. This is contrary to HY plants with both reservoirs and water inflow coming from adjacent rivers. These plants do not pump water back into upper reservoirs, but simply store water by not releasing the water inflow coming into the upper reservoirs (Førsund, 2005). In the following, we formulate a setup that is general enough to include the different storage technologies as special cases in our model. Subsequently, we evaluate the performance of the modelling approach for the case of HY plants.[36]

In the general case we define the linear dynamic programming problem facing plants with storage

[35] See for instance Zerrahn et al. (2018) for an example with two different control variables.
[36] HY plants are chosen due to data availability.

capacity as

$$\max_{\{E_h\}_{h=1}^{H}} W_0 = \sum_{h=1}^{H} \beta^h \left[(p_h - c) E_h \right], \tag{5a}$$

$$\text{s.t.} \quad S_h = S_{h-1} + (1 - b\mathbb{I}_s)(Y_h - E_h), \quad \mathbb{I}_s = \begin{cases} 0, & \text{if } E_h \geq 0 \\ 1, & \text{if } E_h < 0 \end{cases} \tag{5b}$$

$$E_h \in [\underline{E}, \bar{E}] \tag{5c}$$

$$S_h \in [0, \bar{S}], \tag{5d}$$

$$S_0 = S_H \geq 0, \quad \text{given.} \tag{5e}$$

Equation (5a) is the discounted net profits with discount factor β, prices p_h in hour h, unit costs c, and the dispatch/store decision E_h. Note that within a year, unit costs are assumed fixed. Furthermore, they are assumed the same for both storing ($E_h < 0$) and dispatching ($E_h > 0$). To motivate this assumption take for instance pure-pumped hydro plants: When these plants are storing energy ($E_h < 0$) their turbines are running backwards and when they are dispatching energy ($E_h > 0$) their turbines are running forwards. The marginal cost of using the turbines, however, is the same regardless of which way they are running. The main difference, however, comes down to whether they are buying additional electricity to run the turbines backwards ($E_h p_h < 0$) or letting the water flow down through the turbines and selling it ($E_h p_h > 0$).

Equation (5c) is the inequality path constraints on the control variable (E_h), which is determined by the power generation capacity of the plant. For HS and ES technologies, we can think of the lower bound $\underline{E} \leq 0$ as the maximum amount a battery can store/turbine can pump in a given hour, whereas $\underline{E} \geq 0$ for HY may represent a minimum base-load. Equation (5b) is the law of motion with S_h being the stock of stored energy and Y_h an exogenous inflow of energy. Both S_h and Y_h are measured in the same energy units as E_h (e.g MWh).[37] $\mathbb{I}_s$ is a dummy variable, indicating that when a plant stores energy there is a loss of b% of the energy. Equation (5d) is the inequality path constraints on the state variable S_h given by the storage capacity of the plant $\bar{S}$. Finally, (5e) provides a simple terminal condition on the state variable S_h.[38] Note that storage technologies of types ES and HS have no exogenous inflow of water ($Y_h = 0$), but a percentage loss of storing energy of b%. This implies that they are in fact *net consumers* of energy: As these storage plants lose b% of all energy they purchase on the market and put into storage, we have that

$$\frac{\sum_h E_h}{\sum_h E_{h\{E_h<0\}}} - 1 = b, \qquad \sum_h E_h < 0, \quad \sum_h E_{h\{E_h<0\}} < 0. \tag{6}$$

Consequently, b fully determines how much energy ES and HS technologies take of out the system. Given that these plants bring down the total yearly supply of energy, the value they bring to the energy system, is the ability, to move production from hours with low prices to hours with high prices, thus mitigating

[37] For HY and pure-pumped hydro (ES) this is possible, when there is no spillage in reservoirs (Førsund, 2005).

[38] This is a relatively standard assumption in the literature, see for example Danish Energy Agency (2018a) and Zerrahn et al. (2018).

the effects of intermittency.

The general problem in (5) is linear in the control variable (E_h) with multiple occasionally binding constraints. In the dynamic programming literature, a number of suitable solution methods have been developed for that particular class of problems. To the best of our knowledge, however, they all involve some sort of backwards recursion or iteration scheme, which greatly increases the computational burden of solving for an equilibrium.[39] The standard way of tackling these problems is to iterate until convergence between (1) solving the dynamic programming problem, taking equilibrium prices on E and H as given and (2) solving for equilibrium prices, taking the solution from the dynamic programming problem as given (Berkovec, 1985). Although this approach tackles the problem head on, it performs poorly in large-scale CGE models.

The problem of storage technologies is in Ramses simplified to obtain a static representation (Danish Energy Agency, 2018a). The essence of their approach is to capture as much of the optimal solution as possible by coupling the supply to relevant contemporaneous variables (e.g. level of demand and price today) or constraints (e.g. size of storage reservoir). In this way hydro plants dispatch electricity when prices are high and store when prices are low.

Below we present a less drastic simplification that still leaves the solution dynamic and ensures that we respect the occasionally binding constraints in (5c)-(5d). Finally, we illustrate the performance of our dynamic model for storage technologies in section 4.3.2 for HY plants in Sweden.

4.3.1 A smooth simplification of the storage problem

In this section we present a smooth approximation of the general case presented in (5) that can readily be solved by a Newton-based optimizer in a general equilibrium setting. In general, we see three obstacles to achieve this goal: First, the law of motion involves a kink (non-differentiability). Second, there are occasionally binding constraints in both our control and state variable. Third, the objective function is linear in the control variable (E_h), which typically implies kinks in the optimal supply function. Here we offer three approximations that aim at solving each of these issues in turn. In some regards the approach outlined here is novel and non-standard - albeit fairly intuitive. For the interested reader we refer to appendix D for a presentation of alternative methods, we ultimately found inferior to this application.

We start by replacing the kink in the law of motion with a continuously differentiable function, replacing (5b) with

$$S_h = S_{h-1} + f(Y_h - E_h), \tag{7}$$

where $f(\cdot)$ is a function that smoothly switches from 1 to $1 - b$ around $Y_h - E_h = 0$.[40] From this we

[39] Essentially, the problem can be set up as a discrete-choice problem. By using the terminal state condition of the a predetermined reservoir level, the model for storage technologies could be solved by means of backwards induction. That is, given a terminal value tomorrow, the optimal discrete choice today can be solved for using a numerical optimisation algorithm on an exogenous grid of the state variable. Here the terminal value of tomorrow can be determined by standard interpolation techniques. This process continuous by iterating backwards and solving for the entire optimal supply path.

[40] A simple solution is a normal smoothing device, which we have applied to smooth out jumps in the solution in section 4.1. Alternatively, appendix J outlines a method for smoothing out general piece-wise linear functions.

define the Lagrangian function for the problem as:

$$\mathcal{L} = \sum_{i=1}^{H-1} \beta^i \left[E_h(p_h - c) + \theta_h \left[S_{h-1} - S_h + f(Y_h - E_h) \right] + \bar{\mu}_h \left(\bar{S} - S_h \right) + \underline{\mu}_h S_h + \bar{\lambda}_h \left(\bar{E} - E_h \right) + \underline{\lambda}_h \left(E_h - \underline{E} \right) \right]$$
$$+\beta^H \left[E_H(p_H - c) + \theta_H \left[S_{H-1} - S_0 + f(Y_H - E_H) \right] + \bar{\lambda}_H \left(\bar{E} - E_H \right) + \underline{\lambda}_H \left(E_H - \underline{E} \right) \right], \tag{8}$$

where we have explicitly applied $S_H = S_0$ in the terminal period H. We add the Karush-Kuhn-Tucker (KKT) complementary slackness conditions for all inequality constraints and for all h:

$$\bar{\mu}_h \left(\bar{S} - S_h \right) = \underline{\mu}_h S_h = 0, \qquad \bar{\lambda}_h \left(\bar{E} - E_h \right) = \underline{\lambda}_h \left(E_h - \underline{E} \right) = 0, \qquad \bar{\mu}_h, \underline{\mu}_h, \bar{\lambda}_h, \underline{\lambda}_h \geq 0. \tag{9}$$

The first order conditions for the problem are now given by (9), the law of motion for the state variable, and the following system of equations:

$$p_h - c = \bar{\lambda}_h - \underline{\lambda}_h + \theta_h \left[f'(Y_h - E_h) - 1 \right] + \theta_h \qquad \forall h \tag{10a}$$
$$\theta_h \equiv \underline{\mu}_h - \bar{\mu}_h + \beta \theta_{h+1}, \qquad \text{for } h < H \tag{10b}$$

The interpretation of the solution characterized by (10) is straightforward: If $p_h - c$ is large relative to the continuation value of the storage problem, θ_h, the firm should produce as much as possible, implying $\bar{\lambda}_h > 0$. If $p_h - c$ is small compared to the continuation value, the storage firm decreases production towards $\underline{E}$. Finally, there might be intermediate price cases, where it is optimal to produce approximately $E_h \approx Y_h$ in order to avoid the storage loss. Instead of solving this discrete choice problem explicitly, we formulate a production function that inherits these features directly:

$$E_h^* = \underline{E} + (Y_h - \underline{E}) \Phi \left(\frac{p_h - c - a\theta_h}{\sigma} \right) + \left(\bar{E} - Y_h \right) \Phi \left(\frac{p_h - c - \theta_h}{\sigma} \right), \tag{11}$$

where $\Phi(\cdot)$ is the standard normal CDF, σ is a smoothing parameter and a is the efficiency of storage $(1 - b)$.[41] One way to interpret the function in (11) is as follows: Start by ignoring the kink in the law of motion, implying that $f'(Y_h - E_h) = 1$. In this case the optimal dispatch function in (11) follows directly from the first order conditions in (10), by assuming:

$$\bar{\lambda}_h - \underline{\lambda}_h \approx \Phi^{-1} \left(\frac{E_h^* - \underline{E}}{\bar{E} - \underline{E}} \right) \sigma. \tag{12}$$

The approximation thus corresponds to forcing the shadow cost of the capacity constraints $(\underline{E}, \bar{E})$, to follow a specific functional form. The specific functional form is, however, quite intuitive. If the approximate solution (E_h^*) approaches the lower bound $\underline{E}$, the shadow cost of the capacity constraints tends to negative infinity, implying that it is worthless to lower E further. Conversely, when production approaches the upper bound $\bar{E}$ the shadow cost of the constraints tends to infinity making it optimal to keep $E_h^* < \bar{E}$. Finally, note that lowering the smoothing parameter (σ) appropriately, our shadow-cost function is only significantly different from zero when E approaches the bounds $\underline{E}, \bar{E}$. In this way, the

[41] For HS this is near 100%, whereas ES is usually around 90%.

our approach once again nests the discrete choice solution represented by the first order conditions in (10), given that the function in (5a) can come arbitrarily close to the discrete choice case by lowering σ.

With equation (11) in place we still have kinks in our solution from the state constraints in (9), which feed into our solution through the continuation value in (10b). To solve this issue, we start by recognizing that the inequality constraints can be rewritten into equality constraints, using *max* or *min* functions. Thus (5c) can be represented as:

$$\begin{aligned}\max\left\{S_h, \bar{S}\right\} =& \bar{S}\\ \min\left\{S_h, 0\right\} =& 0.\end{aligned}$$

The max/min functions are non-differentiable around $\bar{S}$ or 0. Here we follow the approach that comes recommended with the software we use to solve our model, CONOPT4 in GAMS. Drud (2019) offers a way to smooth this out by adding an approximation error $\delta/2$ such that:[42]

$$\max\left\{S_h, \bar{S}\right\} \approx \frac{S_h + \bar{S} + \left[\left(S_h - \bar{S}\right)^2 + \delta^2\right]^{1/2} - \delta}{2} \equiv S_h^{max} \tag{13}$$

$$\min\left\{S_h, 0\right\} \approx \frac{S_h - \left[S_h^2 + \delta^2\right]^{1/2} + \delta}{2} \equiv S_h^{min}. \tag{14}$$

This approximation is differentiable with analytical derivatives that are straightforward to compute. Letting $\nabla S_h^{max}, \nabla S_h^{min}$ denote these derivatives, the KKT conditions can be dropped. The final system of equations characterising the optimal storage and dispatch path for storage technologies are then given by:

$$\begin{aligned}
E_h^* &= \underline{E} + (Y_h - \underline{E})\Phi\left(\frac{p_h - c - a\theta_h}{\sigma}\right) + \left(\bar{E} - Y_h\right)\Phi\left(\frac{p_h - c - \theta_h}{\sigma}\right),\\
\theta_h &= \beta\theta_{h+1} + \underline{\eta}_h - \bar{\eta}_h\\
S_h &= S_{h-1} + f(Y_h - E_h),\\
\bar{\eta}_h &\equiv \left(S_h^{max} - \bar{S}\right)\nabla S_h^{max}\\
\underline{\eta}_h &\equiv -S_h^{min}\nabla S_h^{min}\\
S_H &= S_0, \quad S_0 > 0 \text{ given.}
\end{aligned} \tag{15}$$

Compared to the original first order conditions, the optimal supply decision (E_h^*) is now represented by a continuously differentiable and closed-form function of exogenous terms, the contemporaneous price (p_h) and the continuation value θ_h. Note in particular, that given prices (p_h) and an initial level of the continuation value θ_1, the system of equations in (15) is straightforward to solve, as the system is no longer simultaneous.[43] Thus, the numerical problem boils down to finding a value of θ_1, such that recursively solving for the system yields a S_H that obeys the terminal condition $S_H = S_0$.

[42] In the documentation it is stated that with a properly scaled state variable (a level of around 1), a δ value of around [0.001; 0.0001] is suitable.

[43] Technically, the model presented here can be ordered topologically, such that given θ_1 (and ignoring the $S_H = S_0$ constraint), the dependency graph associated with the model is a Directed Acyclic Graph. In particular, the topological order is respectively $E_1, S_1, \underline{\eta}_1, \bar{\eta}_1, \theta_2, E_2, ...$ and so on for all h.

4.3.2 Evaluation of the storage model using Swedish hydro power plants

To evaluate our approach to model storage technologies, we consider the case of Swedish hydro power plants. We choose Swedish hydro power plants in part because they are essential for the electricity equilibrium in Denmark and partly due to the data availability.[44] We collect hourly hydro-electric production from the national TSO (Svenska Kraftnät, 2019) and elspot prices from Nord Pool (2018). Water inflow and storage level are only available at the weekly frequency. To get the hourly frequency we allocate the weekly water inflow equally into every hour within the week and calculate the hourly reservoir level using the law of motion $S_h = S_{h-1} + Y_h - E_h$ where Y_h is the allocated hourly water inflow. This method implies a small deviation, when comparing the weekly reservoir level with the imputed hourly reservoir level (see figure 4.4).

Figure 4.4: Calculated hourly reservoir level and water inflow for Sweden, 2017

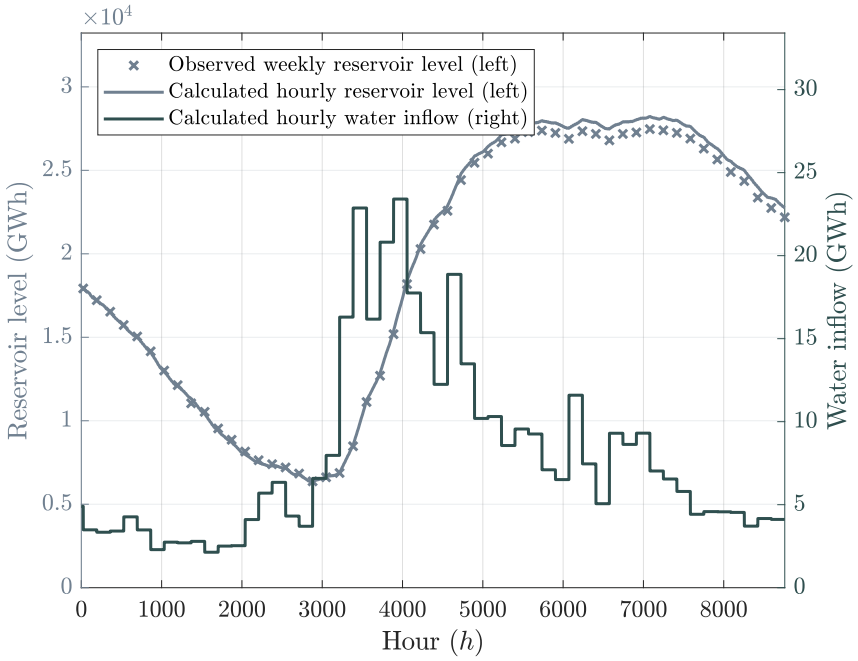

Source: Own calculations based on Nord Pool (2018) and Svenska Kraftnät (2019).

To structurally estimate the model we assume that observed electricity production (E_h) is contaminated with mean-zero i.i.d. normal measurement error

$$x_h(\xi) \equiv E_h - E_h^*(S_{h-1}, p_h; \xi) \sim \mathcal{N}(0, \sigma_\eta^2), \tag{16}$$

where $E_h^*(S_{h-1}, p_h; \xi)$ is the policy function given by the system of equations in (15) and the estimation parameters are $\xi = (\sigma, \beta, c, \underline{E}, \bar{E})'$. Assumption (16) implies that the likelihood of observing the data is

$$\mathcal{L}() = \prod_{h=1}^{H} \phi(x_h(\xi)), \quad \phi(x_h(\xi)) = \frac{1}{\sqrt{2\pi\sigma_\eta^2}} \exp\left(-\frac{x_h(\xi)^2}{2\sigma_\eta^2}\right) \tag{17}$$

[44] To the best of our knowledge, hourly frequency data is only available for Swedish hydro plants and not any other storage plants; at least not any that are included in our model.

The estimation is implemented in GAMS, formulated as a maximization problem, which is similar to the *mathematical program with equilibrium constraints* (MPEC) method proposed by Su and Judd (2012). Formally the problem is set up as follows:

$$\max_{\xi \in \Xi} \log\left(\mathcal{L}(\xi)\right) = \frac{1}{H} \sum_{h=1}^{H} \log(\phi(x_h(\xi))) \quad \text{subject to system (15)} \tag{18}$$

The parameter space (Ξ) is restricted to:

$$\Xi = \left\{ \xi \in \mathbb{R}^5_+ \,\middle|\, \sigma > 0 \ \wedge \ c \geq 0 \ \wedge \underline{E} \in \left[0, \min\{E_h\}\right] \ \wedge \ \bar{E} \in \left[\max\{E_h\}, \infty\right[\right\}.$$

To compute standard errors from this estimation, the model would have to be resolved for each estimate $\hat{\xi}$. As the exercise performed here is meant to illustrate the model formulation's fit compared to observed data, we do not include standard errors in the following. The estimated parameters are presented in table 5 along with the technical information in Ramses for Sweden in 2017 for comparison. The optimal discount factor is set to 1 cf. table 5. Recall that the frequency of data is hourly, thus a discount factor of $\hat{\beta} = 1$ seems somewhat reasonable. Furthermore, the estimate of the marginal cost (c) is almost identical to the cost estimate in Ramses. For the current framework to replicate the observed patterns, the capacity data has to be scaled down by around 22% though.

Table 5: Comparison of estimated parameters and Ramses technical information.

Parameter	Description	Estimate	Ramses
σ	Smoothing parameter	81.56	NA
β	Discount factor	1.00	NA
c	Marginal cost (DKK)	7.54	5.85
$\bar{E}$	Maximum generation capacity (GWh)	12.77	16.27
$\underline{E}$	Minimum base-load (GWh)	2.01	0.00

The model fit is presented in figure 4.5. Figure 4.5a plots power generation for given prices. The model replicates the general upward sloping supply curve, indicating that hydro plants ramp up production when prices increase. The model does not sufficiently capture the variance in observed electricity production. The immediate explanation for this is that the current version of the model, does not include uncertainty. Both future prices as well as the exact inflow of water is to some degree uncertain. Including stochasticity in the model would, however, require a major update. While it might be feasible to include in the BU module, it is not clear whether this could work when coupled to a CGE model.[45]. Another possible explanation is that hydro plants do not plan production according to prices but according to demand; such an assumption is the basis for hydro-electric production in Ramses (Danish Energy Agency, 2018a, p. 33-37). We view this as unlikely, given hydro power managers have access to both projected demand

[45]It is a somewhat straightforward exercise to include expectations on how prices and inflow in the decision rules of the hydro plants. Including the simulation of stochastic processes for each hourly state would, however, increase the dimensionality of the model significantly.

and supply on Nord Pool, enabling them to calculate the expected system spot price.[46]

Figure 4.5: Model fit of hydro power in Sweden, 2017

(a) Power generation for given electricity prices. (b) Reservoir level.

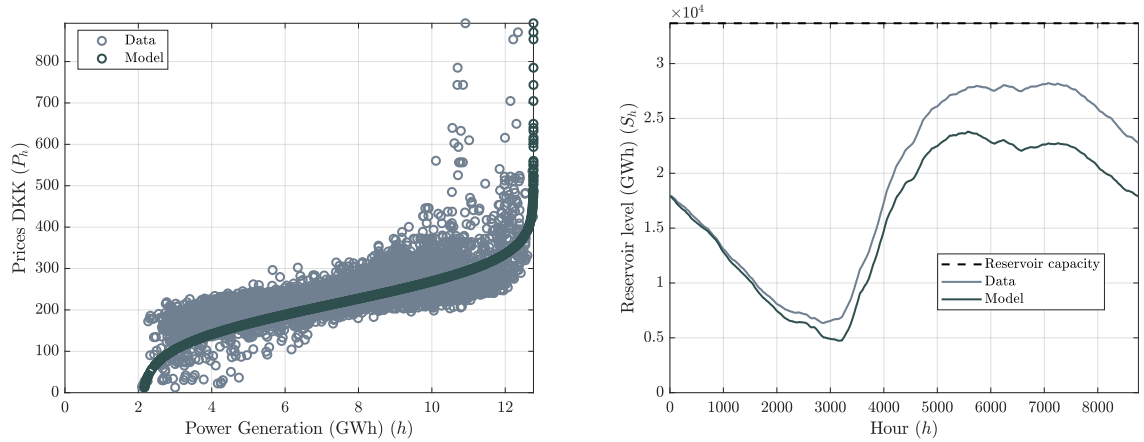

Figure 4.5b plots the reservoir level. The model replicates the general shape and level of the hourly reservoir level. The level difference towards the terminal period is due to the terminal condition in (5e). To fit the reservoir level more accurately an infinite horizon framework could be invoked. This would however make the calibration of our bottom up module far more complicated, as it would have to run simultaneously with the entire CGE model. The reason for this is that managers of storage technologies now take into account the entire price path, even prices in the very long-run, when planning production in the very short-run. Solving the BU-model for one year, thus depends on solution of the BU-model in other years. In the current model version presented in the following sections, the simple terminal conditions is applied.

4.4 Intermittent versus dispatchable technologies

A subset of technologies are characterized as *intermittent*. This means that the productivity of a plant varies deterministically and in part stochastically over the course of a year. In the framework presented here this corresponds to the plant capacity q_i varying across the h hourly states. A second characteristic (albeit not a defining one) of intermittent technologies is that the marginal cost of production is close to zero compared to both investment costs and other technologies' marginal costs. These characteristics of intermittent plants lead to a short run supply that is ultimately controlled by fluctuation in wind speed, cloud cover etc. rather than economic decisions.

In contrast to intermittent plants, *dispatchable* ones generally have an (approximately) constant capacity (q_i) over the year. With (typically) significantly higher marginal costs than intermittent technologies, the short run equilibrium is found by balancing the residual demand after supply from intermittent plants with supply from dispatchable plants. Figure 4.6 illustrates the variation in wind power compared to

[46] See `https://www.nordpoolgroup.com/Market-data1/Power-system-data/Production1/Procuction-Prognosis/ALL1/Hourly/?view=table` and `https://www.nordpoolgroup.com/Market-data1/Power-system-data/Consumption1/Consumption-prognosis/`.

demand in Denmark. Figure 4.7 illustrates the corresponding residual load curve that dispatchable plants face.

Figure 4.6: Demand and intermittent supply variation

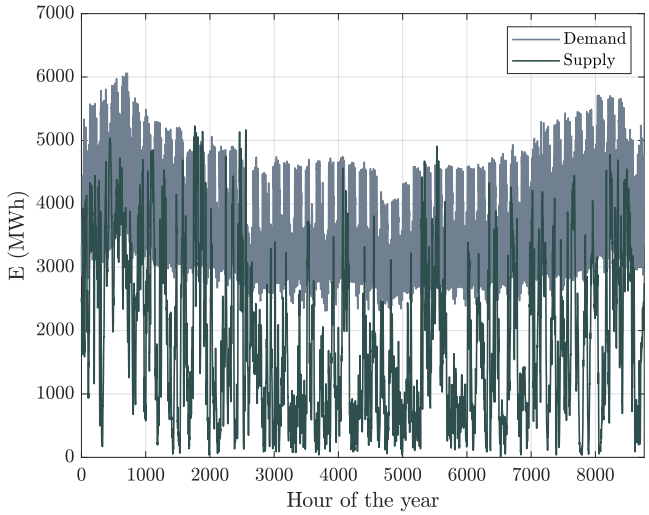

As discussed in section 2, these features of intermittent/dispatchable technologies are essential to the economic value of different types of plants. Ignoring trade and subsidies, the residual load curve for Denmark in figure 4.7 shows that when production is peaking for wind power, prices are driven to almost zero (around 8.5% of the year). Dispatchable plants that work as back-up capacity for intermittent technologies can, on the other hand, charge a considerable higher price in peak load hours, where the residual load is as high as 5500 MWh. These dynamics are essential for the economic value of different technologies and thus for the investment decision (Joskow, 2011).

Figure 4.7: The residual load curve for Denmark, 2017

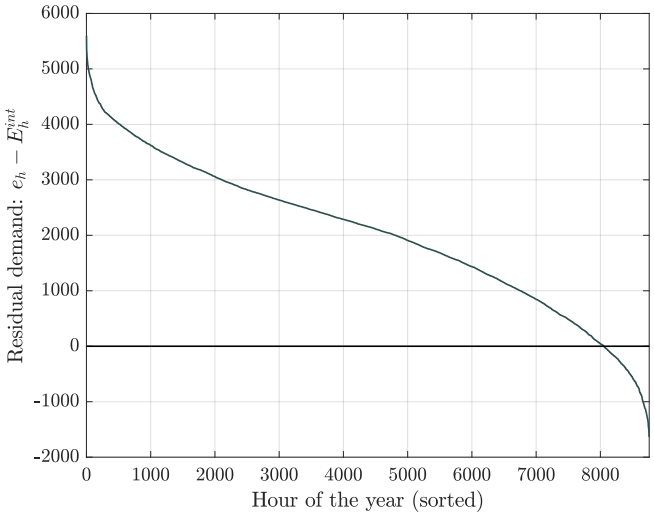

4.5 Energy deficit plants

The final type of plant included in the model is the so-called *energy deficit plants*. We include one of these plants in each heating and electricity area of the model. Technically, these plants are characterized by having a huge electricity or heat production capacity $(\bar{q}_E, \bar{q}_H)$, but also by having by far the highest marginal cost of production $(\bar{c})$. The plants are included in our model only for computational purposes to ensure that there always exists a short run equilibrium. At any given hourly state (h) the model has a maximum supply of electricity and heat available. Furthermore, as we elaborate on in section 5, the hourly demand for energy goods are partly exogenous. This means that we can potentially have states, where demand cannot be satisfied by supply in the very short run. In these states our model activates the EDF plants ensuring that our equilibrium constraints are obeyed.

In Denmark such states are handled by the national transmission system operator (TSO) as so-called *brown-outs*. If the price ceiling on Nord Pool is reached, the TSO will disconnect a share of consumers to ensure that an equilibrium can be reached (Energinet, 2018).[47] The supply from EDF plants is modelled exactly as *standard* plant types with a smoothed normal function:

$$\bar{E} = \bar{q}_E \Phi \left(\frac{p^E - \bar{c}}{\sigma} \right).$$

The production of heating by EDF plants $(\bar{H})$ is modelled similarly. Besides the computational importance of these plants, we can use the amount of production from the EDF plants as a measure for how stable supply is. That is, we can use the production from EDF plants as a measure for the amount of demand that has to be curtailed in order to ensure equilibrium.[48]

4.6 The Danish bottom-up derived supply function

The result of our bottom-up approach is a short run supply curve that depends on a number of considerations. The productivity of intermittent plants depends on exogenous variation. The supply from CHP plants depend on both the price on electricity and the price on heat. The supply from storage firms depends on the entire path of electricity/heating prices in that given year. Finally, the marginal cost of each plant is tied to fuel-prices, taxes etc.. In this way, we can compute the supply at any given time (h) as the sum of supply from all plants in the respective area.

Before we proceed to the demand and short-run equilibrium, we briefly showcase some of the characteristics of the bottom-up supply function for the Danish plants. Recall that electricity is supplied from simple standard plants, CHP plants that plan production, taking heat prices into account and storage plants that consider the entire path of electricity prices throughout the year. Finally intermittent plants' capacity varies exogenously over the hours of the year. To illustrate the supply as simple function of contemporaneous electricity prices, we thus need to impose some assumptions. In the scenario depicted in figure 4.8, heat prices are fixed at 200 DKK/MWh. Electricity prices are then varied exogenously from

[47] This is done to avoid the far more critical scenario of *black-outs*. See Energinet (2017).
[48] For this measure to work, we need the costs $\bar{c}$ to be significantly above all other plants' marginal costs.

Figure 4.8: Average hourly Danish supply curve.

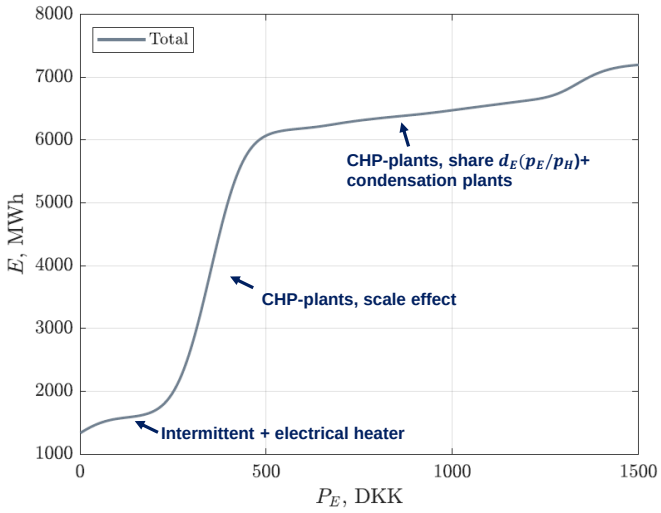

Note: The figure shows the supply from Danish electricity plants varying the price level from 0-1500 DKK. We use yearly average productivity levels for intermittent technologies and a price on heating at 200 DKK/MWh. We use a value of the smoothing parameter described in section 4.1 $\sigma = 50$.

0-1500 DKK/MWh. To keep things simple, we assume that electricity prices are constant throughout the year; thus storage plants are not activated here. Finally to illustrate an average supply function, the capacity of intermittent technologies is given by the hourly average for 2017. In appendix E the supply function is further illustrated for different plant and fuel types.

With fixed heat prices the supply function in figure 4.8 largely consists of three parts: First, when prices are very low, the supply comes primarily from intermittent sources. Given that the price on heat is fixed at around 200 DKK/MWh in this example, electrical heaters supply a significant negative part, when prices are near zero; that is, they are consuming large amounts of cheap electricity and using it to generate heat. Second, when prices are intermediate (250-300 DKK/MWh), the large CHP plants become profitable. Note that the supply curve becomes muc more price elastic around the threshold, where CHP plants become active. Third and final, when prices are high supply adjusts through primarily two channels: The CHP plants endogenously adjust their output split towards more electricity rather than heat output, and the condensation plants become profitable.[49]

Figure 4.9 illustrates the share of Danish supply when split into different fuel types. The figure illustrates that when prices are very low and the hourly capacity is at the yearly average, intermittent technologies produces roughly 85% of the domestic supply. In our model, only biomass and waste production also produce at electricity prices around 0 DKK/MWh. When the large CHP plants become profitable around 250-300 DKK/MWh, the production share of natural gas an oil/coal sharply increases. Not surprisingly, we see that the higher the electricity prices are, the larger is the share of supply coming

[49]Recall that we assume the prices on electricity are constant across hours, i.e. storage firms are not considered here. Furthermore, we only focus on domestic supply and thus ignore trade.

Figure 4.9: Average hourly Danish share of supply on fuel types.

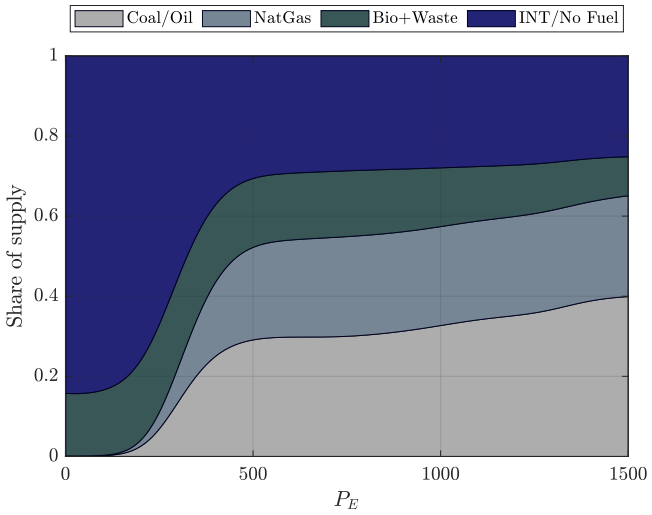

Note: The figure shows the supply from Danish electricity producing plants when varying the price from 0-1500 DKK/MWh. The figure illustrates how large a share of electricity output, is provided by different fuel-types. We use yearly average productivity levels for intermittent technologies and a price on heating at 200 DKK/MWh. We use a value of the smoothing parameter described in section 4.1 $\sigma = 50$.

from fossil fuels.

5 Short run demand for electricity and heating

In the previous section we defined the modelling of the bottom-up derived supply function. In the following, we proceed to describe the specification of demand for electricity and heating *within* a year. In the long-run we assume that both firms and households demand energy goods rationally, e.g. by some maximization principle. The yearly demand functions are thus price-sensitive functions, representing firms and households updating respectively their production processes and consumption patterns in response to relative prices. Importantly, this part can be modelled in a different module or a CGE model that the BU model can be linked to.[50]. We choose to include a rigidity in demand when considering shorter time horizons. This rigidity can reflect imperfect information on hourly electricity and heat prices, behavioral inattention or simply habits in the demand for energy goods. Another reason for including demand rigidity in the short run, is that wholesale prices are currently not passed on to end-consumers in the electricity market.[51] With smart meters however this is expected to change. In the following we thus develop and estimate a demand specification that can capture the expected structural changes in the short run demand for energy goods.

[50]In section 11.1 we provide a simple specification of demand in a CGE model that is used in the counterfactual simulations.

[51]This also applies to market for heat, where prices for end-consumers are usually fixed by long-term agreements.

5.1 A demand specification with habits and partial flexibility

In energy system models the tradition is that short run demand is completely inelastic. While this may be a somewhat reasonable approximation today, this leaves no scope for introducing more flexible demand in the future.[52] On this basis we model short-run demand on the form:

$$e_h\left(p_h, p\right) = \phi \bar{e}_h + (1-\phi)\bar{e}_h f(p_h, p), \qquad f'_{p_h} < 0,\ f'_p > 0,$$

where h indicates the hour within a given year. Time subscript for years is omitted for simplicity, such that p_h is the hourly price and p is the weighted average yearly consumer price. While the parameter ϕ expresses the share of demand that is inelastic, $\bar{e}_h$ captures exogenous preferences for how consumers prefer to allocate consumption on an hourly basis.[53] The share parameter ϕ is a deep parameter that can be altered in policy experiments of *demand flexibility*, but is otherwise considered constant.[54] The share $(1-\phi)$ of the yearly demand represents price-sensitive demand. Thus, $f(p_h, p)$ represents how the price elastic part of demand depends on hourly and yearly average prices. We assume that if prices were constant throughout the year, the price-sensitive part coincides with the inelastic part. Secondly, we assume that the preferences over hourly variation is defined as constant shares of total yearly demand. Thus, we split the exogenous part into $\bar{e}_h = g_h D$, where D is a level component. Defining the total yearly demand (E) as the sum of the short-run components we then have:

$$\begin{aligned} e_h(p_h, p) &= \phi g_h D + (1-\phi) g_h D f(p_h, p), \qquad \sum_h g_h = 1 \\ E &= D \sum g_h \left[\phi + (1-\phi) f(p_h, p)\right], \quad f(p,p) = 1, \\ E &= \sum_h e_h(p_h, p). \end{aligned} \tag{19}$$

If prices were constant across a year, consumers would plan their consumption according to the exogenous weights g_h and consume $g_h D$ in hour h. When prices fluctuate, only a share $(1-\phi)$ of consumers readjust their consumption pattern by reallocating consumption to relatively cheap hours. This may also have a level effect on total consumption.[55] Thus, D here represents the hypothetical level of demand absent price fluctuations, while E is the realised yearly demand level. To motivate the specification of exogenous consumption weights (g_h), the average electricity consumption cycle over a day is plotted in figure 5.1 for 2011-2017. The average daily cycle is almost identical across years, and the 95% highest density interval suggests that the daily cycle is also persistent. The pattern is very much in line with expectation that consumers demand electricity in conjunction with their daily task, which is captured by g_h in our framework.

[52] It is expected that making demand more flexible will mitigate the cost of intermittent energy production (Ambec and Crampes, 2017).

[53] For instance, the demand for electricity spikes in the morning when people wake up.

[54] This specification leaves us open to the well known critique of Calvo versus state-dependent price models in the rigid price-setting literature. One may argue that ϕ indeed should be a function of the volatility in prices. We could quite easily include this in the general equilibrium setting, however, this leaves us with the challenge of identifying parameter values in this relationship. We leave this challenge for future work.

[55] It essentially depends on the way prices fluctuate, as well as the specific functional form of $f(p_h, p)$. More specifically on whether or not the demand is convex or concave.

Figure 5.1: Average daily electricity consumption cycle for Denmark

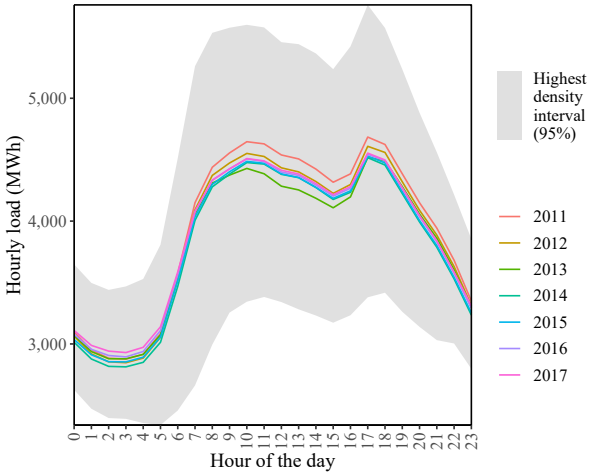

Note: Hourly load for DK-West and DK-East have been aggregated.

Source: Energy Data Service (2018a)

By rewriting (19) we have a demand specification of the form

$$e_h(p_h, p) = E * z_h\left(p_h, p\right), \qquad z_h \equiv \frac{g_h\left[\phi + (1-\phi) f(p_h, p)\right]}{\sum_h g_h\left[\phi + (1-\phi) f(p_h, p)\right]}. \tag{20}$$

Demand in the short run can then be thought of as an allocation problem of yearly demand (E) with solution shares z_h for each hour h. This function guarantees consistency with the top-down model, as $z_h \in (0, 1)$ and $\sum_h z_h = 1$ by construction. We say that (20) is an *integration link* between the top-down and bottom-up model. In section 11.1 we provide a simple specification of yearly demand (E), which is used in the counterfactual simulations to illustrate how the integration link works. Note that this framework allows for a wide class of demand specifications. We work with a couple of parametrized versions for the price elastic part, in particular:

$$f_1(p_h, p) = \left(\frac{p_h}{p}\right)^{-\sigma}, \qquad \sigma > 0, \tag{21}$$

$$f_2(p_h, p) = \underline{D} + \frac{(1-\underline{D})\frac{\bar{D}-\underline{D}}{\bar{D}-1}}{\frac{1-\underline{D}}{\bar{D}-1} + exp(\sigma(p_h - p))}, \qquad \sigma > 0, \qquad \bar{D} > 1 \geq \underline{D} \tag{22}$$

Version (21) is the traditional iso-elastic function, frequently applied in economics. We offer an alternative to this function for two reasons: Firstly, this function does not allow for having negative prices, which occurs in the electricity market in the short run. Secondly, this specification allows for very large re-allocations of energy demand when prices drop. While an appropriately low value of σ may remedy this, we offer a bounded demand function in version (22) as an alternative.[56] The bounded demand version is inspired by a simple logit demand, where $\underline{D}$ and $\bar{D}$ are lower and upper bound, respectively, on the demand function.[57] It has some intuitive features when modelling energy demand, which is illustrated in

[56] We found that because the iso-elastic function is not defined for negative prices, the numerical stability was greater when using the bounded version.

[57] Appendix G elaborates on the specific functional form of (22). The appendix furthermore includes some alternatives to the logit-like demand function.

5.2. First, $\bar{D}$ controls the upper bound on the demand of energy and $\underline{D}$ the minimum demand level. We can think of $\underline{D}$ as controlling the *subsistence* energy consumption. Finally, σ controls the overall price sensitivity around the equilibrium price (for consumers already reacting to the price).

Figure 5.2: Modelling of energy demand in the very short-run.

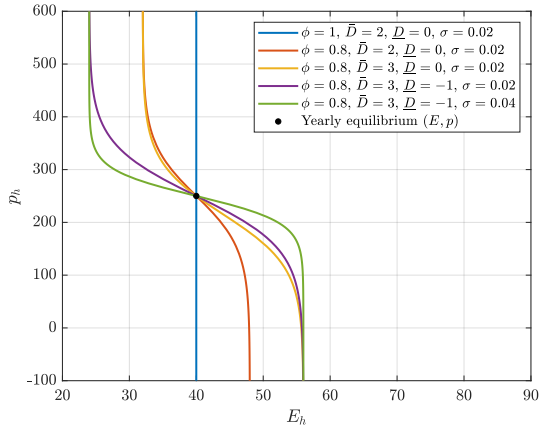

Note: The yearly equilibrium is set at $(E, p) = (40, 250)$.

5.2 Determining the parameters of very short run energy demand

The parameters $\underline{D}$ and $\bar{D}$ are considered deep parameters in the sense that they are policy invariant. The share of yearly inelastic demand (ϕ) and the smoothing parameter (σ), however, are not invariant to policy. In some instances they may even be considered policy variables. For instance, equipping consumers with smart meters will enable them to react to the hourly price, making a larger share of demand elastic (ϕ decreases). Consequently, a lower value of ϕ can be interpreted as making a larger share of demand more price responsive. In other words, ϕ is a policy variable for increasing demand flexibility. Similarly, equipping consumers with 'smart technologies' such as load switching technologies increases the overall price responsiveness of the price-elastic part. While we could, in principle, determine all the parameters of the demand function (at least for electricity demand), using the publicly available data in Nord Pool (2018), we focus below on the determination of ϕ, because this is the key parameter that separates the demand modelling approach in this paper from the standard approach in BU models.

The tradition in energy system models is to assume that energy demand in the very short-run is completely inelastic ($\phi = 1$). Under this assumption, the weights g_h can simply be fixed at the observed levels. For a relatively large share of consumers of electricity this seems like an appropriate assumption, given that end-consumers often face contract prices specified for a longer period of time. Even for the power sector, hourly wholesale prices are not passed through to the majority of end-consumers in the retail market (Zerrahn et al., 2018). For heating the assumption of $\phi = 1$ seems reasonable. For electricity demand, however, there is available data allowing us to pin down the level of ϕ.

Using hourly load data, we show in appendix G.2 that by assuming $\phi = 1$ and estimating (20), we are able to explain a little over 92% of hourly electricity demand variation in Denmark. This supports the

conventional assumption that demand is (nearly) perfectly inelastic in the very short-run. However, it should also be recognized that examining the load curves corresponds to examining an equilibrium outcome. An obvious choice is therefore to examine the price sensitivity of demand on the wholesale market using bid-curves from Nord Pool spot market (Nord Pool, 2018). These bid-curves are price-quantity bid combinations, showing the total aggregate demand curve on the day-ahead market (aggregated over all countries). In this way we target the demand side more directly. There are, however, two important caveats of using this data: First, market members on Nord Pool do not necessarily reflect an average consumer. They are predominately system operators, public and private energy producers, distributors, traders, brokers, financial institutions, and energy intensive companies (i.e. large consumers). Second, the market only encompasses the day-ahead market and hence does not capture total electricity demand (although most electricity is traded on NordPool). Households that are normally considered price inelastic do not operate on the wholesale market. These two caveats both suggest that estimating ϕ on the data from Nord Pool provides a lower bound of the true ϕ.

To calculate ϕ we have to make an assumption. On the day-ahead market on Nord Pool there is a price ceiling of €3.000/MWh[58]. We assume that agents bidding at the maximum price are effectively price independent. We believe this to be a reasonable assumption given the scale of the price ceiling. The average hourly electricity price between 2010-2017 was merely €34.5/MWh and the price-ceiling is more than 86 times that, indicating that these clients are buying electricity no matter the cost. The estimate of ϕ is only based on agents bidding the maximum price and is a very simple exercise; we simply calculate the share of demand over the course of the year that is demanded at the price-ceiling.

The estimate of ϕ is presented in table 6. The share of inelastic demand has been somewhat constant around 86%. Our estimation suggests that while demand for electricity is still largely inelastic, we miss out on some dynamics by setting $\phi = 1$. In particular, we might overestimate the costs of having intermittent supply (with ϕ =1). For now, we stick to the assumption of $\phi = 1$ for the simple reason that this is the convention in energy system models. In section 11.4 we do, however, perform a counterfactual scenario by setting $\phi = 0.9$.

6 Trade in the short run

As discussed in section 2, trade is one potential instrument that can be applied in mitigating the costs of fluctuating supply. With higher penetration rates of wind power in Denmark, we have come to rely to a larger extent on supply from stored hydro power from Norway and Sweden. The competition between domestic and foreign plants depends largely on what type of technology is applied, and furthermore on the composition of future foreign plants. This further affects investment decisions and the economic value of intermittent technologies. As an example instance, consider a scenario where neighboring countries all invested heavily in wind power. As intermittent plants usually provide electricity at very low marginal costs, this would drive down equilibrium prices. As the productivity from intermittent plants in neighboring countries is typically positively correlated with domestic intermittent plants' productivity, prices

[58] Until 28. November 2013 the price ceiling was €2.000/MWh.

Table 6: Estimation of inelastic electricity demand

Year (t)	Share of yearly inelastic electricity demand (ϕ_t)
2010	0,83
2011	0,82
2012	0,88
2013	..
2014	..
2015	0,89
2016	0,89
2017	0,88
2018	0,86
Average	0,86

Note: The data for 2013 and 2014 currently contain unidentified errors. For this reason the results are left out.

Source: Own calculations based on Nord Pool (2018).

would be driven down in hours, where domestic intermittent wind farms dispatch electricity. Furthermore with more foreign investments in intermittent technologies relative to dispatchable, the back-up capacity from trade would be lowered, thus increasing the costs of intermittency in Denmark.

To accurately describe how firms compete across technology types, and how this may evolve in the future, we have to abandon the traditional view of the homogeneous and infinitely large foreign economy. In the following we present a framework that allows for a great level of detail on neighboring countries' electricity supply. For computational purposes we will later simplify some of these aspects, to focus on the application in GREEN REFORM with focus on the Danish economy.

As mentioned previously, we define the set of geographical electricity areas as $\mathcal{G}_E$, with n denoting the number of areas. Table 7 shows the most detailed version available in the Ramses data. For each pair of areas (g_i, g_j), export and import trade capacities are defined by ($T^c_{i,j}$ and $T^c_{j,i}$). We further define indicator variables for whether the capacities are zero or not as $(T_{i,j}, T_{j,i})$.[59] Denote the corresponding matrices containing all capacities $\mathbf{T}^c$ and $\mathbf{T}$. In the short run capacities may vary. The state of transmission capacities at any time (h) is thus given by $\mathbf{T}^c_h = \tau_h \mathbf{T}^c$, where τ_h is a $(n \times n)$ matrix containing transmission line shocks. In our framework the shocks, τ^i_h, are simply independent $(0/1)$ variables indicating a constant probability of line i failing. However, there is nothing that prohibits including other types of transmission line shocks in the framework.

As will become more clear in the following section 8, the trade capacities are essential for how equilibrium prices differ between geographical areas. The main idea is that if plants in one area g_i have access to a foreign market g_j, the equilibrium prices in the two areas can only differ up to the marginal cost of transmission between the two areas. If the transmission line between g_i and g_j is fully utilized, plants in g_i no longer have access on the margin. Whether or not plants in g_i have access to g_j however, depends on more than just the transmission cables $(T_{i,j}, T_{j,i})$: If a third area g_k has free trade capacity between both g_i and g_j, then plants in g_i, g_j can effectively trade with each other.[60] Abstracting from trade costs

[59] Appendix A shows the matrix of all capacities $\mathbf{T}^c$ in 2018.

[60] Rather than thinking of one plant in g_i sending electricity through g_k and into g_j, we think of plants in area g_i exporting to areas in g_k, and plants in g_k in turn exporting to g_j.

Table 7: Set of geographical electricity areas, $\mathcal{G}_E$

Electricity area set $\mathcal{G}_E$:	
Denmark, West	
Denmark, East	
Norway	
Sweden	
Finland	
Germany, Austria, Luxembourg	
Holland	
Great Britain, Norther Ireland, Ireland	
France, Belgium	
Spain, Portugal	
Schweiz	
Italy	
Estonia, Latvia, Lithuania	
Poland, Czech Republic, Slovakia	
Hungary	
Russia	(exogenous trade)
Greece	(exogenous trade)
Slovenia	(exogenous trade)
Macedonia	(exogenous trade)

The choice of geographic splits follow the convention in the RAMSES data set described in section 3. For the last seven areas noted 'exogenous trade' we do not have information on plants, but only on yearly import/export flows.

this implies a trade function on the form:

$$NX_{i,j} \begin{cases} = T_{i,j}, & p_{E,i} < p_{E,j} \\ \in [-T_{j,i}, T_{i,j}], & p_{E,i} = p_{E,j}, \\ = -T_{j,i}, & p_{E,i} > p_{E,j} \end{cases}, \qquad \forall (g_i, g_j) \in (\mathcal{G}_E \times \mathcal{G}_E) \tag{23}$$

where $NX_{i,j}$ is the net export between areas g_i, g_j. Trade with third countries are thus taken into account, as the function in (23) is defined for all combinations of g_i, g_j. With this in mind we define *trade partitions* that capture this idea of having access to neighbouring markets:

Definition 1. *A **simple trade partition** is a partition of $\mathcal{G}_E$ into subsets $(\mathcal{G}_1, ..., \mathcal{G}_{n_g})$ such that:*

i. For all $\mathcal{G}_i \in \mathcal{G}_E$: All $g \in \mathcal{G}_i$ can adjust trade marginally up and *down with any other $g \in \mathcal{G}_i$. Either directly or through other trade partners.*

ii. For all $\mathcal{G}_i \in \mathcal{G}_E$: No $g \in \mathcal{G}_i$ can adjust its trade with any $g \notin \mathcal{G}_i$ neither *upwards and downwards. Either due to zero capacities or trade frictions binding.*

*Furthermore, we add that a **stable trade partition** is a simple trade partition where:*

iii. For all pairs $(\mathcal{G}_i, \mathcal{G}_j) \in \mathcal{G}_E$: If any $g \in \mathcal{G}_i$ is exporting at capacity to a $g \in \mathcal{G}_j$, then regional prices must be lower for exporting areas: $p_{E,i} < p_{E,j}$.

Appendix H outlines an algorithm that defines trade partitions using the indicator matrix $\mathbf{T}$. A trade partition is thus a collection of electricity areas, where trade capacities are sufficiently large, to allow for prices to be equalized across all of them.

7 A small scale simulation model

Before we proceed to presenting solution concepts in the short run, we briefly outline the structure of a small-scale *toy model*. The model is used in section 8 to illustrate how different solution methods perform under different circumstances. In the simplest version of this model - the *baseline* - we have just three electricity areas and ignore the market for heat altogether.[61] The three areas are described by artificial data, but in some ways (trade capacities, demand variation and level) resemble respectively Western Denmark, Eastern Denmark and Norway. We furthermore ignore plants that have access to storage for now. For each country the supply side consists of one *intermittent* and three *dispatchable* plants. We refer to the three types of dispatchables as:

i. *Base load plants:* Relatively cheap plants that cover the residual load after intermittent supply in most states.

ii. *Peak load plants:* Relatively expensive back up plants that only cover hours of peak residual load.

iii. *Energy deficit plants:* Very expensive and very large plants, included only for computational reasons. As explained in section 4.5 these plants are included to ensure that an 'equilibrium' always exists.

The exact data applied in the toy model presented here is outlined in appendix F. Here we present the general features of the model. In the baseline version we assume that the plants in the three electricity areas are roughly similar, both in terms of marginal costs and the capacity relative to the level of demand in the respective country. Figure 7.1 illustrates the supply functions relative to the demand levels for the three areas. As figure 7.1 shows, intermittent plants are assumed to operate at marginal costs around 25-30 DKK/MWh, with yearly average capacities ranging from around 45-60% of the respective country's level of demand.[62] The baseload plants operate with marginal costs of around 250-275 DKK/MWh. As figure 7.1 illustrates, they are able to cover around 60-80% of the average hourly demand. Thus in average states of supply, electricity is supplied entirely by intermittent and base load technologies. Peak load technologies operate at around 500-600 DKK/MWh and are able to cover around 19-23% of demand in an average hour.

Demand follows the specification in (20) with ϕ =0.9 and σ=1.5 for all areas. To keep things simple and easy to illustrate we work with 4 hourly states instead of the full 8760. The four states are constructed to represent respectively January-March, April-June, July-September and October-December. Figure 7.2 illustrates the variation in demand (e_h) and supply (E_h) functions in the four h states for country 1. The intermittent plants' productivity (q_i) as well as the demand components expressing hourly variation (g_h) vary throughout these four states. The variation in the three countries are similarly based roughly on actual data on Western Denmark, Eastern Denmark and Norway. The general pattern is the same across all three countries: In states $h = \{1, 4\}$ the capacity of intermittent plants is above average and vice versa

[61] While the interaction with the market for heat is interesting, the challenge of finding short run equilibria is primarily posed by the interaction of trade with electricity and the non-linear supply and demand components. To keep things as simple as possible here, we thus disregard heat altogether.

[62] As these plants are intermittent, these figures may of course vary over the year.

Figure 7.1: Yearly supply functions relative to demand levels

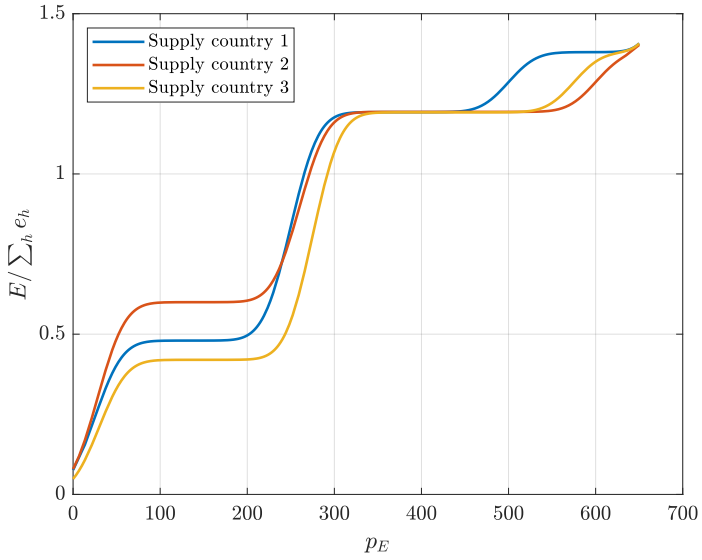

in states $h = \{2, 3\}$. Demand for electricity follows this same pattern albeit with smaller fluctuations in general.[63]

Finally transmission capacities between the three areas are given by

$$\mathbf{T}^c = \begin{pmatrix} \cdot & 1.3 & 3.1 \\ 1.3 & \cdot & 2.4 \\ 3.2 & 2.5 & \cdot \end{pmatrix}, \tag{24}$$

with entry (i, j) denoting the export capacity from country i to j.

In the baseline scenario discussed here, the variations in productivity of intermittent plants and demand over the year are so small that the law of one price holds for all $h = \{1, 2, 3, 4\}$. Figure 7.3 illustrates the equilibrium in the baseline scenario. Part (a) shows that the sum of supply from all three areas equals the sum of demand at prices around 290 DKK/MWh for all states of the year. Part (b) illustrates the domestic surplus production, defined as the difference between domestic production and demand for electricity: $E_h - e_h$. The figure illustrates that to implement the equilibria, where prices are equalized across all areas in all four h states, country 1 exports between 0.2-1.4 TWh, country 2 exports between 0.1-0.7 TWh and country 3 imports between 0.5-2 TWh. This is well within the trade capacities in (24), where e.g. country 1 can export 3.1 TWh of electricity at any h to country 3. Thus the law of one price holds in the baseline.

[63] As appendix G.2 shows, the electricity demand is highly cyclical but with variation covered by e.g. daily frequencies and not as much seasonal.

Figure 7.2: Demand and supply in different h states (country 1)

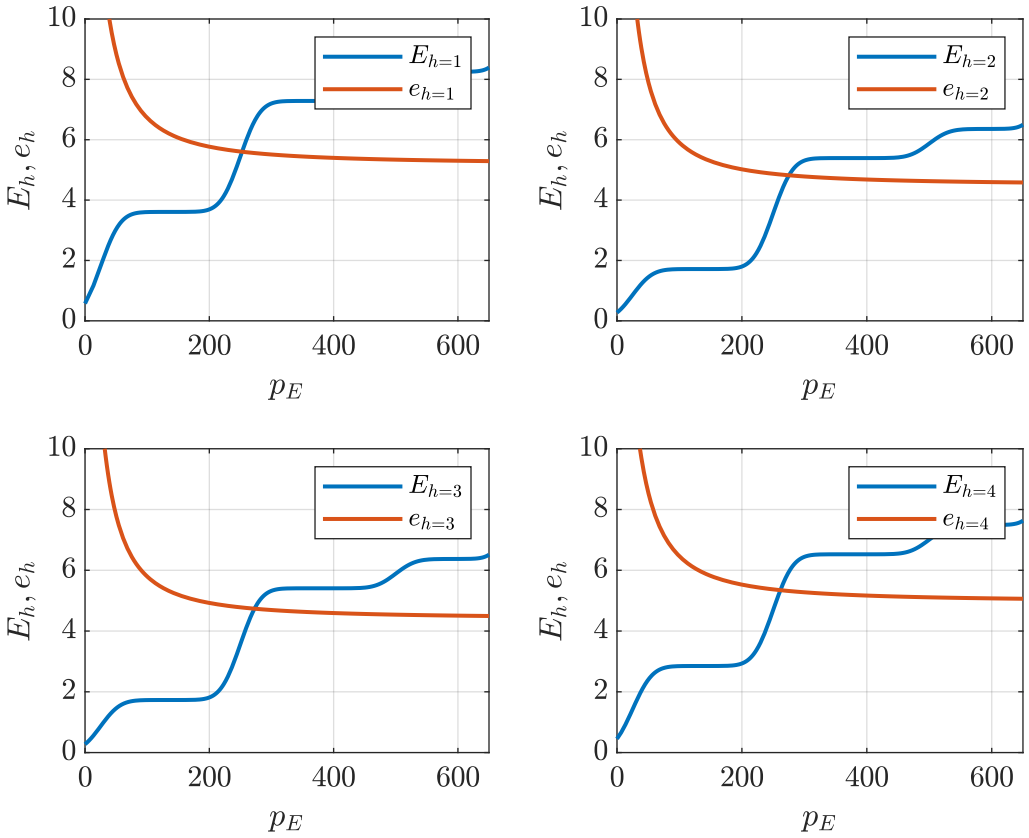

Figure 7.3: Baseline FLE scenario

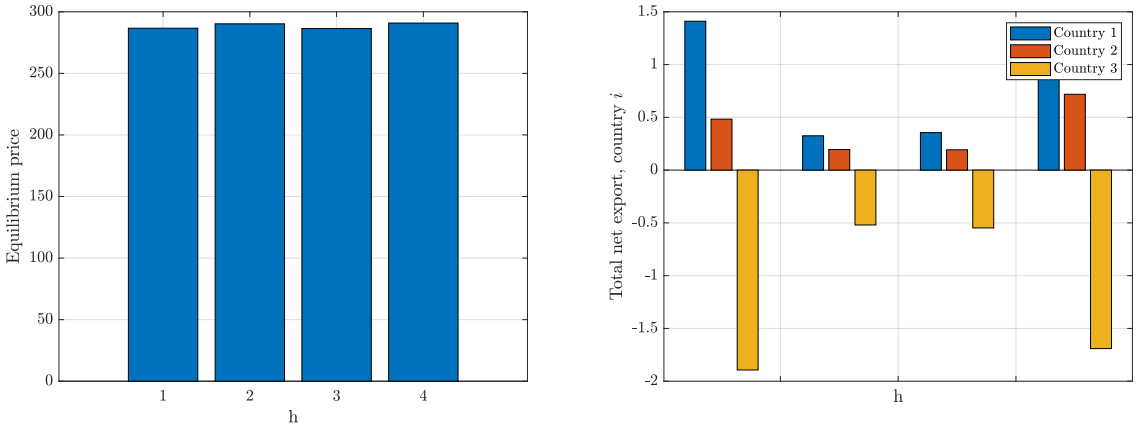

(a) Equilibrium price

(b) Domestic Surplus function

Note: The frictions-less equilibrium (FLE) is defined formally later in section 8. The equilibrium is solved for using the *complex bottom up algorithm* outlined in section 8.1.2. The domestic surplus function is defined as the difference between domestic production and demand: $E_h - e_h$. In other words; it defines the sum of net exports needed, for the FLE to be implemented.

8 The short run equilibrium

With the building blocks of demand, supply and trade in the very short run in place, we proceed to the short run equilibrium. Our fundamental understanding of the short run equilibrium is the very standard one: There is a market clearing price in each pair of electricity and heating areas (g_i^E, g_j^H), for each state h, such that demand, supply and trade clears in all states and areas. Each area's supply function is the sum of individual plants' supply. Recall that this supply consists of storage plants that optimize intertemporally, thus taking all future equilibria prices into consideration, and CHP plants that reacts to both electricity and heating prices.[64] Furthermore, demand for electricity and heat are partly inelastic and partly price-responsive, as discussed in section 5. Electricity is exported to neighbouring countries, until prices on electricity are equalized, or the capacity constraint on trade is reached.

We face a challenge when it comes to numerically solving for such an equilibrium. On one hand, our model contains bottom-up model features, such as discontinuous step-wise supply functions and trade capacities giving rise to jumps in the trade function. If short run demand was constant and the supply from intertemporal optimizing firms linear in prices, this setup could be formulated as a linear programming problem.[65] On the other hand, our model also includes smooth demand and supply components that are best suited to solve with a gradient-based solver. In the following we propose two different solutions: One that is suitable in a partial equilibrium model and a second that can be integrated directly into a larger CGE. Along the way we use the small scale 'toy model', to illustrate both how the solution methods work, and how the solutions are different. To simplify notation slightly, we present the equilibrium concepts and solutions for a single state h. As noted in sections 4 and 5, demand and supply in one state (h) depends on the entire path of equilibrium prices throughout a year; thus a full characterization of equilibrium contains clearing of markets in all h states.

8.1 An Equilibrium Concept of Trade Partitions

The first solution method we present here builds an iterative procedure of searching over possible trade partitions as defined in definition 1, for an allocation that is feasible and minimizes system costs. Before we present the algorithm, we define a couple of useful concepts.

8.1.1 Equilibrium concepts in the very short run

Definition 2. *The friction-less equilibrium consists of an equilibrium price on electricity denoted p_E^*, a set of regional equilibrium heating prices $\left\{p_{g_H}^*\right\}_{g_H \in \mathcal{G}_H}$ and a feasible set of net export flows $\left\{NX_{g_i,g_j}\right\}_{(g_i,g_j)\in \mathcal{G}_E^2}$ such that:*

[64] This is furthermore the case for electrical heaters and heat pumps that produce heat using electricity, when the relative price on heat compared to electricity are sufficiently large.

[65] This is essentially how (at least some of the) models of the energy system solve for an equilibrium, e.g. Ramses and Balmorel (Danish Energy Agency (2018a), EA (2018))

i. Total demand and supply for electricity across all countries $g_E \in \mathcal{G}_E$ are equalized:

$$\sum_{g_E \in \mathcal{G}_E} e_{(t,h,g_E)}\left(p_E^*,\ p_{g_E,t}\right) = \sum_{g_E \in \mathcal{G}_E} \sum_{i \in \mathcal{I}_{g_E}} E_i(p_E^*, p_{g_H}^*) \tag{25}$$

ii. Regional heat demand and supply are equalized. For all $g_H \in \mathcal{G}_H$:

$$h_{(t,h,g_H)}\left(p_{g_H}^*,\ p_{g_H,t}\right) = \sum_{i \in \mathcal{I}_{g_H}} H_i\left(p_E^*, p_{g_H}^*\right). \tag{26}$$

iii. The set of net exports is defined by the identity for each $g_i \in \mathcal{G}_E$:

$$e_{(t,h,g_E)}\left(p_E^*,\ p_{g_E,t}^E\right) + \sum_{g_j \in (\mathcal{G}_E \setminus g_i)} NX_{g_i,g_j} = \sum_{i \in \mathcal{I}_{g_i}} E_i\left(p_E^*, p_{g_H}^*\right), \tag{27}$$

such that trade capacities are satisfied:

$$NX_{g_i,g_j} \leq T_{g_i,g_j}, \qquad \forall (g_i, g_j) \in (\mathcal{G}_E \times \mathcal{G}_E). \tag{28}$$

iv. The equilibrium prices are lower than the unit costs of the energy deficit plants (EDF) $\bar{c}$:

$$\max\left(p_E^*,\ \left\{p_{g_H}^*\right\}_{g_H \in \mathcal{G}_H}\right) < \bar{c}. \tag{29}$$

Without any trade costs or transmission capacity constraints for electricity, the resulting equilibrium price p_E^* along with the regional heat prices $p_{g_H}^*$ balances total demand and supply. In our setup there are two reasons why this might not be the equilibrium outcome. Firstly, trade capacities can prohibit the implementation, if there is no set of net export flows that ensures this allocation, such that (28) holds. Secondly, if (29) does not hold, inelastic short run demand cannot be met by supply and we are in fact in a disequilibrium.

If we cannot implement the friction-less equilibrium, there must be areas with different equilibrium prices. If prices are higher in one area g_j, plants in g_i have an incentive to export to g_j instead of selling domestically. This scenario can only be an equilibrium outcome, if exports are already at full capacity, i.e. if $NX_{g_i,g_j} = T_{g_i,g_j}$. Note furthermore that this has to hold for all trading partners: If there is a third geographic area g_k that can import from area g_i and then export to g_j, there is no argument for g_j and g_i having different prices. Thus solving for the outcome in the general case entails forming a trade partition of $\mathcal{G}_E$, where the outcome *within* subsets is the friction-less equilibrium, but trade *between* subsets are at full capacities.

Next, we consider what happens in cases where demand cannot be satisfied by supply (29 is violated). The characterization of what happens in this case is not straightforward. In a Danish context these scenarios are handled as so-called *brown-outs* by the relevant Transmission System Operator (TSO). In

anticipation of a power shortage the TSO decouples a share of the demand to ensure that an equilibrium is always satisfied. Without explicitly modelling a TSO firm, we attempt to capture such a scenario in the brown-out equilibrium (BOE):

Definition 3. *A brown-out (dis)equilibrium is defined for a subset of countries $\mathcal{G}_i$ as an electricity price, a set of regional heating prices, a subset of countries in equilibrium $\mathcal{G}_{Equi}$ and a brown-out percentage $\{\mathcal{O}_{g_E}\}_{g_E \notin \mathcal{G}_{Equi}}$ where:*

i. Inelastic demand cannot be satisfied by supply in the trade area $\mathcal{G}_i$ implying that (29) is violated.

ii. The electricity price is fixed at most costly technology in the trade area:

$$p_E^{AH} = \max_{c_i \in \mathcal{I}_g} (c_i) \,. \tag{30}$$

iii. Regional heating prices are defined as equilibrium prices:[66]

$$h_{(t,h,g_H)}\left(p_{g_H}^{AH},\ p_{g_H,t}\right) = \sum_{i \in \mathcal{I}_{g_H}} H_i \left(p_E^{AH}, p_{g_H}^{AH}\right). \tag{31}$$

iv. The subset of countries in equilibrium $\mathcal{G}_{Equi}$ is defined by subsets where domestic production covers domestic demand:

$$\mathcal{G}_{Equi} = \left\{ g_E \in \mathcal{G}_i : \sum_{i \in \mathcal{I}_{g_E}} E_i \left(p_E^{AH}, p_{g_H}^{AH}\right) - e_{(t,h,g_E)}\left(p_E^{AH} p_{g_E,t}^{E}\right) \geq 0 \right\} \tag{32}$$

v. Trade is allocated in a way that reduces the percentage of power shortage in all countries equally. Thus for all countries not in $\mathcal{G}_{Equi}$ the power shortage is given by

$$\mathcal{O}_{g_E} = \left[e_{(t,h,g_E)}\left(p_E^{AH}, p_{g,t}^{E}\right) - \sum_{i \in \mathcal{I}_{g_E}} E_i \left(p_E^{AH}, p_{g_H}^{AH}\right) \right] (1 - tr_{reduc}) \tag{33}$$

where tr_{reduc} is the share of the shortage covered by trade, thus given by

$$tr_{reduc} \equiv - \frac{\sum_{g_E \in \mathcal{G}_{Equi}} \left(e_{(t,h,g_E)} \left(p_E^{AH}, p_{g_E,t}\right) - \sum_{i \in \mathcal{I}_{g_E}} E_i \left(p_E^{AH}, p_{g_H}^{AH}\right) \right)}{\sum_{g_E \notin \mathcal{G}_{Equi}} \left(e_{(t,h,g_E)} \left(p_E^{AH}, p_{g_E,t}^{E}\right) - \sum_{i \in \mathcal{I}_{g_E}} E_i \left(p_E^{AH}, p_{g_H}^{AH}\right) \right)}. \tag{34}$$

In the brown-out equilibrium countries where domestic supply and trade cannot cover demand, experience a percentage shortage (requirement *i.*). By fixing prices at the most costly technology operating in the market (requirement *ii.*), we mimic the scenario, where the last share of demand is decoupled from the market. As demand cannot be satisfied in this case, it is not straight forward to conclude which country should suffer the larger brown-out. Here we simply establish two principles: (1) Domestic

[66] If regional heating is not in equilibrium, prices are fixed at highest unit-cost as with electricity, and a share of demand for heat is simply not satisfied. The shortage of heat is straightforwardly calculated, as there is no trade.

demand is favored by the TSOs in an attempt to avoid a brown-out altogether and (2) countries that suffer larger brown outs, buy up more of surrounding countries' surplus production. The first principle is represented in requirement *iv.*, which states that if $g_E \in \mathcal{G}_{Equi}$, i.e. if domestic production at the price p_E^{AH} covers domestic demand, the area g_E does not experience a brown-out at all. The second principle is represented by requirement *v.*. If there is no trade with electricity, the power shortage corresponds to $\mathcal{O}_{g_E}$ with $tr_{reduc} = 0$. If there are countries with excess electricity, i.e. if $\mathcal{G}_{Equi} \neq \emptyset$, this excess electricity (numerator of (34)) is distributed amongst the countries that suffer a brown-out, in a way that is proportional to the magnitude of the respective country's power shortage.[67]

8.1.2 Solving for the short run equilibrium

In the terminology established here, we can think of an equilibrium in the very short run as the cost-minimizing and stable trade partition, where each subset of the partition constitutes either a friction-less or a brown-out equilibrium. Solving for a short run equilibrium then boils down to searching efficiently over feasible trade partitions for the cost-minimizing one.

Definition 4. *The equilibrium in the short run (SRE) is defined as electricity and heating prices, consumption, production, net export, shortage percentages and a trade partition* $\mathcal{G}_E = \left(\mathcal{G}_1, ..., \mathcal{G}_{n_g}\right)$ *where:*[68]

i. Each subset $\mathcal{G}_i$ *is either in a friction-less or brown-out equilibrium, as defined in definition 2 and 3. Prices, consumption, production, net export and shortage percentages are defined accordingly.*

ii. The trade partition is stable, as defined in definition 1.

The naive or 'simple' approach here is to check all feasible candidates of trade partitions. This becomes infeasible very fast though: With n countries there are $2k = 2\sum_{i=1}^{n} i$ potential trade capacity constraints that can bind. With h denoting the number of short run states, this essentially implies $(3^k * h!)$ potential equilibria. Even in the toy model described in section 7 with n=3 and h=4 this corresponds to 648 potential equilibria.[69] While this might be feasible to search over in the toy model, it is not so in models of larger scale. As an alternative to this search, we suggest a (in contrast to the 'simple' one) *complex* solution algorithm for finding the SRE. The main innovation in this algorithm is that we set up an *unconstrained shadow problem*, to determine which trade capacities are likely to bind. The unconstrained shadow problem is formally defined in appendix H in problem 2. The most important features of the problem (also shown formally in appendix H) is that (1) a unique solution always exists and (2) this solution both orders which trade capacities are more likely to bind, but also determine whether or not a constraint is likely to bind at all. As we explain further in the example below, this allows us to efficiently

[67] The numerator in (34) (including the −) sums over excess electricity from areas, where demand is covered by domestic production. The denominator sums the power shortages for all countries affected by the brown-out. Thus if the model is in a brown-out equilibrium and requirement *i.* holds, the reduction percentage tr_{reduc} is in $[0, 1)$ per construction.

[68] Albeit the formalization is slightly different, this is essentially, how bottom up models as Balmorel and RAMSES search for equilibria. With constant unit costs, perfectly inelastic demand and capacity constraints this can be achieved simply by solving a linear programming problem. The linear programming problems are outlined in the user guide for Balmorel: `http://ea-energianalyse.dk/papers/Balmorel_UserGuide.pdf` and the documentation for RAMSES: `https://ens.dk/sites/ens.dk/files/Analyser/ramsesr.pdf`.

[69] At n =5 this becomes 1,417,176 potential equilibria. At n=5 and h=20 this is $1.4*10^{23}$.

bind a lot of trade capacities simultaneously, thus significantly lowering the number of potential trade partitions/equilibria to search over. A rough outline of the *complex* algorithm is given in the following:[70]

i. Solve for friction-less or brown-out equilibrium, as defined in definition 2 and 3 for all subsets of the trade partition $\mathcal{G}_E^i$, disregarding trade capacity restrictions. Verify that the partition is stable according to definition 1.

ii. Check if the allocation is feasible by minimizing trade flows (linear programming problem). Exit if feasible.

iii. If the trade partition is not a feasible equilibrium, solve the unconstrained shadow-problem that indicates which capacity constraints are most likely to bind.

iv. Fix net exports at capacity in the order indicated by the shadow-problem, until it results in a new trade partition. Repeat i.-iv. until exit.

Compared to the simple solution algorithm, this approach searches over feasible trade partitions for the equilibrium outcome, by using a shadow problem that essentially penalizes trade, when it approaches capacity constraints. To illustrate how the complex algorithm works, we consider a simple simulation experiment in the toy model outlined in section 7. As the baseline scenario of the toy model involved no binding trade capacities, we add large positive and negative supply shocks to country 1 and 4 respectively in both period 1 and 4. The specific scenario is described in detail in appendix F.2.

Step *i.*: Compute the friction-less equilibrium prices using the initial trade partition:

$$(\mathcal{G}_E^0)_{h=1} = ... = (\mathcal{G}_E^0)_{h=4} = \{1, 2, 3\}.$$

Ignoring trade initially and simply summing electricity demand and supply in each area, we solve for one electricity price for all areas, for each h. Denote this price vector from the initial round $(p_E)^0$. The scenario is illustrated in figure 8.1. Part (a) illustrates that without any capacity restrictions on trade, prices are equalized across countries with slightly higher prices in $h = \{1, 4\}$ than in $h = \{2, 3\}$. Part (b) indicates that in order to implement this allocation, net export flows are particularly large from country 1 to 3 for $h = \{1, 4\}$.

Step *ii.*: We check whether the trade flows in part (b) of figure 8.1 can be implemented by solving a simple linear programming problem.[71] For $h = \{2, 3\}$ the allocation is feasible, but not for $h = \{1, 4\}$.

Step *iii.*: To identify which trade capacities are binding (for $h = \{1, 4\}$), we set up an unconstrained shadow problem that minimizes trade costs of achieving the net export flows necessary to implement the FLE allocation from step i. We essentially approximate the inequality constraints $NX \leq T$ with

[70] Appendix H provides more detail on each step of this approach.
[71] The linear programming problem is formally defined as problem 1 in appendix H.

Figure 8.1: A non-feasible friction-less equilibrium (FLE) scenario

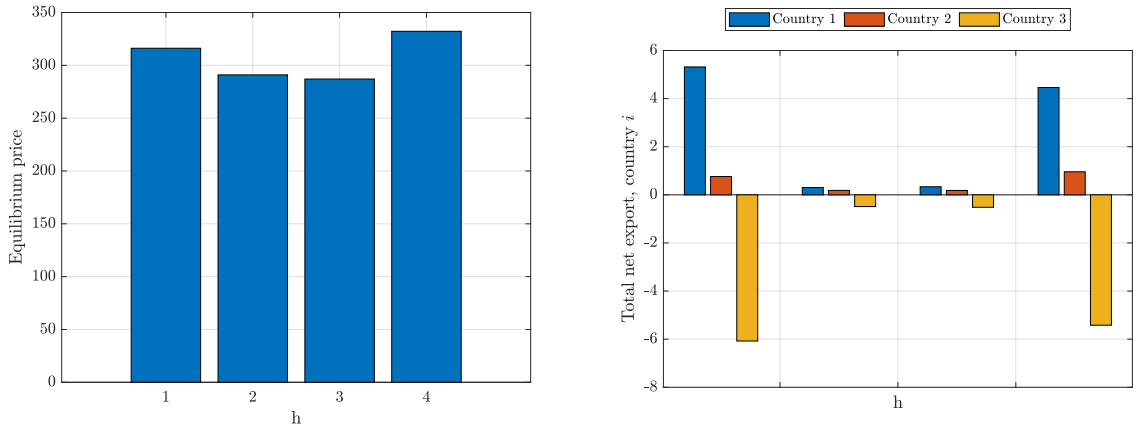

(a) FLE prices, $\mathcal{G}_E^0 = \{1, 2, 3\}$

(b) Domestic surplus function

a continuously differentiable trade cost function ($C(\cdot)$) that increases significantly around the capacity constraint T. The problem is formally defined in problem 2 in appendix H. The result is a marginal trade cost variable ($\mu_{i,j}$) for each trade capacity constraint. For $h = 1$ and $h = 4$ the ranking of these costs are the same:

$$|\mu_{1,3}| > |\mu_{1,2}| > |\mu_{2,3}|.$$

Step *iv.*: We use the marginal trade cost solution to guide which constraints are more likely to bind. We use the information in two steps here: Firstly, we bind all net export flows for which the marginal trade cost ($\mu_{i,j}$) exceeds a threshold $\bar{c}$. In the scenario carried out here we bind 3 constraints in this one step, namely:

$$(NX_{1,2})^{h=1} = T_{1,2}, \qquad (NX_{1,3})^{h=1} = T_{1,3}, \qquad (NX_{1,3})^{h=4} = T_{1,3}.$$

Secondly, we use that for step *i.* to yield a different result in the second round of the algorithms four steps, the imposed constraints must imply a new trade partition. For $h = 1$ the two binding capacities imply a new trade partition; country 1 now exports at full capacity to both country 2 and 3. Thus even if prices are higher in country 2 or 3, there would be no way for plants in country 1 to export anymore and equalize prices. For $h = 4$ the one binding constraint on $NX_{1,3} = T_{1,3}$ does not, however, imply a new trade partition. Before proceeding, we thus fix the net export terms with highest marginal trade costs, ($|\mu_{i,j}|$) aside from $|\mu_{1,3}|$. From the first round of the algorithms four steps we conclude by suggesting the new candidates:

$$(\mathcal{G}_E^1)_{h=1,4} = \Big\{ \{1\},\ \{2, 3\} \Big\}, \qquad (\mathcal{G}_E^1)_{h=2,3} = \{1, 2, 3\}.$$

We then repeat step *i.* computing the FLE for country 1, and another for countries $\{2, 3\}$. The suggested solution is now both feasible and we can confirm that the trade partition is stable (for both $h = 1, 4$) as

defined in definition 1. The solution is illustrated in figure 8.2.

Figure 8.2: Solution after first round of the complex algorithm

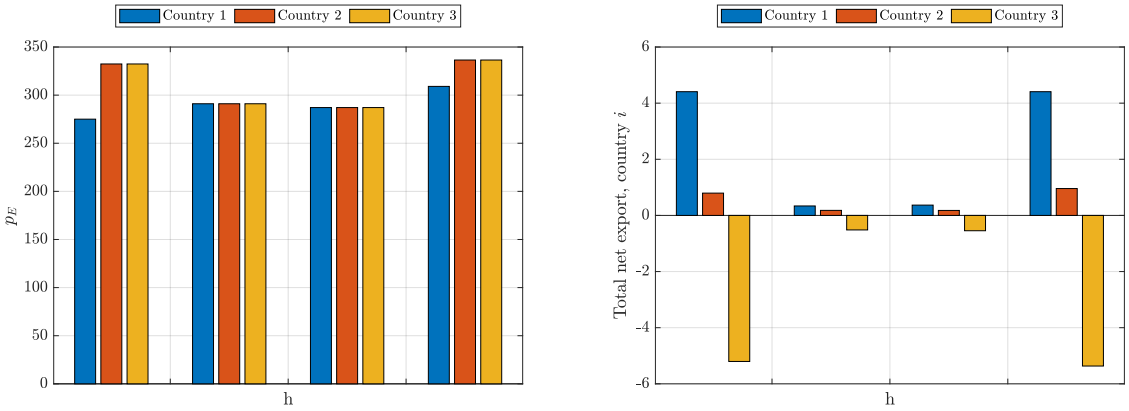

(a) Equilibrium prices

(b) Domestic surplus function

Albeit the explanation of the four steps involved in solving the model using the *complex* algorithm seems cumbersome, the computational costs of carrying these operations out are next to nothing: It only involves a handful of simple *if*-statements and a single (low dimensional) system of equations to be solved numerically. In a partial equilibrium model where the objective is to develop a bottom up module of the sector, this is our preferred solution method. It allows us to solve models that share the technical features of energy system models (non-differentiable supply, capacity constraints), but can also include features such as price-responsive demand and storage plants that maximize profits intertemporally. Furthermore, for all the simulation experiments we ran in the toy model, our algorithm found the solution after just one iteration. The partial equilibrium model here can further be linked to a computable general model. However, it cannot be integrated directly as a system of equations that can be solved simultaneously with a CGE model. For this purpose we develop an approximate equilibrium concept that can.

8.2 An Approximate Equilibrium Concept

The main computational issue of the short run equilibrium is the capacity constraints on trade. To circumvent the iterative procedure outlined above, where we search over feasible trade partitions (i.e. which constraints are binding), we propose two alternatives in this section that always ensure an interior solution in one shot: One approach that builds on including a marginal cost of trading, and a second more direct approximation approach. In doing so we drop the notion of trade partitions; instead we introduce individual country prices on electricity.

8.2.1 A marginal trade-cost function

The main idea of the trade-cost function is to approximate the capacity constraints on trade flows. In the short run equilibrium defined in definition 4 our solution corresponds to minimizing the trade costs,

given prices, where the cost of net exports between country i and j are given by

$$\tilde{C}_{i,j}(NX_{i,j}) = \begin{cases} \infty, & \text{if } NX_{i,j} > T_{i,j} \text{ or } NX_{i,j} < -T_{j,i} \\ 0, & \text{else} \end{cases}$$

To approximate this function we choose a function $C_{i,j}$, such that the marginal cost function is given by

$$\frac{\partial C_{k,j}}{\partial NX_{k,j}} = \begin{cases} \left[1 + \left(\frac{\theta(T_{k,j})}{NX_{k,j}}\right)^{\frac{\sigma-1}{\sigma}}\right]^{1/(1-\sigma)} - 1, & \text{for } NX_{k,j} > 0 \\ -\left[1 + \left(\frac{\theta(T_{j,k})}{-NX_{k,j}}\right)^{\frac{\sigma-1}{\sigma}}\right]^{1/(1-\sigma)} + 1, & \text{for } NX_{k,j} \leq 0 \end{cases}, \qquad \sigma \in (0, 1/2) \tag{35}$$

Appendix H shows that this function is continuously differentiable and overall invertible except at $NX = 0$. Here we calibrate the functions

$$\theta(T_{k,j}) = T_{k,j}\left(\bar{c}^{1-\sigma} - 1\right)^{\frac{\sigma}{\sigma-1}},$$

such that the marginal cost of trading reaches $\bar{c}$ exactly at the trade capacities $T_{k,j}$. Recall that each country's supply curve includes an *energy deficit plant* that automatically kicks in around $\bar{c}$. This ensures that the equilibrium outcome will never feature trading patterns that violate the capacity constraints. Moreover, we can adjust the degree of smoothness by appropriately changing σ: When σ approaches zero $C_{i,j}$ approaches the bottom up version $\tilde{C}_{i,j}$. Figure 8.3 illustrates how a change in σ alters the shape of the marginal trade cost function.

Figure 8.3: The marginal trade-cost function $\partial C/\partial NX$

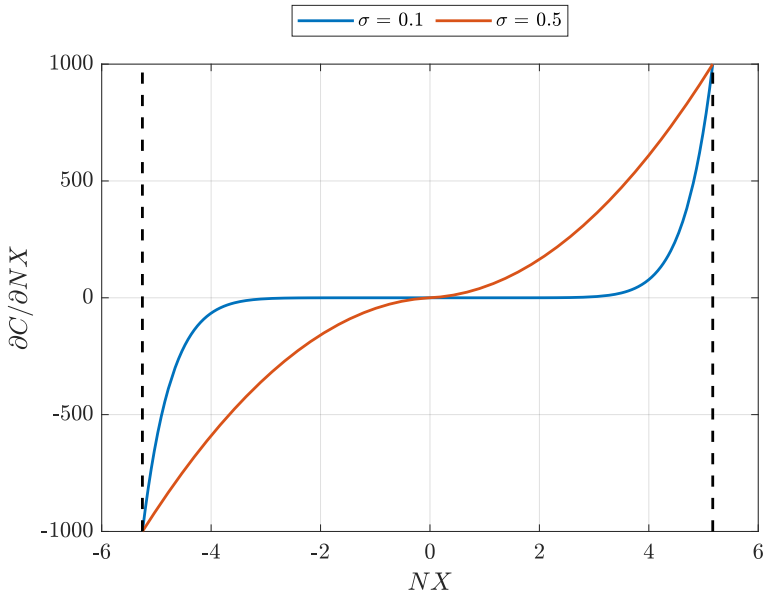

Definition 5. *The approximate equilibrium is defined for a subset $\mathcal{G}_E$ of n countries partitioned into $\mathcal{G}_H$ regional heating areas as: A set of electricity prices, regional heating prices, net export flows and shortage*

percentages $\mathcal{O}_{g_E}$ such that:

i. Total demand and supply for electricity across all countries $g_E \in \mathcal{G}_E$ are equalized:

$$\sum_{g_E \in \mathcal{G}_E} e_{(t,h,g_E)}\big(p_{g_E},\ p_{g_E,t}\big) = \sum_{g_E \in \mathcal{G}_E} \sum_{i \in \mathcal{I}_{g_E}} E_i\left(p_{g_E}, p_{g_H}\right). \tag{36}$$

ii. Regional heat demand and supply are equalized. For all $g_H \in \mathcal{G}_H$:

$$h_{(t,h,g_H)}\big(p_{g_H},\ p_{g_H,t}\big) = \sum_{i \in \mathcal{I}_{g_H}} H_i\left(p_{g_E}, p_{g_H}\right). \tag{37}$$

iii. Net export flows are determined by minimizing trade costs

$$\mathbf{NX}^* \equiv \begin{pmatrix} NX_{1,2} \\ \vdots \\ NX_{n-1,n} \end{pmatrix} = \operatorname{argmin} \sum_{k=1}^{n-1} \sum_{j=k+1}^{n} C_{k,j}\left(NX_{k,j}\right), \tag{38}$$

subject to country-specific equilibrium constraints

$$e_{(t,h,g_j)}\big(p_{g_j},\ p_{g_j,t}\big) + \sum_{g_k \in (\mathcal{G}_E \setminus g_j)} NX_{g_j,g_k} = \sum_{i \in \mathcal{I}_{g_j}} E_j\left(p_{g_j}, p_{g_H}\right), \qquad \forall g_j \in \mathcal{G}_E. \tag{39}$$

iv. Electricity prices differ by exactly the marginal trade costs, for each $g_i \in \mathcal{G}_E$:

$$p_{g_i} = p_{g_j} - \frac{\partial C_{i,j}}{\partial NX_{i,j}}. \tag{40}$$

v. All supply coming from the energy deficit plant ($\bar{E}$) represents power shortage, such that shortage percentages $\mathcal{O}_{g_E}$ are defined for each $g_E \in \mathcal{G}_E$ by

$$\mathcal{O}_{g_E} = \frac{\bar{E}_{g_E}(p_{g_E})}{e_{(t,h,g_E)}\big(p_{g_E},\ p_{g_E,t}\big)}. \tag{41}$$

Appendix H shows that given prices, the problem of minimizing trade costs is well-defined, such that first order conditions are necessary and sufficient. Thus we can present net exports by a simple block of equations that can be immediately included in a larger system of equations (CGE model). Secondly, we show that the pricing rule in (40) is unique, in the respect that comparing g_i with any other area g_j, yields the same price level p_i, when net exports are chosen according to (38). Furthermore, we show that there exists a unique injective mapping $\mathbf{f}^p : \mathbb{R}^n \mapsto \mathbb{R}^k$ from the vector of prices $\bar{p}_E$ to the vector of net export terms $\mathbf{NX}$, such that trade costs are minimized. This mapping has a simple analytical form

$$\mathbf{NX} = (\partial \mathbf{C})^{-1}\left(A \times (p_n - \tilde{p}_E)\right), \qquad \tilde{p}_E \equiv \begin{pmatrix} p_1 & \cdots & p_{n-1} \end{pmatrix}', \tag{42}$$

where $(\partial \mathbf{C})^{-1}(\cdot)$ denotes the inverse marginal trade cost function, defined by inverting (35) applied

element-wise on its arguments, and A is a coefficient matrix of size $(k \times (n-1))$.

To illustrate how trading of electricity depends on prices, consider the simple setup of the toy model from section 7. In this three country setup country 1 can import/export up to around 1.3 TWh with country 2, and around 3.1 TWh with country 3. Figure 8.4 illustrates how total net exports from country 1 depends on prices. The figure illustrates that around the thresholds $p_1 = p_2$ and $p_1 = p_3$ there are large drops in the net export, roughly corresponding to $T_{1,j} + T_{j,1}$. These drops mark the thresholds for when the country goes from exporting to importing from country j.

Figure 8.4: Illustrating the trade function

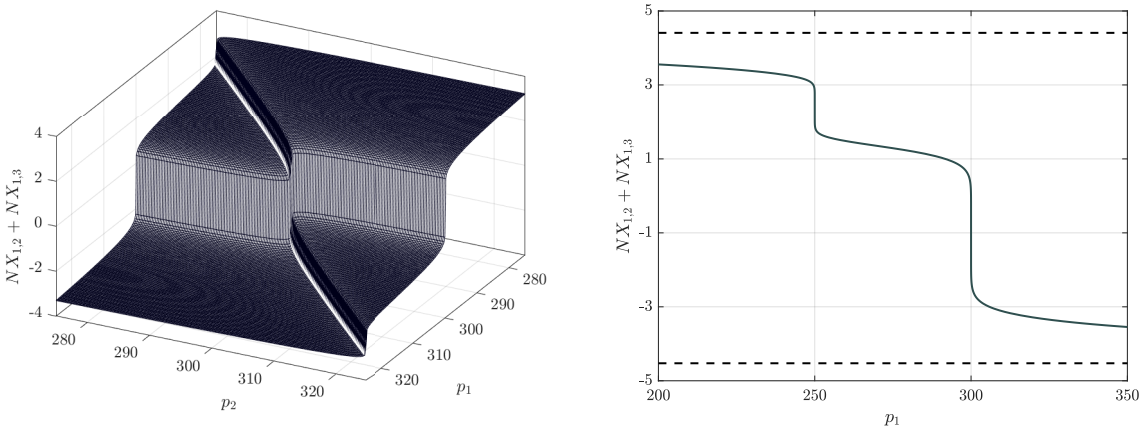

(a) Trade function with $p_3 = 300$, $\sigma = 0.1$. p_1, p_2 exogenously varied between $[200, 350]$.

(b) Trade function with $p_2 = 250$ and $p_3 = 300$. (- -) indicates sum of trade capacities.

One downside to this approach is that the trade function has quite 'heavy tails'. Part (a) of figure 8.4 shows that with a smoothing parameter of around $\sigma = 0.1$, the trade function is very close to the non-differentiable case around the two thresholds; thus the scope of lowering σ further is small. Part (b) however shows that with price differences of around 50 DKK, trade capacities are still not fully utilized. Recognizing this issue of heavy tails in our approximation, we propose a second approximation approach.

8.2.2 A direct approximation of net exports

Instead of approximating trade by including a trade-cost component, we can instead turn directly to the net export functions illustrated in figure 8.4. In the limit when $\sigma \to 0$ we obtain the bottom up net export function:

$$NX_{i,j} = \begin{cases} T_{i,j}, & p_i \leq p_j, \\ -T_{j,i}, & p_j \leq p_i \end{cases} \tag{43}$$

As presented in section 4 on the short run supply, we can approximate this jump function using our normal smoothing function with a few modifications. As we do not (necessarily) have symmetry in our trade function, i.e. $T_{i,j} \neq T_{j,i}$, we include a centering term $\tilde{g}_{i,j}$ that ensures that net exports are zero

when $p_i = p_j$:

$$NX_{i,j} \approx -T_{j,i} + \left(T_{i,j} + T_{j,i}\right) \Phi\left(\frac{p_j - p_i + \tilde{g}_{i,j}}{\sigma}\right), \qquad \tilde{g}_{i,j} \equiv \Phi^{-1}\left(\frac{T_{j,i}}{T_{i,j} + T_{j,i}}\right) \sigma. \tag{44}$$

$\Phi(\cdot)$ denotes the standard normal cumulative density. We note that $\sigma \to 0$ implies the version in (43). To illustrate the difference when using the normal smoother, figure 8.5 replicates the scenario in figure 8.4 with the centered normal smoother. Compared to the trade cost approach outlined above, countries can fully utilize the capacities within reasonable price differentials, while keeping the function relatively smooth around the approximated jumps. The rest of the equilibrium conditions in definition 5 stay the same.

Figure 8.5: Centered normal smoother of trade function

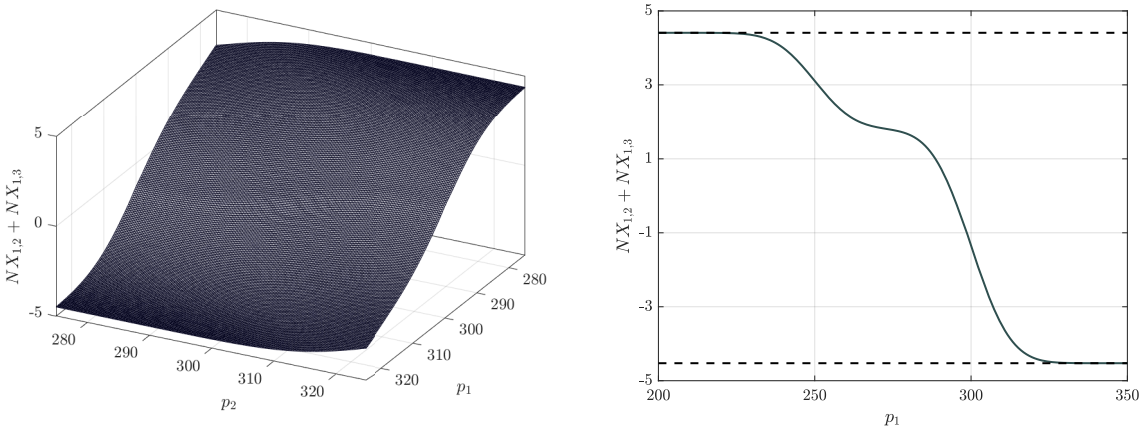

(a) Trade function with $p_3 = 300$, $\sigma = 10$. p_1, p_2 exogenously varied between $[200, 350]$.

(b) Trade function with $p_2 = 250$ and $p_3 = 300$. (- -) indicates sum of trade capacities.

8.2.3 Trade costs or direct approximation?

The figures 8.4-8.5 suggest that the approximation using a centered normal smoother, performs better when net exports are near capacity constraints. To test this assumption, we run a simple experiment in the toy model outlined in section 7. All three solutions have been implemented in this small scale model: (1) The *complex* bottom up algorithm outlined in section 8.1.2 that can deal with discontinuities in the trade function, (2) the approximate equilibrium with trade costs as in equation (42), and (3) the approximate equilibrium with the centered normal smoothing trade function in equation (44). We use the results from the bottom up algorithm as the true outcome, to which we compare the simulations from the two versions of the approximate equilibrium.

We initially consider the *baseline* scenario in the toy model outlined in section 7. We choose smoothing parameter values in the two versions of the approximate equilibrium, such that the solution time for the two methods are similar in this baseline. In one of the short run states ($h = 1$), we simulate the result of a series of supply shocks of varying magnitudes. Specifically, we let ϵ be a multiplicative shock to the capacity of all plants. In order to incentivize trade, we let country 1 be hit by a positive supply shock of

size $\epsilon > 1$ and country 3 by a proportionally negative shock ($1/\epsilon$). Appendix F outlines the exact setup for the baseline scenario, and how the supply shocks are implemented.

Figure 8.6: Comparing solvers with varying supply shocks

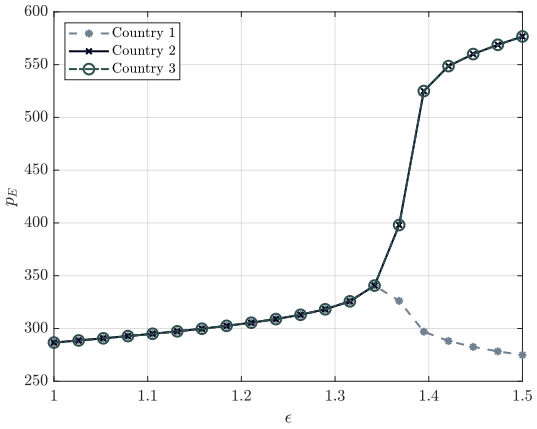

(a) Equilibrium prices in bottom up solution

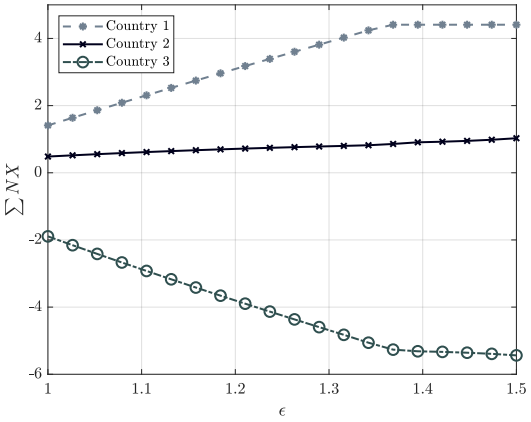

(b) Total net exports in bottom up solution

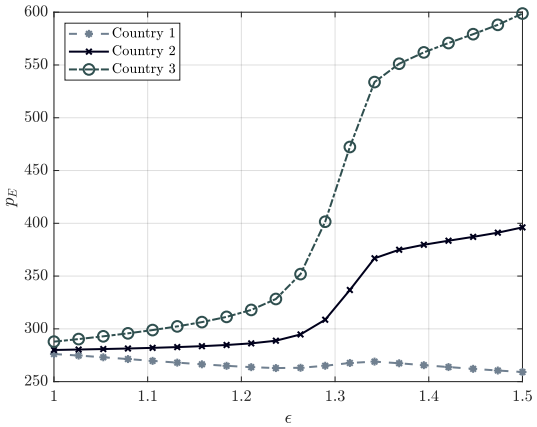

(c) Equilibrium prices in approximate equilibrium

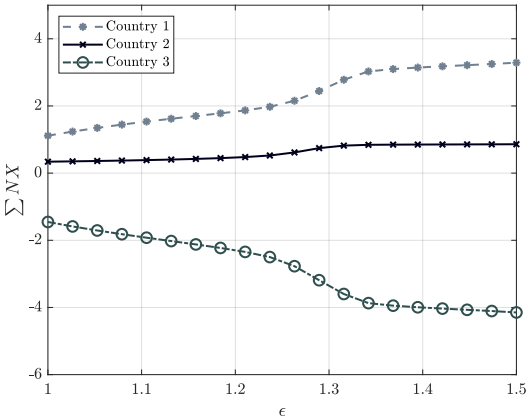

(d) Total net exports in approximate equilibrium

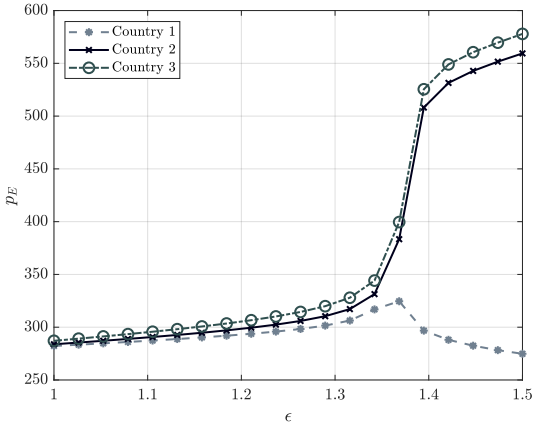

(e) Equilibrium prices in approximate equilibrium with centered normal smoother

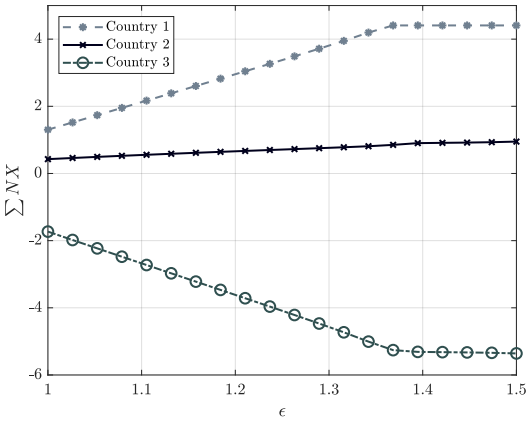

(f) Total net exports in approximate equilibrium with centered normal smoother

Figure 8.6 illustrates the equilibrium prices and total net exports for the three solvers. The bottom

up solution using the 'complex' algorithm shows that as supply shocks increase in magnitude (positive for country 1, negative for country 3), prices increase slightly for all countries initially. When the trade capacity is met for country 1 around $\epsilon = 1.34$, prices fall in country 1, whereas the two other countries experience large increases in prices, as there is no longer any offsetting effect from the cheaper supply of country 1. Interestingly, country 2, which is not affected directly by the supply shocks, follow the price path of country 3 completely. This is due to the relative size of trade capacities between countries 1-2 (which is around only 1.3) and countries 2-3 (which is around 2.5). In particular, this last feature, the price path of country 2, is far better approximated by the centered normal smoothing trade function illustrated in part (e)-(f) of figure 8.6. Thus we conclude that - at least in our application - the centered normal smoothing trade function seems preferable to the trade cost approach.

Part III

Aggregation, Calibration and Validation of Bottom Up Module

In the most dis-aggregated version, the BU module described above includes 15 countries, 34 heating areas, 8760 hours of the year, and several thousand individual plants.[72] When we include the intertemporal supply decision of storage plants and demand decision of flexible consumers, the highly non-linear trade functions and the interaction between electricity and heat supply decisions of CHP plants, all of the $(15 \times 34 \times 8760)$ states - in which we need to find an equilibrium - become interdependent. While we may be able to solve this in a partial equilibrium model, this is far too large a model to work with in a structural estimation, or as a module in a general equilibrium model. As we aim to do both, we have to reduce the dimensionality of this model considerably.

To do this we focus mainly on aggregating the 8760 hours of the year into fewer representative states. This is standard in models of the energy system; in Ramses neighbouring hours are summed (Danish Energy Agency, 2018a), while in TIMES-DK the model runs through 32 time slices representing grouping of hours deemed relevant for the electricity system (Balyk et al., 2019).[73] In the following we present an alternative way of performing this aggregation of hourly data into k states. The main challenge of choosing the right number of states (k) is to weigh the need for computational speed (low k) against capturing the most essential hourly variation in productivity, demand, prices etc. (high k). A first natural step in this direction is to check whether data on this variation, informs us directly on the appropriate number of states. This is done using the K-means approach described in section 9.1. We find that 2800 is the maximum number of states need to describe exogenous hourly variation.

Our further strategy to determine the appropriate number of states (k) in our BU module, is related to our method of integrating it into a CGE model. For a given number of states (k), we require that our model can replicate a number of facts. Data from the yearly Energy Statistics published by the (Danish Energy Agency, 2017a) inform us on a number of statistical targets the BU module has to fit. This includes the use of various fuel inputs, the yearly level of domestic production and trade, as well as average prices on electricity and heating. This is done in section 10.

In a final *validation* step we investigate, whether we can reduce the dimensionality even further. The idea of this step is that the K-means approach informs us on which 8760 hours of the year are similar enough to considered roughly the same. However, this is measured only on the basis of exogenous variation, whereas the relevant criterium should be *equilibrium outcomes* of the model. In other words, the number of states (k) can be reduced as long as the equilibrium outcome of the model, does not change

[72] Although we have information on 22 countries we do not have detailed technical data on the last 7 of them.

[73] Our baseline model will furthermore decrease the number of countries to 8 as it seems to capture the dynamics most relevant for Denmark. Furthermore, we experiment with lowering the number of heating areas to as much as 2, but keep the possibility of increasing this to the full 34.

significantly. In section 11 four counterfactual scenarios are run for varying levels of k. The counterfactual scenarios include policy-induced shocks to intermittency, demand flexibility, energy storage, and trade. In each of the four scenarios we record and compare a number of marginal effects, e.g. the average consumer price level, fuel consumption, emissions, average prices received by intermittent technologies etc.. In essence, we then choose the minimum k, where the marginal effects of the shocks are similar (at least in qualitative terms) to the most dis-aggregated version. Unfortunately, we are only able to calibrate models with $k \leq 168$ states, implying that this our most disaggregated version in this paper. In future work we expect it to be very likely to calibrate the model with $\bar{k} = 2800$ as well, which would provide a much better benchmark model for comparing more aggregated models with.[74]

Finally, in this part we do not work with the most general settings. In particular, we choose to work with 8 of the 15 electricity areas covered in our data. These include the Scandinavian countries (5), Germany, Austria and Luxembourg (1), as well as Great Britain (1) and The Netherlands (1). This is done to focus on the case of Denmark: We include current neighbouring countries, as well as countries with whom transmission lines are already planned. Furthermore, we aggregate all heating areas in DK-west and DK-east, thus going from 34 to 2 heating areas. At the moment we have not formally tested these simplifications. We justify them only on the grounds of simplification. None of the methods presented below are affected by this simplification though.

9 Aggregation of Model

Following Reguant (2019) we reduce the dimensionality of the bottom-up data using K-means clustering. K-means is an unsupervised algorithm that does not require a response variable, making it ideal for clustering the bottom-up data. Furthermore, it does not rely on clustering hours within the year chronologically, implying the dimensionality of the BU-model can potentially be significantly reduced. The non-chronological clustering is essential because most of the intra-year variation is cyclical; that is, January resembles December, Monday resembles Monday, and so forth. Compared to Reguant (2019), however, our BU-model contains plants with storage capacity that optimise inter-temporally. The first-order linear difference equations describing storage firms' behaviour assume time is linear and chronological; an assumption that the K-means clustering is likely to violate. To take this into account we develop a novel aggregation method for storage technologies in section 9.3.

9.1 The K-means algorithm

As outlined in section 4 the BU module includes a number of exogenous variables that vary in the hourly data. In particular, the set of hourly variation ($\mathcal{V}$) contains more than 50 different categories (see appendix A), where each category contains a distinct exogenous variation pattern. As an example

[74] Note, we can easily solve the model with $\bar{k} = 2800$. Calibrating it, however, is a much more high-dimensional problem. We are running the calibration on a standard Dell laptop with an Intel i7 CPU with 2.90 GHz and 16 GB RAM. The main constraint here is RAMs. We are currently working on calibrating the BU module on the internal servers of the Department of Economics (UCPH) where there is basically no RAM limitation for our purposes.

there are currently 11 different Danish off-shore wind variation patterns included in the set $\mathcal{V}$. In our application of the K-means algorithm we reduce this dimensionality significantly.

Firstly, we only use eight electricity areas and not all 15. Secondly, we only compute one exogenous residual load function (demand minus intermittent production) for foreign areas. The residual load function is sufficient, when assessing how equilibrium prices are formed. In doing so we lose some accuracy in assessing the average prices received by different foreign intermittent type of plants. However, as investments in foreign plants are exogenously given in our model, we do not consider this detrimental to the choice of aggregation.[75] We do not, however, sum variation in *domestic* demand and intermittent production into one residual load function, because we need technology-specific prices in order to model investment behavior in Danish plants. To realistically capture the capacity expansion of existing technologies and the market penetration rate of new technologies we need to be able to assess the profitability of specific domestic technologies. For instance, what is the profitability of investing in wind farms and biomass-fired plants?

Thirdly, we aggregate domestic productivity variations for intermittent technologies into fewer representative technologies. As an example, the set of variations ($\mathcal{V}$) includes one pattern of productivity for offshore wind farms at *Horns Rev 2* and another for the offshore wind farms at *Rødsand*. It is at the moment not the ambition, to model investments in 11 different offshore wind farm technologies. For this reason the 11 types of variations are aggregated into one *representative* technology representing Danish offshore wind farms.

Performing the the three steps outlined above, on the original set of hourly variation patterns in $\mathcal{V}$ (outlined in full in table 17, appendix A), the final set of exogenous variation used in the K-means algorithm ($\mathcal{W}$), is reduced from over 50 categories to the 17 categories given in table 8.

Table 8: Set of hourly variation patterns in K-means application, $\mathcal{W}$

Hourly variation set $\mathcal{W}$	Number or patterns
District Heating, demand	1
Electricity demand, DK	2
Residual load, foreign	6
Wind, DK	2
Solar (PV), DK	2
Solar heat, DK	2
Hydro inflow	2

The electricity demand in Danish areas are corrected for industrial surplus production (type EP), as there is no investment function related to industrial surplus of electricity. We only use 2 hydro inflow paths; one for Germany, Austria and Luxembourg, and another for Sweden, Norway and Finland. This follows the convention from Ramses. The hourly variations in wind production is a weighted average of the various types included in the set $\mathcal{V}$, see appendix A table 17 for the full list of sets in the original ste $\mathcal{V}$.

We collect the hourly variation for the 17 different types outlined in table 8 in the data matrix $\mathbf{x} = (x_1, ..., x_{8760})$. Here $x_i \in \mathbb{R}^{17}$ is a data vector that denotes the share of yearly production/demand/inflow

[75] When only using the residual load function for foreign areas, it means that the K-means algorithm sums over productivity from e.g. wind and solar power (of foreign plants). Thus, the K-means approach considers an hour with high wind and low PV productivity as the same as an hour with low wind and high PV productivity: As long as the sum of the two is roughly the same.

that occurs in hour i for the 17 different types. The K-means clustering algorithm partitions 8760 observations into k sets $\mathbf{S} = (S_1, ..., S_k)$, by minimizing the within cluster variation:

$$\mathbf{S} = \underset{\{S_i\}_{i=1}^{k}}{\operatorname{argmin}} \sum_{i=1}^{k} \sum_{x_j \in S_i} \|x_j - \mu_i\|^2, \tag{45}$$

where μ_i is the average of $x_j \in S_i$.[76] Note the objective in (45) is based on the euclidean distance, implying that K-means is sensitive to outliers.[77] We argue that this is a desirable feature in our setting, as intermittency is closely related to outliers: If a few hours within the year is associated with very low or high productivity, we need to capture these hours to realistically assess the cost of intermittency. If outliers are clustered with 'near outliers', we average out some of the very variation we attempt to capture.[78]

The result of the K-means algorithm is a mapping from the original 8760 hours into k new states. The majority of the bottom-up data is not affected by the K-means clustering. This includes technical parameters as efficiency, marginal costs in DKK/MWh etc.. Other variables, such as capacity variables in general, are clustered by summing over the relevant hours in each state k. Finally, it should be noted that the individual clusters (S_i) are sensitive to the initial random selection of cluster centers. We circumvent this problem by drawing initial random cluster centers 25 times for each value of k (Kassambara, 2017).

9.2 Identifying the maximum number of states within a year

As briefly outlined in the introduction to part III we initially use the K-means algorithm to decrease the number of states while preserving the relevant intra-year exogenous variation in the data. A drawback of the K-means algorithm is that the numbers of clusters k is set a priori. Unfortunately, there are no formal test to determine the 'optimal' number clusters needed to represent the full data ($\bar{k}$). Instead we resort to two informal tests: The Elbow Method and the Average Silhouette Method (Kassambara, 2017).

Recall from equation (45) in section 9.1 that the objective of the K-means algorithm is to minimise the total within cluster variation. The Elbow method is based on a simple visual inspection of how the total within-cluster variation changes, when we exogenously change k. The informal test is straightforward: If this plot features a sharp increase in the within cluster variation when decreasing k, we should not lower k further. Part (a) of figure 9.1 illustrates the relevant plot for our data. While it does provide some information on the relation between the number of clusters, and how well we fit the data, this does not provide us with a clear guideline for $\bar{k}$: As k is lowered towards 0, the within cluster variation seems to somewhat smoothly increase.

[76] The method can easily weigh the various variation patterns in x_i differently; i.e. we can emphasize the variation pattern in domestic areas, and lower the importance of technology types that are *a priori* not expected to be essential.

[77] K-means will tend to allocate these "outlier" hours into a separate cluster.

[78] For instance, we found that using the K-mediods algorithm, also known as partitioning around mediods (PAM), tend to cluster outlier hours characterised by intermittency with more 'normal' hours. This is not the case for the K-means algorithm although some averaging of hours is bound to take place.

The Average Silhouette Method is based on the silhouette value, which is a measure of how similar an hour is to its own cluster, relative to other clusters. For each hour h in cluster S_i define the average (euclidean) distance between h and any other hour in the same cluster, h_{-1}, as

$$d(h) = \frac{1}{|S_i| - 1} \sum_{h_{-1} \in S_i,\ h \neq h_{-1}} \|x_h - x_{h_{-1}}\|^2, \tag{46}$$

where $|S_i| - 1$ is the number of hours in state i, not counting the given state h. Then $d(h)$ is a measure of how well hour h is assigned to cluster S_i. Furthermore, define $n(h)$ as the smallest average distance of hour h to all points in any other cluster that h is not a member of:

$$n(h) = \min_{h \neq h_{-1}} \frac{1}{|S_j|} \sum_{h_{-1} \in S_j} \|x_h - x_{h_{-1}}\|^2. \tag{47}$$

Here the sum measures the average dissimilarity between h (belonging to state i) and the hours in state j. $n(h)$ thus measures the average distance between h and the second-best cluster available. The silhouette *value* is then defined as

$$s(h) = \begin{cases} \frac{n(h) - d(h)}{\max\{n(h), d(h)\}}, & |S_i| > 1, \\ 0, & |S_i| = 1, \end{cases} \tag{48}$$

Note here that $s(h) = 0$ for states with only one hour in it, whereas the variable in general can attain values in the range of [-1,1]. A high value indicates a good fit, while a negative value indicates that the hour resembles the hours of a different cluster better, than the one it is assigned to by the K-means algorithm. By assigning $s(h) = 0$ for states with only one hour in it, the method essentially penalizes values of k, where hours are not clustered. The average silhouette value is then simply given by

$$\bar{s(h)} = 1/H \sum_h s(h) \tag{49}$$

Finally the average silhouette method prescribes that the optimal number of clusters, $\bar{k}$, is given by the number of cluster that maximises the average silhouette:

$$\bar{k} = \underset{k \in \mathcal{K}}{\operatorname{argmin}}\, \bar{s(h)}, \qquad \mathcal{K} = \left\{ k \in \mathbb{N}_{++} \mid k \leq 8760 \right\} \tag{50}$$

As k is defined for positive natural numbers, we simply solve this using a coarse grid search. Compared to the Elbow method, this provides a more unique recommendation of $\bar{k} = 2800$, as illustrated in part (b) of figure 9.1. We also assessed the fit of $k = 2800$ manually and find that it seems to represent the full hourly data satisfactory.[79] Compared to part (a), illustrating the Elbow Method, 2800 states seems rather large where the sharpest bend occur for k <1000.

As these tests are informal, we use the results from this inspection with caution. The number $\bar{k}$=2800

[79] In appendix I we plot the clustered value x_{k_i} for $i \in S_i$ against the true, hourly value, x_h, for each variable x. If the clusters are appropriate, observations should be closely centered around the diagonal. This seems to be the case for all exogenous variables.

(a) The elbow method.

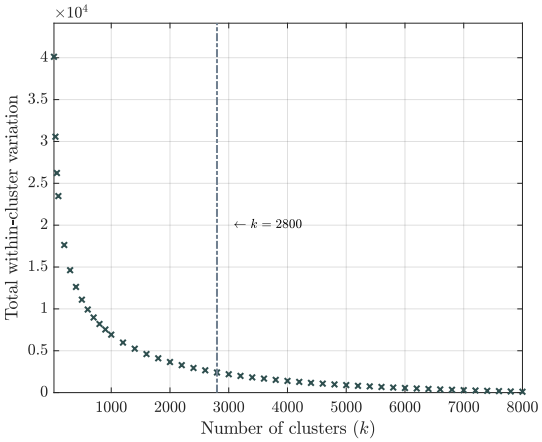

(b) The average silhouette method.

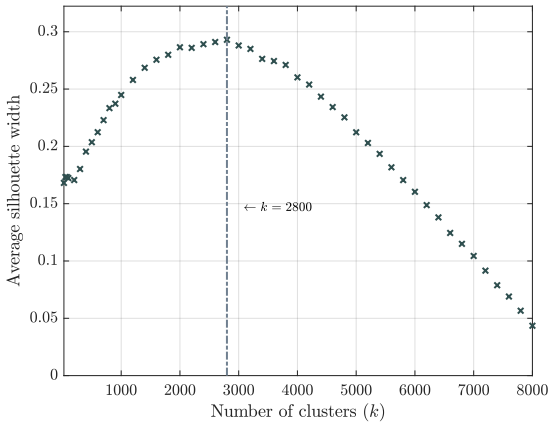

Note: According to the elbow method the optimal value of clusters is given by the location of a bend. The average silhouette method states that the optimal number of clusters is given by the value maximising the average silhouette.

Figure 9.1: The determination of the maximum number of clusters, $\bar{k}$.

should only be used as the maximum number of hours, for which we should calibrate and run the BU model. In the end it does not matter, how large the within cluster variation is, for exogenous variation patterns. It is the marginal effects of shocks to the calibrated model that needs to be realistic. We return to this issue later.

As mentioned in the beginning of part III, we are only able to calibrate models with $k \leq$168 clusters, implying that this our most disaggregate version in this paper. In future work, however, we expect it to be very likely to calibrate the model with $\bar{k}$ =2800. For this reasons, the suggested approach above is included in the paper, although it is not put to use at the moment.

9.3 Aggregation of supply from storage firms

For the most part, the model solution is straightforwardly altered to the aggregated version with k clusters: Quantities are generally *summed* into new states, whereas price and cost variables are *averaged*. For instance, if state k contains 2 hours the capacity of a plant in state k is given by the sum of capacity from the 2 hours, whereas the marginal cost of production in state k is the same as in the two hours. For plants without storage capacity, each k state is independent, as for the case with the 8760 hours, and thus their supply functions remain the same. For storage firms that optimize intertemporally, this is not the case.

Recall from section 4.3 that the solution to a storage plant's maximization problem depends on the entire year's path of equilibrium prices. In the K-means aggregation scheme hours that are similar in terms of productivity and demand are clustered. However, the aggregation does not take into account, how endogenous storage behavior might differ between otherwise similar hours within an aggregate k_i state. Furthermore, the aggregation into states does not preserve the chronology of hours. In the following, we propose a number of ways to deal with this.

9.3.1 Folding all 8760 hours into k states

Consider a state h in the hourly model. Let k_h denote the state that hour h is a subset of. Let $f_h = \{f_{-h}, f_{+h}\}$ denote the history of preceding states (f_{-h}) and future path of states (f_{+h}). Following the outline for storage firms in section 4.3, the supply in hour h from a storage plant is then given by:

$$E_h = \underline{E} + (Y_h - \underline{E})\Phi\left(\frac{p_h - c - a\theta_{f_h}}{\sigma}\right) + \left(\bar{E} - Y_h\right)\Phi\left(\frac{p_h - c - \theta_{f_h}}{\sigma}\right).$$

In particular, the continuation value θ_{f_h} depends implicitly on the entire history of states. The simplest (but computationally most costly) way to aggregate this into the k states is to solve for a value E_h for all hours and then sum into the k states. In other words simply compute

$$E_{k_i} = \sum_{h \in S_i} E_h.$$

This, however, would require solving the intertemporal storage problem described in section 4.3 for all 8760 hours, for all storage plants in our data. Albeit storage plants are important, given they mitigate the effects of intermittency, we offer below an alternative aggregation method that lowers the computational cost.

9.3.2 A state-average aggregation

Consider a plant in a particular state k_i. To plan production optimally over time, it needs information on both the previous state (stored energy going into the state) as well as the entire future path of prices to determine the continuation value θ_{k_i}. However, because hours are disorderly clustered within states, it can both arrive in state k_i from multiple states and likewise transition into multiple states - even state k_i itself. We can describe these transition dynamics by transition matrices. Let $\mathbf{P}$ be the $(k+1 \times k+1)$ matrix of forward-looking transition probabilities. The last column and row $(k+1)$ represents the terminal state of the model. Element (i,j) of the matrix identifies the probability that state i transitions to state j. Similarly, we define the backwards looking transition matrix $\mathbf{P}_{-1}$. Here element (i,j) identifies the probability of state j transitioning to state i. Without clustering the hours into smaller states, i.e.

k =8760, the transition matrices are given by:

$$\mathbf{P} \equiv \begin{pmatrix} p_{0|0}, & p_{0|1}, & p_{0|2}, & \cdots & p_{0|k-1}, & p_{0|k} \\ p_{1|0}, & p_{1|1}, & p_{1|2}, & \cdots & p_{1|k-1}, & p_{1|k} \\ \vdots & \vdots & \vdots & p_{k_i|k_j} & \vdots & \vdots \\ p_{k-1|0}, & p_{k-1|1}, & p_{k-1|2}, & \cdots & p_{k-1|k-1}, & p_{k-1|k} \\ p_{k|0}, & p_{k|1}, & p_{k|2}, & \cdots & p_{k|k-1}, & p_{k|k} \end{pmatrix} = \begin{pmatrix} 0, & 1, & 0, & \cdots & 0, & 0 \\ 0, & 0, & 1, & \cdots & 0, & 0 \\ \vdots & \vdots & \vdots & \vdots & \vdots & \vdots \\ 0, & 0, & 0, & \cdots & 0, & 1 \\ 0, & 0, & 0, & \cdots & 0, & 1 \end{pmatrix},$$

$$\mathbf{P}_{-1} \equiv \begin{pmatrix} p_{0|0}, & p_{0|1}, & \cdots & p_{0|k-2}, & p_{0|k-1}, & p_{0|k} \\ p_{1|0}, & p_{1|1}, & \cdots & p_{1|k-2}, & p_{1|k-1}, & p_{1|k} \\ \vdots & \vdots & p_{k_i|k_j} & \vdots & \vdots & \vdots \\ p_{k-1|0}, & p_{k-1|1}, & \cdots & p_{k-1|k-2}, & p_{k-1|k-1} & p_{k-1|k} \\ p_{k|0}, & p_{k|1}, & \cdots & p_{k|k-2}, & p_{k|k-1}, & p_{k|k} \end{pmatrix} = \begin{pmatrix} 1, & 0, & \cdots & 0, & 0, & 0 \\ 1, & 0, & \cdots & 0, & 0, & 0 \\ \vdots & \vdots & \vdots & \vdots & \vdots & \vdots \\ 0, & 0, & \cdots & 1, & 0, & 0 \\ 0, & 0, & \cdots & 0, & 1, & 0 \end{pmatrix}.$$

For $\mathbf{P}$ the last row indicates that the terminal state transitions into itself such that the terminal state is an absorbing state. Furthermore, note for $\mathbf{P}$ that the first column sums to zero as there is no state transitioning into hour zero[80]. For $\mathbf{P}_{-1}$ the second row indicates that it is only the initial state that transitions into hour 1[81]. In the simple case where the transition probability matrix consists entirely of ones and zeros, the transition dynamics are identical to full model described in section 4.3 with $k = 8760$ states.

Replacing the simple chronology with transition matrices, we can define a system of equations for each state that simply looks at state-average values. By doing so, we can replace the first order conditions in (15) with:

$$\begin{aligned} E_{k_i} &= \underline{E} + \left(Y_{k_i} - \underline{E}\right) \Phi\left(\frac{p_{k_i} - c - a\theta_{k_i}}{\sigma}\right) + \left(\bar{E} - Y_{k_i}\right) \Phi\left(\frac{p_{k_i} - c - \theta_{k_i}}{\sigma}\right) \\ \theta_{k_i} &= \beta\theta_{k_i+1} + \underline{\eta}_{k_i} - \bar{\eta}_{k_i} \\ S_{k_i} &= S_{k_i-1} + f\left(Y_{k_i} - E_{k_i}\right) \\ \bar{\eta}_{k_i} &\equiv \left(S_{k_i}^{max} - \bar{S}\right) \nabla S_{k_i}^{max} \\ \underline{\eta}_{k_i} &\equiv -S_{k_i}^{min} \nabla S_{k_i}^{min} \end{aligned} \tag{51}$$

Here we let E_{k_i} be the hourly average production in state k_i. Thus the total production in the state k_i is given by scaling up with the number of hours n_i, i.e. $\mathbf{E}_{k_i} = n_i E_{k_i}$. The state-average variables are then defined by

$$S_{k_i-1} \equiv \mathbf{P}_{-1,k_i} \times \begin{pmatrix} S_0, & S_{k_1}, & \cdots, & S_{k_k} \end{pmatrix}, \tag{52}$$

$$\theta_{k_{i+1}} \equiv \mathbf{P}_{k_i} \times \begin{pmatrix} 0, & \theta_{k_1}, & \cdots, & \theta_{k_k} \end{pmatrix} \tag{53}$$

and where $\mathbf{P}_{-1,k_i}$, $\mathbf{P}_{k_i}$ refers to row k_i in the respective transition matrices.

[80] In technical terms, state zero is the terminal state in the previous year, which is given.

[81] Note that the two are simply each other transposed. This need not be the case in the aggregated case; there can easily be different number of hours in each state k_i, making the weights different in the backward and forward looking transition matrices.

9.3.3 A state-transition-contingent aggregation

As a third option we aim for the middle ground between computing all 8760 hours and summing them into k states, and only computing k average states. Our idea is to decompose the production in an aggregate state k_i by letting the storage plant always know exactly which state it transitions into at $k_i + 1$. The reason behind this approach is that the supply from our storage firms is highly non-linear. To illustrate the gains from this approach, consider the case illustrated in figure 9.2. Part (a) plots the optimal production scheme as a function of current profits minus the continuation value θ_k. Recall from the storage section 4.3 that the dispatch solution involved two smoothed thresholds: When prices are low compared to the continuation value ($p_k - c < a\theta_k$), the storage plant should approximately choose the minimum $\underline{E}$. In intermediate price ranges the inefficiency of storage implies a solution of exactly zero storage, with production around the inflow Y_k. At high prices ($p_k - c > \theta_k$) it is optimal to produce at max capacity $\bar{E}$. Now consider a plant that from state k_i either transitions into an average-price state k_j or a high-price state k_g. Part (b) in figure 9.2 illustrates how this translates into a low θ_{k_j} and a high θ_{k_g}. In the simple state-average approach, we would compute an average continuation value over the two states. Due to the non-linearities of the supply, this can lead to large errors in the production decision. Part (b) in figure 9.2 illustrates an example where applying an average state $\theta_{k_i} = 0.5(\theta_{k_j} + \theta_{k_g})$ in the production function erroneously ignore the low-future-price continuation value θ_{k_j}, and thus leads to a sub-optimal low production level. In other words, applying a non-linear function to an averaged variable can often be a bad approximation to averaging over said function applied on individual observations.

Figure 9.2: Illustration of state-average aggregation

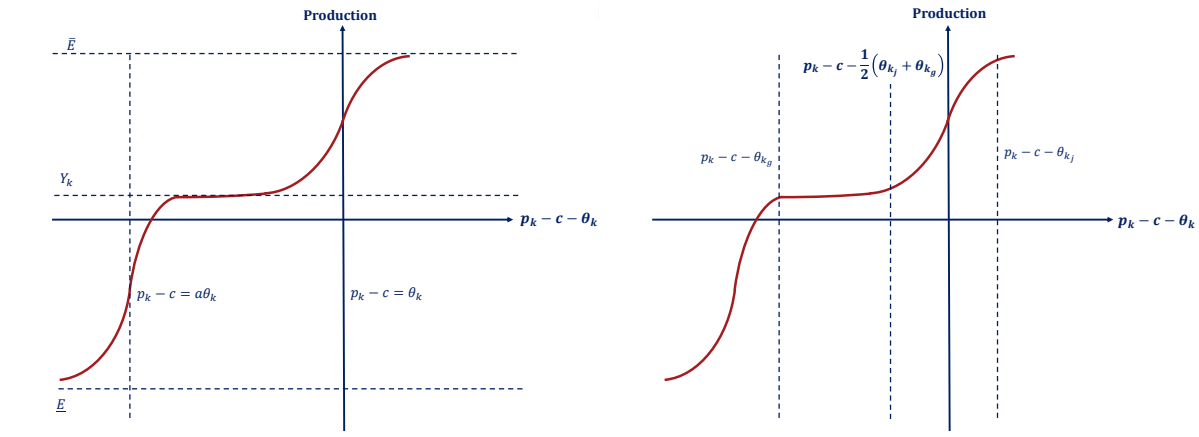

(a) Smoothed jump-thresholds in storage production

(b) The state-average solution

Now consider a storage plant in state k_i that knows for certain that it transitions into state k_j in the next period. Allowing production to be contingent on the state tomorrow, the first order conditions for this plant is then given by:

$$E_{k_i|k_j} = \underline{E} + (Y_{k_i} - \underline{E})\,\Phi\left(\frac{p_{k_i} - c - a\theta_{k_i|k_j}}{\sigma}\right) + (\bar{E} - Y_{k_i})\,\Phi\left(\frac{p_{k_i} - c - \theta_{k_i|k_j}}{\sigma}\right) \tag{54a}$$

$$\theta_{k_i|k_j} = \beta\theta_{k_j} + \underline{\eta}_{k_i|k_j} - \bar{\eta}_{k_i|k_j} \tag{54b}$$

$$S_{k_i|k_j} = S_{k_i-1} + f\left(Y_{k_i} - E_{k_i|k_j}\right) \tag{54c}$$

$$\bar{\eta}_{k_i|k_j} = \left(S^{max}_{k_i|k_j} - \bar{S}\right)\nabla S^{max}_{k_i|k_j} \tag{54d}$$

$$\underline{\eta}_{k_i|k_j} = -S^{min}_{k_i|k_j}\nabla S^{min}_{k_i|k_j}. \tag{54e}$$

Here $E_{k_i|k_j}$ is the production in state k_i given that it transitions into k_j and $\theta_{k_i|k_j}$ the relevant continuation value. With production being state-contingent we also get a state-contingent reservoir level ($S_{k_i|k_j}$) and corresponding shadow values on the reservoir constraints ($\bar{\eta}_{k_i|k_j}, \underline{\eta}_{k_i|k_j}$). Note that to limit the number of equations, we still use the simple weighted average continuation value θ_{k_j} in the law of motion (54a), as well as the simple average initial reservoir level $S_{k_i} - 1$ in (69). These averages are defined in a manner similar to the state-average approach:

$$S_{k_i-1} \equiv \mathbf{P}_{-1,k_i} \times \left(S_0, \quad S_{k_1|k_i}, \quad \cdots, \quad S_{k_k|k_i}\right)'$$
$$\theta_{k_i} \equiv \mathbf{P}_{k_i} \times \left(0, \quad \theta_{k_i|k_1}, \quad \cdots, \quad \theta_{k_i|k_k}\right)'.$$

In this way storage plants make decisions knowing which aggregate state they enter in the following period, but only the probability distribution for which states to enter in subsequent periods. Figure 9.3 illustrates how the state-transition-contingent aggregation better captures the non-linearity of the supply than the state-average aggregation displayed in figure 9.2.

Figure 9.3: Difference between state-average and state-transition-contingent supply

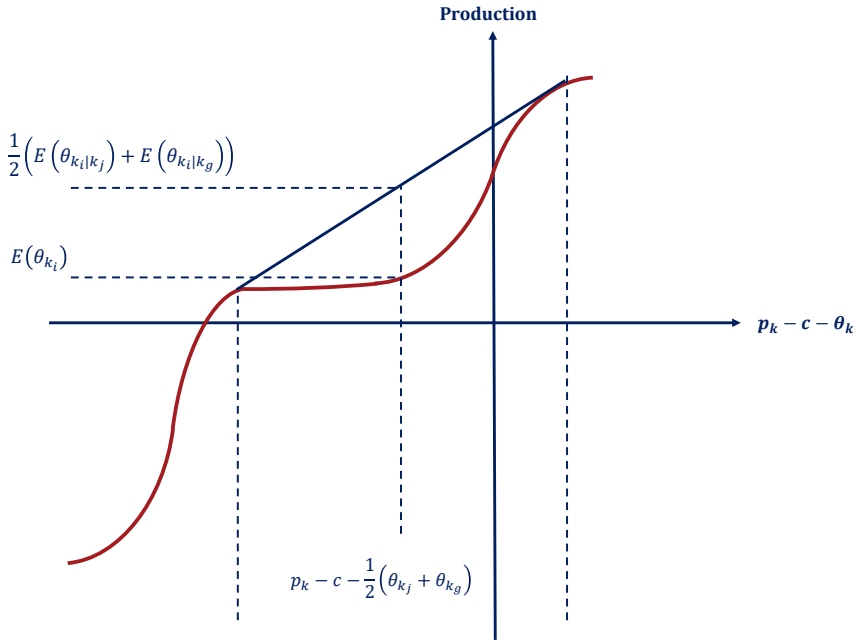

Compared to the state-average approach this adds some accuracy, but at the cost of having to solve for an $E_{k_i|k_j}$ for all entries with strictly positive weights in the transition matrix $\mathbf{P}$. Below we illustrate the performance of the state-transition-contingent aggregation method.

9.3.4 Example: Hourly aggregation of Swedish hydro plants

Given that the BU model is so high-dimensional we cannot test the aggregation scheme for the model with all 8760 hours at the moment.[82] Instead we focus on evaluating the performance of the aggregation using the case of Swedish hydro plants described in section 4.3.2. Given this is a partial equilibrium model, taking prices as constants, the clustered exogenous data consists of prices (p) and water inflow (Y).[83] We solve and estimate the model presented in section 9.3.3 for $k = \{25, 500\}$. The full model with 8760 states is included to show that our state-transition-contingent aggregation nests the full model in section 4.3.1. The estimation method is identical to the one described in section 4.3.2 with the only change that the probability density function in the log-likehood objective, $\phi(x_h(\theta))$, now depends on the hourly random variable $x_h(\theta) = E_h - E_h^*(S_{k_i}, p_{k_i}; \theta)$ where average state dependent production, $E_{k_i}^*(S_{k_i}, p_{k_i}; \theta)$, has been mapped into the hours contained in cluster k_i.[84]

The performance of the K-means clustering in this two-dimensional framework is presented in figure 9.4 for k =25. The algorithm seems to be picking up the central states over all 8760 hours. Clustered hours in the North-West part of the diagram can be described as *storage*-states in which prices are low and water inflow is high. Conversely, clusters in the South-East part of the diagram are states containing high prices and low water inflow.

Figure 9.4: K-means clustering in two dimensions ($k = 25$).

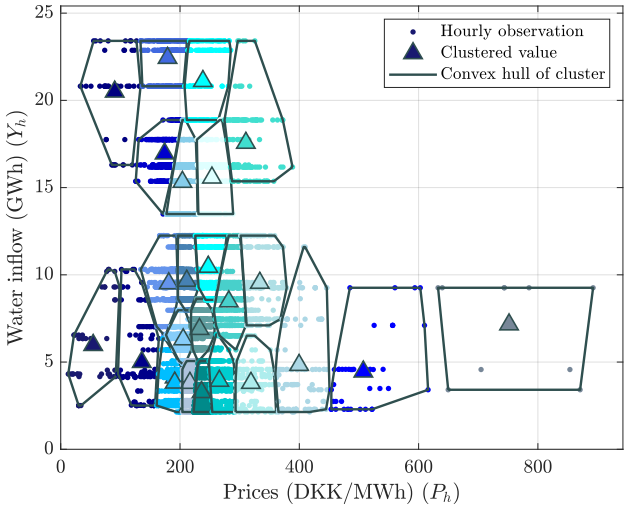

Note: Dots ($\cdot$) indicate the hourly observation of (p_h, Y_h)-pairs. Closed areas ($--$) indicate the convex hull of a given cluster containing h hours. Triangles ($\triangle$) are centroids of the cluster, i.e. the clustered pair (p_{k_i}, Y_{k_i}).

The model prediction of $k = \{25, 500\}$ and the full model with all 8760 hours are illustrated in 9.5.

[82] We are running the computations on a Dell laptop with an Intel i7 CPU with 2.80 GHz and 16 GB RAM. We are currently awaiting to have the software we use installed on the Department of Economics' internal servers. Thus the plan is to run the model with 8760 hours in the future.

[83] What really should matter for the performance of the aggregation scheme is the clustering of prices. Water inflow only matters for the dynamic profit maximisation if the upper or lower bound reservoir constraint is binding. However, we take a neutral stand and let prices (DKK/MWh) and inflow (GWh) have equal weight in the clustering algorithm. Consequently, they are scaled into the same units with mean zero and variance one.

[84] Note that $E_h^*(S_{k_i}, p_{k_i}; \theta)$ still depends of the clustered exogenous data and not the actual hourly data.

We see the overall shape of inter-temporal supply curve is well preserved in figure 9.5a. The shape of the hourly reservoir curve, however, changes considerably fast whenever down-scaling k. As such, the control variable (electricity production) behaves almost identical to the full model but the state variable (reservoir level) is far from the full model. This is due to the non-chronological clustering of the K-means algorithm and the state-transition-contingent aggregation scheme. It is not the averaging effect of the clustering that is at play. With 25 clusters the dispersion in the electricity production still reproduces nearly as 'extreme' observations as the full model (see part (a) of figure 9.5).[85] Instead, because the K-means algorithm is essentially clustering hours in the beginning of the year together with hours in the end of the year, the state-transition-contingent aggregation implies that the *average* reservoir level that the hydro plant manager enters the state with (S_{k_i-1}) is the same in the beginning and end of the year. For the model with few clusters ($k = 25$) this effect is more extreme since the reservoir level is averaged over many hours, almost removing the entire shape of the reservoir curve. For the case with ($k = 500$) we get the increase in reservoir level during summer but hours in the beginning and end of the year are still clustered together. Consequently, the average of the low reservoir level in the start of year and the high reservoir level in the beginning of the year is averaged out. The aggregation method is thus, at the moment, an unresolved issue. Section 14 discusses possible solutions to the issue of aggregating the model.

Figure 9.5: Performance of the state-contingent aggregation scheme.

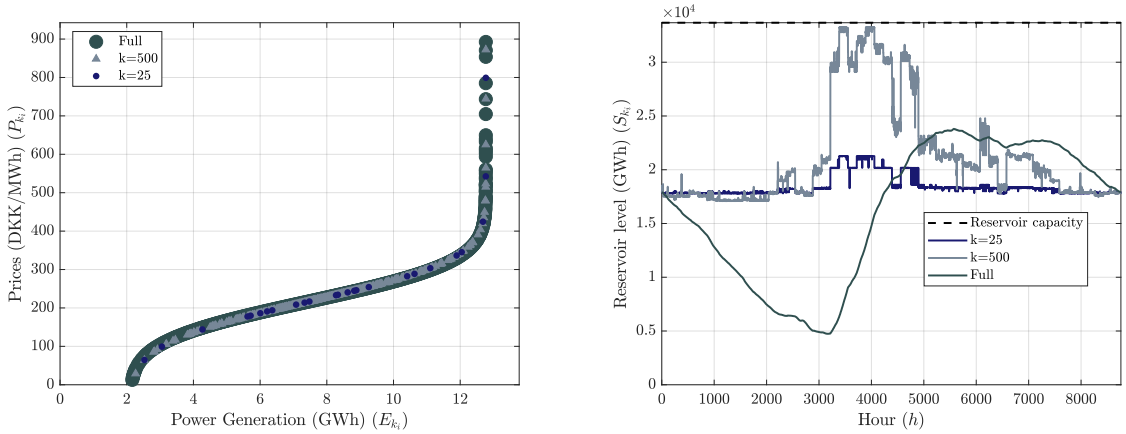

(a) Power generation (GWh).

(b) Reservoir level (GWh).

[85] We also solved the model with the 'folding all 8760 hours into k states' approach in section 9.3.1. We found that the model prediction of this approach was almost identical to the model using actual data. Given that the only difference between these two predictions is the data they use, the averaging effect of the K-means clustering is neglible.

10 Solution and Calibration of the Bottom Up Module

In the following we outline how the model is solved and calibrated. Given that considerable effort has been put into formulating the model in a computational efficient environment and that we aim at making the model code open source as part of the larger research project (SUSY Project, 2019), we describe the software used for solving and calibrating the model. Similarly, we describe in detail the calibration process that ensures that the BU module reproduces empirical facts in a base year (here 2017), which is necessary for it to be integrated with a standard CGE model. Although the model could be calibrated to several more empirical facts, we have selected a set of statistics that ensures that the model reproduces the energy statistics that a CGE model is calibrated to as well. Consequently, the information between the CGE and the BU module is aligned in the base year. Additional calibration is beyond the scope of this paper.

10.1 Solving the model

The model is solved using open source software R and Python, with the core of the model written in GAMS. The model is run from Python, where the relevant settings are defined for the model. The settings are parsed to either R or GAMS, where data manipulation and model solutions are carried out. The main advantage is that the model user can use the model from the main Python script, taking the underlying R and GAMS scripts for granted.

Figure 10.1: An Overview of the Model Code

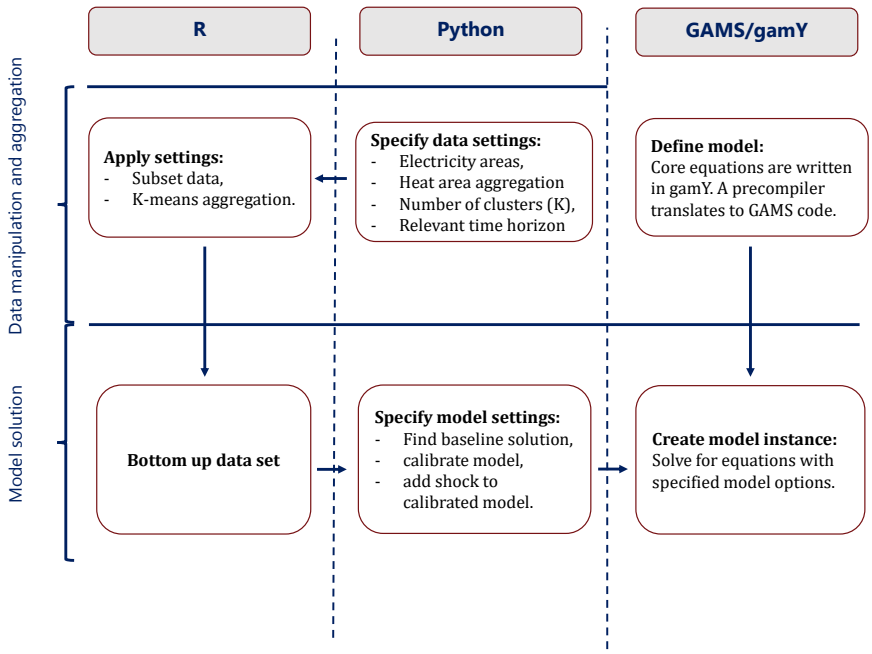

The code can roughly be broken into two parts: A data manipulation and clustering part and a model solution part. Figure 10.1 illustrates the structure of the code. In the first part a number of settings is chosen in the main Python script, such as the number of countries to include, which years to

consider, aggregation of heating areas etc.. The main Python scripts parses settings to various R-scripts that subsets the technical bottom-up data and aggregates the chosen data using the K-means algorithm. Finally, the data is arranged and written as Gams Data eXhange (gdx) files, in a way that is consistent with the core equations in the BU model. In the second part, model settings are specified in Python. The core model equations are specified in gamY.[86] The model is called from Python, translated to GAMS code using a pre-compiler in gamY and finally run using the relevant solver from the GAMS software.[87] This setup allows us to use R as the main tool for processing and manipulating data and the potent numerical tools from GAMS, while maintaining the flexibility of Python.[88]

The BU model is solved as a square system of continuously differentiable equations. As outlined in part II, a number of free *smoothing* variables (σ) are available for the researcher to specify. If these are set appropriately close to zero, the supply of various types of plants as well as the trade mechanism, becomes highly non-linear, approaching kinked functions. When this is the case, the *global convergence* property of the solution algorithm in CONOPT4 in GAMS, is far from guaranteed. To ensure the global convergence of the solution, a N-step algorithm is applied when solving for the baseline model. Initially, the σ values are set at relatively high values. At sufficiently high levels the supply function essentially becomes linear in the range of plausible equilibrium prices. If the share of inelastic demand is initially set at $\phi = 1$, the entire bottom up problem is (approximately) linear, ensuring the global convergence of the gradient-based solver CONOPT4. Once an initial solution has been acquired, the smoothing variables (σ) can gradually be lowered towards the researcher's preferred level.[89] Once a baseline solution has been identified, relatively large shocks can be carried out, without using the N-step approach.

10.2 Calibrating the model

The BU module is calibrated to fit a number of moments, including the sum of production, net exports and use of various fuel inputs. For 2017 we use the moments from the Danish Energy Agency's yearly energy statistics (Danish Energy Agency, 2017a), displayed in table 9. The average spot price is computed from hourly consumption and price data from Energy Data Service (2018a,b).

To achieve this calibration, the model is adjusted in a number of ways. As a first step three adjustments are performed. Table 10 outlines the relevant targets and parameters affected here. First, we target the overall price level by including a correction factor in the marginal cost function for all dispatchable domestic plants. Second, we include a marginal cost correction variable for all foreign dispatchable plants. Given that the total energy consumption throughout a year enters exogenously in the demand

[86] The use of gamY and the pre-compiler translating the equations to GAMS code is the work of the Danish modeling group DREAM. See `https://github.com/MartinBonde/gamY_sublime` for an introduction to the gamY package. Unfortunately, the complete source-code for gamY is currently not publicly available.

[87] For most of our purposes the model is solved using the solver CNS option in the CONOPT4 algorithm. See Drud (2019).

[88] Python includes several useful packages that could perform the data manipulation part of the model instead of R. It is solely the personal preference of the authors for using R and the convention in the DREAM modelling group that led to this choice.

[89] Experience so far shows that initially setting σ around 400 in the normal smoothing function, ensures that the algorithm finds a solution very fast. From here our standard settings use $N = 12$ steps to gradually decrease σ towards 50 in smoothing Danish plants' supply an approximating the linear programming solution. We have not experimented much with these values, but for now simply set them in ranges, to ensure that the algorithm always works.

Table 9: Calibration targets, 2017

Variable	**Target** (PJ)
Coal (input)	60.66
Oil (input)	3.75
NatGas (input)	31.38
Straw (input)	15.26
Wood (input)	66,03
Waste (input)	37.46
Bio gas (input)	7.01
Bio oil (input)	0.189
Electricity for heating (input)	1.211
District heating from electricity (output)	1.14
Surplus heating (output)	3.74
Wind, PV, hydro (output)	55.98
Solar heating (output)	1.81
Gross production, electricity	111.47
Gross production, district heating	135.59
Net import (DK)	16.43
	Target
Average spot price (DK)	236.23 DKK/MWh

Note: At the moment we do not fit the yearly price of district heating for end-consumers. Given that the BU module does not contain the distribution of heat to consumers the price for end-consumers will be specified in the CGE model. Similarly, the average electricity spot price is not the price for end-consumers of electricity. However, the average spot price is calibrated because it is instrumental for determining electricity trade.

function (see section 5), we do not need to include a calibration parameter to fit energy consumption; it is always guaranteed to be at the correct level. Thus, we only have to target either gross production of electricity or the total net imports in order to fit both in our model. To achieve this target, there is a number of alternatives to the marginal cost component of foreign plants. These include adjustment of trade capacities, trade smoothing parameters and the price elasticity of domestic demand for electricity. As is illustrated in the sections to come, including a marginal cost component constant across all foreign plants achieves the target very easily. Reassuringly, the adjustment to marginal costs of foreign plant, in order to achieve the target of trade with electricity, is generally very small (less than 5 DKK/MWh). Third, we adjust the production capacities for a set of plants. This includes intermittent technologies that have (near) zero marginal costs as wind, solar and hydro.[90]

With the first three adjustments just described, the model is relatively close to the targets for all relevant endogeous variables. For the model to fit the rest of the targets, we add correction parameters to a number of technical parameters obtained from the Ramses data. These include: (1) efficiency corrections, (2) marginal cost corrections, (3) production capacity corrections and (4) fuel mix coefficient matrix corrections. We allow all four types of corrections to be on a fuel type specific level in order to ensure that we reach the fuel input targets in table 9. In contrast to a structural estimation, the

[90]We also allow for the adjustment of production capacity for plants using biogas and waste as primary input factors. The reason for this is the same as for intermittent technologies mentioned here: Note from the fuel-specific supply functions in figure E.1 that with prices ranging from 0-1500 DKK/MWh, the supply is basically fixed at the capacity levels. Thus, the only way to affect the supply from these firms, is basically through an adjustment of the capacity variable.

Table 10: Calibration target and parameters, step 1

Target	**Adjustment of parameter**
Average spot price (DK):	Marginal cost parameter added to all dispatchable Danish plants
Sum of net import (DK):	Marginal cost parameter added to all dispatchable foreign plants
Output targets (DK)	
Electricity, intermittent plants	⋮
Heat, intermittent plants	⋮
Surplus heating	Correction of yearly average capacity for relevant plant/fuel type
Electricity + heat, waste	⋮
Electricity + heat, bio gas	⋮

parameters we unfix here are clearly not identified from the targets above: We have approximately 3500 technical parameters that are endogenized and only eight fuel input targets to hit. Our reasoning behind this approach is that technical parameters should more or less be identified directly from our data. As we *a priori* have no information on which of the technical parameters best explain the discrepancy between the model solution and the targets in table 9, we formulate a criterium function to be minimized, which penalizes large deviations from the original Ramses data. This is done subject to the model being in equilibrium and that all targets in table 9 are met. The criterium function used here is given by

$$\min \mathcal{Q} \equiv \sum_{i \in \mathscr{F}_B} \sum_{j \in \mathscr{F}_F} \left(C_{i,j}^{MC}\right)^2 + w_{FM} \left(C_{i,j}^{FM} - FM_{i,j}^{data}\right)^2 + w_{Eff} \left(C_{i,j}^{Eff} - 1\right)^2 + w_{Cap} \left(C_{i,j}^{cap} - 1\right)^2,$$

where $\mathscr{F}_B$ and $\mathscr{F}_F$ are the two fuel mix sets defined in the data. The marginal cost correction $C_{i,j}^{MC}$ is added to all plants' marginal costs and is thus measured in DKK. C^{FM} is the corrected fuel-mix matrix. It consists of variables between zero and one, with entry (i, j) denoting the amount of basic fuel i that is used for a plant of fuel-type j. We only allow for non-zero values in the fuel-matrix to be adjusted. To remedy that the corrections in $C_{i,j}^{FM}$ are not measured in DKK as the marginal cost corrections, we include a weight w_{FM}. A large value of w_{FM} indicates that we should change the marginal costs of the plant, rather than coefficients in the fuel-mix matrix given by the Ramses data. $C_{i,j}^{Eff}$ is a multiplicative correction term on plants' fuel efficiency. $C_{i,j}^{Cap}$ is a similar multiplicative correction term on plants' production capacity.

To illustrate the effect of the calibration, we plot the domestic supply functions split into technology- and fuel types. Figure 10.2 illustrates the supply of electricity in an average hourly state for Denmark. The *baseline* included in the figure, represents the supply function prior to any calibration of the model. We include three calibrated versions with varying levels of the weight w_{Cap} to illustrate the importance of the exogenous weights. Part (a) illustrates that the sum of supply is hardly changed after the calibration. Part (b)-(f) further confirms that our calibration generally does not alter the supply from any one type of technology too severely. In other words, for our BU model to reproduce the data in table 9, the technical parameters from Ramses barely have to be adjusted. In so far as the data from Ramses is reliable, this

indicates that our model approach, captures the most relevant features of equilibria on the electricity market and in the district heating system.

Figure 10.2: Danish supply of electricity on technology types

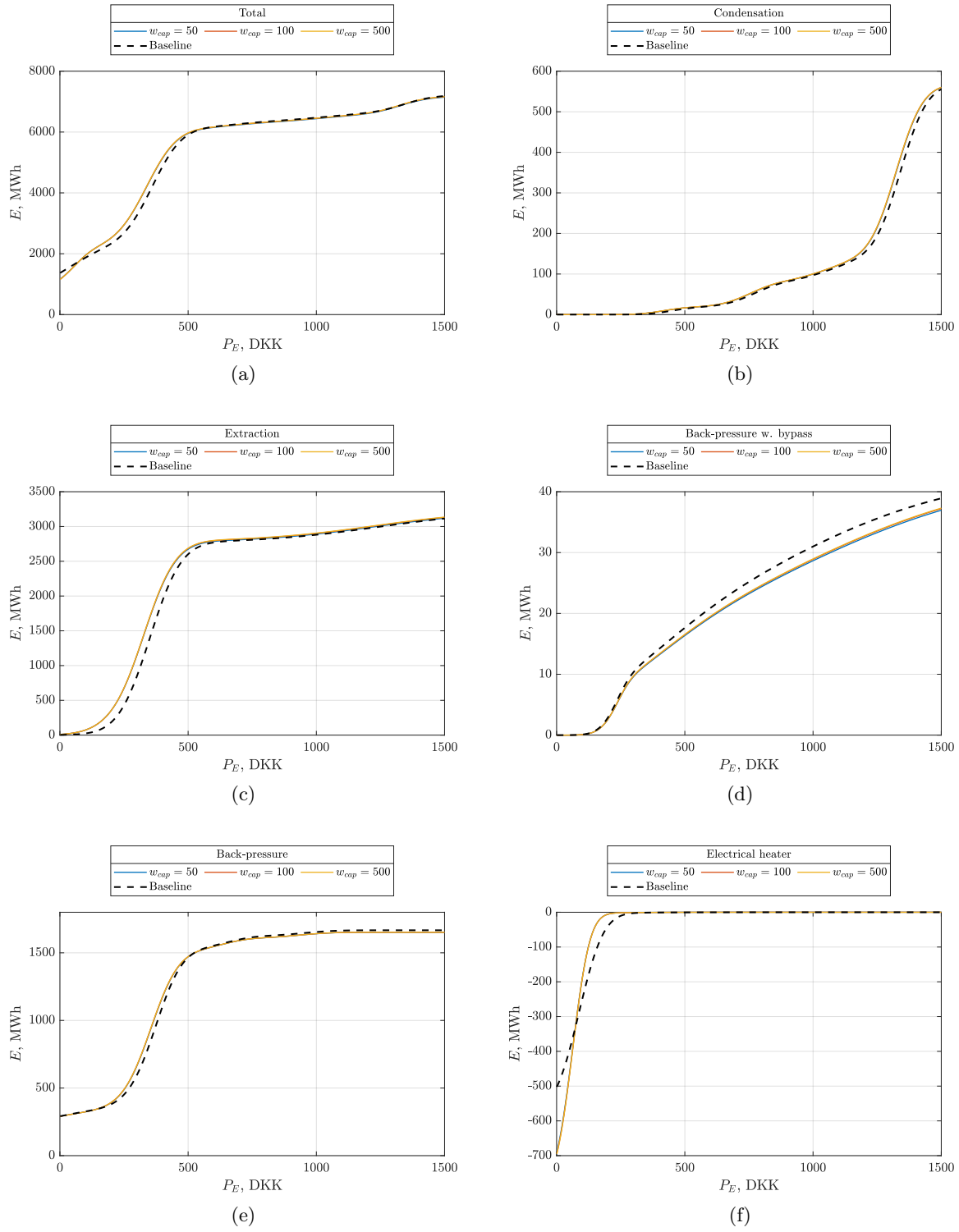

Note: The figure shows the supply from Danish electricity plants varying the price level from 0-1500 DKK. We use yearly average productivity levels for intermittent technologies and a price on heating at 200 DKK/MWh. The smoothing parameter σ described in section 4.1 is set to 50 here.

Figure 10.3 illustrates the Danish supply on electricity split onto fuel types. Compared to the technology split in figure 10.2, these figures illustrate slightly larger corrections of the model from the calibration of it. Note that for waste plants, we have to decrease the capacity quite a bit (around 10%) to fit the amount of waste used for production of energy in 2017. This is simply because waste plants - in our representation at least - are highly profitable. Thus, adjustments to marginal cost components would have to be very large for the production from waste plants to go down in equilibrium.

The biggest correction, however, is for the supply based on biomass. In particular, the supply function for plants using wood in production is somewhat different, at least at prices above 350 DKK/MWh. When prices increase from around 350 to 500 DKK/MWh the calibrated model implies a small additional supply from wood compared to the baseline (uncalibrated model). Furthermore, changing the weight w_{cap} does not seem to alleviate this issue. We note, howevre, that he supply still decreases when prices increase above 500 DKK/MWh. This is due to the plants in our data that can apply more than one fuel-mix, and the way taxation is levied on production of heat compared to electricity. When electricity prices increase above 500 DKK/MWh, two types of CHP plants (wood- and straw-based) increase the relative production of electricity compared to heat. As the use of coal is taxed higher in the production of heat relative to electricity, this induces CHP plants to substitute towards the use of coal instead of wood an straw.

Figure 10.3: Danish supply of electricity on fuel types

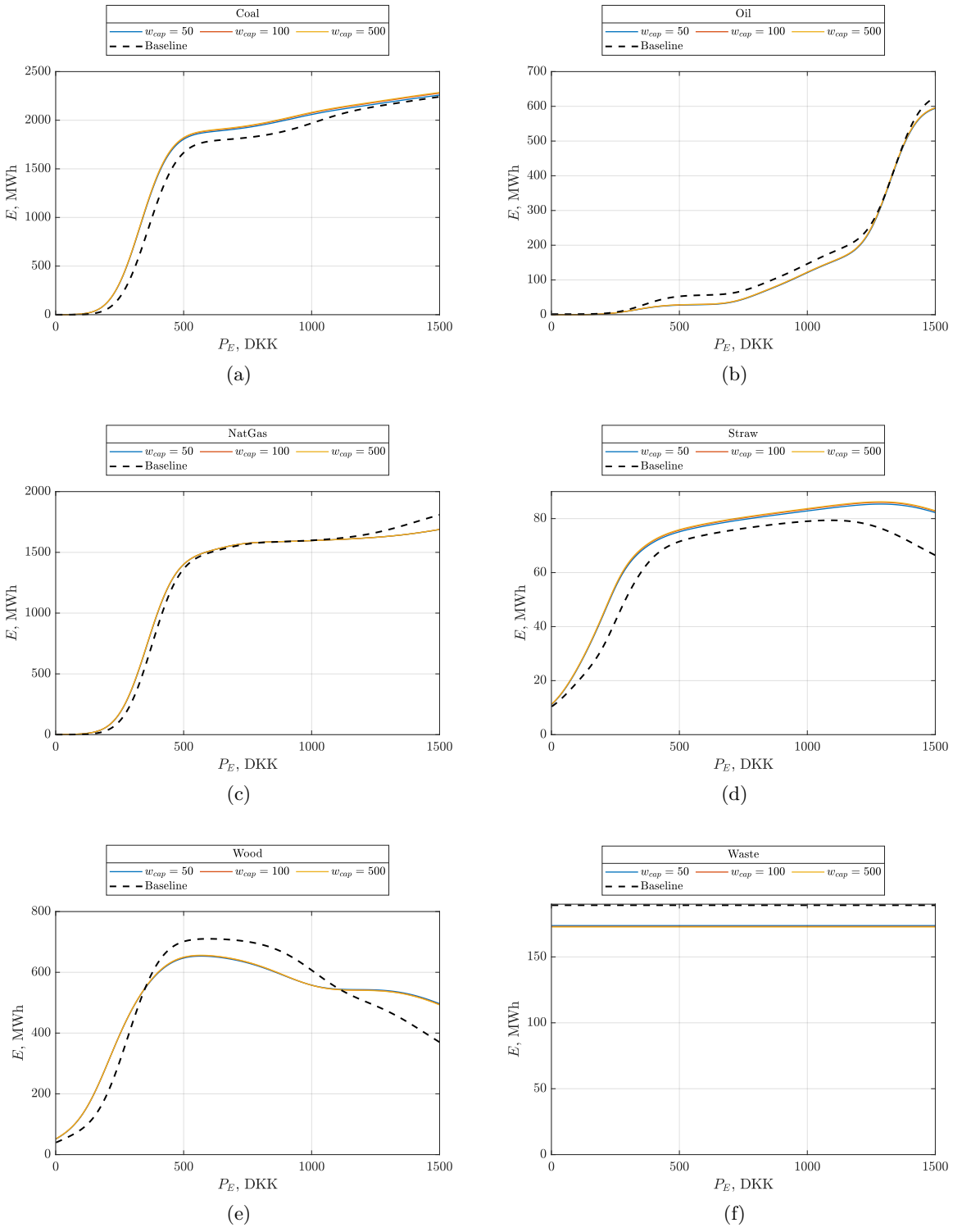

continues on the next page...

Figure 10.3: Danish supply of electricity on fuel types

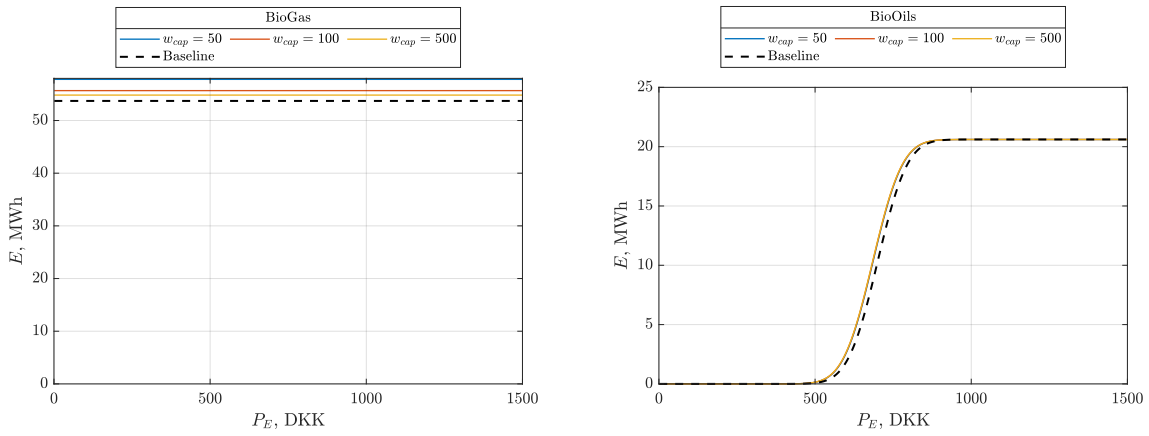

(g) (h)

Note: The figure shows the supply from Danish electricity plants varying the price level from 0-1500 DKK. We use yearly average productivity levels for intermittent technologies and a price on heating at 200 DKK/MWh. The smoothing parameter σ described in section 4.1 is set to 50 here.

11 Policy experiments: Validation of aggregated model

In this section we use the BU model of the energy system to simulate how the system responds to a number of exogenous (policy-induced) shocks that are expected to be key parts of the transition to a carbon-neutral society: (1) An increase in the supply of energy from intermittent renewable sources, (2) an increase in the flexibility of energy demand, (3) an increase in the capacity for energy storage, and (4) an increase of transmission lines' capacity for international trade in electricity. The counterfactual scenarios illustrate the usefulness of our approach. Furthermore, they serve as a validation for the 'efficient' choice of cluster number (k), by which we mean the value of k that balances the trade-off between accurate policy effects and computational efficiency. We will argue that the efficient number of cluster is k =40. However, as we will show in the baseline scenario of the BU model and in experiment (2), this level of aggregation dampens the degree of intermittency, although the qualitative patterns are preserved compared to the most disaggregated model of k =168.

Finally, note that in previous sections yearly energy demand has been considered fixed. In the counterfactual scenarios presented here, the BU module is coupled to a simple top down price-elastic demand function. This serves to illustrate the simplicity of the *integration link* from the BU module to a top down CGE model.[91]

[91] We only link the BU module to a domestic demand function. The yearly consumption in foreign countries is exogenously given.

11.1 Price-elastic top-down demand

We choose a simple iso-elastic function given that the yearly demand function is only included to illustrate one of the essential links between BU and top down models:

$$X = \gamma_X p_X^{\epsilon_X}, \qquad X = \{E, H\}, \tag{55}$$

where $\epsilon \leq 0$ is the exogenous short-run (one-year) price elasticity and γ is a calibrated scale parameter. Deryugina et al. (2017) estimate the price elasticity using a permanent natural experiment, suitable for identifying a value of ϵ. Illinois implemented a municipal aggregation program, allowing individual communities to select new electricity suppliers on behalf of their residents. This created long-lasting price drops in communities that adopted the aggregation scheme. Using a difference-in-difference estimator with communities that did not implement the aggregation as control groups, they find a one-year price-elasticity of -0.227.[92] This estimate is close to the price elasticity used for residential consumers in the Balmorel model (-0.3, Grohnheit and Larsen (2001)).[93] For now the elasticity in demand for heating is also set to -0.227. As the model is calibrated to fit the average prices and consumption in the baseline year 2017, the parameters γ_E and γ_H are calibrated to reflect this equilibrium, implying the scale parameters in (55) are γ_E=123.01 and γ_H=132.33.

11.2 The baseline scenario (DK, 2017)

We initially report the domestic levels of some key endogenous variables in the baseline scenario. In the baseline scenario, most of the variables included here are the same across the models with different number of clusters (k). This is because the calibration of (exogenous) structural parameters presented in section 10 ensures that the model reproduces selected statistics for the Danish transformation sector in 2017. Cf. table 9, this includes domestic fuel consumption, net export, average yearly consumer price of electricity, and consumption of electricity and heating. Given the model replicates the current state of supply, the brief outline of the baseline scenario in this section largely resembles the description of the transformation sector in section 3.2. For convenience however, some of the main facts are repeated here. The calibrated fuel consumption is illustrated in figure 11.1a. It shows that of the five fuel types, electricity and district heating are primarily produced using coal and bio fuels.[94] Recall from section 3.2 that bio fuels have been essential in particular for the district heating sector, whereas wind power is the primary source of energy, driving the green transition of electricity generation (with bio fuels being secondary). Finally, waste is widely used in both the production of electricity and district heating.[95]

[92] Note that this is still consistent with the modelling of energy demand in the present paper. Deryugina et al. (2017) estimate (numerically) much lower price elasticities for shorter time horizons. The shortest horizon is three months, where the price elasticity is merely -0.061. Consequently, this is still consistent with our assumption of hourly demand being perfectly inelastic.

[93] We are aware that the price elasticity for private sectors is not necessarily the same as for households. For simplicity we abstract from this issue.

[94] To simplify the presentation of the results, fuel types have been aggregated. Bio fuels consist of straw, wood, bio oil and bio gas.

[95] The category waste consists of 55% renewable-based biodegradable waste and 45% non-renewable. Following the convention in Ramses this share is assumed fixed.

Figure 11.1b illustrates consumption of electricity and district heat as well as net exports of electricity in the baseline scenario. The model replicates the fact that Denmark is a net importer of electricity, where roughly 13% of domestic consumption is satisfied by imports. The yearly consumer price of electricity of p_E=236.2 DKK/MWh is included in part (c) of figure 11.1.

Parts (c)-(e) of figure 11.1 report various yearly (weighted) price indices. As none of these endogenous variables (except p_E) have been fitted to data for 2017, the indices are plotted for all values of k. In other words, they are not necessarily equal across different values of k. Part (c) shows the producer price for Danish electricity producing plants that are based on intermittent energy sources. To simplify the presentation, the figure does not distinguish between wind, photovoltaics, nor ROR hydro power. It shows that intermittent plants generally produce electricity, when prices are below the yearly average consumer price. This is consistent with hourly data from Energy Data Service (2018a) and Energy Data Service (2018b): The weighted average producer price received by intermittent technologies in the electricity market in Denmark was roughly 200 DKK/MWh in 2017. This observation is primarily driven by wind power that receives below yearly average prices (198.5), whereas solar power receives prices slightly above the yearly average (238.1). Importantly, the difference between the yearly average prices and the one intermittent technologies receive implies that the model reproduces the important characteristic of a downlift in the producer price of intermittent technologies (see section 2.1). However, part (c) of figure 11.1 also illustrates that the BU model is currently not able to create a sufficiently large downlift. For higher values of k the model is closer to data. However, even at k=168 the predicted downlift is still only at 22.4 DKK/MWh, whereas the actual downlift is at 37.5. The result that a larger k yields more realistic prices for intermittent technologies, is straightforward to explain: Whenever the number of states is reduced, each representative state includes more of the 8760 hours. Thus the k states become increasingly average, as k decreases. This dampens the effect of intermittency and yields a smaller downlift for intermittent power. While the fit illustrated in part (c) of figure 11.1 is reasonable, section 14.1 discusses how to remedy the discrepancy between model and data in the clustered version of the model.

Part (d) illustrates the yearly average price for solar heat production. Similar to intermittent technologies producing power, the producer for solar heat production is decreasing in the number of states (k) and, in particular, when going from k=48 to k=72 and again to k=96. However, note that this pattern is also present in part (e) of figure 11.1, illustrating the average weighted producer price for heating in general.[96] Similar to the electricity market, the district heating system demonstrates a downlift in the producer price of intermittent technologies across all levels of k. Furthermore, it seems that the downlift increases with the number of states k. One possible explanation for this could come from CHP plants: When the number of states increases, the electricity prices fluctuate more over the course of a year. In general, low electricity prices imply that (marginal) CHP plants are only profitable, if the price on heating

[96]The producer price for heat is not calibrated, but the yearly average **consumer price** is calibrated in the model, c.f. table 9. The consumer price for heat is simply calibrated, by adjusting a (economically) standard markup factor. For electricity however, it is the producer price (spot price) that is relevant for determining trade etc.. Thus, we cannot apply this simple calibration approach for electricity generation plants.

Figure 11.1: Baseline scenario (DK, 2017)

(a) Calibrated fuel consumption

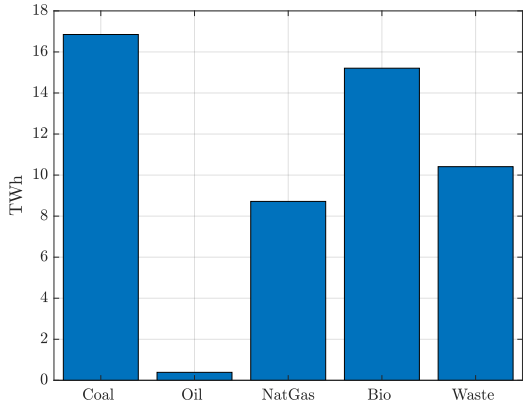

Note: Fuels are aggregated. Bio consist of straw, wood, bio-oil and biogas. Waste consists of both renewables and non-renewables.

(b) Calibrated energy consumption and net-export of electricity

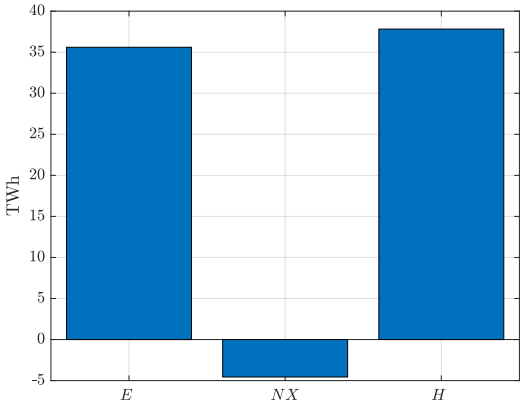

Note: E is electricity consumption, H is district heat, and NX is net-export of electricity.

(c) Uncalibrated intermittent electricity producer price

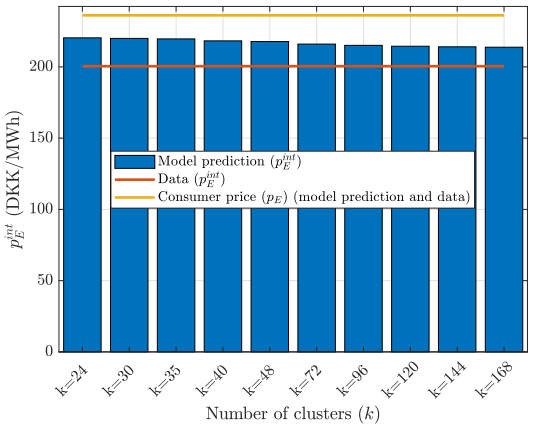

Note: p_E^{int} is the (weighted) average producer price for intermittent technologies producing electricity (wind, solar, ROR hydro).

(d) Uncalibrated intermittent district heating producer price

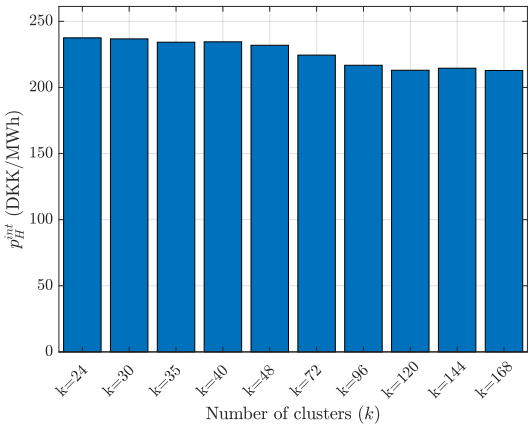

Note: p_H^{int} is the (weighted) average producer price for intermittent technologies producing heat (solar only).

(e) Uncalibrated district heating producer price

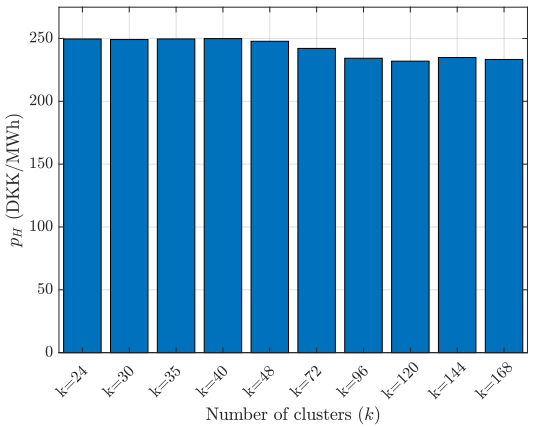

Note: p_H is the (weighted) producer price for district heat.

(f) Uncalibrated CO_2 emissions

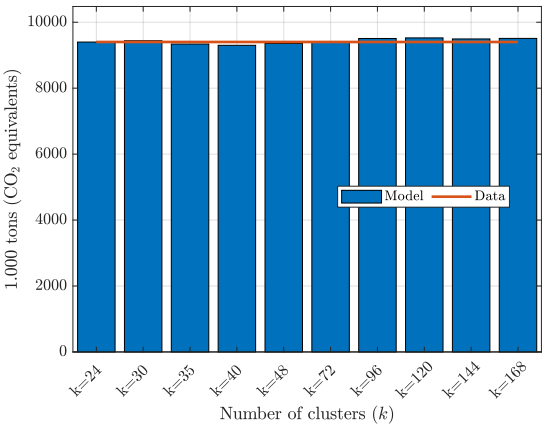

Note: CO_2 emission are measured in CO_2 equivalents.

Source: Data is based on Danish Energy Agency (2017a) and Energy Data Service (2018a,b).

increases. From this effect alone, we expect low electricity prices to be associated with high prices for heating. When the number of clusters increases, there are more outlier states of electricity prices. If the outlier states of high electricity prices correlates positively with demand for heating, the effect from CHP plants would drive down the price on heating, in hours where demand is large.

Finally part (f) of figure 11.1 reports the actual CO_2 emissions for 2017 along with the model emissions implied by the model for all clusters (k). In 2017 CO_2 emissions (measured in CO_2 equivalents) associated with the production of electricity and district heat were 9.401 million tons (Danish Energy Agency, 2017a). The model predictions are virtually identical to this level for all clusters. An important reason for this is that the fuel consumption levels have been fitted to observed fuel consumption. However, the emissions from the energy sector depends not only on the fuel mix, but also on the technology installed at the individual plants, implying that emissions may differ from actual emissions and across clusters.[97] However, part (f) of figure 11.1 shows that the number of clusters (k) does not seem to influence this fit.[98]

In the following the four counterfactual scenarios are presented. To increase readability, the results of these scenarios are mostly reported for clusters k=40 and k=168, only. While we have run the scenarios for all clusters, k=40 is our preferred candidate, for what we in the introduction to section 11 referred to as the 'efficient' value of k. As will be shown in the counterfactual scenarios the value of k=40 produces virtually the same results as the disaggregated model. In particular, section 11.4 shows that for k less than 40, the effect of increasing flexibility of short run demand is no longer qualitatively similar to models with larger k.

11.3 Expansion of intermittent electricity production

In the baseline scenario the share of intermittent production of domestic electricity production is 50.1%. We now consider a scenario where this share is exogenously increased to 75%, by increasing the capacity for all wind, solar, and ROR hydro plants by the same factor. With a reduction target of 70% of GHG emissions in 2030 compared to the 1990 level announced by the Danish government, this is a scenario that can be expected within a relatively short time horizon. Figure 11.2 illustrates the effects of the expanding the share of intermittent electricity production.

Part (a) of figure 11.2 illustrates the effect on prices. With the increased capacity of intermittent technologies, the yearly average price on electricity (p_E) drops significantly with around 22-23%. As noted previously, this is expected given that intermittent technologies generally have near zero marginal costs of production. Furthermore, the producer price for intermittent technologies drops even more significantly with around 33-34%. Thus the economic value of intermittent supply decreases in this short run framework. Part (a) of figure 11.2 further illustrates that when average electricity prices drop, it has

[97] At the moment this does not include carbon capture and storage (CCS) technologies (however, this information is available and applied in the model formulation, should it be used more in the future). The technology referred to here is for instance what type of turbine e.g. a specific coal-fired CHP plant uses.

[98] We note that while this is the case for GHG emissions, it is not the case for NOX and SO_2 emissions. Here, plant-specific technology plays a much larger role in determining the amount of polluting emissions.

Figure 11.2: Effects of increased intermittency

(a) Domestic prices

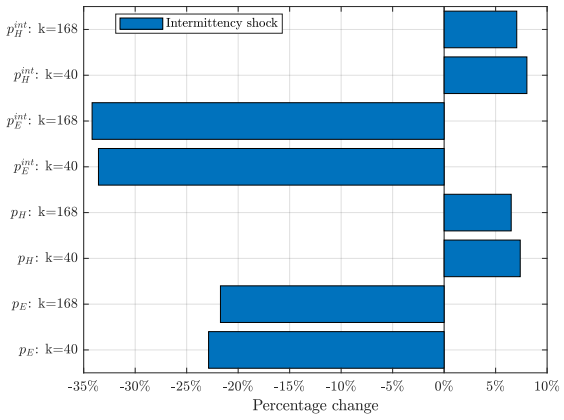

(b) Domestic energy consumption and net export of electricity

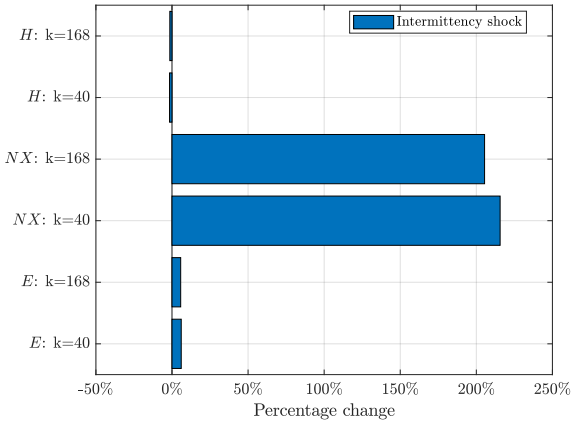

(c) Domestic fuel consumption

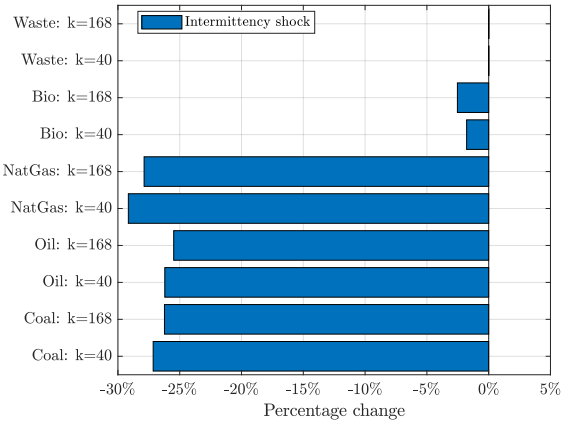

(d) Domestic CO_2 emissions

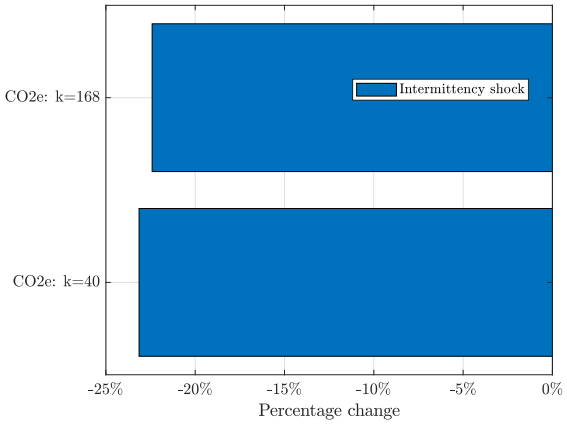

Note: In this counterfactual scenario DK becomes a net exporter ($NX > 0$). Given the sign of the net-exports change, there is less meaning of the percentage change. We therefore note that in levels (TWh) NX=4.8 and NX =5.3 for k =168 and k =40, respectively, in the counterfactual scenario.

a significant effect on heat prices as well. The price for heating increases by roughly 6-7%. There are two opposing effects at play here. For CHP plants the lower price on electricity implies that they are less profitable in general. Thus the price on heating has to increase, to keep them active. On the other hand electrical heaters and heat pumps, can generally profit from the lower electricity prices. *Ceteris paribus*, this drives down the price for heating. Recall from section 3.2 that in 2017 only around 1% of the Danish supply of district heat is covered by electrical heaters and heat pumps, whereas CHP plants covers more than 60%. Thus, the effect from CHP plants (increasing prices) naturally dominates. Finally, we note that the results are very similar for k=40 and k=168.

Part (b) of figure 11.2 illustrates the effect of the shock on consumption and net exports.[99] The qualitative results here are straightforward: With lower electricity prices total consumption increases (≈6%). With higher prices on heating the consumption decreases (≈1.5%). With the huge increase in cheap Danish electricity net exports increase. For the consumption part, the quantitative effects are entirely controlled by the change in consumer prices as explained above and the elasticity of the top down iso-elastic demand functions. The dramatic increase in net exports illustrates that Denmark goes from being a net importer to a net exporter of electricity. Instead of importing around 5 TWh of electricity, the increased intermittency implies exports of around 5 TWh. This shows that with trade capacities at the 2017 levels and the current composition of foreign electricity generating plants, trade offers quite a potent channel for mitigating the negative price effects of intermittency for Danish plants. In other words: One would expect far larger price drops for domestic intermittent plants, if not for the large potential to increase exports to neighboring countries. Another observation with relevant policy implications is that the cheap Danish electricity from the expansion of intermittent renewable energy, largely seems to be exported to foreign countries; at least in the short run. In fact, at most 42% of the additional intermittent electricity production is consumed domestically.[100] This result illustrates that when designing policy instruments and targets, there can significant effects, e.g. on emissions from foreign consumption of electricity, that should be taken into account.

Part (c) of figure 11.2 illustrates the effect of the shock on domestic fuel consumption. Naturally there is a crowding out effect on all types of fuels, when the capacity of cheap intermittent electricity generating plants increases. Recall from earlier that waste plants in our model are particularly profitable, c.f. section 10. Thus they are hardly affected by the intermittency shock. Part (c) confirms that in 2017, the marginal supply of electricity generally comes from coal fired and natural gas fired plants: Thus the consumption of these types drop by 25-30%. The consumption of oil similarly drops by a large percentage, however, as oil only constitutes a tiny share of the Danish transformation sector's consumption, this effect

[99] Note that $NX < 0$ in the baseline scenario. In the figure we compute the percentage change ϵ as:

$$\epsilon = \frac{X_1 - X_0}{|X_0|} \quad \Rightarrow \quad \text{sign}(\epsilon) = \text{sign}(X_1 - X_0).$$

Thus a positive ϵ reflects that net exports have increased.

[100] At this point, we have not identified the fuel mix composition of electricity sold to domestic or foreign consumers. However, if we assume that (i) the 4.9 TWh decrease of domestic fuel based electricity is for domestic consumers only, and (ii) the increase in domestic electricity consumption of 2 TWh consists solely of intermittent energy, this leaves 6.9 TWh of the additional intermittent electricity to be sold to domestic consumers. Given that domestic intermittent electricity production increases by 16.3 TWh, the increase in domestic consumption of renewable energy thus corresponds to 42% of the total increase.

is negligible in absolute terms. With the large drop in consumption of natural gas, coal, and oil presented in part (c), the CO_2 emissions from the domestic transformation sector drops significantly at around 22-24%.

11.4 Increased flexibility of short run electricity demand

In this section we perform a counterfactual scenario in which the share of yearly inelastic electricity demand (ϕ) is lowered from 100% to 90%. In other words demand in the very short run becomes more flexible. Recall from section 5 that by observing the bid-curves from the Nord Pool wholesale market of electricity, it is likely that ϕ is currently less than 1. The conclusion in section 5.2 was that a lower bound estimate of ϕ for Denmark is around 85% in 2017. With the implementation of smart meters and other technologies in the near future, this is expected to decrease further in the future. The counterfactual scenario presented in this section, investigates what this might entail for equilibrium prices and consumption.

Note that the flexible demand specification outlined in equation (20) requires information on three parameters: (1) the lower bound of demand ($\underline{D}$), (2) the upper bound on demand ($\bar{D}$) and (3) the price-responsive parameter σ. All three parameters can be structurally estimated on market data, as discussed in section 5.2; this however remains a task for future work. Thus in the current version presented here, the parameter values are set more or less arbitrarily with $\bar{D} = 2$, $\underline{D} = 0$ and $\sigma = 0.02$. This means that the magnitudes of the results in the following should be interpreted with caution.

The main results of the scenario are illustrated in figure 11.3. Part (a) shows that when 10% of domestic electricity demand becomes flexible, the price of electricity drops by around 1%. This is the direct effect of consumers reallocating their consumption from hours with high prices towards hours with low prices. Recall that with the parameter values for the flexible demand function applied here, lowering ϕ implies that 10% of electricity demand can *at most* double in states with low prices and tend to zero if the price tends to infinity. This could at least in part explain the small magnitude of the change, compared to e.g. the intermittency shock in the previous section.

Increasing the demand flexibility furthermore increases the producer price for intermittent plants. As discussed in the previous section as well, intermittent plants are characterized by a downlift of roughly 36 DKK/MWh, implying that they produce more in low-price hours. Thus we expect that the flexible demand re-allocates towards these hours, driving up the equilibrium prices. Interestingly, part (b) of figure 11.4 shows that the producer price for intermittent plants only increases in the demand flexibility scenario, when k is 40 or larger. Part (a) of the figure reassuringly illustrates that the yearly average producer price for all plants decreases significantly more than for intermittent plants. Thus the the downlift for intermittent plants still decreases for all k. In quantitative terms it is the general trend that the *reduction* in the downlift for intermittent plants increases with k. Section 14 discusses ways that can potentially remedy the issue of dampened intermittency in aggregated models in future work.

Figure 11.3: Effects of increased demand flexibility

(a) Domestic prices

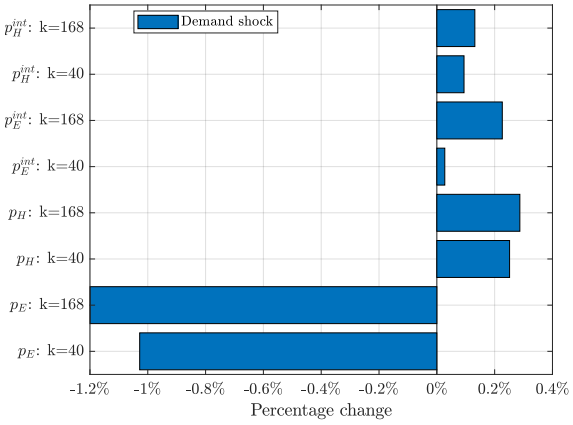

(b) Domestic energy consumption and net exports of electricity.

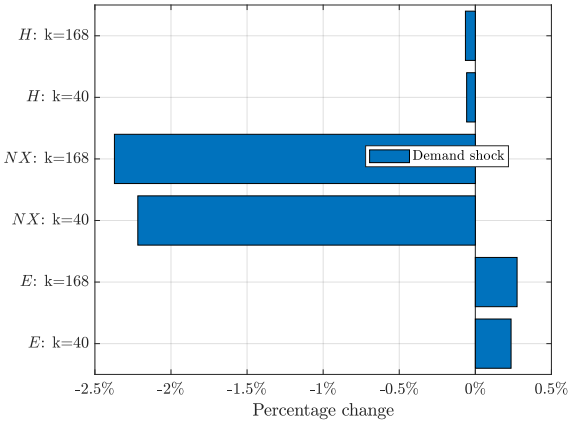

(c) Domestic fuel consumption

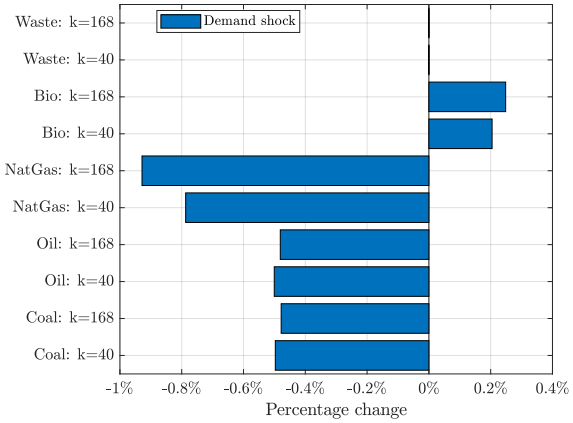

(d) Domestic CO_2 emissions

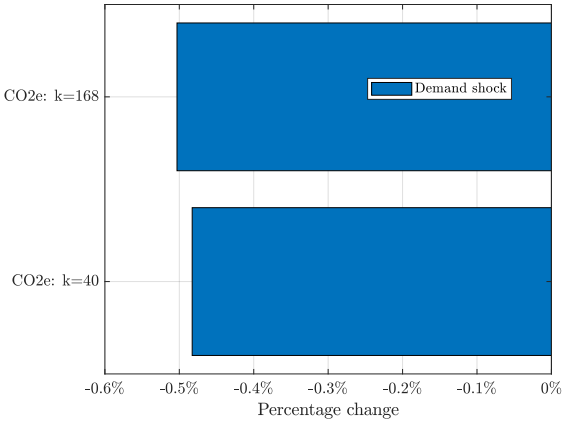

Figure 11.4: Change in yearly electricity prices in demand flexibility scenario.

(a) Yearly average consumer price

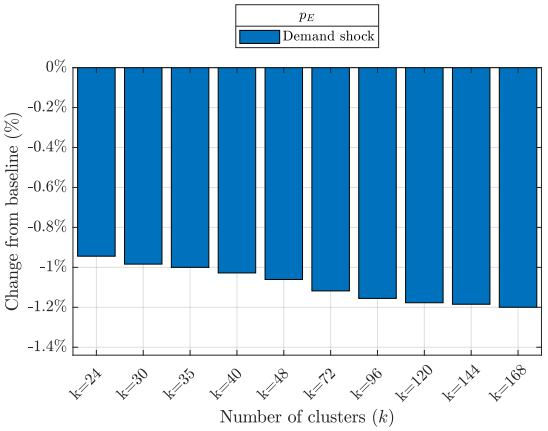

(b) Yearly average intermittent producer price

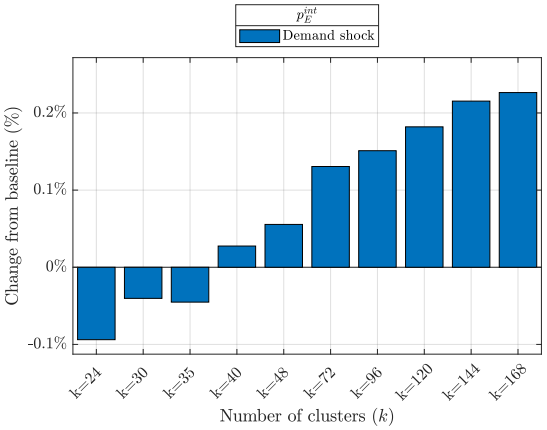

Finally part (a) in figure 11.3 also illustrates that the yearly average price level on heating increases slightly as a result of the lower electricity prices. The intuition for these dynamics is identical to the one given in the previous section 11.3.

Part (b) in figure 11.3 illustrates the effect on consumption and trade. With the simple TD demand functions applied here, the changes in consumption of electricity and heating follow mechanically from the changes in yearly average prices. Interestingly, the net export decreases by 2.2-2.4%. This is not straightforward to explain, but essentially hinges on the non-linearity of the trade function, implying that the marginal effect of a change in demand on trade is close to zero in some regions. To see this, consider initially the states where electricity prices are relatively low domestically. The increased flexibility reallocates more demand towards these states. Roughly speaking, the low electricity prices can either be due to cheap supply from domestic or foreign plants. If this is driven primarily by cheap domestic electricity, the consumption of this increases and the export of electricity is likely to decrease as well, unless export is already at full capacity. If the low price state is due to cheap foreign electricity, import of electricity will increase as long as the import capacities are not fully utilized yet. Thus we expect net export to decrease in these states. Second consider the states, where electricity prices are relatively high domestically. the increased flexibility lowers the domestic demand for electricity in these states. The high electricity prices can either be because (1) both domestic and foreign electricity is expensive, or (2) because domestic electricity is expensive and import capacity is fully utilized. In the first case, it is not clear whether net export should increase or decrease, when domestic demand drops. This is because both domestic and foreign plants can be the marginal plant in our framework. If domestic and foreign prices are both high it indicates that transmission capacities are not binding. A decrease in demand can therefore imply both an increase and a decrease in net exports, depending on which plant is the marginal plant. In the second case, it is the domestically produced electricity that is expensive and drives up the equilibrium price. To see this, recall that relatively high domestic prices implies that import capacities are binding. Thus when demand drops, it is primarily domestic production of electricity that is crowded out and not the import. To sum up, the increased domestic demand flexibility, is likely to increase import or lower export of electricity, in hours where prices are low, thus driving down net exports. However, it is not clear whether net export increases or decreases in states, where electricity prices are high.

Part (c)-(d) in figure 11.3 confirms the result from the previous section: When the domestic electricity prices decrease, it is primarily supply from plants using natural gas, oil and coal that is reduced. This results in lower CO_2 emissions, although the effects are small.

11.5 Increased capacity for energy storage

To examine the effects of increased capacity for energy storage, we exogenously increase the generation and storage capacity of already existing domestic heat storage technologies by 300 %.[101] The district heating sector in Denmark includes technologies for short and long term storage (Danish Energy Agency,

[101] There are currently no electricity storage technologies of significant size available in Denmark. Thus we chose to perform the shock to the heat market instead.

2013). In our model, however, we do not distinguish between the two types. The effects of the shock are shown in figure 11.5.

Figure 11.5: Effects of increased capacity for heat storage

(a) Domestic prices

(b) Domestic consumption and net-export of electricity

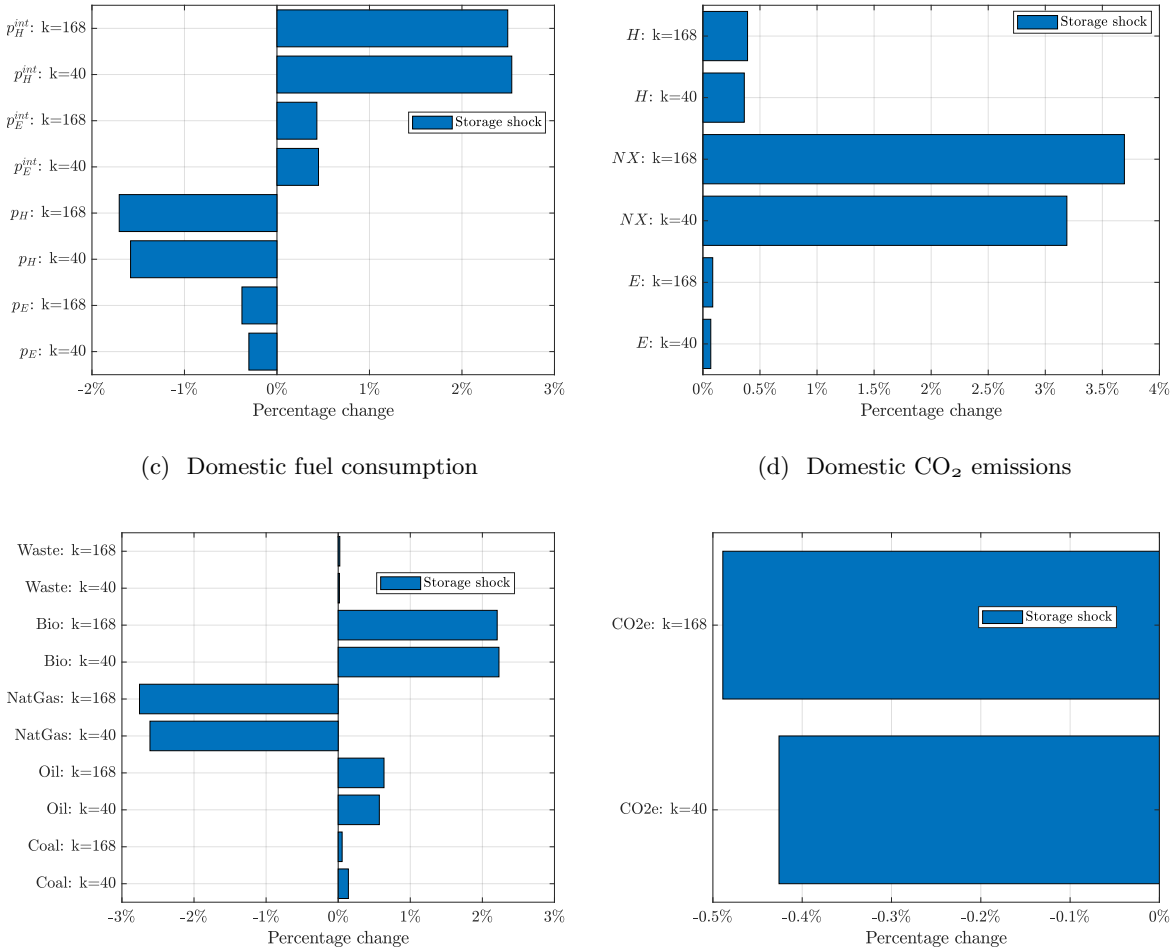

(c) Domestic fuel consumption

(d) Domestic CO_2 emissions

Part (a) of figure 11.5 illustrates the effect on domestic equilibrium prices. Note initially that the increased ability to store heat, entails lower prices on heating in the range of 1.5-1.7%. Here, prices decrease because storage technologies are storing (buying) heat in low price states and dispatching it in high price states. Given that they are net consumers of heat they are not able to dispacth as much heat as they are buying. Consequently, average prices decrease. Furthermore, note that the price decrease might seem unreasonably small compared to the 300% increase in storage capacity. We see three main reasons for the small magnitude: Firstly, the intermittency of heat production is quite low, compared to the electricity market. Recall from section 3.2 that the CO_2 reductions achieved from the district heating sector was primarily due to increased use of biomass and much less due to solar heating. Thus, there is no significant intermittency in production for the storage plants to smooth out. The reason why there is an effect, however, is the variation in demand, which exhibits both seasonal and daily cycles. Secondly,

there is already a significant capacity of heat storage available in the Danish district heating sector. Thus the largest fluctuations in heat prices have already been smoothed out, by the existing capacity. Thirdly, the Danish district heating system has a very large capacity from dispatchable plants, compared to the level of demand (Danish Energy Agency, 2017a). In our model the variance of the marginal costs across these plants is relatively small; consequently, the supply of district heat is very price elastic around the equilibrium price.

Importantly part (a) of figure 11.5 also shows that the increased storage capacity, increases the equilibrium price for intermittent heat plants at around 2.2-2.3%. Recall from the baseline in section 11.2 that intermittent heat production experiences a significant downlift, with prices roughly 15-30 DKK/MWh lower than the yearly average prices. Note that heat storage plants are essentially a part of the demand side when prices are low, and part of the supply side when prices are high. Thus the increased capacity effectively increases demand in hours where production of solar heat production is high, thus driving up equilibrium prices. Finally part (a) of figure 11.5 illustrates that the same pattern is evident for electricity, albeit more dampened: Average electricity prices drop slightly, whereas intermittent producers receive slightly higher prices. Thus, albeit the magnitudes are relatively small, the effect of more storage capacity is generally lower prices and mitigation of intermittency through a reduced downlift for intermittent producers.

Part (b) of figure 11.5 shows that with the lower electricity and heat prices, the consumption of both energy goods increase. Furthermore, as domestic electricity becomes cheaper, net exports of electricity increases. Part (c) of figure 11.5 shows that when it comes to the supply of district heat, the marginal supply in high price states comes primarily from dispatchable plants that use natural gas in production. In turn the increased production in low price states, comes primarily from dispatchable plants using bio fuels. Albeit the use of coal and oil slightly increase, the net effect is still that CO_2 emissions decrease in this scenario.

11.6 Expansion of network capacity for trade in electricity

In the final counterfactual scenario, we exogenously increase the network capacity for trade in electricity. Specifically, the transmissions line connection between DK-West and the Netherlands planned for 2020 is opened. Before proceeding to the results, we briefly note that electricity prices in Netherlands have not been calibrated. In the baseline run the prices are significantly higher than Danish electricity prices. While the price has not been calibrated, this price differential is realistic; it is mentioned as one of the main reasons for constructing the transmission line in the first place.[102] Figure 11.6 sums up the effects of the *trade shock*.

As expected the additional trade partner with higher electricity prices increases the domestic prices significantly with roughly 5%, cf. part (a) of figure 11.6. Interestingly the price received by intermittent technologies increases by almost 7%. The reason for this increase is that the correlation between wind production in Denmark and The Netherlands is quite low; in fact this is one of the other main reasons

[102] See the project sheet for the COBRA cable here: `https://tyndp.entsoe.eu/tyndp2018/projects/projects/71`.

Figure 11.6: Effects of increased network capacity in electricity trade

(a) Domestic prices

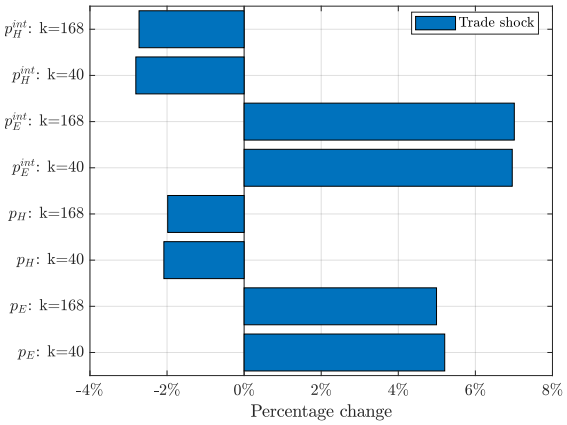

(b) Domestic consumption and net-export of electricity

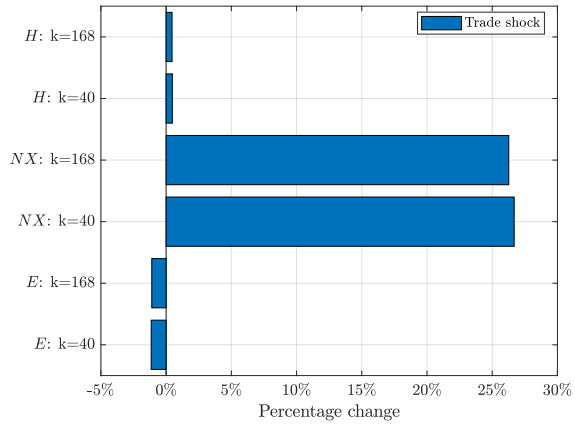

(c) Domestic fuel consumption

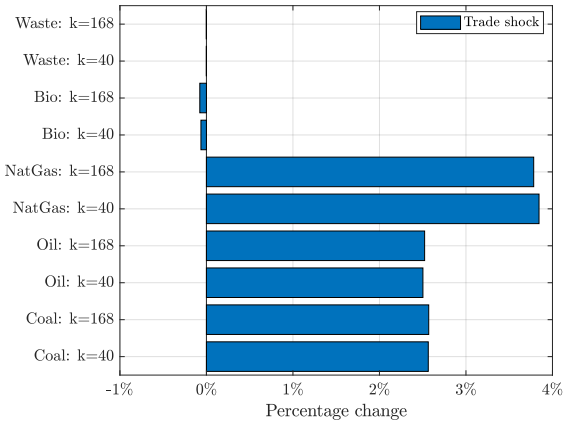

(d) Domestic CO_2 emissions

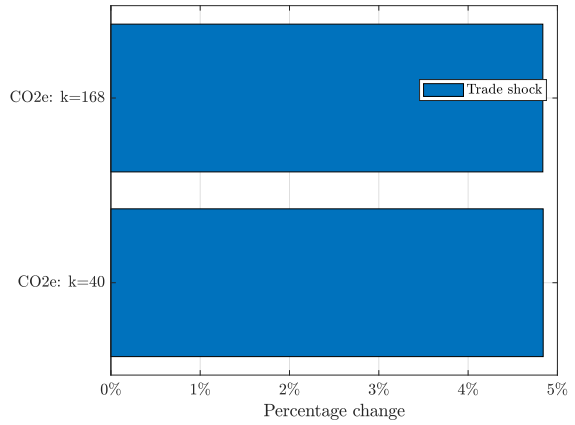

for construction of the transmission line. Part (a) of the figure finally illustrates that the price on heat is driven down. This is the same dynamic as explained in sections 11.3-11.4.

Part (b) of figure 11.6 illustrates that the transmission line to a high price area, increases the net exports dramatically by more than 25%. As our simulation experiment is carried out in the static BU model, this additional production is covered by dispatchable domestic plants. Part (c) of figure 11.6 illustrates that when prices increase in general, the idle capacity is mostly found in plants that use natural gas, oil and coal. Thus the result in this static model is a quite significant increase in CO_2 emissions as illustrated in part (d) of figure 11.6. Note, however, that this result is not likely to prevail in a dynamic model with endogenous investment behavior: As part (a) of the figure clearly illustrates, the added trade capacity significantly increases the value of domestic intermittent plants. This is particularly the case when the correlation between the two areas' intermittent production is low, as is the case for the Netherlands and Denmark. Thus, while the connection to a high price electricity area at a first glance increases the CO_2 emissions, the simulation experiment carried out here suggests that it is highly efficient in mitigating the costs of intermittency.

11.7 Savings in computational cost from aggregating the model

Besides providing information on how effective various tools are in mitigating the costs of intermittency, the previous sections show that aggregating the model, to include only around k=40 short run states instead of e.g. k=168, yields highly similar results. We end this part of the paper by briefly illustrating, why it is so essential to achieve a well-fitted model with a low number of k states. Figure 11.7 shows the time it takes to carry out the various counterfactual scenarios in the model with k=40 and k=168. For all four scenarios, the decrease in computational time is at least 75%. In particular for the large increase of intermittent electricity production, the computational time required to solve the model is more than an order of magnitude larger for k =168 compared to k =40. Once again, we reiterate that running a model in 300 seconds is not in itself an issue. The problem comes when the model is to be dynamic, in which case the curse of dimensionality kicks in.

As mentioned throughout the sections in this part, there are features of the aggregation scheme that are unsatisfactory at the current stage; including the fact that the downlift for intermittent producers of electricity is not sufficiently large. The next part discusses avenues for future work, amongst other things in this area.

Figure 11.7: Computation time of k =168 and k =40.

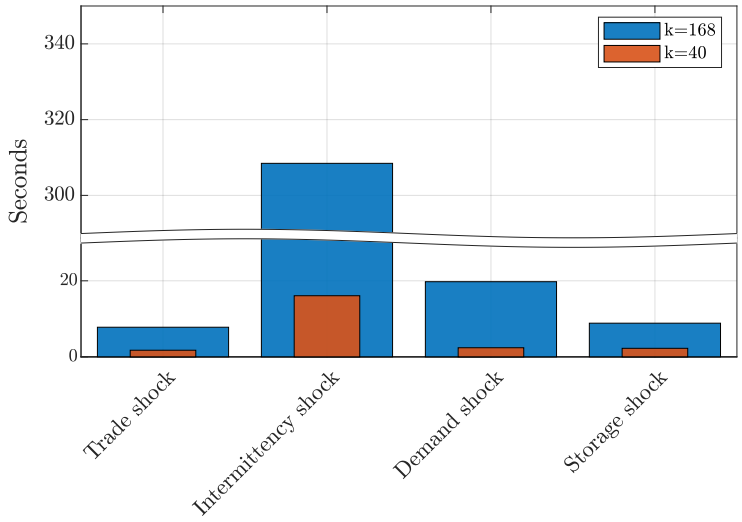

Part IV

Future work and model prospects

This part outlines the path for future work in the model. While a large part of this is naturally focused on linking the BU module to a CGE model, there are a few unresolved issues that need to be addressed in future work, in particular the aggregation of the model into fewer states. Finally, this part includes a section on possible extensions to the model that could be of interest.

12 Investment in electricity and heat producing firms

The BU module developed in part II takes the existing capacity of various plants as given. In this section the investment and maintenance decision of plants is explained. While investment decisions have not been implemented in the model yet, the section shows how the level of detail enables us to use expert information from technology catalogues and energy system models in determining investment in capacity. Furthermore, the presentation of investment decisions points exactly to the links needed to couple the model to a CGE model.

With the level of detail on existing plants, the endogenous investment decisions can be modelled quite detailed. It can depend on the composition of various competing technologies, taking into account the variations in their productivity throughout a year. It can depend on the effectiveness of mitigating the effects of intermittency; either through flexible demand, storage capacity, or trade. Furthermore, the investment decision can depend on the current stock of existing plant capacity. For example, if the economic viability of e.g. coal-fired power plants ends in 2025, such that a plant owner is better off scrapping the plant rather than supplying in the short run, investments to replace this body of capacity can be undertaken in advance in more economically profitable technologies. Finally, with the current

level of detail the model can use *expert information* in the calibration of technology-specific capacities.[103]

12.1 Existing plants, scrapping decision, and re-investments

The BU-module computes on a plant-specific level the total yearly revenue and short run costs associated with its production. For a plant i that is scheduled to be decommissioned in T_i years, leaving the plant operational for the entire horizon, yields the discounted profits from time t an on wards:

$$D_t^i = \sum_{j=0}^{T_i} R_{t+j}\pi_{t+j} \tag{56}$$
$$\pi_{t+j} = E_{t+j}^i \left(p_{t+j}^i - \mathbf{c}_{t+j}^i\right) - FC_{t+j}^i.$$

where R_{t+j} is the accumulated discount factor, $E_{t+j}^i p_{t+j}^i$ is the plant-specific revenue computed from the BU-module, $\mathbf{c}_{t+j}^i$ denotes the short unit costs of production (including taxation) and FC_{t+j}^i is a yearly operational and maintenance cost that is not included in the hourly supply decision, but influences the sum of discounted dividends D_t^i.[104] The optimal timing for scrapping a plant is in principle a discrete-choice problem that is not suited for a standard CGE model. Furthermore, some types of plants can be re-purposed. Thus, they face a third option of investing in order to e.g. increase efficiency or to be able to use a different fuel input in production.

12.1.1 Rule-of-thumbs for optimal scrapping-decision

Assume that a plant of type τ has a scrapping value per capacity (q) of V_t^τ in year t. If energy prices are increasing and the short run costs of the existing plant are relatively constant, potential benefits of not scrapping the plant lies in the future. In this case it suffices to compute whether or not long run profits are larger than the scrapping value today. Alternatively, if energy prices are known to decrease in the future, the largest benefits from not scrapping the plant occurs in the beginning of the planning horizon. In this case it suffices to compute whether or not current profits are higher than the scrapping value today. Consequently, we get the simple scrapping decision

$$\text{Scrap at time } t \text{ if:} \quad \begin{cases} \text{output prices are increasing over time:} & D_t^i < q_t^i V_t^\tau \\ \text{output prices are decreasing over time:} & \pi_t < q_t^i V_t^\tau \end{cases},$$

where a more robust rule would require both to hold before scrapping the plant. For the ad-hoc rules to be applicable, however, we need to assume a monotonicity in the stream of profits over time; either profits are primarily in the first or the last periods of the planning horizon. One way to apply the endogenous scrapping decision in our CGE model, using one of the two ad-hoc rules is to include a law of motion for

[103] We use 'expert information' loosely to refer to bodies of information collected e.g. in technology catalogues on expected potential for technologies, or information provided by simulations from technical models.

[104] For existing plants we have a variable from the technical data FOM that informs us on the size of this variable.

existing plants on the form:

$$q^i_{t+1} = \begin{cases} q^i_t \Phi\left(\frac{\pi^i_t - q^i_t V^\tau_t}{\sigma}\right) & \text{for } t+1 < t_0 + T_i \\ 0 & \text{for } t+1 \geq t_0 + T_i \end{cases},$$

where t_0 is the base year of the model. We note that if we expect electricity prices to be increasing (relative to short run costs) the decision should ideally include D^i_t in place of π^i_t.

12.1.2 Re-purposing the plant: From coal to biomass fired power plants

Existing plants can alternatively be rebuild, for instance in order to use a different fuel-mix input. As with the scrapping decision, this is essentially a discrete-choice problem that is not suited well to run inside a CGE model. Similarly to the scrapping decision, we can find well-suited rule-of-thumbs to represent the optimal discrete choice, if we are able to conclude whether the profitability of the existing plant relative to a rebuilt one is largest in the first or last periods of the relevant time horizon.

In the case of rebuilding a coal-fired power plant to a biomass-fired one, we expect the relative profitability of the biomass to be increasing over time.[105] The decision to rebuild the power plant, however, then depends on two criteria: (i) The first year in which the short run profits are larger for a biomass-fired power plant and (ii) whether the gain exceeds investment costs. Rebuilding a plant at time t at the investment costs I^τ_t per unit of capacity q^i_t then yields the dividends

$$D^{i,rebuild}_t = \sum_{j=0}^{T_i^{rebuild}} \left(R^i_{t+j}\pi^{i,rebuild}_{t+j}\right) - q^i_t I^{bio}_t,$$

where I^{bio}_t denotes investment costs per capacity unit for rebuilding the plant. Note that rebuilding the power plant, with the purpose of using biomass instead of coal, is usually combined with an extension of the plant's lifetime. Thus, the time horizon in $T^{rebuild}_i$ is not the same is the one that enters D^i_t. This means that we should ideally also take into that the lifetime of the coal plant could be extended, i.e. the value of rebuilding should not be compared to D^i_t, but rather:

$$D^{i,coal}_t = \max\left\{\sum_{j=0}^{T_i^{rebuild}} \left(R_{t+j}\pi^{i,rebuild,coal}_{t+j}\right) - q^i_t(1+r_t)I^{coal}_t,\ D^i_t\right\}.$$

Under the assumption that the relative profitability of the biomass plant increases over time, the following decision rule captures the optimal timing as well:

Rebuild at some $t+j$ **if**:	$D^{i,rebuild}_t - D^{i,coal}_t - q^i_t\,(1+r_t)\,I^{bio}_t \geq 0$
and at time $t+j$ **when**:	$(\pi^{i,rebuild}_{t+j} - \pi^i_{t+j}) \geq 0$

[105] When prices of coal and biomass are forecasted by IEA, the relative price of coal and biomass inputs are almost constant over time. With an increasing tax on emissions, we expect biomass' profitability to increase relative to coal. This outlook can, however, change with regulation of the sector, in particular if there is put further restrictions on what is considered *sustainable* use of biomass.

This decision rule states that the plant should be rebuild if the current profits are larger for a biomass plant, and the payoff from rebuilding the plant to a biomass plant exceeds investment costs as well as the alternative cost of the investment. This decision rule is still relatively complex, compared to how investment decisions are made in standard CGE models. Thus, we might need to simplify the decision rule even further in future work.[106]

In the scrapping decision, the decision rule can be caught relatively straightforward in the law of motion for the plant. In the case of rebuilding a coal-fired power plant into a biomass-fired one, this is not as straightforward. The problem is that we need to circumvent the irreversible discrete-choice of *rebuild if*, in a way that involves only smooth and differentiable functions. In other words, once the decision has been made to rebuild the plant, the decision rule is no longer valid. This entails that if the inequality in the decision rule reverse at a later time, the plant should not be rebuild back into a coal-fired plant. One way of ensuring this is to model all coal-fired power plants, which are eligible for being rebuild as biomass-fired plants, with both a coal capacity $q_t^{i,coal}$ and a biomass capacity variable $q_t^{i,bio}$.[107] We let q_t^i be the exogenous installed capacity in coal in the baseline year of the model. The decision to irreversibly invest could then be made on the basis of the mapping:

$$
\begin{aligned}
q_{t+j}^{i,bio} &= q_t^i \Phi \left(\frac{D_{t+j}^{i,rebuild} - D_{t+j}^{i,coal} + \left[q_{t+j-1}^{i,bio} - q_{t+j-1}^{i,coal} \right] (1 + r_{t+j}) I_{t+j}^{bio}}{\sigma} \right) \\
q_{t+j}^{i,coal} &= q_t^i - q_{t+j}^{i,bio},
\end{aligned}
$$

for $j > 0$. Note that for $j = 1$ we nest the decision rule outlined above for $\sigma \to 0$. If the plant is rebuild entirely then $q_{t+j}^{i,bio}$ is approximately q_t^i and $q_{t+j}^{i,coal}$ is near zero. Due to the endogenous weighting in the subsequent period, the investment cost I_{t+j}^{bio} now represents a cost of switching back from biomass to coal. In this way the investment decision becomes *de facto* irreversible, at least for σ appropriately close to zero.

12.2 Investment and construction of new plants

12.2.1 Construction of new plants with known lifetimes

On the basis of technology catalogues a number of technology-specific discounted profit functions are computed as in (56). Investments are assumed to be a continuous variable that produces new capacity (q) according to some capital production function. The production of new capacity is currently made with a one-period lag, as is the convention in homogeneous capital formation models.[108] Investments undertaken at time $t-1$ thus results in a plant of size q_t^τ at time t, where τ refers to the specific technology.

[106] Some of the possible simplifications we have considered are: (1) Drop the second constraint on $(\pi_t^{i,rebuild} - \pi_t^i)$. The first inequality automatically includes this if the development in relative profitability is somewhat stable over time. (2) Approximate the sum in the first inequality imposing $\pi_{t+j}^i \approx \pi_t^i$ for both the rebuild and not rebuild plant. With exponential discounting this gives a very simple decision rule.

[107] In the technology catalogue published by the Danish Energy Agency this includes coal-fired extraction and back-pressure plants. While the number of these coal-fired plants is relatively small, they still supply a relatively large share of the supply.

[108] It could be advantageous to implement a *time to build* lag in the model, resulting in longer time horizons than one before the capacity is realized. We leave this for future work as well.

This investment generates short run profits just as existing plants given by:

$$D(q_t^\tau) = q_\tau \sum_{j=0}^{T_\tau} R_{t+j}\pi_{t+j}^\tau \left(p_{t+j}^\tau\right) \tag{57}$$
$$\pi_{t+j}^\tau = E_{t+j}^\tau \left(p_{t+j}^\tau - \mathbf{c}_{t+j}^\tau\right) - FC_{t+j}^\tau$$

where R_{t+j} is the accumulated discount factor. This consists of the product of year-specific factors, i.e. we can decompose it into year-specific discount factors β_t:

$$R_{t+j} \equiv \prod_{i=0}^{j} \beta_{t+i}.$$

Note that from the perspective of the investor, the discounted sum of short run profits is linear in the size q_t^τ. Furthermore, note that the average/marginal short run benefits D/q can be written recursively as:

$$\left(\frac{D}{q^\tau}\right)_t = \pi_t^\tau + \beta_{t+1}\left(\frac{D}{q^\tau}\right)_{t+1} - \beta_{t+T_\tau+1}\pi_{t+T_\tau+1}^\tau. \tag{58}$$

With this in mind, investment costs must be formulated such that new capacity is build in a reasonable pace. Furthermore, investment costs are modelled such that unprofitable technologies can endogenously be shut down in the model.[109] To allow for shutting down investments entirely, we add a fixed cost component to an otherwise standard quadratic installation cost function:

$$C_t(q_t^\tau) = p_t^{I,E}\left(c_f^\tau \mathbb{I}_{q_t^\tau>0} + c_1^\tau q_t^\tau + \frac{c_2^\tau}{2}\left(q_t^\tau\right)^2\right), \qquad \mathbb{I}_{q_t^\tau>0} = \begin{cases} 0, & q_t^\tau \le 0 \\ 1, & q_t^\tau > 0 \end{cases}, \tag{59}$$

The coefficients $c_f^\tau, c_1^\tau, c_2^\tau$ are technical parameters, whereas $p_t^{I,E}$ is an investment cost price in the energy sector. Maximizing (57) minus investment costs in (59) leads to the optimal investment behavior:

$$(q_t^\tau)^* = \begin{cases} 0, & \text{for } \dfrac{D(q_t^\tau)}{q_t^\tau} < \vartheta^\tau \\ \dfrac{1}{c_2^\tau}\left(\left(\dfrac{D(q_t^\tau)}{q_t^\tau}\right)/p_t^{I,E} - c_1^\tau\right), & \text{for } \dfrac{D(q_t^\tau)}{q_t^\tau} > \vartheta^\tau \end{cases}, \qquad \vartheta^\tau \equiv p_t^{I,E}\left(\sqrt{2c_f^\tau c_2^\tau} + c_1^\tau\right). \tag{60}$$

The solution describes how the size of the plant must be of a particular size before breaking even, which is due to the fixed investment cost c_f^τ. Note that this investment rule involves a linear function with slope 0, until it reaches the discontinuity around ϑ_t^τ, after which the slope changes from zero to $1/c_2^\tau$. To model this in a flexible and smooth manner, we use two approximation functions. First, we split up the investment function into the smoothed jump part, as well as a piece-wise linear part:

$$(q_t^\tau)^* \approx \sqrt{2c_f^\tau/c_2^\tau} * \Phi\left(\frac{(D/q^\tau)_t - \vartheta_t^\tau}{\sigma}\right) + f\left(\frac{D}{q_t^\tau}\right),$$

[109] As is the general case of the model, the decision will not be a discrete one; rather we model a non-linearity that makes unprofitable technologies shut x% down, where the modeller can let x tend to 100% at the cost of an increased solution time.

where $f(\cdot)$ is a piece-wise linear function on the form

$$f\left(\frac{D}{q_t^\tau}\right) = \begin{cases} 0, & \frac{D}{q_t^\tau} \leq \vartheta_t^\tau \\ \frac{1}{c_2^\tau}\left(\frac{D}{q_t^\tau} - \vartheta_t^\tau\right), & \frac{D}{q_t^\tau} > \vartheta_t^\tau \end{cases}$$

The piece-wise linear part is then approximated as:

$$g\left(\frac{D}{q_t^\tau}\right) = -\frac{\vartheta_t^\tau}{2c_2^\tau} + \frac{1}{2c_2^\tau}\left[\frac{D}{q_t^\tau} + \sqrt{\left(\frac{D}{q_t^\tau} - \vartheta_t^\tau\right)^2 + \epsilon^2}\right].$$

Appendix J provides some information on how kinks in piece-wise linear functions can be smoothed. The approximation error from the smoothed kink function is largest around the kink, with an error of $\epsilon/(2c_2^\tau)$. Consequently, the error tends to zero for $\epsilon \to 0$.[110] The approximate investment rule is thus defined by:[111]

$$(q_t^\tau)^* \approx \sqrt{2c_f^\tau/c_2^\tau} * \Phi\left(\frac{(D/q^\tau)_t - \vartheta_t^\tau}{\sigma}\right) - \frac{\vartheta_t^\tau}{2c_2^\tau} + \frac{1}{2c_2^\tau}\left[\frac{D}{q_t^\tau} + \sqrt{\left(\frac{D}{q_t^\tau} - \vartheta_t^\tau\right)^2 + \epsilon^2}\right]. \tag{61}$$

We highlight three advantages of this investment rule: First, it is based directly on discounted sum of profits computed in the BU module. In this way it deals with the concerns voiced by Joskow (2011) and others with only using levelized cost of energy (LCoE) as a metric to compare profitability of different technologies. Second, by appropriately adjusting parameters, the researcher can obtain the standard quadratic installation cost function ($c_f = 0$) to increase computational speed, or smoothly approach the fixed cost discrete choice case that allows for corner solutions ($\sigma, \epsilon \to 0$). Third and final, the technical parameters (c_f, c_1, c_2) can be used to influence investment behavior to conform to 'expert' information (see section 12.2.3).

12.2.2 Construction of new plants with constant depreciation rates

The presentation of investment in new plants implies the same structure of depreciation as that of existing plants: The capacity of a plant i stays constant for T^τ periods and then drops to zero. In other words,

[110] The modeller should be aware that, compared to the normal-smoothing of jumps, the kink-smoothing function applied here, has far heavier 'tails'. Thus, even for relatively large values of σ in the normal smoothing function, the approximation error goes relatively fast to zero, when we move away from the threshold around which the jump occurs. This is not the case for the kink-smoothing variable ϵ. Therefore, ϵ should be kept appropriately low throughout the analysis.

[111] An alternative version is the multiplicative one where

$$g\left(\frac{D}{Q^\tau}\right)_t = -\frac{c_1}{2c_2} + \frac{1}{2c_2}\left[\left(\frac{D}{q^\tau}\right)_t + \sqrt{\left(\left(\frac{D}{q^\tau}\right)_t - c_1^\tau\right)^2 + \epsilon^2}\right].$$

and

$$(q_t^\tau)^* \approx \Phi\left(\frac{(D/q^\tau)_t - \vartheta_t^\tau}{\sigma}\right) g\left(\frac{D}{q^\tau}\right)_t.$$

In this version the kinked function starts increasing from zero approximately around c_1^τ. The level is however generally dampened by the smoothed jump-function as well.

we have the very simple structure:

$$q^i_{t+1} = \begin{cases} q^i_t, & t - t_0 \leq T^\tau \\ 0, & t - t_0 > T^\tau \end{cases},$$

where t_0 is the time of construction. In CGE models the convention is that capital, in general, is assumed to depreciate with a constant factor δ each year. This may be preferred due to its simplicity. As in the previous section, the fundamental value of a firm investing in technology τ is still given by the discounted sum of dividends. Here, dividends consist of short run profits minus the investment- and installation costs. For a firm investing in new capacity in technology τ each year, the relevant Lagrangian function is straightforwardly given by:

$$\mathcal{L}_t = \sum_{s=t} R_s \Big[Q^\tau_s \pi^\tau_s \left(p^\tau_s\right) - C^\tau_s \left(q^\tau_s\right) + \lambda^\tau_s \left(q^\tau_s + (1-\delta^\tau) Q^\tau_{s-1} - Q^\tau_s\right) \Big], \tag{62}$$

where Q^τ_t denotes the total capacity of technology τ at time t and λ^τ_s is the shadow value of capacity. Note that because we per definition start with zero new plants, we have $\mathcal{Q}^\tau_{t_0} = 0$ in the baseline year t_0. The short run profits $\pi^\tau_s(p^\tau_s)$ are still determined in the BU module and given as in equation (57). With the constant depreciation rate, however, the recursive formulation of average discounted dividends become much simpler:

$$\begin{aligned} \left(\frac{D}{q^\tau}\right)_t &= \sum_{j=0}^{\infty} R_{t+j} (1-\delta^\tau)^j \pi^\tau_{t+j}(p^\tau_{t+j}) \\ &= \pi^\tau_t \left(p^\tau_t\right) + \beta_{t+1}(1-\delta^\tau) \left(\frac{D}{q^\tau}\right)_{t+1}. \end{aligned}$$

The optimal investment scheme then follows the same rule as in equation (60) and can therefire be smoothed in the same way as in equation (61).[112]

12.2.3 Using expert information and imposing bottom-up restrictions

The cost parameters of the investment function in (61) should be identified using technical/expert information. Here we briefly outline how to apply information, e.g. from a technology catalogue as the one available from the Danish Energy Agency (2016), to identify the parameters. Note that the investment function is constructed, such that it is linear once the average dividends exceeds the threshold ϑ^τ_t. The slope of this linear part is determined by c^τ_2. Thus, this parameter informs us on the rate a profitable technology penetrates the market. This type of installation cost parameters are currently used in standard CGE models.[113]

Secondly, the investment function has the feature that capacity is approximately zero as long as the average dividend is lower than the the threshold ϑ^τ_t. Let $\underline{q}$ denote the investment size around this

[112] The discounted sum of profits corresponds to the shadow value of capacity in (62). We arrive at the exact same investment rules by maximizing (62) with respect to q_s and Q_s and recalling that the cost function $C^\tau_s(q^\tau_s)$ is not continuous in q around 0. The investment rule in (60) is derived by comparing $\mathcal{L}_t(q_s = 0) - \mathcal{L}_t(q^*_s)$ with q^*_s, denoting the optimal choice of q_s conditional on $q_s > 0$.

[113] An example of this is the new MAKRO model for the Danish economy (The MAKRO modelling Group, 2018).

threshold, for which investments start to increase:

$$\underline{q}_t^\tau = \sqrt{c_f^\tau/(2c_2^\tau)} + \epsilon/(2c_2^\tau).$$

Given c_2^τ the fixed cost level, c_f^τ , can be calibrated to reflect this level. Most of the technologies described in the technology catalogue includes a *typical capacity*, referencing a minimum level. Furthermore, the technology catalogue includes estimates of the investment costs per capacity of the different technologies. Let $\bar{C}_t^\tau$ be the investment costs reported for an investment of size $\underline{q}^\tau$ in the given technology. The parameter c_1^τ can then be determined by

$$\bar{C}_t^\tau = \left(c_f^\tau + c_1^\tau \underline{q}_t^\tau + \frac{c_2^\tau}{2} \left(\underline{q}_t^\tau \right)^2 \right).$$

With this calibration, a technology type τ would then shut down whenever the discounted sum of dividends from the BU module does not cover the investment costs as reported in the technology catalogue.

Finally, the framework presented here allows for a straightforward implementation of bottom-up capacity restrictions. In energy system models it is standard to impose an overall potential restriction on some technologies. The reason for this is that for most energy technologies, some essential input factor can be considered scarce. As an example, consider the hydro power plants of Norway and Sweden. The plants are in many ways hugely profitable; they provide renewable energy relatively cheap and often with storage options, thus not subject to intermittency. However, the scarce resource of suitable locations for such plants in Denmark implies that there should not be significant investments in increasing the share of hydro power. As the resource of suitable geographical location for a given technology is not straightforward to include, we can instead use more *ad-hoc* approaches to impose the relevant constraints.

13 Links between the bottom-up and top-down model

With the investment specification in place, all the relevant components of the BU module are described. As the BU model is yet to be integrated into a CGE model, we do not include a description of an economic CGE model here. Instead, this section briefly details how the BU and TD models can be coupled in a straightforward fashion.

Figure 13.1 illustrates the basic linking of the BU and TD model, when abstracting from the additional links formed in the dynamic version outlined in section 12. For the BU model to run it needs the input of fuels, labor, and other materials from the rest of the economy. Furthermore, the BU module takes yearly demand of electricity and heating as given. Finally, fuel prices, wages, interest rates, and tax rates are taken as given in the BU module. All of these are, however, are endogenous in the CGE model.[114] With the BU model presented in this paper, including the description of the dynamic investment behavior in section 12, the interactions between the BU and TD models can roughly be summed up by two effects: (1)

[114]Tax rates can of course also be exogenous to the TD model.

Figure 13.1: Illustration of linking between BU and top down model

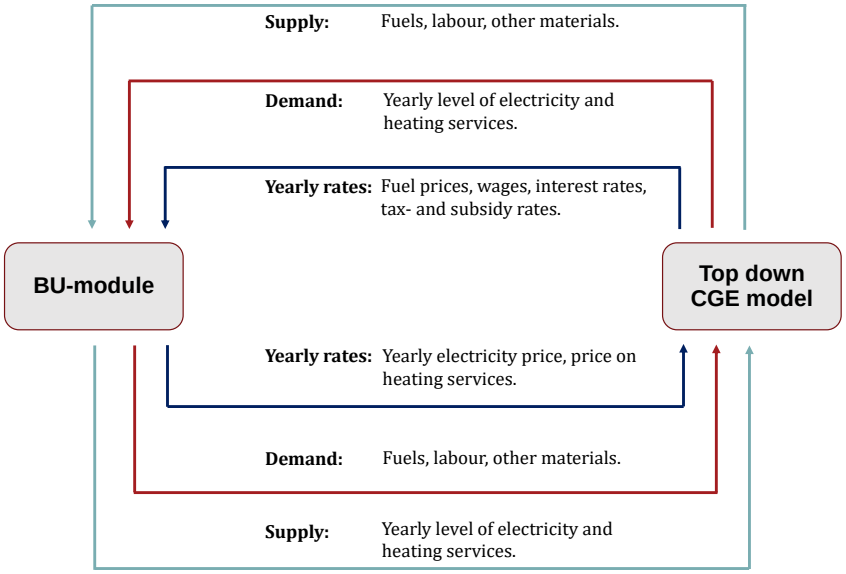

Endogenizing the cost of energy production and (2) feedback effects from energy demand. We comment of these two effects below.

The cost components in the BU module are endogenized: In the BU model the short run costs ($\mathbf{c}_i$) consist of fuel costs, taxation, and other costs (e.g. labour cost). In section 12 we further added a cost component (FC_t) that contains yearly costs of operation and maintenance. Finally, the BU sector incurs costs when it invests in new plants (function $C(q)$ in (59)). When coupling this to an economic CGE model, all of these components become endogenous; the yearly maintenance costs of a plant consists of purchases of materials from other sectors as well as wages to households supplying labor. When investments are undertaken to produce new capacity, this capital is purchased from other various sectors such that the investment price on capacity ($p_t^{I,E}$) becomes endogenous.

Feedback/general equilibrium effects from demand: The BU model deals with intra-year variation of demand for electricity and heating. However, the yearly level of demand should be derived from profit-maximizing firms in other sectors and utility-maximizing households. Some of the straightforward general equilibrium effects, for instance from the introduction of more wind power in the system, is that lower average electricity prices drives up the yearly demand. If the CGE model contains sufficient information on other key sectors such as waste management and transportation, one could imagine other hugely important general equilibrium effects. In the case of transportation, electrification would not only imply an increase in the yearly demand for electricity, but also increase the value of so-called *power-to-X* technologies that produce renewable fuels using electricity. If these technologies in turn become profitable, the value of e.g. intermittent wind power will likely increase, as the peak hours of wind production can then be used to produce renewable fuels that can be stored (Energinet, 2019).

14 Unresolved issues: The aggregation methods

One of the major challenges of constructing the BU model is to reduce the dimensionality sufficiently to enable the integration with a CGE model. However, the reduction of dimensionality is still an unresolved issue at this point. First, in section 9 the dimension of *time* (8760 hours) is aggregated into K representative states. The application of the K-means algorithm is based on the property that the K-means approach efficiently clusters cyclical variation into aggregated representative states. The immediate downside of this approach is, however, that the clustering is not chronological. This poses a problem when it comes to characterizing the behavior of plants with storage capacity, which maximizes profits inter-temporally. As discussed in section 9.3.4, the *state-transition-contingent* aggregation scheme does not sufficiently capture the variation in the state variable (storage level). In the following, a number of potential fixes to the aggregation of time is discussed. Finally, we briefly discuss the potential for aggregating plants into *representative types*.[115]

14.1 Alternative methods of aggregating time

Adjusting the storage plants' behavior

One approach for capturing the development in the storage level is to add the variation in the state variable directly to the plants' solution. Recall that in the version outlined in section 9, the law of motion for the state variable is given by (repeated here for convenience)

$$S_{k_i|k_j} = S_{k_i-1} + f\left(Y_{k_i} - E_{k_i|k_j}\right).$$

The initial level of stored energy, available when entering the state, is defined by the weighted average:

$$S_{k_i-1} = P_{-1,(0,k_i)}S_0 + P_{-1,(k_1,k_i)}S_{k_1|k_i} + \ \ldots \ + P_{-1,(k_k,k_i)}S_{k_k|k_i},$$

where $P_{-1,(k_j,k_i)}$ denotes the probability of transitioning to state k_i from state k_j. The *transition-contingent* aggregation derived the optimal choice of production ($E_{k_i|k_j}$) in state k_i contingent on knowing the subsequent state would be k_j. In the way this is currently modelled, the variables Y_{k_i} and $E_{k_i|k_j}$ are scaled as hourly variables. In other words, if 20 hours are aggregated in state k_i, the choice of production $E_{k_i|k_j}$ is bounded by the **hourly** production capacity (and not 20 times that). This effectively means that difference between the initial level of stored energy (S_{k_i-1}) and the end-of-period stored energy ($S_{k_i|k_j}$), are also scaled as **hourly** changes. Given that the main issue with the aggregation method is the insufficient variation in the state variable (S), this hourly scaling of variables in the law of motion is a potential source to the problem.

Before we simply scale up the law of motion by the number of hours in each state (n_{k_i}), we note that this problem seems less likely if states are aggregated to represent seasonal storage behavior. To see this,

[115] In a dynamic CGE model with an elaborate description of e.g. the transportation, waste management, and agricultural sector, the BU model of the energy system presented here needs to be scaled down further in order for the integrated model to be solved on a standard laptop.

note that by using the definition of $S_{k_i|k_i}$ in the weighted average, defining S_{k_i-1}, we can write:[116]

$$S_{k_i-1} = \frac{1}{1-P_{-1,(k_i|k_i)}} \left[P_{-1,(k_i|k_i)} f\left(Y_{k_i} - E_{k_i|k_j}\right) + \sum_{j\neq i} P_{-1,(k_j|k_i)} S_{k_j|k_i} \right] \tag{63}$$

Consider for example the case where state k_i represents pure seasonal variation, e.g. all hours in winter. In this case there are two states that transitions into winter: The state containing the last hour of fall (1/2190 hours) and winter (2189/2190 hours). In this case the probability $P_{-1,(k_i|k_i)}$ is near one, in which case the hourly scaled variables $(Y_{k_i}, E_{k_i|k_j})$ are scaled up appropriately i.e. by the factor:

$$\frac{P_{-1,(k_i|k_i)}}{1-P_{-1,(k_i,k_i)}} = \frac{2189/2190}{1-2189/2190} = 2189.$$

This suggests that the problem of insufficient variation of the state variable in the aggregated version of the model might be related to how often the state repeats itself, i.e. the value of the scale factor

$$\frac{P_{-1,(k_i|k_i)}}{1-P_{-1,(k_i,k_i)}}.$$

Appendix K shows that in general the state variable can be written on the form

$$S_{k_i-1} = \sum_j \alpha_{j,k_i} f\left(Y_{k_j} - E_{k_j|k_i}\right) + \sum_{j\neq i} \alpha_{j,k_i} S_{k_j-1}, \qquad \text{where } \alpha_{j,k_i} \equiv \frac{P_{-1,(k_j|k_i)}}{1-P_{-1,(k_i|k_i)}}, \tag{64}$$

and where $\sum_{j\neq i} \alpha_{j,k_i} = 1$. This shows that the state variable S_{k_i-1} is a linear combination of other states (S_{k_j-1}) with weights summing to 1, but with weights on the storage decisions $(Y_{k_j} - E_{k_j|k_i})$ with a sum that depends on the scale factor α_{i,k_i}. In appendix K we further show that our aggregation method always dampens the variation in the state variable (the empirical problem we are facing), except for the purely seasonal variation case. Appendix K finally shows that fixing this problem is straightforward, by including exogenous weights (χ_i) in the law of motions:

$$S_{k_i|k_j} = S_{k_i-1} + \chi_i f\left(Y_{k_i} - E_{k_i|k_j}\right), \qquad \chi_i \equiv \frac{n_{k_i}}{1+\alpha_{i,k_i}}. \tag{65}$$

where n_{k_i} is the number of hours in state k_i.[117]

Alternatives to the K-means clustering:

Another alternative is to find a way that aggregates time in a way that ensures chronology. First, there is the possibility of using a constrained clustering that restricts the ordering of hours to be chronological. A popular method for chronological aggregation is conditional inference trees (cTree). Typically, this method is only applicable for univariate models (i.e. models with only one outcome variable) but Hothorn et al. (2006) provides an interesting framework for using cTree with multiple outcome variables readily

[116] Note that S_{k_i-1} does not enter the other $S_{k_j|k_i}$ expressions that are defined by $S_{k_j|k_i} = S_{k_j-1} + Y_{k_j} - E_{k_j|k_i}$.

[117] As an alternative, the weights χ_i could be simply be estimated to fit the variation in the state variable. This ad-hoc approach could provide a significantly better bit, but at the expense that the estimated χ_i's might not be invariant to equilibrium outcomes.

implemented in R - the software we are using for handling data already. As opposed to K-means the cTree method is a *supervised* machine learning algorithm, as it is based on a regression model with both outcome and predictive variables. Consequently, in order to apply the cTree method in the current setting, additional work on setting up a correct regression model for predicting the intra-year variational data is required.[118] The chronological clustering is, however, likely to come with the computational cost of having to add more states (k) in order to capture the *cyclical* intra-year variation, precisely because the clustering is constrained. A second possibility is to let the clustering be less data-driven; for instance by restricting the K-means clustering to hourly categories created by the researcher. One such example could take its basis on the aggregation procedure used in TIMES-DK (Balyk et al., 2019). TIMES-DK consists of 32 clusters within a year. This is illustrated in fig. 14.1. At the top level hours are divided into seasons. At the second level hours are divided into non-work day and work-day. Thus chronology is broken at this level. At the third and final level, hours are divided into four representative states: (A) 'high wind production - low power demand', (B) 'high power demand - low wind production', (C) 'no photovoltaics', and (D) 'rest'. The final clustering also breaks with chronology. We note that a similar procedure can be implemented in the BU module, but where the K-means algorithm is allowed to decide the final four clusters.

Figure 14.1: Time aggregation in TIMES-DK.

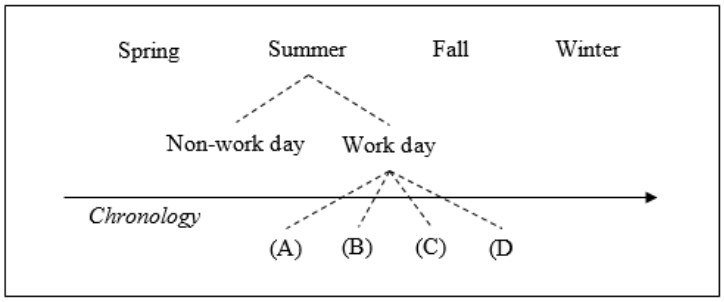

Note: Initially, hours are divided into seasons. In the second level, hours are divided into non-work and work-day. At the third level, hours are aggregated into four representative states: (A) 'high wind production - low power demand', (B) 'high power demand - low wind production', (C) 'no photovoltaics', and (D) 'rest'.

Source: Balyk et al. (2019, p. 16)

Selection of exogenous intra-year variational data:

The selection of the final four clusters in TIMES-DK is only based on domestic data, albeit the model does include exogenous intra-yearly variation in foreign prices as well. In this paper we have stressed the importance of modelling trade realistically: In section 3.2 we showed that the importance of import and export of electricity had grown in recent decades, and section 11 carried out simulation experiments showing the large effects from domestic policies on trade in electricity. In our attempt to aggregate time into k states we therefor use data on both domestic and foreign exogenous hourly variation, as only focusing on domestic intra-year variation might create unrealistic trade patterns. Applying only domestic

[118] For inspiration we refer to appendix G.2 for how such a model could be set up using either harmonic or dummy regressors.

data as in TIMES-DK or a sub-selection of foreign data should therefore be examined with caution. In the current version, however, the K-means algorithm weighs the exogenous variation from all countries equally. There is an argument to be made that at least these weights should be adjusted to reflect that domestic variation is more important for maintaining the degree of intermittency in aggregated models.

Alternatives to the state-transition-contingent aggregation:

An alternative to using both the K-means algorithm and the state-transition-contingent aggregation is to let the time aggregation follow TIMES-DK completely. Even though chronology is broken at two levels in the TIMES-DK clustering, Balyk et al. (2019) assume that plant managers optimize intra-year as if states were chronologically ordered. We note that such an assumption can also be implemented in the current BU module. However, because time is assumed chronological (even though it is not) the connection between clusters and hours are disconnected. In other words, it is not possible to compare the aggregate model to a model with all 8760 hours because it does account for non-chronological ordering. Even so, implementing this assumption could be explored.

14.2 Explaining price drops with outlier states

The previous section focused on how to aggregate the model in order to realistically capture behavior of plants with storage capacity. However, as mentioned in section 11.2, another unresolved issue with the aggregation method is that the model does not sufficiently capture the relevant price drops throughout the year. The average price of electricity received by Danish intermittent plants is roughly 10-25 DKK/MWh higher than the observed level for k between 25-168. However, this average producer price for intermittent plants is decreasing in the number of hourly states (k), suggesting that the problem of price drops is coupled to the chosen aggregation procedure outlined in section 9: The K-means aggregation simply averages out too much of the relevant outlier hours of demand and intermittent energy production.

The suggestion in the previous section 14.1 to put more weight on Danish data on hourly variation, might be one potential solution to this problem. If this is not sufficient, however, one alternative could be to explicitly model *outlier* states. Prior to applying the K-means algorithm, we could manually pick the x% of hours, where domestic residual demand is lowest and collect them in one state, and similarly for the x% with highest domestic residual demand. At the moment when computing yearly variables (e.g. yearly average producer price for intermittent technologies), each k is weighted by the number of hours collected in the relevant state by the K-means algorithm. By including a parameter that adjusts the weight on outlier states, the average yearly price of electricity received by intermittent plants could be added to the list of moments in table 9 that the model is calibrated to. This would guarantee that the model in the baseline scenario replicates the observed downlift in producer prices as discussed in section 11.

14.3 Aggregation of domestic plants

While the discussion above relates to the aggregation of *time*, the model may also benefit from an aggregation of *plants*. A model where all individual plants are explicitly represented allows a huge level of detail. For instance, the BU model can describe relatively old plants' decision on whether to scrap its existing capacity, or update it to reflect new technology standards as explored briefly in section 12. However, there are significant computational gains from aggregating plants into *representative types*. In the static framework presented in this paper, the BU model for 2017 is comprised of roughly 55.000 equations and variables. A dynamic version from 2017-2040 would increase the size of the BU model to around 1.265 million equations. While this is still feasible to solve, the computational costs start to get significant here; so significant that when coupled to a large CGE model it would not be realistic to solve on a standard laptop.

The aggregation of plants should be relatively straightforward: For plants that are of a similar type and use the same fuel mix, the capacity variables should be summed and the technical coefficients averaged.

15 Future extensions to the BU model

15.1 The carbon leakage rate in the transformation sector

One of the features of the BU model outlined in this paper is the detailed description of trade with electricity. In particular, the model includes information on the composition of neighboring plants and the fuel mix they apply in production of electricity. Thus, the structure of the model is well suited to investigate the carbon leakage rate from Danish environmental policies aimed at reducing CO_2 emissions in the transformation sector. Consider for instance a subsidy scheme that increases the investment in Danish wind capacity by $x\%$. As explained in the simulation experiment of the *increased intermittency scenario* in section 11.3, this would significantly lower both domestic and potentially affects foreign electricity prices as well. Furthermore, the net export of electricity would increase significantly, implying that a part of foreign production is no longer competitive. With the framework developed here, we can track which foreign plants are no longer competitive in what hours. In this way the model can simulate the marginal effect on GHG emissions from a domestic environmental policy, including the effect it has on neighboring countries. In this way, simulating the carbon leakage rate can provide an estimate of the *marginal* and not only the *average* carbon leakage rate.

In order to use the model for this purpose, however, two extensions are needed. First of all, while the information on foreign plants are a part of the technical data gathered by the Danish Energy Agency, the model is not calibrated to reflect the actual GHG emissions or fuel consumption in foreign countries' transformation sectors. Secondly, as the transformation sector is included in the EU ETS for CO_2 quotas, any convincing estimation of the carbon leakage rate needs to include a model for the market for CO_2 quotas.

15.2 Adding an intra-day market to the electricity market

One of the issues with the current version of the model is that it is not able to sufficiently capture the observed price peaks and drops. Section 14 outlines suggestions for how to alter the K-means aggregation method in order to replicate the relevant price drops. Albeit we have not tested this yet, we do not suspect the K-means aggregation approach to be the only reason for the lack of sufficient price peaks in the model. Instead, we also attribute this problem to the fact that the model currently does not include uncertainty: Productivity and demand fluctuate exogenously throughout the year but the TSO firm, balancing demand and supply, is always certain about exactly how much supply must be secured in order to satisfy residual demand.[119]

By not including uncertainty and a reserve market, the model does not take into account that short run adjustments of production are typically constrained in some way; different types of plants are characterized by having a *ramp-up time* as well as *ramp-up costs*. On Nord Pool, the intra-day market supplements the day-ahead market with trade of electricity down to one hour before delivery. With only an hour to ramp up production, some dispatchable plants simply cannot react due to its ramp-up time, while others have significantly ramp-up costs associated with the adjustment.[120]

To model such a reserve market requires a number of extensions. First, the size of the reserve market needs to be modelled. The size and hourly variation of the market today can roughly be observed by data from Nord Pool. However, the importance of the intraday market is expected to increase with the use of intermittent energy and conversely, it is expected to decrease with the implementation of storage technologies. Second, the various plant types included in the model should be categorized according to their *regulating abilities*; that is, if the start-up time technically prohibits them from participating in the intra-day market. Third, we need to formalize the supply decision from plants that have the necessary regulating abilities to participate in the intra-day market. This poses a challenge, however, as plants with *ramp-up costs* essentially have a fixed cost of adjusting their supply compared to the previous period. The challenge is that a fixed cost component creates a kink in the value function of the given plant. Furthermore, the position of the kink depends on the solution in the previous hourly equilibrium.[121] While this problem is similar to the ones dealt with throughout this paper, we have not yet developed an appropriate solution to include it in the BU model.

[119] The residual demand/the residual load is defined as demand after supply from intermittent plants.

[120] The technology catalogue published by the Danish Energy Agency, describes that an *extraction plant* using a *gas turbine* of the type *combined cycle*, has a warm start-up time of 1 hour, and a cold start-up time of 2.5 hours (Danish Energy Agency (2016), page 79).

[121] The plant can choose to adjust its production compared to the previous hour and incur the adjustment cost, or keep production at $E_h = E_{h-1}$ and not pay the adjustment costs. The value of not adjusting however obviously depends on E_{h-1}; i.e. the position of the kink in the value function depends on previous equilibria. See Iskhakov et al. (2017) for an introduction to these kinds of problems.

Part V

Conclusion

16 Conclusion

This thesis developed a detailed BU model of the electricity and district heating sector (the transformation sector) that can be directly integrated in standard CGE models. The formulation allows for a rich description of competing technologies and accounts for intermittent energy production in a general equilibrium framework. The model was calibrated to data on the Danish transformation sector for 2017, where several simulation experiments were undertaken to illustrate the usefulness and assess the validity of our approach.

Firstly, the BU framework for the energy sector was developed. The formulation of the BU model is in particular focused on five aspects that are expected to be key elements in coming decades. *First*, the BU model accounted for the interaction between electricity and heat markets, by including CHP plants as well as electricity-to-heat technologies as heat pumps. *Second*, the model accounts for intermittency of electricity and heat production by modelling equilibria on the hourly basis. *Third*, the model further included storage technologies that are expected to mitigate the cost of intermittency by storing energy in low value (price) states and dispatching it in high value (price) states. The thesis presented a novel general modelling approach for a large range of energy storage technologies, including hydro power plants, electricity batteries, solar heat etc., in a single mathematical format. The approach allows for multiple occasionally binding constraints and is fully compatible with CGE models that are solved numerically using gradient-based algorithms. The specification was evaluated through a structural estimation of Swedish hydro power plants. *Fourth*, an intuitive and analytically convenient way of modelling an increase in the flexibility of hourly energy demand was presented. The approach allowed for an evaluation of the effects of introducing new technologies such as smart meters and load-switching devices. The demand specification further formed integration links between the BU model and a CGE model. These integration links ensure consistency between the two models in terms of yearly levels of demand, supply and prices. *Fifth* and final, to realistically capture the effects of increased network capacity in electricity trade, we developed a novel trade mechanism that emulates the trade algorithm used on the Nordic electricity exchange Nord Pool spot market. The approach computes endogenous electricity prices for each country included in the model. In a small-scale toy model, we showed that the trade mechanism was computationally efficient and easily captured highly non-linear effects from changes in relative prices between neighboring countries.

We presented a solution method for the BU model that allows for the integration into a CGE model that is formulated in the standard non-linear programming format. It was shown that the solution method nests the linear programming format conventionally applied in BU models. It was further argued that the solution method is ideal for coupling the BU model to a large-scale CGE model and ensures global convergence under very mild conditions.

Next, the BU model was aggregated from including 8760 hourly equilibria within a year to k representative states. The aggregation followed three steps. Firstly, given the number of states k, a K-means algorithm was applied to detect which hours of the year were most similar in terms of intermittent plants' capacity and level of demand for energy goods. Secondly, the aggregated model was calibrated to replicate statistics for the Danish transformation sector in 2017. Third and finally, a number of simulation experiments were carried out. The preferred number of representative states (k) was determined by lowering k as long as the simulation experiments implied similar results as the most disaggregated model. As part of the aggregation step, we developed a *state-transition-contingent aggregation scheme* for energy storage technologies to take into account that the k representative states were non-chronological ordered. We showed that the aggregation scheme captured intra-year variation in production well; however, it did not sufficiently capture development in the stock of stored energy. Several potential solutions to this problem were proposed for future work.

The usefulness of the model was also illustrated in the simulation experiments. In the baseline scenario the model replicated a downlift in the producer price for technologies based on intermittent renewable sources. In the energy economic literature this downlift is generally viewed as essential to assess the cost of intermittency. The model further closely predicted the observed CO_2 emissions in the base year without being calibrated to this target. We then simulated the effects of increasing the share of domestic production of electricity from intermittent renewables from 50% to 75%. Domestic electricity prices dropped by 22.5%, and producer prices for intermittent technologies decreased even further (34%). Thus, the value of intermittent electricity fell significantly in this scenario, without investments in any tools to mitigate these effects. The increased production of renewable electricity increased net export dramatically (approximately 10 TWh). We concluded that installing new capacity of intermittent energy production has a large impact on not only domestic emissions, but potentially also on emissions from neighboring countries' production of electricity.

Next, three simulation experiments were carried out to illustrate how demand flexibility, energy storage, and trade can mitigate the effects of intermittent energy production. With higher demand flexibility, we found that consumers allocate consumption from hours with high prices towards low prices, thus effectively lowering the yearly average energy price. The producer price for intermittent technologies increased, thereby reducing the downlift. When increasing the capacity for energy storage we found similar effects as for increased demand flexibility; a conclusion also reached by Ambec and Crampes (2017). Finally, we increased the network capacity for trade in electricity, by including the planned COBRA transmission cable between Denmark and the Netherlands. The prices between the two areas were partially equalized as expected, which led to an increase in net exports by 25%. In this static framework the CO_2 emissions from Danish plants increased significantly, due to the larger export to the Netherlands. However, as the producer price for intermittent technologies rose by more than average prices, it suggested that in a dynamic model, it would entail increased investments into more renewables. With the simulation experiments outlined here the most effective tool in mitigating the effects of intermittency was the added trade capacity. However, we note that the results should be interpreted with caution, as the model does not include endogenous investments and time dynamics.

Finally, while the BU model developed in this thesis is static, it was stressed that important features of the green transition are time dynamics and the coupling to a general equilibrium. Although not yet implemented, the thesis presented a framework for modelling endogenous investments in energy technologies and calibrating it in a general equilibrium framework. Thus a path for the future work of integrating the BU model in a CGE model was outlined.

References

Ambec, S. and C. Crampes

2012. Electricity provision with intermittent sources of energy. *Resource and Energy Economics*, 34(3):319–336.

Ambec, S. and C. Crampes

2017. Decarbonizing electricity generation with intermittent sources of energy. Working paper, n. 15-603, Toulouse School of Economic, Toulouse, France.

Andersen, K. S., L. B. Termansen, M. Gargiulo, and B. P. Gallachóirc

2019. Bridging the gap using energy services: Demonstrating a novel framework for soft linking top-down and bottom-up models. *Energy*, 169:277 – 293.

Andreas Bloess, W.-P. S. and A. Zerrahn

2018. Power-to-heat for renewable energy integration: A review of technologies, modeling approaches and flexibility potentials. *Applied Energy*, 212:1611–1626.

Armington, P. S.

1969. A theory of demand for products distinguished by place of production. *Staff Papers (International Monetary Fund)*, 16(1):159–178.

Balyk, O., K. S. Andersen, S. Dockweiler, M. Gargiulo, K. Karlsson, R. Næraa, S. Petrović, J. Tattini, L. B. Termansen, and G. Venturini

2019. Times-dk: Technology-rich multi-sectoral optimisation model of the danish energy system. *Energy Strategy Reviews*, 23:13 – 22.

Berg, R. and J. Eskildsen

2019. Modelling the energy sector in a computable general equilibrium framework: A new approach to integrated bottom-up and top-down modelling.

Berkovec, J.

1985. New car sales and used car stocks: A model of the automobile market. *The RAND Journal of Economics*, 16(2):195–214.

Bloomfield, P.

2004. *Fourier Analysis of Time Series: An Introduction*, Wiley Series in Probability and Statistics. Wiley.

Böhringer, C.

1998. The synthesis of bottom-up and top-down in energy policy modeling. *Energy Economics*, 20(3):233 – 248.

Böhringer, C. and T. F. Rutherford

2008. Combining bottom-up and top-down. *Energy Economics*, 30(2):574 – 596.

Böhringer, C. and T. F. Rutherford

2009. Integrated assessment of energy policies: Decomposing top-down and bottom-up. *Journal of Economic Dynamics and Control*, 33(9):1648 – 1661.

Calmfors, L., J. Hassler, N. Nasiritousi, K. Bäckstrand, F. Silbye, P. B. Sørensen, B. Carle;n, B. Kriström, M. Greaker, R. Golombek, M. Hoel, and K. Holtsmark

2019. Nordic economic policy review 2019: Climate policies in the nordics.

Danish Energy Agency

2013. Smart grid strategy. `https://ens.dk/sites/ens.dk/files/Globalcooperation/smart_grid_strategy_eng.pdf`. Downloaded 04-07-2019.

Danish Energy Agency

2014a. Denmark's heat supply 2014. `https://ens.dk/sites/ens.dk/files/Statistik/denmarks_heat_supply_2014_uk.pdf`. Downloaded 17 November 2018.

Danish Energy Agency

2014b. Fjernvarms rolle i den fremtidige energiforsyning. Technical report, Danish Energy Agency.

Danish Energy Agency

2016. Technology data for energy plants for electricity and district heating generation. Technical report, Danish Energy Agency.

Danish Energy Agency

2017a. Energistatistik 2017. `https://ens.dk/sites/ens.dk/files/Statistik/pub2017dk.pdf`. Accessed: 04-09-2018.

Danish Energy Agency

2017b. From centralized to decentralized power production. `https://ens.dk/sites/ens.dk/files/Statistik/foer_efter_uk.pdf`. Downloaded 17 November 2018.

Danish Energy Agency

2018a. Ramsesr docomentation. `https://ens.dk/sites/ens.dk/files/Analyser/ramsesr.pdf`. Accessed: 03-09-2018.

Danish Energy Agency

2018b. Regulering af varmeforsyningssektoren. `https://ens.dk/ansvarsomraader/varme/regulering-af-varmeomraadet`. Accessed: 05-07-2019.

Dansk Energi

2018. Varme outlook 2018: Perspektiver for fremtidens varme i danmark. `https://www.danskenergi.dk/sites/danskenergi.dk/files/media/dokumenter/2018-11/Varme_Outlook_2018_perspektiver_for_fremtidens_varme_i_Danmark.pdf`. Accessed: 14-07-2019.

Delarue, E. and J. Morris

2015. Renewables intermittency: Operational limits and implications for long-term energy system models.

Deryugina, T., A. MacKay, and J. Reif

2017. The long-run dynamics of electricity demand: Evidence from municipal aggregation. Working Paper 23483, National Bureau of Economic Research.

Drud, A.

2019. Gams documentation 27, conopt manual. https://www.gams.com/latest/docs/S_CONOPT.html.

EA, E. A.

2018. Balmorel userguide. https://ea-energianalyse.dk/papers/Balmorel_UserGuide.pdf. Accessed: 04-07-2019.

Energinet

2018. Security of eletricity supply report 2018. Technical report, Energinet, Fredericia, Denmark.

Energinet

2019. Ptx i danmark før 2030. Technical report, Energinet, Fredericia, Denmark.

Energinet.dk

2016. Introduktion til elmarkedet. https://energinet.dk/-/media/9D31DCCA764B42B5A292FECCFA847E49.pdf. Downloaded 17 November 2018.

Energy Commission

2016. Baggrundsnotat med fakta om den danske energisektor i dag. https://efkm.dk/media/8283/baggrundsnotat-med-fakta-om-energisektoren-i-dag.pdf. Downloaded 18 November 2018.

Energy Data Service

2018a. Electricity balance data. https://www.energidataservice.dk/dataset/electricitybalance/resource_extract/498c68e3-d248-4965-b36f-3aa738130adc. [Online; accessed 02-10-2018].

Energy Data Service

2018b. Elspot prices. https://www.energidataservice.dk/dataset/elspotprices/resource_extract/c86859d2-942e-4029-aec1-32d56f1a2e5d.

ENTSO-E

2018. Completing the map. the ten-year network development plan. Technical report, ENTSO-E.

European Commission

2018. Antitrust: Commission imposes binding obligations on tennet to increase electricity trading capacity between denmark and germany. Accessed 14-07-2019.

Førsund, F.

2005. *Hydropower Economics*, volume 112.

Gowrisankaran, G., S. S. Reynolds, and M. Samano

2016. Intermittency and the value of renewable energy. Technical Report 4.

Grohnheit, P. E. and H. V. Larsen

2001. Balmorel - data and calibration. Model documentation Version 2.05, Balmmorel.

Helgesen, P. I., A. Lind, O. Ivanova, and A. Tomasgard

2018. Using a hybrid hard-linked model to analyze reduced climate gas emissions from transport. *Energy*, 156:196 – 212.

Hirth, L., F. Ueckerdt, and O. Edenhofer

2015. Integration costs revisited – an economic framework for wind and solar variability. *Renewable Energy*, 74:925 – 939.

Hothorn, T., K. Hornik, and A. Zeileis

2006. Unbiased recursive partitioning: A conditional inference framework. *Journal of Computational and Graphical Statistics*, 15(3):651–674.

IPCC

2014. Climate change 2014: Synthesis report. contribution of working groups i, ii and iii to the fifth assessment report of the intergovernmental panel on climate change. Technical report, IPCC, Geneva, Switzerland. Core Writing Team, R.K. Pachauri and L.A. Meyer (eds.).

Iskhakov, F., T. H. Jørgensen, J. Rust, and B. Schjerning

2017. The endogenous grid method for discrete-continuous dynamic choice models with (or without) taste shocks. *Quantitative Economics*, 8(2):317–365.

Joskow, P. L.

2011. Comparing the costs of intermittent and dispatchable electricity generating technologies. *The American Economic Review*, 101(3):238–241.

Kassambara, A.

2017. *Practical Guide to Cluster Analysis in R: Unsupervised Machine Learning*, Multivariate Analysis. STHDA.

Klimarådet

2017. Omstilling frem mod 2030. Technical report, Klimarådet, Copenhagen, Denmark.

Klimarådet

2018a. Fremtidens grønne afgifter på energiområdet. Technical report, Klimarådet, Copenhagen, Denmark.

Klimarådet

2018b. Status for danmarks klimamålsætninger og forpligtelser 2018. Technical report, Klimarådet, Copenhagen, Denmark.

Loulou et al.

2016. Documentation for the times model. `https://iea-etsap.org/docs/Documentation_for_the_TIMES_Model-Part-II_July-2016.pdf`. Accessed: 04-07-2019.

Nord Pool

2018. Nord pool ftp server. `ftp.nordpoolgroup.com`. Accessed: 12-11-2018.

Pindyck, R. S. and J. J. Rotemberg

1983. Dynamic factor demands and the effects of energy price shocks. *The American Economic Review*, 73(5):1066–1079.

Reguant, M.

2019. The efficiency and sectoral distributional impacts of large-scale renewable energy policies. *Journal of the Association of Environmental and Resource Economists*, 6(S1):129–168.

Silbye, F. and P. B. Sørensen

2019. National climate policies and the european emissions trading system. In *Nordic Economic Policy Review 2019: Climate Policies in the Nordics*, chapter Chapter 3, Pp. 63–101. Nordic Council of Ministers.

Sinn, H.-W.

2017. Buffering volatility: A study on the limits of germany's energy revolution. *European Economic Review*, 99:130 – 150. Combating Climate Change. Lessons from Macroeconomics, Political Economy and Public Finance.

Stephensen, P., C. Huss, R. B. Jensen, G. Høgh, and P. Bache

2019. Reform-modellen. Technical report, DREAM, Copenhagen, Denmark.

Stern, N.

2008. The economics of climate change. *American Economic Review*, 98(2):1–37.

Su, C.-L. and K. L. Judd

2012. Constrained optimization approaches to estimation of structural models. *Econometrica*, 80(5):2213–2230.

SUSY Project

2019. The green reform model: A model of the interaction of the environment and the danish economy. `https://susy.ku.dk/phd-projects/green-reform-model/`. Accessed: 03-07-2019.

Svenska Kraftnät

2019. Statistics per el area and hour, 2017.

The MAKRO modelling Group

2018. Makro. http://www.makromodel.dk/upl/website/materiale/Documentation1.pdf. Documentation of version MAKRO 18AUG.

Wene, C.-O.

1996. Energy-economy analysis: Linking the macroeconomic and systems engineering approaches. *Energy*, 21(9):809 – 824.

Zerrahn, A., W.-P. Schill, and C. Kemfert

2018. On the economics of electrical storage for variable renewable energy sources. *European Economic Review*, 108:259 – 279.

Appendices

A Relevant Sets and data for bottom up module

A.1 A comprehensive list of set and set-values in bottom up module

Table 11: Set of basic fuel types $\mathscr{F}_B$ in plants' marginal cost computation

Basic fuel types $\mathscr{F}_B$:	
Coal	
Lignite	(not used in DK)
Fuel oil	
Gas oil	
Natural Gas	
Peat	(not used in DK)
Straw	
Wood pellets	
Wood chips	
Wood waste	
Waste	
Bio gas	
Bio oil	
SNG	(not used in DK)
Uranium	(not used in DK)

The set *full fuel types* is defined as a linear combination of the basic fuel type set $\mathscr{F}_B$. The full set includes 97 elements with simple elements that maps 1-to-1 with a basic fuel type and other fuel-mixes that combines several of the basic fuels.

Table 12: Set of multiple fuel-mix use $\mathcal{M}$ / number of fuel-mixes a plant can use.

Multiple fuel-mix $\mathcal{M}$:	
1	(vast majority is type 1)
2	

At the moment the 'multiple fuel-mix' set identifies whether plants are restricted to the use of one or more fuel-mix (at the moment only 1 or 2 fuel-mixes appear in data). This is relevant as a number of Danish plants can either use a coal-type fuel-mix or a biomass type of fuel-mix in its production. This adds a flexibility to the profitability of the given plant; if CO_2 prices increase, it may still be profitable using biomass inputs.

Table 13: Set of time/years, t in bottom up module

Years	$t \in \mathbb{N}$:	$\{2014, ..., 2040\}$

There are no restrictions on our model **in general** in terms of what years we can work over. The set 'years' that is restricted to $2014 - 2040$ is the set of years our bottom up data covers from *Energiproducenttællingen*. For foreign plants we use data from our baseline year to 2040 to exogenously model the change in supply from these plants. For Danish plants however we only use the data to model current plants and calibrate our bottom up module. Future plants are commissioned as a result of endogenous investment, c.f. section **??**. When we run the model past the year 2040, the sector evolves more or less according to a standard economic CGE model.

Table 14: Set of electricity areas, $\mathcal{G}_E$ in the model

Electricity area set $\mathcal{G}_E$:	
Denmark West	
Denmark East	
Norway	
Sweden	
Finland	
Germany, Austria, Luxembourg	
Holland	
Great Britain, Norther Ireland, Ireland	
France, Belgium	
Spain, Portugal	
Schweiz	
Italy	
Estonia, Latvia, Lithuania	
Poland, Czech Republic, Slovakia	
Hungary	
Russia	(exogenous trade)
SLGR	(exogenous trade)
ROHRRS	(exogenous trade)
Greece	(exogenous trade)
Slovenia	(exogenous trade)
UKRBLR	(exogenous trade)
Macedonia	(exogenous trade)

The choice of geographic splits follow the convention in the RAMSES data set described in section 3. For the last seven areas noted 'exogenous trade' we do not have information on plants, but only on yearly import/export flows. If we wish to include these plants in the model, we can at most hope for a rule-of-thumb trading function.

The set of subsidies $\mathcal{S}$ contains around 90 types (not all of them active though). A list of subsidies can be produced on request, but is omitted even from the appendix. It covers various feed-in tariffs, mainly covering production coming from types of wind, solar, hydro, biomass and biogas.

Full datatables for transmission lines:

Table 15: Set of heating regions $\mathcal{G}_H$

Heating area set $\mathcal{G}_H$:	**Subset of g_E:**
Copenhagen	DK-East
Kalundborg	DK-East
Vordingborg	DK-East
Rønne	DK-East
Helsingør	DK-East
Hillerød	DK-East
Næstved	DK-East
Slagelse	DK-East
Nykøbing Falster	DK-East
DTU	DK-East
Odense	DK-West
Aarhus	DK-West
Aalborg	DK-West
TVIS	DK-West
Esbjerg	DK-West
Herning	DK-West
Thisted	DK-West
Svendborg	DK-West
Frederikshavn	DK-West
Hjørring	DK-West
Holstebro, Struer	DK-West
Horsens	DK-West
Silkeborg	DK-West
Sønderborg	DK-West
Viborg	DK-West
Brønderslev	DK-West
Grenå	DK-West
NG_DK-West	DK-West
BIO_DK-West	DK-West
Other_DK-West	DK-West
NG_DK-East	DK-East
BIO_DK-East	DK-East
Other_DK-East	DK-East

The choice of geographic splits follow the convention in the RAMSES data set described in section 3. Due to data limitations we do not have heating sectors outside of Denmark in the model.

Table 16: Technology Sets in bottom up module:

Technology set $\mathcal{T}$:[122]	
Condensation plant (electricity only)	(standard)
Extraction plant (CHP)	(non-standard)
Backpressure plant with bypass (CHP)	(non-standard)
Backpressure plant (CHP)	(non-standard)
Electric heater (heat only)	(standard)
Intermittent electricity	(standard)
Boiler heating plant (heat only)	(standard)
Solar heating plant (heat only)	(standard)
Heat storage	(non-standard)
Exogenous production (industry surplus)	(standard)
Electricity storage	(non-standard)
Hydro with storage	(non-standard)
Electricity deficit plant	
Heating deficit plant	

'Standard' technology types are modeled using the same supply function approach, but differ in the way marginal costs of production are calculated. 'Non-standard' technologies are modeled differently in both marginal cost calculation as well as supply function modeling.

Table 17: Set of hourly variation patterns

Hourly variation set $\mathcal{V}$	
District Heating, demand	(same for all heating areas)
Electricity demand, one for each $\mathcal{G}_E$	(unique for each area)
Onshore Wind, DK1	
Onshore Wind, DK2	
Offshore wind, DK:	
VestEksKyst	
Horns Rev 1	
Horns Rev 2	
Anholt	
VestLand, pre 2008	
VestLand, 2008-2013	
ØstEksKyst	
Nysted	
Rødsand	
ØstLand, pre 2008	
ØstLand, 2008-2013	
Wind, foreign, 1 for each $\mathcal{G}_E$	(unique for each area)
Photo Voltaics, 1 for each $\mathcal{G}_E$	(unique, for each area)
Solar heating, DK1	
Solar heating, DK2	
Hydro inflow, SE/NO/FI	(3 countries share the same)
Hydro inflow, DE	(Germany)
Industrial Surplus production	(same for all $\mathcal{G}_E$)

Table 18: Set of bid type for Danish plants

Bid types $\mathcal{B}$:	Explanation
Marginal	Supply from plant depends on marginal costs of production relative to spot price on the market.
Prioritized	Marginal revenue of supply of electricity is constant (given by a subsidy rate). Only reacts to changes in spot price if it approaches the lower bound (cf. section 3.4).

Table 19: Transmission line capacity data for 2018, MW capacity per hour.

	DKW	DKE	NO	SE	FI	DEATLU	NL	GBNIIE	FRBE	ES	CH	IT	EELVLT	CZSK	HU	RU	SLGR	ROHRRS	GR	SL	UKRBLR	MAC
DKW	1	590	1424	641	0	24493	700	1400	0	0	0	0	0	0	0	0	0	0	0	0	0	0
DKE	600	1	0	1324	0	1343	0	0	0	0	0	0	0	0	0	0	0	0	0	0	0	0
NO	1467	0	1	3889	100	1400	700	4200	0	0	0	0	0	0	0	50	0	0	0	0	0	0
SE	641	1524	4205	1	5900	1930	0	0	0	0	0	0	700	600	0	0	0	0	0	0	0	0
FI	0	0	100	5100	1	0	0	0	0	0	0	0	1000	0	0	3120	0	0	0	0	0	0
DEATLU	28461	1365	1400	1930	0	1	4479	0	11432	0	2421	2158	0	5316	516	0	0	0	0	680	0	0
NL	700	0	700	0	0	4539	1	1200	2432	0	0	0	0	0	0	0	0	0	0	0	0	0
GBNIIE	1400	0	4200	0	0	0	1200	1	20400	0	0	0	0	0	0	0	0	0	0	0	0	0
FRBE	0	0	0	0	0	6800	2263	20400	1	31800	3147	6505	0	0	0	0	0	0	0	0	0	0
ES	0	0	0	0	0	0	0	0	33295	1	0	0	0	0	0	0	0	0	0	0	0	0
CH	0	0	0	0	0	6105	0	0	1895	0	1	15645	0	0	0	0	0	0	0	0	0	0
IT	0	0	0	0	0	1616	0	0	3126	0	9700	1	0	0	0	0	1020	0	0	0	0	0
EELVLT	0	0	0	700	1000	0	0	0	0	0	0	0	1	500	0	0	0	0	0	0	0	0
CZSK	0	0	0	600	0	10326	0	0	0	0	0	0	500	1	4653	0	0	0	0	0	150	0
HU	0	0	0	0	0	632	0	0	0	0	0	0	0	2634	1	0	0	2800	0	0	0	0
RU	0	0	50	0	3120	0	0	0	0	0	0	0	0	0	0	1	0	0	0	0	0	0
SLGR	0	0	0	0	0	0	0	0	0	0	0	920	0	0	0	0	1	0	0	0	0	0
ROHRRS	0	0	0	0	0	0	0	0	0	0	0	0	0	0	2550	0	0	1	0	0	0	0
GR	0	0	0	0	0	0	0	0	0	0	0	0	0	0	0	0	0	0	1	0	0	0
SL	0	0	0	0	0	930	0	0	0	0	0	0	0	0	0	0	0	0	0	1	0	0
UKRBLR	0	0	0	0	0	0	0	0	0	0	0	0	0	150	0	0	0	0	0	0	1	0
MAC	0	0	0	0	0	0	0	0	0	0	0	0	0	0	0	0	0	0	0	0	0	1

B Technical information on competing technologies

In modelling competing technologies, we distinguish between several types identified in the RAMSES data. In the following we present selected relevant technologies and how the marginal costs of these are derived. We start by presenting a *standard* plant. Other types are explained by how they differ from this standard plant. Throughout we distinguish between element-wise multiplication/division "$*$, /" and matrix multiplication "$\times$".

B.1 The standard electricity producing plant

The simplest fuel-driven electricity producing plant has a marginal cost structure like a *condensing plant* (CD). As in the model section, we distinguish between plant-marginal costs c_i and costs incurred through taxation $F^i(\mathbf{t})$.

Marginal costs c_i:

- Fuel costs excluding taxation:

  We distinguish between 15 types of basic fuels (FB), which can be combined in various ways into 97 types of fuel mixes (FM). In the baseline scenario we are considering we have data from 2014-2040. Furthermore, different CD plants may vary in efficiency (Eff) of transforming the energy content of the fuel input into energy units of output. To calculate the marginal cost of producing 1 MWh in terms of fuel use, we define the $(N \times T)$ matrix c_F with plant-specific marginal costs of fuel-use for each $t \in T$ years as:

  $$\underbrace{c_F}_{(N\times T)} = \underbrace{\mathbf{FM}}_{(N\times 97)} \times \underbrace{\mathbf{FB}}_{(97\times 15)} \times \underbrace{\mathbf{FB}_P}_{(15\times T)} \,/\, \underbrace{\mathbf{Eff}}_{(N\times T)} .$$

  Here **FM** contains fuel mix dummies for each plant, **FB** contains each fuel mix shares of the 15 types of basic fuels, $\mathbf{FB}_P$ contains time-paths of prices for each basic fuel and **Eff** contains plant- and time specific efficiency.[123]

- Other marginal costs of production:

  In the data other marginal costs of production is aggregated into one variable: VOM. This includes costs as "*... consumption of auxiliary materials (water, lubricants, fuel additives), treatment and disposal of residuals, spare parts and output related repair and maintenance*".[124] We interpret the VOM variable as the result of a Leontief production function, such that it is given by a linear

[123] In a general equilibrium model with a small open economy the basic fuel prices are exogenous and thus this c_F measure can be seen as an exogenous feature. If the basic fuels produced in the model as well (and not traded freely in a large world market), these prices should be endogenized in a general equilibrium framework.

[124] Excerpt from Danish Energy Agency's technology catalogue from https://ens.dk/service/fremskrivninger-analyser-modeller/teknologikataloger/teknologikatalog-produktion-af-el.

combination of input prices:

$$VOM_i \equiv \sum_{j \in M} a_j p_j,$$

where M is the set of inputs used in production, a_j is the input-output coefficient of input j and p_j the price on this input. In a general equilibrium framework the shares a_j should be identified from national accounts and accounting data and p_j's should be endogenous. For now we take the VOM as given.[125]

$$c = c_F + VOM.$$

Marginal costs incurred through taxation $F^i(\mathbf{t})$:

- Emission taxes (ET):

  We track 3 types of emissions from plants: CO_2 equivalents, NO_x and SO_2.[126] CO_2 equivalents are calculated from CO_2, CH_4 and $N2O$ emissions with conversion factors 1, 25 and 298 respectively.[127] For CO_2 and SO_2 we further allow for use of end-of-pipe abatement equipment use. In particular we let CO_2^A, SO_2^A be share of emissions abated. Furthermore, we have information on whether or not the plant is part of the ETS, letting CO_2^{CAP} denote the share of emissions included.

$$ET = \Bigg(\left[1 - CO_2^A\right] * CO_2^{equi} * \left[CO_2^{CAP} \times CO_2^{ETS} + \left(1 - CO_2^{CAP}\right) \times CO_2^{Tax}\right] + \left[1 - SO_2^A\right] * SO_2 \times SO_2^P + NO_x \times NO_x^P \Bigg) / \mathbf{Eff}$$

  As with c_F these are matrices with plant or time specific information. CO_2^A, CO_2^{EQUI}, CO_2^{CAP}, SO_2^A, NO_x are all matrices with plant-specific information, based on what type of fuel mix the plant is using. CO_2^{ETS}, CO_2^{TAX}, SO_2^P and NO_x^P are matrices containing time-paths for tax levels. In the Danish context we add that plants not subject to ETS is subject to another tax, CO_2-*afgiften*. This level of detail is not included for foreign plants.

- Non-fuel taxes and subsidies (TS):

  We include 89 types of taxes/subsidies depending on geographic area, fuel-type, electricity / heat production, etc..[128] To allow for exogenous changes in these tax paths as follows:

$$TS = - \underbrace{\mathbf{SD}}_{(N \times 89)} \times \underbrace{\mathbf{S}}_{(89 \times T)},$$

[125] It is comforting to note that the VOM variable is only a significant cost component for plants that have very small (or negative) marginal costs. Thus it seems that endogenizing the VOM variable would not lead to different conclusions when it comes to the equilibrium prices on electricity or heating.

[126] For foreign plants we only have the CO_2 emissions.

[127] We use guidelines from https://ec.europa.eu/eurostat/statistics-explained/pdfscache/1180.pdf

[128] Far from all types are relevant for the CD plants though.

where **SD** is a dummy matrix indicating the individual plant's access to the subsidy and **S** is a matrix with time-paths for each subsidy (taxes enter negatively). From this we define marginal costs from taxation:

$$F(\mathbf{t}) = ET + TS.$$

B.2 Combined Heat and Power production (CHP) plants

We have 3 different type of CHP plants in the data. For all three types we define the marginal cost without taxation c_i as the marginal cost of producing one unit of electricity. A second step then defines how much of this unit of electricity is 'used' for production of heat. In the model section we explain this step by share functions $d_E(p_E/p_H)$ and $d_H(p_E/p_H)$. We start by explaining this step a bit further for the three types.

B.2.1 Share functions for an *extraction plant* (EX)

In the bottom up literature, an approximate way of defining the joint production possibility set of an extraction plant is as follows: (i) The plant can at most produce q_i electricity at a unit cost of c_i. (ii) There is an approximate linear transformation rate of electricity-to-heating defined by C_v. (iii) There is a minimum of electricity-to-heating co-production of C_b.

We replace the linear transformation assumption and the minimum co-production inequality with a normalized constant elasticity of transformation. This gives us an interior solution that can come arbitrarily close to the bottom up solution, when $\sigma \to -\infty$. The CHP plant now maximizes:

$$\max_{E,H} p_E E + p_H H - q_i c_i,$$
$$\text{s.t. } q_i = \frac{C_v + C_b}{C_v}\left[\left(E - \frac{q_i C_b}{C_v + C_b}\right)^{\frac{\sigma-1}{\sigma}} + C_v^{\frac{\sigma-1}{\sigma}} H^{\frac{\sigma-1}{\sigma}}\right]^{\frac{\sigma}{\sigma-1}}, \qquad \sigma < 0.$$

The solution to this problem is given as in the main section with share functions given by:

$$d_E\left(\frac{p_E}{p_H}\right) = \frac{1}{C_v + C_b}\frac{C_v + C_b\left[1 + C_v^{\sigma-1}\left(\frac{p_E}{p_H}\right)^{\sigma-1}\right]^{\frac{\sigma}{\sigma-1}}}{\left[1 + C_v^{\sigma-1}\left(\frac{p_E}{p_H}\right)^{\sigma-1}\right]^{\frac{\sigma}{\sigma-1}}}$$
$$d_H\left(\frac{p_E}{p_H}\right) = \frac{1}{C_v + C_b}\frac{C_v^{\sigma}\left(\frac{p_E}{p_H}\right)^{\sigma}}{\left[1 + C_v^{\sigma-1}\left(\frac{p_E}{p_H}\right)^{\sigma-1}\right]^{\frac{\sigma}{\sigma-1}}}$$

In the limit when $\sigma \to -\infty$ these shares tend to $(1, 0)$ or $C_b/(C_v + C_b)$ and $1/(C_v + C_b)$ depending on whether heat or power production is most profitable, i.e. whether $C_v p_E/p_H$ is larger or smaller than 1. This corresponds to the bottom-up case.

On the technical data side we note the following (some of this may only be relevant if you actually

look at the data):

- For some plants there might be an additional constraint on the co-production of electricity-to-heat, besides the one defined by the C_b parameter. Specifically the dotted triangle in figure B.1 is not attainable. To circumvent modelling another discontinuity, we re-define C_b as

$$C_b \equiv \frac{q_E - C_v q_H}{q_H},$$

  where $q_E - C_v q_H$ is the electricity production in full back-pressure mode.

Figure B.1: Adjustment of electricity-to-heating ratio

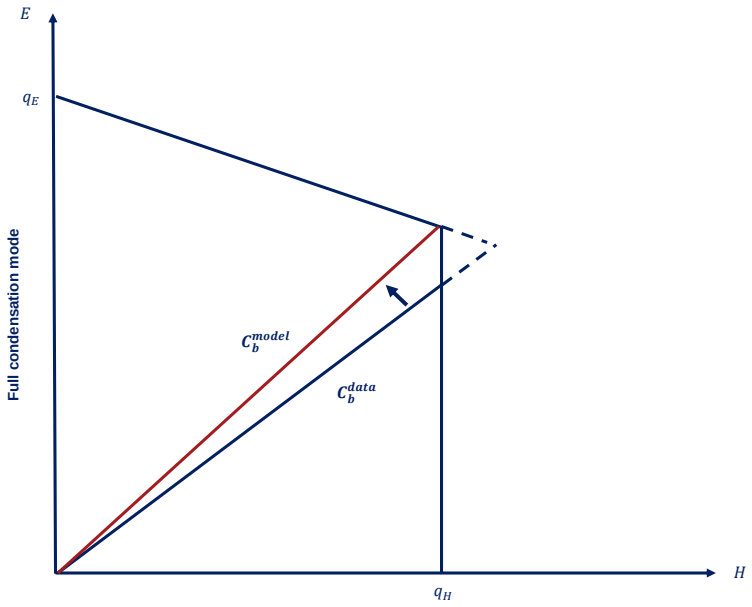

- Taxation of heating $F_H^i(\mathbf{t})$ is not entirely straightforward, as it in principle depends on the share of the inputs that goes to production of heating and what goes to electricity. To simplify matter we simply assume that all plants use the V-formula for computing this share.[129] This V-formula states that the share can be approximated by measuring the **output** of heating divided by 1.2.

- The efficiency parameter in data defines the fuel-efficiency in condensation mode (CD). In other words $\Delta Input = 1 \Rightarrow \Delta E^{CD} = Eff$. Thus unit costs are constructed by increasing $\Delta Input = 1/Eff$, as this increases output marginally (in condensation mode).

B.2.2 Share functions for a *back pressure plant* (BP)

Can only produce a fixed ratio of (E/H) only. Thus the shares d_E, d_H becomes constants given by technical information. We finally add that the efficiency measure for this type of plants give electricity outcome / energy input. As these plants usually co-produce a high level of heating, this efficiency measure

[129] For an example of calculation of fuel taxation, see here.

is misleading in the calculation of marginal costs c. For the share of marginal costs not associated with specific use (not that it matters as these shares are fixed here), 1 MWh input yields

$$\Delta E = Eff, \quad \Delta H = Eff/C_b.$$

Consequently, increasing inputs with $1/Eff$ yields $\Delta E = 1$ and $\Delta H = 1/C_b$. As with the extraction plants, the share of input fuels purposed for heating is taxed. We assume they follow the V-formula here as well.

B.2.3 Share functions for a *back pressure plant with bypass* (BB)

Can produce as a back pressure plant with a certain ratio of (E/H), or use bypass and transform E linearly and 1-to-1 to H. Thus this is essentially a CHP plant, with a maximum co-production constraint on electricity production / minimum co-production constraint on heating. The electricity-to-heating production can thus be between 0 and C_b. With a rate of transformation between heat and electricity of $C_v = 1$ this implies that:

- The minimum co-production of heat is given by $\underline{q}_H = q_E/C_b$.
- The capacity constraint on heat is $q_H = \underline{q}_H + q_E = q_E(1 + 1/C_b)$. In the minimum co-production constraint the plant produces $\underline{q}_H$ units of heat and q_E of electricity. With a transformation of $1 - to - 1$ the plant can transform the q_E units into heat.[130]
- In the data Eff measures ΔE when increasing input energy with one unit, when the plant operates as a back-pressure plant. In back-pressure mode the ratio of $\Delta E/\Delta H = C_b$. Thus the efficiency measured as ΔH, when increasing energy input marginally is given by Eff/C_b.

Using this information we can write the co-production function as a CET as with the extraction plant:

$$q_E\left(1 + \frac{1}{C_b}\right) = \frac{1 + 1/C_b}{1}\left[\left(H - \frac{q_E}{C_b}\right)^{\frac{\sigma-1}{\sigma}} + E^{\frac{\sigma-1}{\sigma}}\right]^{\frac{\sigma}{\sigma-1}},$$

This gives share functions of the type:

$$\begin{aligned} d_H\left(\frac{p_H}{p_E}\right) &= \frac{1}{1 + 1/C_b}\frac{1 + 1/C_b\left[1 + \left(\frac{p_H}{p_E}\right)^{\sigma-1}\right]^{\frac{\sigma}{\sigma-1}}}{\left[1 + \left(\frac{p_H}{p_E}\right)^{\sigma-1}\right]^{\frac{\sigma}{\sigma-1}}}. \\ d_E\left(\frac{p_H}{p_E}\right) &= \frac{1}{1 + 1/C_b}\frac{\left(\frac{p_H}{p_E}\right)^{\sigma}}{\left[1 + \left(\frac{p_H}{p_E}\right)^{\sigma-1}\right]^{\frac{\sigma}{\sigma-1}}} \; / \end{aligned} \tag{66}$$

The share functions here (approximately) sums to one here, which is not (necessarily) the case for EX and BP types.

[130] In the data we observe a $\underline{q}_H$ as heat capacities. This is not the actual capacities, if the bypass function is utilized. This little computation corrects for this.

B.3 Electrical Heater

This type of production does not have an exogenous unit-cost measure $\mathbf{c}_i$, as it clearly depends on the equilibrium price p_E. The unit-cost measure is given by:

$$\mathbf{c}_i = VOM + \frac{PtH}{TaxEff} - \frac{p_E}{C_m},$$

where VOM is the usual residual marginal cost measure, PtH is a power-to-heat tax (2 relevant types in Denmark) measured in DKK/MWh heating, $TaxEff$ adjusts individual 'plants' tax payment and finally C_m is defined as the ratio of power-to-heat production.

In data C_m is negative as the power-production is negative, and it seems that in general $TaxEff = 1/C_m$, such that $TaxEff$ only adjusts for efficiency of the technology. Thus for a plant that uses X MWh power to produce 1 MWh heating $TaxEff = X$.

B.4 Wind and solar power

The marginal costs of wind and solar technically follows the general formulas of the *standard electricity generating plant* (CD type). The only difference is that the fuel-mix matrix **FM** only contains zeros here.

The productivity of these technologies are intermittent and follows geographic-and-time specific distributions.

B.5 Hydro electric power

There are tree types of hydro power plants: run-off-river (ROR) plants without storage capacity, hydro plants with reservoirs, and pure-pumped storage (PPS) plants. For domestic plants (DK), RAMSES contains information on individual plants.[131] For foreign countries, RAMSES contain information on country aggregated hydro plants associated with the following information (amongst other):

- A *variation* pattern that defines the yearly pattern of water inflow.
- A *storage capacity* giving a maximum size of the reservoir storage.
- A *generation capacity* giving a maximum power generation capacity of the hydro plant's turbines (for PPS plants the constraint is the same for pumping and power generation).
- A *filling level* giving an initial level of storage.
- Subsidy, tax and unit-cost information as all other plants,
- For pumped storage (standard hydro power plant technology) the efficiency is around $70 - 85\%$ (not in RAMSES data though).

[131] There are a few ROW hydro plants included in our data.

ROR plants operate as intermittent technologies since power generation follows directly from water inflow. Thus in modelling terms ROR plants operate simply as an intermittent technology, e.g. as wind power. PPS plants operate as simple storage technologies in our model, as they do not face any water inflow.[132]

To model hydro power plants as discussed in the main section 4.3 and appendix D, we need parameter values on discounting (β) and 'smoothing' parameter (σ). As we cannot identify them in the RAMSES data, these parameters are instead estimated. We leave a more detailed discussion of the modelling approach for appendix D

B.6 Boiler heating plant (BH)

The plant operates as a straightforward plant with marginal costs consisting of fuel prices, taxes on emissions and taxes on production of heat.

B.7 Solar heating plant (SH)

Operates as an intermittent production technology. Marginal costs are straightforward given by VOM share and potential subsidies/taxes.

B.8 Heat storage (HS) and electricity storage (ES) technologies

RAMSES include the following characteristics of HS and ES technologies:

- A *storage capacity* giving a maximum size of the storage.
- A *generation capacity* giving a maximum power generation capacity, which is the same for storing and dispatching electricity/heat.
- A *filing level* giving an initial level of storage.
- Subsidy, tax and unit-cost information as all other plants,
- An efficiency parameter indicating the loss of energy when storing.

It should be noted that the storage efficiency is around 90% in the base year in RAMSES and that there is no storage loss when dispatching energy. As mentioned in section 4.3 it is commonly assumed that the efficiency of storing energy is 81% and the storage loss when dispacthing is 8% (Zerrahn et al., 2018).

The dynamic problem closely follows the dynamic optimisation problem of hydro plants with reservoirs (albeit without energy inflow). We initially formulate the linear (discrete choice) problem, which is given by:

$$\max_{\{E\}_{h=0}^{h=H}} W_0 = \sum_{h=0}^{H} \beta^h p_h E_h \tag{67}$$

$$\text{st.} \tag{68}$$

[132] For more on PPS and simple technologies, see section D.

$$S_h = S_{h-1} - (1 - b\mathbb{I})\, E_h, \quad \mathbb{I} = \begin{cases} 0, & E_h \geq 0 \\ 1, & E_h < 0 \end{cases} \tag{69}$$

$$S_h \in [0; \bar{S}] \tag{70}$$

$$E_h \in [-\bar{E}; \bar{E}] \tag{71}$$

$$S_H = S_0, \quad S_0 > 0 given. \tag{72}$$

Note from equation 71 that E_h is allowed to be negative; this corresponds to buying and storing energy. The term $1 - b$ in the transition equation in 69 is the storage efficiency. To circumvent the kink created by the indicator variable $\mathbb{I}$ we choose a smooth approximation

$$S_h = S_{h-1} - \big[1 - b\Phi\left(-E_h\right)\big] E_h, \tag{73}$$

with the negative derivative

$$\nabla S_h^E \equiv -\frac{\partial S_h}{\partial E_h} = 1 - b\big[\Phi\left(-E_h\right) - \phi\left(-E_h\right) E_h\big]. \tag{74}$$

As for hydro plants with reservoirs and water inflow we impose CRRA-type smoother in the storing/dispatching choice:

$$(p_h - \gamma)\frac{\left(E_h + \bar{E}\right)^{1-\alpha}}{1-\alpha}, \qquad \alpha > 1 \tag{75}$$

Here $\bar{E}$ is included to handle "negative production" (storage) and the parameter γ is a calibration constant included to allow for negative prices. Finally, we substitute the inequality path constraints in (70) and (71) for the smooth max approximation and arrive at the smooth dynamic optimisation problem:

$$\max_{\{E\}_{h=0}^{h=H}} W_0 = \sum_{h=0}^{H} \beta^h (p_h - \gamma)\frac{\left(E_h + \bar{E}\right)^{1-\alpha}}{1-\alpha} \tag{76}$$

$$\text{st.} \tag{77}$$

$$S_h = S_{h-1} - \left[1 - b\Phi\left(-E_h\right)\right] E_h \tag{78}$$

$$S_h^{\max} = \bar{S} \tag{79}$$

$$S_h^{\min} = 0 \tag{80}$$

$$E_h^{\max} = \bar{E} \tag{81}$$

$$S_H = S_0, \quad S_0 > 0 \text{ given.} \tag{82}$$

The optimality conditions for this problem are given by the system of equations in (83):

$$\begin{aligned}
\frac{(p_{h+1}-\gamma)\left(E_{h+1}+\bar{E}\right)^{-\alpha}-\theta_{h+1}\nabla E_{h+1}^{\max}}{\nabla S_{h+1}^{E}} &= \frac{1}{\beta}\left(\frac{(p_h-\gamma)\left(E_h+\bar{E}\right)^{-\alpha}-\theta_h\nabla E_h^{\max}}{\nabla S_h^{E}}+\mu_h\nabla S_h^{\max}-\nu_h S_h^{min}\right)\\
S_h &= S_{h-1}-\left[1-b\Phi\left(-E_h\right)\right]E_h\\
\theta_h &= E_h^{\max}-\bar{E}\\
\mu_h &= S_h^{\max}-\bar{S}\\
\nu_h &= 0-S_h^{\min}\\
S_H &= S_0
\end{aligned} \tag{83}$$

A comment on the storage/dispatch decision introduced by the system in (83) is warranted. In a *technologically unconstrained world* storage plants should simply look at the average price and store whenever prices are below this. Similarly, they should dispatch when prices are above average prices. This might, however, not always be the case due to CRRA-smoother. The CRRA-smoother creates auto-correlation in the store/dispatch choice since production is smoothed over time. The auto-correlation property is controlled by the intertemporal elasticity of substitution $\epsilon = 1/\alpha$. Since $\alpha > 1$ there is bound to be some auto-correlation because $\epsilon < \infty$. This property, however, can only create problems when prices are consecutively crossing the average price. To be more precise, let $\tilde{p}_h$ be the price in period h minus the average price, $1/H\sum_h p_h$. The problem then occurs in period h where:

$$\text{sign}(\tilde{p}_{h-1}) \neq \text{sign}(\tilde{p}_h) \neq \text{sign}(\tilde{p}_{h+1}) \tag{84}$$

Furthermore, the problem also only arise if the quantitative change in $\tilde{p}_h$ is small enough. The auto-correlation in the dispacth/store choice is not necessarily unrealistic when looking at the very short-run, since ramping production up and down with complete flexibility is impossible or, at the least, costly. This is certainly true for ES technologies since these are exclusively PPS technologies at the moment. Finally, when taking into account technological constraints the strategy of looking only at $\tilde{p}$ is not necessarily optimal any more since this may violate the inequality path constraints.

B.9 Exogenous production

This production consists usually of surplus electricity or heating, from industrial processes. The assumption is that the profits in industries from these activities are secondary and thus supply from these plants is exogenous.

C Profit maximization with joint production technologies

Let the joint production consist of n outputs and m outputs denoted respectively by vectors $\mathbf{y}$ and $\mathbf{x}$. The joint production function is then defined by the correspondence $F : \mathbb{R}^m_+ \rightrightarrows \mathbb{R}^n_+$:

$$F(\mathbf{x}) = \left\{ \mathbf{y} \middle| \ \mathbf{x} \text{ can produce } \mathbf{y} \right\},$$

where we assume the usual regularity conditions such as continuity. We define the maximum-value correspondence $\mathcal{F} : \mathbb{R}^m_+ \rightrightarrows \mathbb{R}^n_+$ as

$$\mathcal{F}(\mathbf{x}) = \underset{\mathbf{y} \in F(\mathbf{x})}{\operatorname{argmax}} \, \mathbf{p}\mathbf{y},$$

where $\mathbf{p}$ is a vector of output prices. Given that all prices are positive it follows immediately that the $\mathcal{F}(\mathbf{x}) \subseteq \partial F(\mathbf{x})$. The optimal choice of $\mathbf{x}$ and correspondingly $\mathbf{y}$ is then found by solving

$$\max_{\mathbf{x}} \mathcal{F}(\mathbf{x}) - \mathbf{c}\mathbf{x},$$

where $\mathbf{c}$ is a vector of input prices. A traditional bottom up construction of the CHP plant is to assume a correspondence of the type below:

Figure C.1: A sketch of the production possibility set of an extraction plant

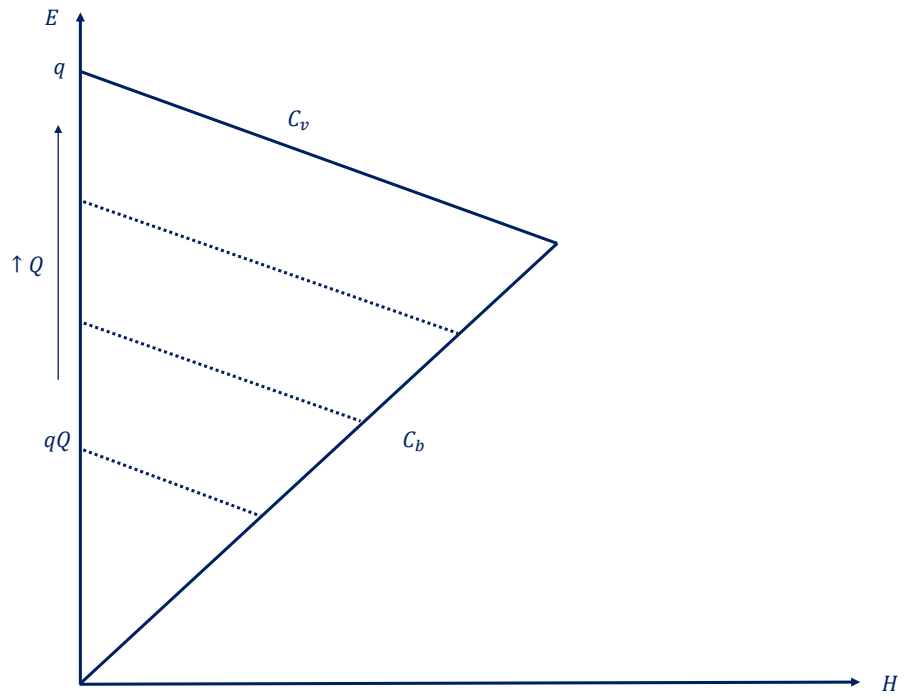

Here q denotes the capacity constraint formulated in terms of electricity production, C_v the linear transformation and C_b the minimum co-production of electricity per unit of heating produced. This assumes that: (1) The input-factor elasticity is zero (Leontief), (2) the rate of transformation between

electricity- and heat is linear, (3) there is an upper capacity on production of total electricity and (4) there is a minimal relative production of electricity compared to heat.[133] With the assumed Leontief production function, we can think of production in terms of a single unit cost of expanding E (denoted c) and a scale parameter $\mathcal{Q} \in [0, 1]$. This yields the relevant correspondence:[134]

$$\partial F(\mathcal{Q}) = \left\{ (E, H) \in R^2_+ : \mathcal{Q}q = E + C_v H \ \wedge \ H \leq \frac{\mathcal{Q}q}{C_b + C_v} \right\},$$

and the maximization problem:

$$\max_{\mathcal{Q} \in [0,1]} \left\{ \underset{(E,H) \in \partial F(\mathcal{Q})}{\operatorname{argmax}} \Big(p_E E + p_H H \Big) - c\mathcal{Q}q \right\}.$$

The solution to this linear problem is a combination of two corner solutions:

- Increasing $\mathcal{Q}$ marginally can to go to production of electricity at a price of p_E or heating - which when transformed at rate $1/C_v$ - brings in p_H/C_v. Thus the split of production between electricity and heating is given by

$$d_E = \begin{cases} 1, & \text{if } p_E C_v > p_H \\ \dfrac{C_b}{C_v + C_b}, & \text{if } p_E C_v < p_H. \end{cases}, \qquad d_H = \begin{cases} 0, & \text{if } p_E C_v > p_H \\ \dfrac{1}{C_v + C_b}, & \text{if } p_E C_v < p_H. \end{cases}$$

  with the price per unit of increase in production in optimum is then given by $p_E d_E + p_H d_H$.

- If the plant is profitable, i.e. if $p_E d_E + p_H d_H > c$, then the plant should work at full capacity, $\mathcal{Q} = 1$. If not then the plant should produce nothing, $\mathcal{Q} = 0$.

To circumvent the first type of corner solution (the second is dealt with in the main text) we replace the linear transformation rate, C_v with an assumption of constant elasticity of transformation (CET). Secondly, in order to naturally obey the minimum co-production constraint, we use a normalized version of the CET assuming that:

$$\mathcal{Q}q = \frac{C_v + C_b}{C_v} \left[\left(E - \frac{\mathcal{Q}q C_b}{C_v + C_b} \right)^{\frac{\sigma-1}{\sigma}} + (C_v H)^{\frac{\sigma-1}{\sigma}} \right]^{\frac{\sigma}{\sigma-1}}, \qquad \sigma < 0, \qquad \mathcal{Q} \in [0, 1].$$

Doing so allows us to simplify the problem to a two-step maximization over functions instead of correspondences:

i. Given the scale of production, $\mathcal{Q}$, find the optimal production split between E and H:

$$\max_{E,H} p_E E + p_H H - \mathcal{Q}qc,$$

   subject to the normalized CET function above. With the CET assumption we can ignore inequality constraints and the first order conditions will be necessary and sufficient. The optimal production

[133] See Ramses and TIMES documentation: Danish Energy Agency (2018a), Loulou et al. (2016).

[134] As prices are positive note that we do not need to search over the entire correspondence F, it is sufficient to determine the boundary ∂F, as the maximum-correspondence is always a subset of this correspondence.

split functions are now given by

$$d_E\left(\frac{p_E}{p_H}\right) = \frac{1}{C_v + C_b} \frac{C_v + C_b\left[\left(\frac{C_v p_E}{p_H}\right)^{\sigma-1}\right]^{\frac{\sigma}{\sigma-1}}}{\left[1 + \left(\frac{C_v p_E}{p_H}\right)^{\sigma-1}\right]^{\frac{\sigma}{\sigma-1}}},$$

$$d_H\left(\frac{p_E}{p_H}\right) = \frac{1}{C_v + C_b} \frac{\left(\frac{C_v p_E}{p_H}\right)^{\sigma}}{\left[1 + \left(\frac{C_v p_E}{p_H}\right)^{\sigma-1}\right]^{\frac{\sigma}{\sigma-1}}}.$$

Note that letting $\sigma \to -\infty$ gives the corner solution with linear transformation rate, such that we can come arbitrarily close to the 'bottom up' case described above.

ii. Secondly, maximize choosing $\mathcal{Q} \in [0, 1]$ with optimal output-split functions as above. It is straightforward to show that profits are still linear in $\mathcal{Q}$ and that (as in the bottom up case) we have that

$$\mathcal{Q}^* = \begin{cases} 1, & \text{if } p_{EH} > c \\ 0, & \text{if } p_{EH} < c \end{cases}, \qquad p_{EH} \equiv p_E d_E + p_H d_H.$$

C.1 An alternative with negative prices

As an alternative to the normalized constant elasticity of transformation function, we may consider the normal distribution smoother (for handling negative prices). We then have share functions

$$d_E = \frac{C_b}{C_v + C_b} + \Phi\left(\frac{p_E C_v - p_H}{\sigma}\right)\left(1 - \frac{C_b}{C_v + C_b}\right).$$

$$d_H = \frac{1}{C_v + C_b}\Phi\left(\frac{p_H - p_E C_v}{\sigma}\right)$$

The assumption is still implicitly that we can split up the problem into a scale and an output split problem. In the NCET approach the assumption of the output split problem is that electricity can be transformed into heating at a constant elasticity. With the normal smoothing assumption, the rate of transformation is also highest around the threshold $p_E C_v - p_H$, but in a way that does not involve a constant elasticity though.

D Modelling Storage Technologies

In this section we present a couple of approaches that we have tested, before ending up with our preferred specification in section 4.3. For now we have included the model formulations along with some remarks on, why we found the approach inferior to our preferred specification. Further information can be obtained about specific approaches upon request.

D.1 A CRRA smoothing approach

One of the approaches we tried out, was to consider the dynamic problem of the hydro power plant and draw on the resemblances to a borrowing constrained consumer. Albeit the hydro power plants are probably not risk averse, when it comes to maximizing profits, we find other reasons for smoothing production in the literature (see e.g. Førsund (2005)). First, our model does not take ramp-up/adjustment costs into consideration. Secondly, the marginal cost of production might not be exactly constant, but more likely increasing slightly as production increases towards the bound $\bar{E}$. Thirdly, hydro plants (as well as other plants) have perfect foresight in our model. If they are only able to foresee price peaks and drops partially, we expect storage plants to have smoother production paths.

The upside of assuming that hydro plants have CRRA preferences over profits, instead of modelling - what we see as - more plausible explanation for smoothing production, is that it allow us to draw directly on a broad existing literature. We simply replace the linear instantaneous profit function with

$$(p_h - c)\frac{E_h^{1-\alpha}}{1-\alpha}, \qquad \alpha > 0$$

where $\epsilon = 1/\alpha$ is the intertemporal elasticity of electricity production. Adopting the same notation for approximate reservoir constraints , this would entail a Lagrangian function given by:

$$\mathcal{L} = \sum_{h=0}^{H} \beta^h \left\{ (p_h - c)\frac{E_h^{1-\alpha}}{1-\alpha} + \lambda_h(S_{h-1} + Y_h - E_h - S_h) - \theta_h(E_h^{\max} - \bar{E}) - \mu_h(S_h^{\max} - \bar{S}) + \nu_h(S_h^{\min} - 0) \right\},$$

where E_h^{max} is an approximate generation capacity constraint, defined in the same way as S_h^{max} is defined in the main section 4.3. The first order conditions for this problem are then given by:

$$\frac{\partial \mathcal{L}}{\partial E_h} = 0: \quad (p_h - c)E_h^{-\alpha} - \theta_h \nabla E_h^{\max} = \lambda_h \tag{85}$$

$$\frac{\partial \mathcal{L}}{\partial S_h} = 0: \quad \lambda_h = \beta\lambda_{h+1} - \mu_h \nabla S_h^{\max} + \nu_h \nabla S_h^{\min} \tag{86}$$

$$\frac{\partial \mathcal{L}}{\partial \lambda_h} = 0: \quad S_h = S_{h-1} + Y_h - E_h, \tag{87}$$

with the Kuhn-Tucker complementary like conditions:

$$\theta_h = E_h^{\max} - \bar{E} \tag{88}$$

$$\mu_h = S_h^{\max} - \bar{S} \tag{89}$$

$$\nu_h = S_h^{\min} - 0 \tag{90}$$

$$\lambda_h \geq 0, \quad \theta_h, \mu_h, \nu_h \geq -\delta/2 \tag{91}$$

The constraint $\theta_h, \mu_h, \nu_h \geq -\delta/2$ is due to the smooth approximation with error $\delta/2$. In other words, with a discontinuous max/min-function the constraint would be $\theta_h, \mu_h, \nu_h \geq 0$. Combining equation (85) and (86) provides the Euler equation:

$$E_{h+1}^{-\alpha} - \frac{\theta_{h+1}\nabla E_{h+1}^{\max}}{p_{h+1} - c} = \frac{1}{\beta(p_{h+1} - c)} \left((p_h - c)E_h^{-\alpha} - \theta_h \nabla E_h^{\max} + \mu_h \nabla S_h^{\max} - \nu_h \nabla S_h^{\min} \right) \tag{92}$$

It is important to note that even though $\theta_h, \mu_h, \nu_h \geq -\delta/2$ the derivatives of the smooth max function, $\nabla S_h^{\max}, \nabla S_h^{\min}$, and $\nabla E_h^{\max}$ are zero when the constraint is non-binding and therefore the approximation error $\delta/2$ is cancelled in the Euler equation. To sum up, the final model for hydro plants with reservoirs is given by the system of equations:

$$\begin{aligned}
E_{h+1}^{-\alpha} - \frac{\theta_{h+1}\nabla E_{h+1}^{\max}}{p_{h+1} - c} &= \frac{1}{\beta(p_{h+1} - c)} \left((p_h - c)E_h^{-\alpha} - \theta_h \nabla E_h^{\max} + \mu_h \nabla S_h^{\max} - \nu_h \nabla S_h^{\min} \right) \\
S_h &= S_{h-1} + Y_h - E_h \\
\theta_h &= E_h^{\max} - \bar{E} \\
\mu_h &= S_h^{\max} - \bar{S} \\
\nu_h &= 0 - S_h^{\min} \\
S_H &= S_0
\end{aligned} \tag{93}$$

This approach is possible to run as an alternative to our preferred specification for storage technologies. However, in comparing the two methods, there are several ways, in which this approach is inferior:

- The approach allows for a dynamic characterization of the hydro plants' production, but in a less intuitive way: The CRRA assumption offers a smooth optimal supply choice, but not through the a cost or information channel, which we intuitively think of, as the real reasons for this.
- We have two (smoothed) Kuhn-Tucker constraints in this version, compared to only one in our preferred specification. All things equal this makes it harder for a gradient-based solver to work properly.
- Simulation experiments show that the CRRA approach have difficulties nesting the 'true' solution, when price peaks or drops are exacerbated. In other words: Adjusting the normal smoothing parameter σ in our preferred specification, makes it easier to fit large responses to price changes than changing our CRRA parameter α, while still ensuring that the gradient-based succeeds in finding the optimum.

D.2 Altering the marginal cost and law of motion functions

As mentioned in the CRRA section, one reason that we observe a relatively smooth production path for hydro plants, is that marginal costs of production are not exactly constant. Thus to avoid having

inequality constraints in our model, and having profits that are linear in our control variable E_h, we could modify the cost structure. Similarly, we can avoid including reservoir inequality constraints, either by including this in the cost structure, or by having non-linear law of motions ensuring the inequality constraints are always obeyed.

There are a number of ways to modify our setup, within the general idea outlined above. We have worked with several variations of the following general form of Lagrangian function:

$$\mathcal{L} = \sum_{h=1}^{H} \beta^h \Big[p_h E_h - C\left(cE_h\right) + \lambda_h g\left(S_{h-1} + Y_h - E_h - S_h\right) \Big],$$

where $C(\cdot)$ is a transformation of the constant marginal cost assumption and $g(\cdot)$ is the transformation of the law of motion. Some examples of the modifications we have tested includes:

- **Ensure that marginal costs spike and drops to ensure constraints using normal smoothing:**

  We can make sure that $E_h \in [\underline{E}, \bar{E}]$ with a marginal cost function on the form:

  $$C'(cE_h) = c + \bar{c}\left[\Phi\left(\frac{E_h - \underline{E}}{\sigma_1}\right) + \Phi\left(\frac{\bar{E} - E_h}{\sigma_2}\right) - 1\right],$$

  where $\bar{c}$ is the marginal costs of the energy deficit plants (see section 4.5), $\Phi(\cdot)$ is the standard normal CDF and σ_1, σ_2 are smoothing parameters. This marginal cost function does not ensure that $S_h \in [0, \bar{S}]$ though. Thus we would need to smooth these constraints using the technique outlined in the main section 4.3. For this specification to run in our model, we needed to have unreasonable large smoothing parameters (σ_1, σ_2) compared to our preferred specification.

- **Ensuring that state constraints hold using non-linear law of motion:**

  Our approach draws on inspiration from the consumption-savings literature. If the storage technology have decreasing returns to energy savings in a suitable way, we can ensure that $S_h \in [0, \bar{S}]$. One way to do this is to model storage as a fixed-factor CES function with an elasticity of substitution lower than 1.[135] As this does not ensure that $E_h \in [\underline{E}, \bar{E}]$ this approach has to be combined with some other fix to this problem, e.g. the marginal cost transformation outlined above. When testing this we found that the 'smoothed state constraints' outlined in the main text, was superior to this transformation of the law of motion.

[135] A function on the form $f(x) = (k_1 + k_2 x^{1/\rho})^{\rho}$ can easily be calibrated to convergence to a fixed level. Thus the marginal return to storage can be calibrated to approach zero around a fixed level of x. When x is around zero the marginal return tends to ∞, ensuring that it is never optimal to deplete the reservoir entirely. Alternatively we can once again model this directly using a normal smoother.

E Description of the short run supply

Figure E.1: Danish supply on technology types

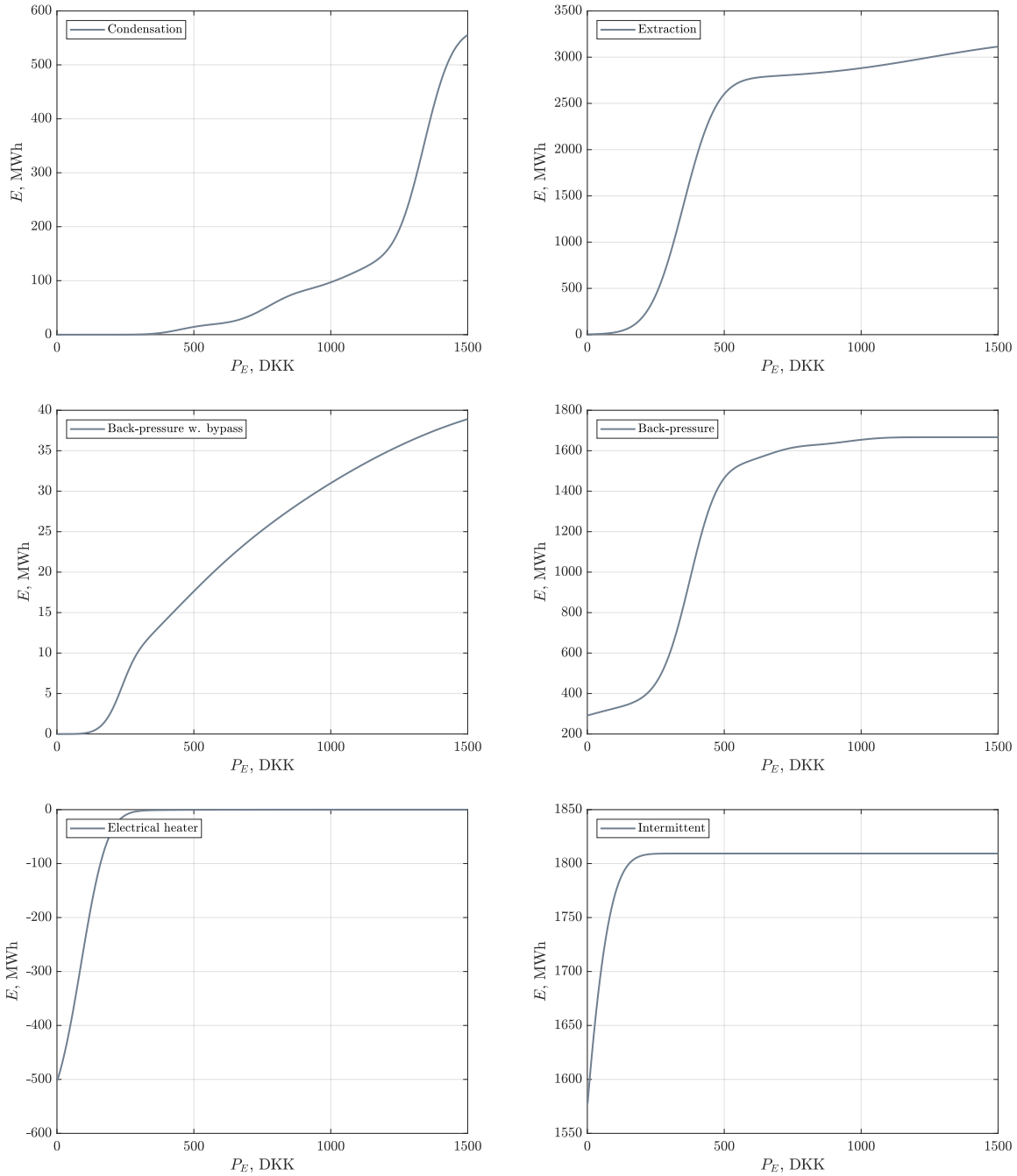

Note: The figure shows the supply from Danish electricity plants varying the price level from 0-1500 DKK. We use yearly average productivity levels for intermittent technologies and a price on heating at 200 DKK/MWh. The smoothing parameter σ described in section 4.1 is set to 50 here.

Figure E.2: Danish supply on fuel types

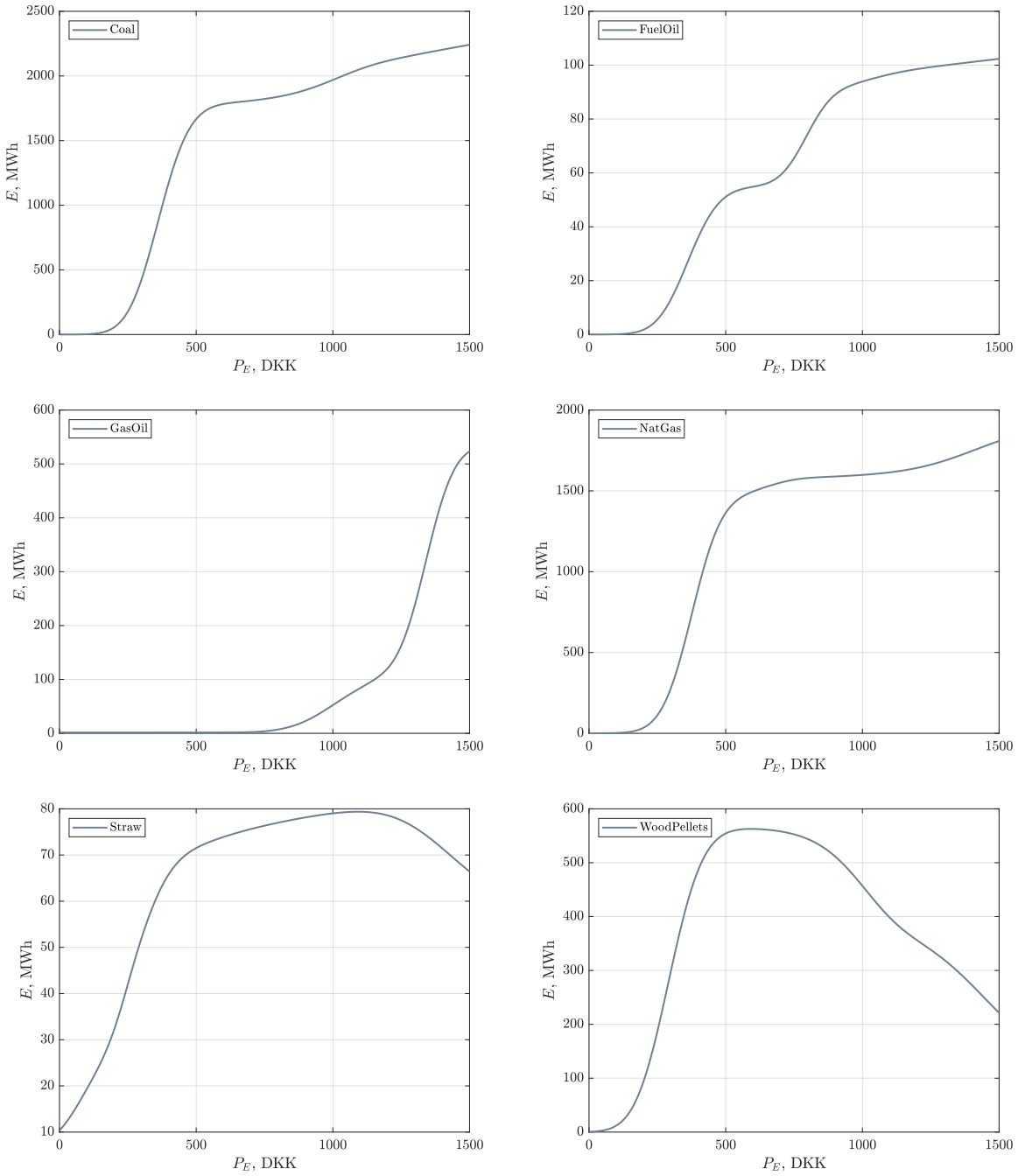

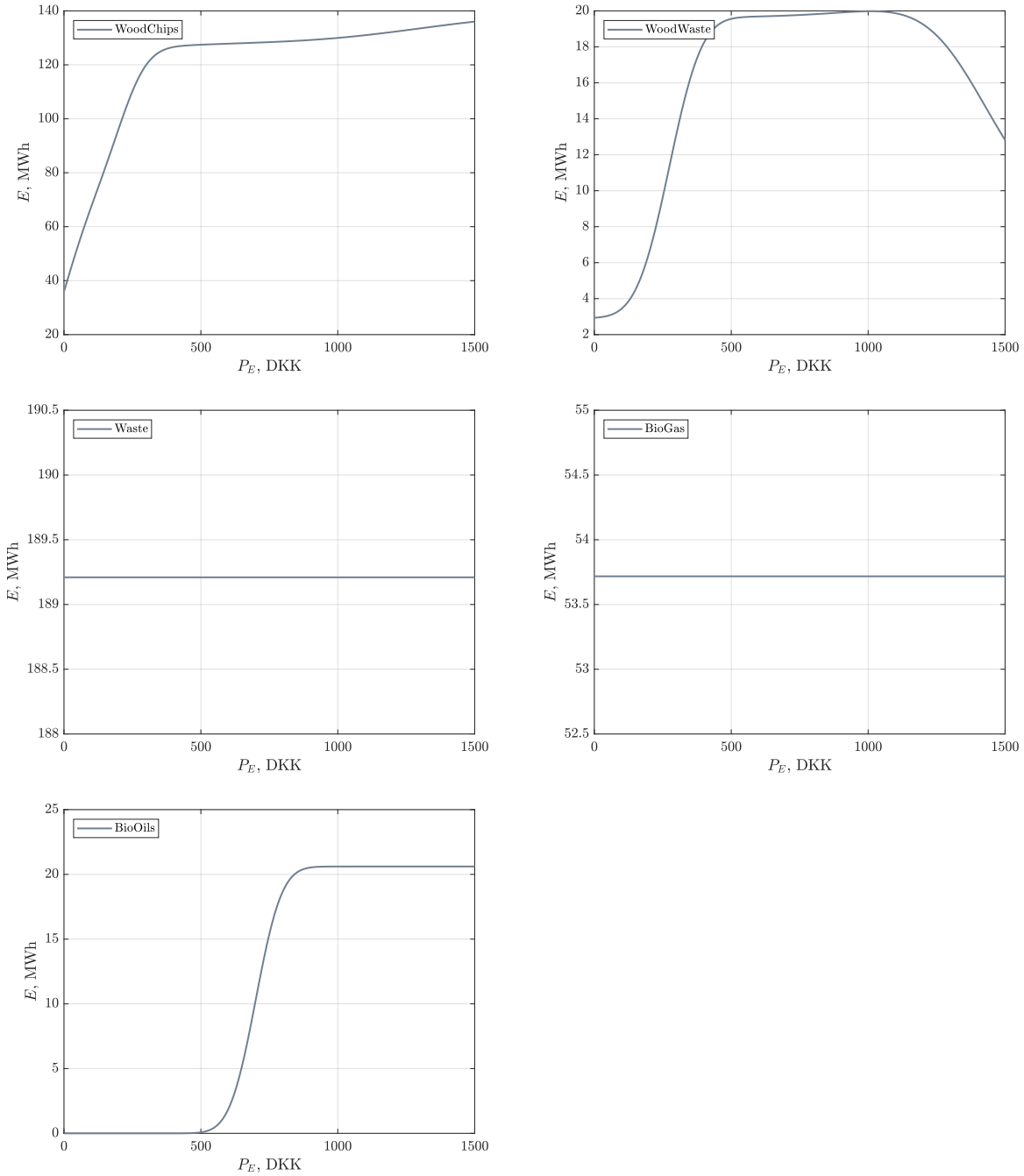

Note: The figure shows the supply from Danish electricity plants varying the price level from 0-1500 DKK. We use yearly average productivity levels for intermittent technologies and a price on heating at 200 DKK/MWh. The smoothing parameter σ described in section 4.1 is set to 50 here.

F A toy model of the short run equilibrium

In this appendix we present the toy model used in simulations in section 8. Depending on the relevant section, we use slightly different setups.

F.1 The baseline model

In the baseline model we use an almost arbitrary setup. On the demand side we use actual data from areas Denmark-West, Denmark-East and Norway. The hourly patterns are computed by aggregating the observed pattern of 2014 into four states. The trade capacities also resembles that of actual transmission capacities, with the exception of the trade between Denmark-East and Norway (which is zero). The productivity of the 'intermittent' technologies are similarly found by looking at actual patterns for wind production in the respective areas. The cost structure is arbitrarily chosen here.

Table 20: Plant-specific information in baseline simulation model

Country	c_i	q_i	Type	Hourly variation in q_i			
1	25	10	Int	36%	17%	17%	29%
	250	15	Base	25%	25%	25%	25%
	500	4	Peak	25%	25%	25%	25%
	700	25	EDP	25%	25%	25%	25%
2	28	8	Int	33%	19%	19%	29%
	260	8	Base	25%	25%	25%	25%
	600	3	Peak	25%	25%	25%	25%
	700	16	EDP	25%	25%	25%	25%
3	30	55	Int	37%	18%	15%	30%
	275	102	Base	25%	25%	25%	25%
	575	25	Peak	25%	25%	25%	25%
	700	159	EDP	25%	25%	25%	25%

Table 21: Demand data in baseline simulation model

Country	Demand level	Hourly variation in demand			
1	21	27%	24%	23%	26%
2	13	29%	23%	23%	25%
3	132	30%	22%	20%	28%

In the baseline case we define the trade capacity matrix $\mathbf{T}^c$ as:

$$\mathbf{T}^c = \begin{pmatrix} \cdot & 1.3 & 3.1 \\ 1.3 & \cdot & 2.4 \\ 3.2 & 2.5 & \cdot \end{pmatrix},$$

with entry (i, j) indicating the export transmission constraint from country i to country j. Finally, we use baseline parameter settings:

Table 22: Parameter values in baseline model

	Notation	Value
Number of countries	n	3
Number of hours	h	4
Number of net export terms	k	3
Elasticity of demand	σ_d	1.5
Inelastic share of demand	ϕ	0.9
Supply smoothing parameter	σ_s	25
Marginal trade cost at capacity	$\bar{c}$	700
Trade cost smoothing parameter	σ_T	0.3

In the baseline case the market clearing in all 4 states of the year is a friction-less equilibrium (FLE) as defined in definition 2. Even with the variation in demand and supply, we construct the baseline-scenario such that the baseload plants are the marginal plants and thus price setters. This give a roughly constant price across the year. Part (b) of figure 7.3 illustrates that with these prices country 1-2 are generally net exporters and country 3 importer. The FLE is feasible in the baseline scenario, as the total net export flows in part (b) is well below the trade capacities between different countries specified in $\mathbf{T}^c$ above.

Figure F.1: Baseline FLE scenario

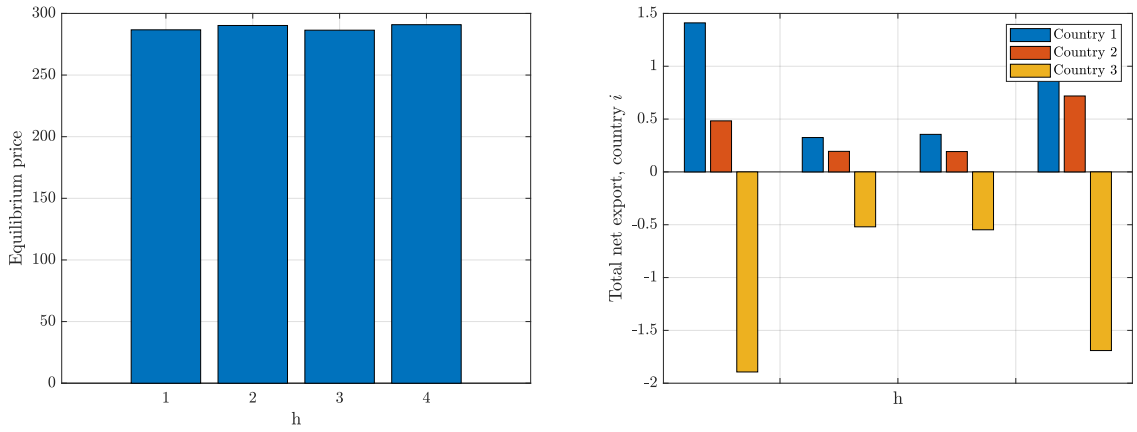

(a) Equilibrium price

(b) Domestic Surplus function

F.2 Supply shock scenarios

Compared to the baseline case, where the friction-less equilibrium (FLE) is feasible, we giv a mix of positive and negative supply shocks, varying across hours and countries. Specifically we alter the plant capacities as follows:

$$\mathbf{q}^{shock} = \left(\mathbf{D}_{g_E} \times \begin{pmatrix} 1.5 & 1 & 1 & 1.5 \\ 1 & 1 & 1 & 1 \\ 0.75 & 1 & 1 & 0.75 \end{pmatrix} \right) * \mathbf{q}^{base},$$

where $\mathbf{D}_{g_E}$ is a $(n_p \times n)$ dummy matrix indicating the relevant plant's country, $\mathbf{q}^{base}$ is a $(n_p \times h)$ matrix of capacities for the plants in the baseline scenario. Following the steps of the *complex* algorithm 1, we proceed:

i. The initial trade partition in all h states, $\left(\mathcal{G}_E^0\right)_{h=\{1,2,3,4\}}$ includes all countries. Solving for the FLE prices as in definition 2, the outcome is given by prices and domestic surplus functions (export needs):

$$(p_{FLE})^0 = \begin{pmatrix} 316 & 291 & 287 & 332 \\ \vdots & \vdots & \vdots & \vdots \\ 316 & 291 & 287 & 332 \end{pmatrix}, \qquad (DSF)^0 = \begin{pmatrix} 5 & 0.3 & 0.3 & 4.5 \\ 0.8 & 0.2 & 0.2 & 1.0 \\ -6.1 & -0.5 & -0.5 & -5.4 \end{pmatrix}.$$

ii. Next we check whether or not this is feasible, i.e. if there for each h exists a vector $\mathbf{NX}$ that obeys the trade capacities $\mathbf{T}$, such that:

$$(DSF)^0 - B \times \begin{pmatrix} \mathbf{NX}_1 & \mathbf{NX}_2 & \mathbf{NX}_3 & \mathbf{NX}_4 \end{pmatrix} = 0, \qquad B \equiv \begin{pmatrix} 1 & 1 & 0 \\ -1 & 0 & 1 \\ 0 & -1 & -1 \end{pmatrix}.$$

Problem 1 formally defines this linear programming problem. For $h = 1, 4$ the implementation is not feasible; thus we proceed to step iii.

iii. Taking $(DSF)^0$ as given, we approximate the inequality constraints

$$-T_{j,i} \leq NX_{i,j} \leq T_{i,j},$$

with continuously differentiable functions, that penalizes trade when it approaches the capacity constraints. The problem is formally set up and solved in problem 2. Solving this problem we obtain shadow-costs of each constraint $T_{i,j}$ given by

$$\mu_{i,j} \equiv \left| \frac{\partial C_{i,j}}{\partial NX_{i,j}} \right|.$$

Furthermore, we construct the problem 2 such that we have a criteria function for when a constraint should be binding:

$$\begin{aligned} \text{if } \mu_{i,j} > \bar{c} \text{ and } \frac{\partial C_{i,j}}{\partial NX_{i,j}} > 0 \qquad &\Rightarrow \qquad NX_{i,j} = T_{i,j}, \\ \text{if } \mu_{i,j} > \bar{c} \text{ and } \frac{\partial C_{i,j}}{\partial NX_{i,j}} < 0 \qquad &\Rightarrow \qquad NX_{i,j} = -T_{j,i}. \end{aligned}$$

This means that we can rank the likelihood of binding for all constraints **and** we have a criteria function that allows us to bind multiple constraints in one step.

iv. Given $\mu_{i,j}$ for all constraints we fix the suggested net export flows at capacity constraints. For $h = 1$ fixing $NX_{1,2} = T_{1,2}$ and $NX_{1,3} = T_{1,3}$ creates a new trade partition, which is a necessary

prerequisite, for arriving at a new FLE guess in step i. For $h = 4$ we only fix $NX_{1,3} = T_{1,3}$ initially. However, as this does not imply a new trade partition, we fix the next likely candidate as suggested by the ranking of the shadow costs $\mu_{i,j}$. Thus we fix $NX_{1,2} = T_{1,2}$ as well. Denote the new candidates $\left(\mathcal{G}_E^1\right)_h$:

$$(\mathcal{G}_E^1)_{h=1} = (\mathcal{G}_E^1)_{h=4} = \Big\{\{1\},\ \{2,3\}\Big\}, \qquad (\mathcal{G}_E^1)_{h=2} = (\mathcal{G}_E^1)_{h=3} = \{1,2,3\}.$$

v. Before repeating steps $i.-iv.$ with the updated guess of the trade partition, we check whether or not the newly suggested trade partitions are stable as defined in definition 1. Deriving the FLE for each $(\mathcal{G}_E^1)_h$ we get prices

$$(p_{FLE})^1 = \begin{pmatrix} 275 & 291 & 287 & 309 \\ 332 & 291 & 287 & 336 \\ 332 & 291 & 287 & 336 \end{pmatrix}.$$

We verify that the new trade partitions are stable, by checking whether a constraint $NX_{i,j} = T_{i,j}$ implies a price-differential $p_j \geq p_i$. If this is not the case, we drop the constraint before repeating steps $i.-v.$

With the proposed $(p_{FLE})^1$, the allocation is feasible and we conclude this is the short run equilibrium.

G Energy demand in the very short-run

G.1 The price elastic part of short-run energy demand

When dealing with the energy market the researcher should acknowledge the presence of relatively low (and even negative) prices at times. In economics there is a long tradition of using functions that exhibits constant elasticity of substitution. As discussed with regards to the short run supply of electricity and heating, the very short run (hourly frequency) is often characterized by some capacity restrictions. This is also true for firms and households that ultimately demand the produced electricity; some firms might be able to adjust some of their production according to when electricity prices drop, but there still seem to be some capacity restriction in place.

As an alternative to the iso-elastic function, we thus provide some alternative demand functions that are characterized by being bounded from above (and below). We take the following three criteria, for the price-sensitive part of the short-run energy demand function ($f(p_h, p)$ in equation (20)) as given:

i. Around the price average $p_h = p$ the function returns 1.

ii. When $p_h \to \infty$ demand tends to zero.

iii. When p_h goes to zero (and becomes negative even), demand does not become infinitely large. I.e. the demand function is bounded from above.

From an economic perspective it is conventional to assume demand is convex and satisfy $d'(p) < 0, d''(p) \geq 0$. However, from an engineering perspective, it seems rational to have an upper bound on short run energy demand such that demand does not go to infinity at any point. Unfortunately, it is not possible to have both. Here we propose two simple specifications that allow for one or the other:

Version 1: Convex demand

In the following, we therefore assume $d'(p) < 0, d''(p) \geq 0$ and the only way for demand to tend to infinity is for large negative prices.

Recalling that we in general have:

$$e_h = \phi g_h D + (1 - \phi) g_h D f(p_h/p), \tag{94}$$

A demand function where $d'(p) < 0$, $d''(p) \geq 0$ we need:

$$f(p_h) = \begin{cases} a_1 - c p_h, & p_h < 0 \\ a_2 \frac{1}{(\eta + p_h)^\sigma}, & p_h \geq 0 \end{cases}$$

Ad i we now require that

$$f(p_h = p_t) = 1 \qquad \Rightarrow \qquad a_2 = (\eta + p)^\sigma.$$

Furthermore, we require that the function is differentiable such that

$$f'_{-}(0) = -c = -\frac{a_2\sigma}{\eta^{\sigma+1}} = f'_{+}(0).$$

Plugging in the expression for a_2 we have

$$c = \frac{\sigma(\eta+p)^{\sigma}}{\eta^{\sigma+1}}.$$

Continuity in the point $p_h = 0$ further requires

$$a_1 = \frac{a_2}{\eta^{\sigma}} = \left(1+\frac{p}{\eta}\right)^{\sigma}.$$

We restrict both a and η to positive domains. Likewise for σ, c. Note that $f(p_h, p)$ is a function to be multiplied onto $g_h D$. We then have:

$$f(p_h) = \begin{cases} \left(1+\frac{p}{\eta}\right)^{\sigma}\left(1-\frac{\sigma}{\eta}p_h\right), & p_h < 0 \\ \left(\frac{\eta+p}{\eta+p_h}\right)^{\sigma}, & p_h \geq 0 \end{cases}$$

Version 2: A demand specification with upper and lower bound

Alternatively we propose a demand function where $d'(p) < 0$ but $d''(p) \lesseqgtr 0$. The attractive feature of this approach is that we have a clear upper and lower bound on the demand. Denote these $\bar{D}, \underline{D}$. In general we still want to restrict the model to return $f(p_h = p) = 1$. This is consistent with our specification of g_h weights being purely exogenous preference weights in absence of price fluctuations. Here we propose a number of specifications:

- A simple symmetric scaling function:

$$f^1(p_h) = \underline{D} + \bar{D}\Phi\left(\frac{p-p_h}{\sigma}\right).$$

  Restricting the function to be one around $p_h = p$ this entails:

$$\bar{D} = 2(1-\underline{D}).$$
$$\lim_{p_h\to\infty}(f^1(p_h)) = \underline{D}$$
$$\lim_{p_h\to-\infty}(f^1(p_h)) = 2-\underline{D}.$$

  This implies that setting $\underline{D} = 0$ implies the highest possible $\bar{D}$ with an upper limit of 2. This function also inherits the feature that demand is most price-sensitive exactly around $p = p_h$.

- Asymmetric scaling: Consider instead the function

$$f^2(p_h) = \underline{D} + \bar{D}\Phi\left(\frac{p-g(p_h)}{\sigma}\right).$$

We assume:

$$\frac{\partial g}{\partial p_h} > 0, \qquad \lim_{p_h \to -\infty} (g(p_h)) = -\infty, \qquad \lim_{p_h \to \infty} (g(p_h)) = \infty.$$

Restricting $f^2(p_h = p) = 1$ this entails

$$\underline{D} + \bar{D}\Phi\left(\frac{p - g(p)}{\sigma}\right) = 1, \qquad \Rightarrow \qquad \bar{D} = \frac{1}{\gamma(p)}\left(1 - \underline{D}\right), \qquad \gamma(p) \equiv \Phi\left(\frac{p - g(p)}{\sigma}\right).$$

This entails that

$$\lim_{p_h \to \infty} (f^2(p_h)) = \underline{D}$$
$$\lim_{p_h \to -\infty} (f^2(p_h)) = \underline{D} + \frac{1}{\gamma(p)}(1 - \underline{D}).$$

Thus we can arbitrarily push up the upper bound on the scale function, by choosing $\gamma(p)$.

- A special case of the asymmetric scaling function:

$$f^3(p_h) = \underline{D} + \bar{D}\Phi\left(\frac{p - p_h + \tilde{g}}{\sigma}\right).$$

Denote the target of the upper bar as η. In this case we can simply fit $\tilde{g}$:

$$\underline{D} + \frac{1}{\gamma}(1 - \underline{D}) = \eta \qquad \Rightarrow \qquad \Phi\left(\frac{\tilde{g}}{\sigma}\right) = \frac{1 - \underline{D}}{\eta - \underline{D}}, \qquad \Rightarrow \qquad \tilde{g} = \sigma\Phi^{-1}\left(\frac{1 - \underline{D}}{\eta - \underline{D}}\right).$$

- Asymmetric scaling with logit inspiration:

$$f^4(p_h) = \underline{D} + \frac{\bar{D}_1}{\bar{D}_2 + exp(\sigma(p_h - p))}.$$

Restricting $f^4(p_h = p) = 1$ we have:

$$\bar{D}_1 = (1 - \underline{D})(1 + \bar{D}_2).$$

The logit bounds are simply given by

$$\begin{aligned} \lim_{p_h \to \infty} &= \underline{D} \\ \eta \equiv \lim_{p_h \to -\infty} &= \underline{D} + \frac{\bar{D}_1}{\bar{D}_2} \\ &= 1 + \frac{1 - \underline{D}}{\bar{D}_2}. \end{aligned}$$

Thus lowering $\bar{D}_2$ increases the maximum demand. We then have:

$$f^4(p_h) = \underline{D} + \frac{(1 - \underline{D})(1 + \bar{D}_2)}{\bar{D}_2 + exp(\sigma(p_h - p))},$$

or in terms of the upper bound η:

$$f^4(p_h) = \underline{D} + \frac{(1-\underline{D})\frac{\eta-\underline{D}}{\eta-1}}{\frac{1-\underline{D}}{\eta-1} + exp(\sigma(p_h - p))}.$$

G.2 Estimation of hourly electricity demand in Denmark

Assuming $\phi = 1$ implies that (20) simplifies to

$$e_{h,t} = E_t g_{h,t}, \tag{95}$$

as $\sum_h g_{h,t} = 1$ by construction. The specification in (95) assumes that the hourly load is perfectly inelastic, where $g_{h,t}$ can be interpreted as purely habitual consumption patterns repeating itself as cycles (seasonality): consumers have a preference for allocating their consumption at specific hours of the year due to e.g. labour/leisure time and holiday effects[136].

To illustrate the idea of $g_{h,t}$ the average daily consumption cycle per year is plotted in figure G.1. The average daily cycle is almost identical across year and the 95% highest density interval suggests that the daily cycle is also persistent. Furthermore, the pattern is very much in line with expectation that consumers demand electricity in conjunction with their daily task without consideration for prices. Finally, note from (95) that seasonalities are assumed to be multiplicative and that $g_{h,t}$ is allowed to

Figure G.1: Average daily electricity consumption cycle for Denmark

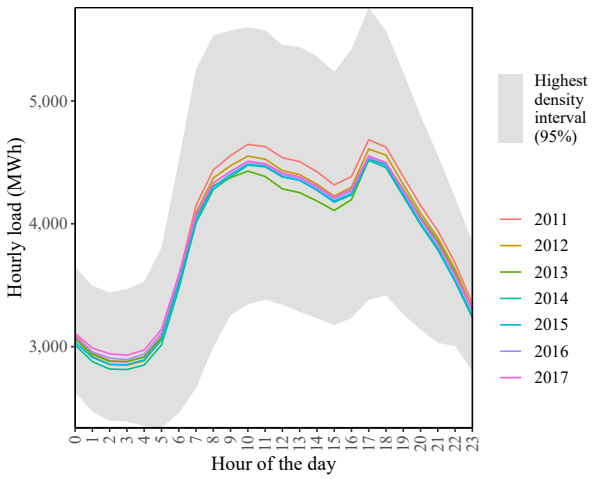

Note: Hourly load for DK-West and DK-East has been aggregated.
Source: Energy Data Service (2018a)

depend on year t. One reason for this is e.g. that the seventh hour of a Monday can fall at different hours, h, within year t assuming demand is the same in this state over time. It should be noted that such a distinction seems unnecessary in the bottom-up model for the forecast to be realistic, however, it might be important in the estimation of the demand.

[136] Remember we only assume a perfectly inelastic demand on the very short-run (hourly frequency), since the yearly consumption level E_t is price dependent in the top-down model

In a regression framework we evaluate two different assumptions on the structure of the irregular component, $\epsilon_{h,t}$:

$$e_{h,t} = E_t g_{h,t} + \epsilon^A_{h,t} \tag{96}$$

$$e_{h,t} = E_t g_{h,t} \epsilon^M_{h,t} \tag{97}$$

In (96) the error term is assumed additive and in (97) the error term is multiplicative. From equation (96) and (97) we get two regression models:

$$y^1_{h,t} = g_{h,t} + \eta^1_{h,t}, \qquad y^1_{h,t} \equiv \frac{e_{h,t}}{E_t}, \qquad \eta^1_{h,t} \equiv \frac{\epsilon^A_{h,t}}{E_t} \qquad \text{(Model 1)}$$

$$y^2_{h,t} = \ln g_{h,t} + \eta^2_{h,t}, \qquad y^2_{h,t} \equiv \ln\left(\frac{e_{h,t}}{E_t}\right), \qquad \eta^2_{h,t} \equiv \ln \epsilon^M_{h,t} \qquad \text{(Model 2)}$$

Model 1 is a run off of the additive model in (96) and Model 2 follows from the multiplicative model in (97). Model 1 and Model 2 have the advantage of estimating the function $g_{h,t}$ directly[137].

The hourly load, $e_{h,t}$, is collected from Energy Data Service (2018a) for the period 2011-2017. The time-series of the transformed dependent variables in Model 1 and Model 2 are illustrated in figure G.2.

[137] We disregarded the option of estimating the logarithmic level of the hourly electricity load given by $\ln e_{h,t} = \ln E_t + \ln g_{h,t} + \ln \epsilon^M_{h,t}$. We are only interested in the allocation shares captured by $g_{h,t}$ as the yearly load level is coming from the top-down model in the integrated model.

Figure G.2: Time-series data for Model 1 and Model 2

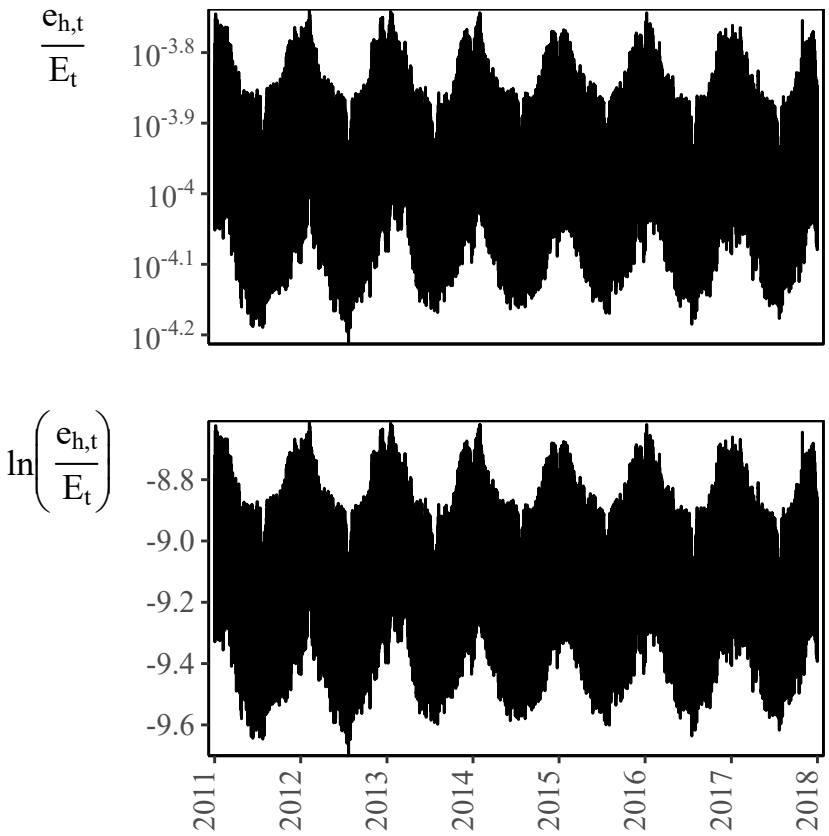

Note: Hourly load for DK-West and DK-East has been aggregated.
Source: Energy Data Service (2018a)

Remembering that we want to evaluate how well (95) explains or rather predicts electricity demand, we split the data into a training and a test set. The training data consists of 2011-2016. We test the forecast on data from 2017. The benchmark for choosing between models is the mean-squared-error (MSE) on the test set, defined as

$$\text{MSE}_i = \frac{1}{8760} \sum_{h}^{8760} \left(e_{h,t} - \tilde{y}^i_{h,t} \right)^2, \qquad i = \{1, 2, 3\} \tag{98}$$

$$\tilde{y}^1_{h,t} \equiv E_t \widehat{y}^1_{h,t} = \widehat{e}_{h,t} \tag{99}$$

$$\tilde{y}^3_{h,t} \equiv E_t exp\left(\widehat{y}^2_{h,t} \right) = \widehat{e}_{h,t}, \tag{100}$$

where $t = 2017$. The transformations in (99) and (100) ensures that the MSE is measured in the units of the hourly load $e_{h,t}$ for both models.

Before estimation we have computed the auto-correlation function (ACF) and the partial auto-correlation function (PACF) of the transformed time-series to examine stationarity. These are illustrate in figure G.3 and suggest that the process is stationary although with considerable seasonalities.

Figure G.3: ACF and PACF for $y^2_{h,t} = e_{h,t}/E_t$

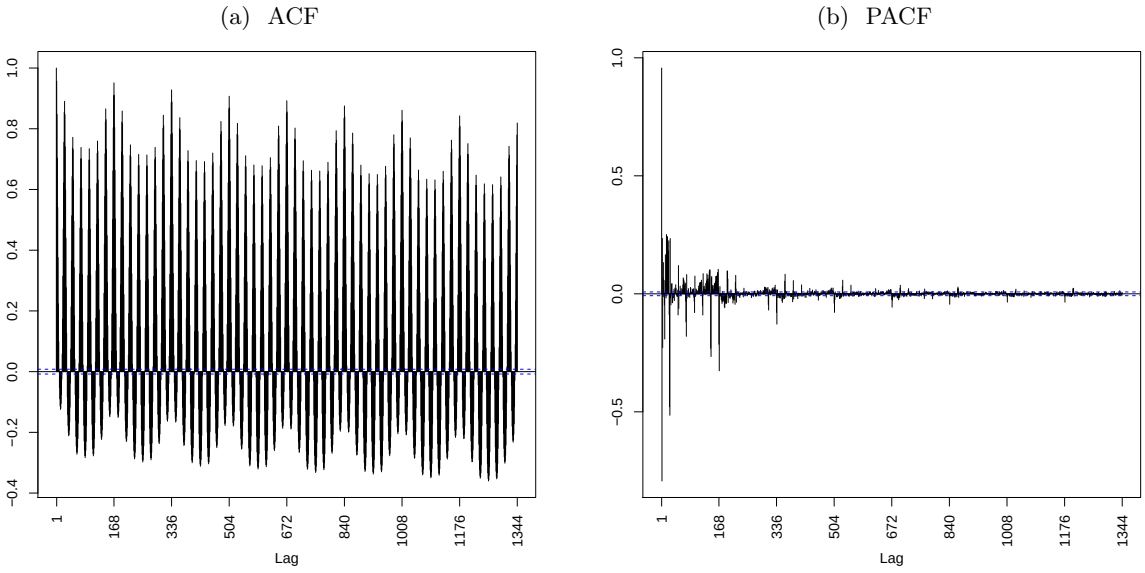

Note: Although not shown here, the ACF and PACF for $y^1_{h,t} = \ln(e_{h,t}/E_t)$ show identical patterns.
Source: Energy Data Service (2018a)

The ACF and PACF for $e_{h,t}/E_t$ (Model 1) is plotted in figure G.3 with a lag of 8 weeks (1.344 hours). The ACF in figure G.3a shows a high degree of auto-correlation, however, it is diminishing rather quickly. Similarly the PACF in figure G.3b converges quickly to zero. These two observations indicate that the time-series are stationary[138]. The ACF also shows clear seasonalities. The ACF is peaking every 24 hours and 168 hours, suggesting a daily and weekly seasonality, respectively. Looking at the time-series in figure G.2 also suggest a yearly cycle.

The patterns of seasonality are exactly what the function $g_{h,t}$ is trying to capture. A more formal examination of these seasonalities can carried out by means of a periodogram Bloomfield (2004). The basic idea of the periodogram is to measure the spectral density (or spectrum power) running on a certain frequency where the frequency is the inverse of the seasonality, e.g. $1/24$ for the daily frequency. The periodogram for $e_{h,t}/E_t$ is shown in figure G.4, and suggests there are clear consumption cycles within every 12 hour (half-daily seasonality), 24 hour (daily seasonality), 168 hour (weekly seasonality), and every 8760 hour (yearly seasonality)[139]. These findings are consistent with the ACF and PACF in figure G.3 with the exception of the cycle every 12 hour; for this reason the 12^{th} hour is not included in $g_{h,t}$[140].

[138] Similarly patterns hold for $\ln\left(e_{h,t}/E_t\right)$ although not shown here.
[139] Although not shown, the result for $\ln(e_{h,t}/E_t)$ is similar.
[140] We have also examined sub-series plots of the 12^{th} hour and there does not seem to be any consistent cycle running at this frequency.

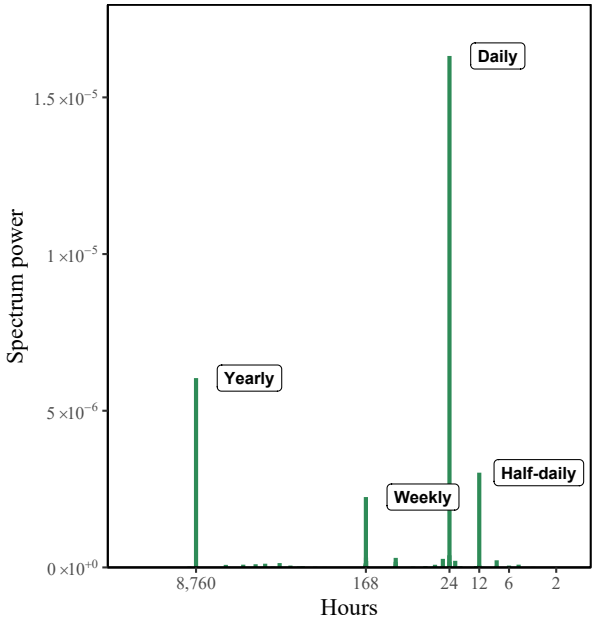

Figure G.4: Periodogram of $e_{h,t}/E_t$

In the modelling of $g_{h,t}$ we evaluate two different sets of regressors based on the findings of seasonality. The first set includes harmonic regressors following Bloomfield (2004). The intuition is that a wave can be approximated using trigonometric functions. A sinusoidal function, $x(h)$, on a certain frequency, $f = 1/s$, where s is the seasonality period in units of time (e.g. $s = 24$) is given by

$$x(h) = A\cos 2\pi\left(\frac{h}{s} + \phi\right) \tag{101}$$

$$= \beta_1 \cos\left(2\pi\frac{h}{s}\right) + \beta_2 \sin\left(2\pi\frac{h}{s}\right), \qquad \beta_1 \equiv A\cos 2\pi\phi, \quad \beta_2 \equiv -A\sin 2\pi\phi \tag{102}$$

In (102) A is the amplitude, ϕ is the phase, h is the indicator for hour, and, finally, β_1 and β_2 are the parameters to be estimated. To approximate a complex cycle such as in figure G.1 we include multiple fourier terms, ω_s, for the same seasonality although with the limitation that $omega_s \in [1; s/2]$. Consequently, the harmonic regressor set is given by

$$\begin{aligned} y^i_{h,t} = \beta_0 + \overbrace{\sum_{s}\sum_{\omega_s}^{\Omega_s}\left[\beta_{1\omega_s}\cos\left(\frac{2\pi\omega_s h}{s}\right) + \beta_{2\omega_s}\sin\left(\frac{2\pi\omega_s h}{s}\right)\right]}^{\text{Fourier series}} \\ + \beta_3 h + \text{WeekDay} + \eta^i_{h,t} \\ \forall \quad s = \{24, 168, 8670\} \text{ and } \omega_s \in [1; \Omega_s] \text{ with } \Omega_s \leq \frac{s}{2} \end{aligned} \tag{X-Harmonic}$$

A dummy for the day of the week (excluding Monday), WeekDay, is included in (X-Dummy) because the weekly cycle is relatively complex and the set of dummies aids the fourier terms in capturing the weekly

seasonality[141]. The second specification consist of a set of dummy variables given by:

$$y^i_{h,t} = \beta_0 + \underbrace{\text{HourOfDay}}_{K=23} + \underbrace{\text{WeekDay}}_{K=6} + \underbrace{\text{Week}}_{K=51} + \underbrace{\text{HourOfDay} \times \text{WeekDay}}_{K=23\times 7} + \underbrace{\text{WeekDay} \times \text{Week}}_{K=6\times 52}, \tag{X-Dummy}$$

where K indicates the number of regressors for each variable. The intercept β_0 is level of y_i on Monday in the first week of the 2011 at hour 0.

Model 1 and Model 2 are estimated using OLS, Ridge, and Lasso since this is an prediction exercise. The objective of lasso and ridge is to minimise the prediction error subject to a tuning parameter:

$$\min_{\beta}(y_t - x_t\beta)^2, \qquad \sum_{k=1}^{K} \beta_k^2 \leq \lambda \tag{Ridge-Problem}$$

$$\min_{\beta}(y_t - x_t\beta)^2, \qquad \sum_{k=1}^{K} |\beta| \leq \lambda \tag{Lasso-Problem}$$

where K is the length of the vector β. The tuning parameter, λ, is the "penalty" on parameters sizes (i.e. the shrinkage effect). When $\lambda = 0$ Ridge is equivalent to OLS. The attractive feature of Ridge and Lasso is the possibility of choosing λ optimally by minimising the MSE of the model. In other words, it chooses the optimal balance between bias and variance of the model's prediction error:

$$\begin{aligned} \hat{\lambda} &= \underset{\lambda \in \Lambda}{\operatorname{argmin}} \operatorname{MSE}(\hat{\eta}(\lambda)) \\ &st. \\ \operatorname{MSE}(\hat{\eta}(\lambda)) &\equiv \mathbb{E}[(\hat{\eta}(\lambda))^2] = \mathbb{E}[(y - \hat{y}(\lambda))^2] \\ &= \operatorname{Bias}(\hat{y}(\lambda))^2 + \sigma^2 + Var(\hat{y}(\lambda)), \end{aligned} \tag{103}$$

where Λ is the set of tuning parameters and σ^2 is the variance of y. The bias-variance trade-off can also be interpreted as a problem of over- and under-fitting the model on the training data. If the bias is high the model is under-fitted and the model can miss important relations on the training data important for predicting the test data. Conversely, if the variance is high the model is over-fitted and can use what essentially is random noise in the training data to predict the hourly load on the test data. The optimal choice $\hat{\lambda}$ balances these two trade-offs and it is implemented by means of cross-validation where 525 observations are left out in each estimation, implying the model is estimated roughlu $(2016 - 2011 + 1) * 8760/525 \approx 100$ times. The tuning set consists of 102 elements and is defined as $\Lambda = 0 \cup \left\{n \in \{0, 0.1, 0.2, ..., 10, \} \ : \ f(n) = 10^{-n}\right\}$.

Finally, we have two different regression models (Model 1 and Model 2) with two sets of different regressors (Dummy and Harmonic) each estimated using three different methods (OLS, Ridge, and Lasso), implyinh we evaluate $2 * 2 * 3 = 12$ different models in total.

It should be noted that the error term of all models are auto-correlated and heteroschedastic suggesting that the models are not fully specified. For instance, we are not accounting for temperature, although

[141] Another way of formulating it is that $\Omega_1 68 = 84$ is too few regressors to fully capture the weekly cycle.

this has been shown to be important in determining electricity demand. Temperature is not included in $g_{h,t}$ (although it easily could be be) because it is a difficult variable to forecast. Importantly, the error term does not contain a unit root.[142]

The prediction performances of the 12 different models are presented in figure G.5. The specifications performs virtually the same albeit the dummy regressors generally outperforms the harmonic regressors. The best prediction is Model 1 with the set of dummy regressors using Lasso. This specification explains a little over 92% of the test data indicating the the assumption of $\phi_t = 1$ is not an unreasonable assumption.

Figure G.5: Prediction performance on test data (2017)

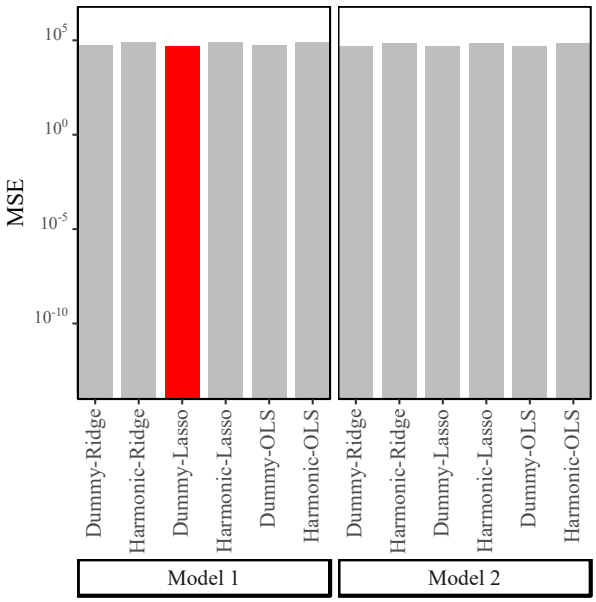

Note: The specification with the lowest MSE is indicated by red.

[142]The ACF and PACF of all estimations suggest a stationary series since lag-terms are converging to zero. Both plots indicates seasonality at the 24th and 168th lag suggesting that seasonality at these two frequencies has not been completely accounted for.

H Algorithms for Equilibrium in the very short run

H.1 Trade Partitions

Define a $(\mathcal{G}_E \times \mathcal{G}_E)$ matrix $\mathbf{T}$ of indicators (1/0) for whether trade capacities $T_{i,j} > 0$ or not. Impose zeros if trade capacities are binding as well. The subset of countries that country i can trade with is then found by:

- For each $g_j \in \mathcal{G}_E$: If $\mathbf{T}_{i,j} = 0$ do nothing. If $\mathbf{T}_{i,j} = 1$ then country i can trade with all of country j's connections, indirectly through j. To capture this add:

  i. Define matrix $\mathbf{X}_j^1$ as the repeated vector of $j'th$ row in $\mathbf{T}$.

  ii. Define $\mathbf{X}_j^2 \equiv \mathbf{X}_j^1 * \mathbf{T}$ where $*$ indicates element-wise multiplication.

  iii. Define $\mathbf{X}_j^3$ as the $(\mathcal{G}_E \times 1)$ vector indicating strictly positive values in $\mathbf{X}_j^2$.

  iv. Update $i'th$ vector in $\mathbf{T}$ with max value in existing vector $\mathbf{T}_i$ and $\mathbf{X}_j^3$.

  When carried out for all $g_j \in \mathcal{G}_E$ define updated vector $\mathbf{T}_i^1$.

- Repeat step above with new vector $\mathbf{T}_i^1$: If resulting vector $\mathbf{T}_i^2 = \mathbf{T}_i^1$ we are done, otherwise repeat.

Note that we do not have to do this for all i, only for the number of subsets in the partition. Furthermore, note that the process above ends after at most $\mathcal{G}_E - 1$ iterations: We have monotonicity in iterations on $\mathbf{T}_i$ (values either increases or stay the same) and the values are bounded below (0) and above (1) ensuring convergence.

H.2 Equilibrium with Trade Partition

Algorithm 1 below outlines in more detail, how we identity the short run equilibrium in cases where the number of countries n, is prohibitively large, to apply the simple algorithm of the main text. The main idea is to search over trade partitions, where each subset constitutes either a frictions-less (FLE) or ad-hoc equilibrium (AHE). To do this we refer to two problems formally defined separately below the algorithm: Problem 1 checks whether a trade-partition candidate can be implemented, without violating trade capacities. Problem 2 is used to rank which trade capacities are most likely to bind. This is used when searching over different trade partition candidates.

Algorithm 1 The Equilibrium in the short run (SRE)

Define initial trade partition $\mathcal{G}_E^{\mathrm{o}} \equiv (\mathcal{G}_1^{\mathrm{o}}, ..., \mathcal{G}_n^{\mathrm{o}})$.
for each $\mathcal{G}_i^{\mathrm{o}} \in \mathcal{G}_E^{\mathrm{o}}$ **do**
  Solve for FLE prices as in definition 2. Next we check if FLE is feasible.
  Given p_E^* and $\left\{p_{H,g_H}^*\right\}_{g_H \in \mathcal{G}_i^{\mathrm{o}}}$ solve linear problem 1.
  if allocation is feasible **then**
    if $p_E^* < \bar{c}$ conclude FLE and **exit**.
    else conclude BOE and **exit**.
  end if
Update trade partition:
  Solve problem 2 yielding trade costs $C(NX_{k,j})$ (*see problem 2 for elaboration*).
  Rank trade costs from highest-to-lowest, indicating likelihood of binding trade capacities.
  repeat
    For remaining transmission line w. highest cost fix: $NX_{k,j} \equiv T_{k,j}$.
    Update trade partition $\mathcal{G}_i^1$.
  until $\mathcal{G}_i^1 \neq \mathcal{G}_i^{\mathrm{o}}$ and $\mathcal{G}_i^1$ is stable as defined in definition 1.
end for
repeat steps above for all $\mathcal{G}_i^j \in \mathcal{G}_E^j$
until exit by either FLE or AHE.

Problem 1 below checks whether or not the FLE is feasible:

Problem 1 (Minimize trade flows: Linear FLE problem)**.**

$$\min \sum_{g_k \in \mathcal{G}_i^{\mathrm{o}}} \sum_{j \in (\mathcal{G}_i^{\mathrm{o}} \setminus k)} X_{k,j},$$

$$s.t. \quad \sum_{g_j \in \mathcal{G}_i^{\mathrm{o}}} e_{(t,h,g_j)} \left(\frac{p_E^*}{p_{g_j,t}^E} \right) = \sum_{g_j \in \mathcal{G}_i^{\mathrm{o}}} \sum_{j \in \mathcal{I}_{g_j}} E_j \left(p_E^*, p_{H,g_H}^* \right),$$

$$h_{(t,h,g_j)} \left(\frac{p_{H,g_j}^*}{p_{g_j,t}^H} \right) = \sum_{j \in \mathcal{I}_{g_j}} H_j \left(p_E^*, p_{H,g_j}^* \right), \qquad \forall g_j \in \mathcal{G}_i^{\mathrm{o}}$$

$$e_{(t,h,g_j)} \left(\frac{p_E^*}{p_{g_j,t}^E} \right) + \sum_{g_k \in (\mathcal{G}_i^{\mathrm{o}} \setminus g_j)} NX_{g_j,g_k} = \sum_{i \in \mathcal{I}_{g_j}} E_j \left(p_E^*, p_{H,g_H}^* \right)$$

$$\mathrm{o} \leq X_{k,j} \leq T_{k,j}, \qquad NX_{k,j} \equiv X_{k,j} - X_{j,k}, \qquad \forall (g_k, g_j) \in (\mathcal{G}_i^{\mathrm{o}} \times \mathcal{G}_i^{\mathrm{o}})$$

The unconstrained shadow problem applied in algorithm 1:

Problem 2 (Minimize non-linear cost of trade: guiding trade partition)**.**

$$\min \sum_{g_k \in \mathcal{G}_i^{\mathrm{o}}} \sum_{j \in (\mathcal{G}_i^{\mathrm{o}} \setminus k)} C_{k,j} \left(NX_{k,j} \right),$$

$$s.t. \quad \sum_{g_j \in \mathcal{G}_i^{\mathrm{o}}} e_{(t,h,g_j)} \left(\frac{p_E^*}{p_{g_j,t}^E} \right) = \sum_{g_j \in \mathcal{G}_i^{\mathrm{o}}} \sum_{j \in \mathcal{I}_{g_j}} E_j \left(p_E^*, p_{H,g_H}^* \right),$$

$$h_{(t,h,g_j)} \left(\frac{p_{H,g_j}^*}{p_{g_j,t}^H} \right) = \sum_{j \in \mathcal{I}_{g_j}} H_j \left(p_E^*, p_{H,g_j}^* \right), \qquad \forall g_j \in \mathcal{G}_i^{\mathrm{o}}$$

$$e_{(t,h,g_j)}\left(\frac{p_E^*}{p_{g_j,t}^E}\right)+\sum_{g_k\in(\mathcal{G}_i^o\setminus g_j)}NX_{g_j,g_k}=\sum_{i\in\mathcal{I}_{g_j}}E_j\left(p_E^*,p_{H,g_H}^*\right),$$

where cost function $C_{k,j}$ is assumed to follow

$$\frac{\partial C_{k,j}}{\partial NX_{k,j}}=\begin{cases}\left[1+\left(\frac{\theta(T_{k,j})}{NX_{k,j}}\right)^{\frac{\sigma-1}{\sigma}}\right]^{1/(1-\sigma)}-1, & for\ \ NX_{k,j}>0\\ -\left[1+\left(\frac{\theta(T_{j,k})}{-NX_{k,j}}\right)^{\frac{\sigma-1}{\sigma}}\right]^{1/(1-\sigma)}+1, & for\ \ NX_{k,j}\leq 0\end{cases},\qquad \sigma\in(0,1/2)$$

and $\theta(T_{k,j})$ is calibrated after

$$\theta(T_{k,j})=T_{k,j}\left((\bar{c}+1)^{1-\sigma}-1\right)^{\frac{\sigma}{\sigma-1}}.$$

Problem 2 implicitly imposes the inequality constraints in trade capacities by the calibration of the cost function $C_{k,j}$. Note in particular that it is cheaper to use the fictional large plant at costs $\bar{c}$ then import more than capacity $\mathcal{T}_{k,j}$. With all supply and demand functions being continuously differentiable, the assumptions on $C_{k,j}$ further renders a somewhat simple solution. From the solution to this problem, we define the shadow cost of a set of transmission constraints, $(T_{i,j},T_{j,i})$, as

$$\mu_{i,j}\equiv\left|\frac{\partial C_{i,j}}{\partial NX_{i,j}}\right|.$$

From the construction of the cost function we note that when $NX_{i,j}$ is not near the constraints, we have $\mu_{i,j}\approx 0$. Furthermore, as then spikes around $\bar{c}$ we can use this cut-off as a criteria for when the constraint is likely to hold or not. Below we establish some results for the solution to this problem:

Taking prices as given we can rewrite budgets in the form:

$$\underbrace{\begin{pmatrix}\sum_{i\in\mathcal{I}_{g_1}}E_i\left(p_E^*,P_{H,g_H}^*\right)-e_{(t,h,g_1)}\\ \vdots\\ \sum_{i\in\mathcal{I}_{g_n}}E_i\left(p_E^*,P_{H,g_H}^*\right)-e_{(t,h,g_n)}\end{pmatrix}}_{\equiv\mu}=b\mathbf{NX},$$

where b is a coefficient matrix and $\mathbf{NX}$ is a vector of stacked $NX_{k,j}$ terms. Dimensions are given by:

$$dim(b)=n\times m,\qquad dim(\mathbf{NX})=m\times 1,\qquad m\equiv\sum_{i=1}^{n-1}i.$$

We note that b has rank $n-1$ when $\sum\mu_i=0$.[143] Dropping the $n'th$ row in μ and b we now write

[143]Particularly we can show that row sum of b is zero, i.e. such that the n'th row $b^n=-\sum_{i\neq n}b^i$.

constraints as $\zeta = B\ \mathbf{NX}$. The corresponding Lagrangian is given by:

$$\mathcal{L} = \sum_{k=1}^{n-1} \sum_{j=k+1}^{n} C_{k,j}(NX_{k,j}) + \sum_{k=1}^{n-1} \lambda_E^k \left[B^k * \mathbf{NX} - \zeta \right],$$

with B^k denoting $k'th$ row of B. The first order conditions for each $k \in \{1, ..., n-1\}$:

$$\begin{aligned} &\text{For } j < n: && \frac{\partial C_{k,j}}{\partial NX_{k,j}} = \lambda_E^j - \lambda_E^k, \\ &\text{For } j = n: && \frac{\partial C_{k,j}}{\partial NX_{k,j}} = -\lambda_E^k. \end{aligned}$$

Letting $\partial \mathbf{C}(\cdot)/\partial \mathbf{NX}$ denote the marginal cost function applied on each element of a vector input, we can sum up the first order conditions on the form

$$\frac{\partial \mathbf{C}}{\partial \mathbf{NX}} = A\lambda,$$

where A is a $m \times n-1$ coefficient matrix and λ is a vector of shadow-values. The matrices A and B are of full rank $(n-1)$ per construction.

The first order conditions are necessary and sufficient for a minimum

For $n = 2$ the solution is uniquely determined by the constraints. For $n \geq 3$:

i. *The objective function and constraints are twice continuously differentiable.* Note in particular that

$$\lim_{NX_{k,j} \to 0^+} \left(\frac{\partial C_{k,j}}{\partial NX_{k,j}} \right) = \lim_{NX_{k,j} \to 0^-} \left(\frac{\partial C_{k,j}}{\partial NX_{k,j}} \right) = 0,$$

and furthermore that

$$\frac{\partial C_{k,j}^2}{\partial NX_{k,j}} = \begin{cases} \frac{1}{\sigma NX_{k.j}} \left(\frac{\partial C_{k,j}}{\partial NX_{k,j}} + 1 \right)^{\sigma} \left(\frac{\theta(T_{k,j})}{NX_{k,j}} \right)^{\frac{\sigma-1}{\sigma}}, & \text{for } NX_{k,j} > 0 \\ \frac{-1}{\sigma NX_{k,j}} \left(1 - \frac{\partial C_{k,j}}{\partial NX_{k,j}} \right)^{\sigma} \left(\frac{\theta(T_{j,k})}{-NX_{k,j}} \right)^{\frac{\sigma-1}{\sigma}}, & \text{for } NX_{k,j} \leq 0 \end{cases}.$$

As long as $\sigma \in (0,\ 1/2)$ we have

$$\lim_{NX\_k,j \to 0^+} \left(\frac{\partial^2 C_{k,j}}{\partial NX_{k,j}^2} \right) = \lim_{NX_{k,j} \to 0^-} \left(\frac{\partial^2 C_{k,j}}{\partial NX_{k,j}^2} \right) = 0.$$

ii. *Gradients of constraints are linearly independent, i.e. the Jacobian matrix B is of full (row) rank.* This implies that the null space of B can be defined by

$$Null(B) = span\left\{ \left(Z \right) \right\},$$

where Z is a basis matrix of dimensions $m \times (m - (n-1))$. We can produce a basis matrix Z by the following steps:

- Define for $k \in \{1, ..., n-2\}$ matrices on the form:

$$z_k = \begin{bmatrix} \mathbf{0}_{(k-1)\times(n-1-k)} \\ \mathbf{1}_{1\times(n-1-k)} \\ -\mathbf{I}_{(n-1-k)} \end{bmatrix}$$

  where we note that z_k is of dimensions $(n-1) \times (n-1-k)$.

- Now define Z as

$$Z = \left\{ \begin{bmatrix} z_1 & \cdots & z_{n-2} \end{bmatrix} \right\}$$
$$\mathbf{I}_{m-(n-1)\cdot}$$

iii. *The matrix* $\mathcal{H} \equiv Z' \left(\nabla^2_{\mathbf{NX},\mathbf{NX}} \mathcal{L} \right) Z$ *is positive semi definite.* We note that $\nabla^2_{\mathbf{NX},\mathbf{NX}} \mathcal{L}$ is a $(m \times m)$ diagonal matrix with diagonal elements $\lambda_i \geq 0$. Thus $\mathcal{H}$ is defined in its diagonalized form, with eigenvalues λ_i and eigenvectors in Z.[144]

iv. *The matrix* $\mathcal{H}$ *is positive definite for all non-zero vector* $\mathbf{NX}$. If $\mathbf{NX} = 0$ is feasible then there exists a $\epsilon > 0$ for which all $\mathbf{NX}$ in the neighbourhood $B_\epsilon(0)$ attains the global minimum. In this case the solution identified by constraints and first order conditions is not unique, but $\mathbf{NX} = 0$ is one of them.

H.3 The approximate equilibrium

In this section we show basic properties of the approximate equilibrium in definition 5. Formally this involves solving problem 3 below:

Problem 3 (Solving for approximate equilibrium)**.**

$$\min \sum_{k=1}^{n-1} \sum_{j=k+1}^{n} C_{k,j}(NX_{k,j}),$$

$$s.t. \sum_{g_j \in \mathcal{G}_E} e_{(t,h,g_j)} \left(\frac{p_{g_j}}{p_{g_j,t}} \right) = \sum_{g_j \in \mathcal{G}_E} \sum_{i \in \mathcal{I}_{g_j}} E_i \left(p_{g_j}, p_{g_H} \right)$$

$$h_{(t,h,g_H)} \left(\frac{p_{g_H}}{p_{g_H,t}} \right) = \sum_{i \in \mathcal{I}_{g_H}} H_i \left(p_{g_E}, p_{g_H} \right) \qquad \forall g_H \in \mathcal{G}_H$$

$$e_{(t,h,g_j)} \left(\frac{p_{g_j}}{p_{g_j,t}} \right) + \sum_{g_k \in (\mathcal{G}_E \setminus g_j)} NX_{g_j,g_k} = \sum_{i \in \mathcal{I}_{g_j}} E_i \left(p_{g_j}, p_{g_H} \right),$$

[144] Technically the vectors in Z are not *orthonormal*, but a scaling of $\sqrt{3}$ makes them so:

$$\mathcal{H} = \left(\sqrt{3}^{-1} Z \right)' \left(3 \nabla^2_{\mathbf{NX},\mathbf{NX}} \mathcal{L} \right) \left(\sqrt{3}^{-1} Z \right),$$

implying that eigenvalues of $\mathcal{H}$ are scaled values of $(\nabla^2_{\mathbf{NX},\mathbf{NX}} \mathcal{L})$, but with unchanged signs.

where the cost function $C_{k,j}$ is defined such that

$$\frac{\partial C_{k,j}}{\partial NX_{k,j}} = \begin{cases} \left[1 + \left(\frac{\theta(T_{k,j})}{NX_{k,j}}\right)^{\frac{\sigma-1}{\sigma}}\right]^{1/(1-\sigma)} - 1, & \textit{for} \;\; NX_{k,j} > 0 \\ -\left[1 + \left(\frac{\theta(T_{j,k})}{-NX_{k,j}}\right)^{\frac{\sigma-1}{\sigma}}\right]^{1/(1-\sigma)} + 1, & \textit{for} \;\; NX_{k,j} \leq 0 \end{cases}, \qquad \sigma \in (0, 1/2).$$

Relative electricity prices are then defined as:

$$p_{g_i} = p_{g_j} - \frac{\partial C_{i,j}}{\partial NX_{i,j}}.$$

In the following we show:

i. The global minimum to problem problem 3 exists and obeys trade capacities.

ii. Taking prices as given, the first order conditions to problem 3 are necessary and sufficient to minimize trade costs.

iii. The relative electricity pricing rule is unique, such that comparing country i with any other two countries (j, k), yields the same price p_i.

iv. In the unconstrained case the first order conditions yields an injective mapping $\mathbf{f}^{NX} : \mathbb{R}^{n-1} \rightarrow \mathbb{R}^m$ from choice of a basis vector to a vector of all net export elements: $\mathbf{NX}_n \mapsto \mathbf{NX}$.[145] This mapping has a simple analytical form.

v. In the unconstrained case the first order conditions can alternatively be used to present an injective mapping $\mathbf{f}^p : \mathbb{R}^{n-1} \rightarrow \mathbb{R}^m$, from a vector of country-specific prices p_E to entire a vector of all net export elements: $p_E \mapsto \mathbf{NX}$. This mapping has a similar simple analytical form.

vi. In a constrained case the first order conditions yields a similar mapping $\tilde{\mathbf{f}}^{NX} : \mathbb{R}^{n-1} \mapsto \mathbb{R}^m$ from a basis vector to all net export elements; the new basis vector $\tilde{\mathbf{NX}}_n$ is straightforward to identify. In the constrained case it turns out the mapping from a price vector to $\mathbf{NX}$ given by $\mathbf{f}^p$ is identical to the unconstrained case.

H.3.1 The global minimum exists and obeys trade capacities

Note that all functions are continuously differentiable in prices and $NX_{i,j}$.[146]. By assumption each area includes a fictional plant with sufficient large capacity to cover entire equilibrium, but highest cost at $\bar{c}$. With the cost function defined as above it will never be optimal to choose a $NX_{i,j} > T_{i,j}$ as marginal costs of trade is greater than $\bar{c}$ around trade capacities. We can thus without loss of generality define the problem on a compact set defined by $\mathbf{NX}_{i,j} \leq T_{i,j}$. By the extreme value theorem our objective function is thus bounded and the global minimum exists.

[145] We define the *unconstrained case* as the case where at least one country, has strictly positive trade capacities $T_{i,j} > 0$ with all other countries.

[146] For the differentiability of $C_{k,j}$ see problem 2

H.3.2 Taking prices as given, the first order conditions are necessary and sufficient to minimize trade costs.

Following the solution to problem 2 the first order conditions for the vector of **NX** can be written on the form:

$$\frac{\partial \mathbf{C}}{\partial \mathbf{NX}} = A \times \lambda$$
$$B \times \mathbf{NX} = \zeta(p_E)$$

Here **NX** is a stacked vector of all $m = \sum_{i=1}^{n-1} i$ net export terms. $\partial \mathbf{C}/\partial \mathbf{NX}$ applies the marginal trade cost function element-wise on **NX**. A and B are suitable coefficient matrices. λ is the vector of Lagrangian variables from the country-specific equilibrium constraints. Finally $\zeta(p_E)$ is defined as *domestic surplus production functions* (DSF) given prices; the difference between domestic supply and demand. Problem 2 shows that these conditions are indeed necessary and sufficient for a minimum.

H.3.3 Uniqueness of relative prices

The relative price rule of $p_{g_i} = p_{g_j} - \partial \mathbf{C}/\partial NX_{i,j}$ identifies the same price p_{g_i} for all (i,k) equations with $k \neq i$ when **NX** is chosen according to the minimization problem. Consider any two pairs $(i,j),(i,k)$ of countries and note that the pricing equation implies that

$$\begin{aligned} p_{g_i} =& p_{g_j} - \frac{\partial C_{i,j}}{\partial NX_{i,j}}, \\ p_{g_i} =& p_{g_k} - \frac{\partial C_{i,k}}{\partial NX_{i,k}}, \\ p_{g_j} =& p_{g_k} - \frac{\partial C_{j,k}}{\partial NX_{j,k}}. \end{aligned}$$

Combining the three this implies that

$$\frac{\partial C_{j,k}}{\partial NX_{j,k}} + \frac{\partial C_{i,j}}{\partial NX_{i,j}} = \frac{\partial C_{i,k}}{\partial NX_{i,k}}.$$

Substituting for the first order conditions this yields:

$$\underbrace{\lambda_E^k - \lambda_E^j}_{\equiv \partial C_{j,k}/\partial NX_{j,k}} + \lambda_E^j - \lambda_E^i = \lambda_E^k - \lambda_E^i,$$

which holds per construction.

H.3.4 The injective mapping from basis vector of net exports to full allocation

Assume that there is one country, for which trade capacities with all other countries are strictly positive. Let this be the n'th country. The first order conditions are then given for $k \in \{1, ..., n-1\}$:

$$\begin{aligned} \text{For } j < n: \qquad & \frac{\partial C_{k,j}}{\partial NX_{k,j}} = \lambda_E^j - \lambda_E^k \\ \text{For } j = n: \qquad & \frac{\partial C_{k,j}}{\partial NX_{k,j}} = -\lambda_E^k. \end{aligned}$$

Using the n'th country's net export terms we can thus rewrite first order conditions without λ:

$$\frac{\partial \mathbf{C}}{\partial \mathbf{NX}} = -A \times \frac{\partial \mathbf{C}}{\partial \mathbf{NX}_n}, \qquad \mathbf{NX}_n \equiv \begin{pmatrix} NX_{1,n}, & \cdots & NX_{n-1,n} \end{pmatrix}'.$$

Note in particular that the marginal trade cost function is a bijection and the inverse function, $(\partial \mathbf{C})^{-1}$, is naturally is as well. Problem 2 establishes that A is of full row rank, but is not square, implying that this mapping is injective. As the composite function of two injective functions is injective itself, this establishes that the mapping $\mathbf{f}^{NX}: \mathbb{R}^{n-1} \to \mathbb{R}^m$ defined by

$$\mathbf{NX} = (\partial \mathbf{C})^{-1} \left(-A \times \frac{\partial \mathbf{C}}{\partial \mathbf{NX}_n} \right),$$

is injective as well. In other words; given a candidate vector of $\mathbf{NX}_n$ there is a unique corresponding vector of all net exports, $\mathbf{NX}$, that obeys the first order conditions.

H.3.5 The injective mapping from prices to net exports

The solution to problem 3 implies the mapping $\mathbf{f}^{NX}$ established above as well as the price function

$$\tilde{p}_E \equiv \begin{pmatrix} p_1 \\ \vdots \\ p_{n-1} \end{pmatrix} = p_n - \frac{\partial \mathbf{C}}{\partial \mathbf{NX}_n}.$$

As the partial trade cost function is bijective, we can invert this

$$\mathbf{NX}_n = (\partial \mathbf{C}_n)^{-1} (p_n - \tilde{p}_E) \qquad \Rightarrow \qquad \frac{\partial \mathbf{C}}{\partial \mathbf{NX}_n} = p_n - \tilde{p}_E.$$

where $(\partial \mathbf{C}_n)^{-1}$ is the inverse of the vector function, taking the derivative of the marginal trade cost function in arguments $NX_{i,n}$. Substituting this into the function $\mathbf{f}^{NX}$ established above we have

$$\mathbf{NX} = (\partial \mathbf{C})^{-1} (A \times (p_n - \tilde{p}_E)).$$

By the same argument as for $\mathbf{f}^{NX}$ this establishes an injective mapping from p_E to $\mathbf{NX}$.

H.3.6 The constrained solution

Consider the case where two countries cannot trade, i.e. $T_{i,j} = T_{j,i} = 0$. In the simple case we assume that there is still a country that can trade with all other countries. In this case the solution is simply to fix the relevant net export terms at zero; the rest of the solution is identical. Recall that we utilized the linear dependence of the n countries' equilibria constraints, to drop exactly one of them, and write the n'th first order conditions, simply as

$$\frac{\partial C_{i,n}}{\partial NX_{i,n}} = -\lambda_E^i.$$

In the case where there is no n'th country to identify the entire λ_E vector, the solution is slightly altered. The first order conditions can now be written in the form

$$\frac{\partial \mathbf{C}}{\partial \mathbf{NX}} = -A \times D \times \frac{\partial \mathbf{C}}{\partial \mathbf{NX}},$$

where D is a suitable $(n \times m)$ coefficient matrix.[147] As in the unrestricted case, the right hand side of this equation essentially only picks out $n-1$ relevant net export flows; which elements are chosen however, depends on the restricted transmission lines. Before proceeding, we note that this representation only holds as long as transmission shocks does not imply new trade partitions. In such scenarios the solution approach outlined here should be carried out separately for each subset of the trade partition. Following the same steps as in the unconstrained case we now have

- The net export vector can be found by an injective mapping $\tilde{\mathbf{f}}^{NX} : \mathbb{R}^{n-1} \mapsto \mathbb{R}^m$ defined by:

  $$\mathbf{NX} = (\partial \mathbf{C})^{-1} \left(-A \times \frac{\partial \mathbf{C}}{\partial \tilde{\mathbf{NX}}_n} \right),$$

  where the new 'basis' vector $\tilde{\mathbf{NX}}_n$ now consists of elements picked out by the D matrix.

- We can define the relative price rule as

  $$p_{g_i} = p_{g_j} - \frac{\partial C_{i,j}}{\partial NX_{i,j}}, \qquad \forall (g_i, g_j) : T_{i,j} > 0,$$

  or equivalently

  $$\tilde{p}_E = p_n - D \times \frac{\partial \mathbf{C}}{\partial \mathbf{NX}} = p_n - \frac{\partial \mathbf{C}}{\partial \tilde{\mathbf{NX}}_n}$$

- The marginal trade cost function is invertible such that

  $$\tilde{\mathbf{NX}}_n = (\partial \tilde{\mathbf{C}}_n)^{-1} (p_n - \tilde{p}_E), \qquad \Rightarrow \qquad \frac{\partial \mathbf{C}}{\partial \tilde{\mathbf{NX}}_n} = p_n - \tilde{p}_E$$

  where $(\partial \tilde{\mathbf{C}}_n)^{-1}$ is the inverse of the vector function, taking the derivative of the marginal trade cost function in the arguments picked out in $\mathbf{NX}$ by the D coefficient matrix.

[147] At the end of this appendix we provide an example of how to construct coefficient matrices as A, B, D applied here.

- Substituting this into the $\tilde{\mathbf{f}}^{NX}$ function we have

$$\mathbf{NX} = (\partial \mathbf{C})^{-1} \left(A \times (p_n - \tilde{p}_E) \right),$$

which is identical to the net export / price function in the unconstrained case.

H.3.7 Constructing coefficient matrices

The D matrix is formed such that the price p_{g_i} are determined by a linear combination of marginal costs that eventually relates to the level p_n, but without relying on any NX terms fixed at zero. One way of doing so is outlined below:

i. Load $n'th$ column vector of $\mathbf{T}$ into a matrix E (of dimension $n \times n$). Row-vectors with a one in E are done, the rest are yet to be filled out. In the matrix D this translates into rows containing unit vectors:

$$D_i = e'_{k_1} \qquad\qquad k_1 \equiv \sum_{j=n-i}^{n-1} j.$$

Only the $n'th$ row of D naturally contains only zeros.

ii. In matrix E: Define i_0 as rows with sum equal zero, and i_1 as rows with 1 in $n'th$ column. Add:

$$\text{For } i \in i_0, j \in i_1: \quad \text{if } T(i,j) = 1 \quad \text{then set} \quad E(i,j) = 1 \quad \text{and then add} \quad E(i,\cdot) = E(i,\cdot) + E(j,\cdot)$$

For rows D_i where $T(i,j) = 1$ as identified above:

- If $i < j$ then set

$$D(i, k_2) = 1, \qquad\qquad k_2 \equiv \sum_{s=n-i}^{n-1} [s] - (n-j).$$

- If $i > j$ then set

$$D_{i,k_3} = -1, \qquad\qquad k_3 \equiv \sum_{s=n-j}^{n-1} [s] - (n-i).$$

- Finally, add the $j'th$ row to the $i'th$ row.

iii. Update sets i_0, i_1 by defining: i_0 contains the rows without ones in E, and i_1 contains rows with ones in column $n-1$.

Repeat this until i_0 is an empty set.

An example of a 4×4 matrix $\mathbf{T}$ scenario is:

$$\mathbf{T} = \begin{pmatrix} 1 & 1 & 0 & 0 \\ 1 & 1 & 1 & 0 \\ 0 & 1 & 1 & 1 \\ 0 & 0 & 1 & 1 \end{pmatrix} \quad \Rightarrow \quad E \equiv \begin{pmatrix} 0 & 1 & 1 & 1 \\ 0 & 0 & 1 & 1 \\ 0 & 0 & 0 & 1 \\ 0 & 0 & 0 & 1 \end{pmatrix} \quad \text{and} \quad D \equiv \begin{pmatrix} 1 & 0 & 0 & 1 & 0 & 1 \\ 0 & 0 & 0 & 1 & 0 & 1 \\ 0 & 0 & 0 & 0 & 0 & 1 \\ & \cdots & \mathbf{0}_6 & \cdots & & \end{pmatrix}$$

The trade coefficient matrix $\mathbf{T}$ states that country 1 can trade with country 2, who trades with country 3 as well, who finally trades with country 4. The established D matrix then states that to tie p_1 to the level of p_n we write this as:

$$p_1 = p_n - \frac{\partial C_{1,2}}{\partial NX_{1,2}} - \frac{\partial C_{2,3}}{\partial NX_{2,3}} - \frac{\partial C_{3,4}}{\partial NX_{3,4}}.$$

This ensures that all NX terms evaluated are not constrained to zero.

H.4 Approximating cost functions with standard normal distributions

As an alternative to the marginal trade cost function, we can attempt to approximate the solution function directly. If we think of the bottom up trade function as

$$NX_{i,j} = \begin{cases} T_{i,j}, & p_i \leq p_j \\ -T_{j,i}, & p_j \leq p_i \end{cases},$$

then we can approximate this directly as

$$NX_{i,j} \approx T_{i,j} - (T_{i,j} + T_{j,i})\Phi\left(\frac{p_j - p_i}{\sigma}\right),$$

where $\sigma \to 0$ nests the bottom up solution. If $T_{i,j} \neq T_{j,i}$ this does not enter origo though. For this function to enter through origo, we use the same specification as the asymmetric normal demand specification outlined in appendix G. In particular we define the approximation

$$NX_{i,j} \approx -T_{j,i} + \left(T_{i,j} + T_{j,i}\right)\Phi\left(\frac{p_j - p_i + \tilde{g}}{\sigma}\right),$$

where we define $\tilde{g}$ such that the function enters origo, i.e. such that

$$\tilde{g} = \Phi^{-1}\left(\frac{T_{j,i}}{T_{i,j} + T_{j,i}}\right)\sigma.$$

I Results from K-means clustering using $\bar{k} = 2800$

The results from the K-means clustering using k =2800 is presented in fig. I.1. For each variable (16 in total) we plot the clustered value against the hourly variable in RAMSES. The diagrams should be read from left to right: Observation on the same horizontal line defines a cluster. Observations on the diagonal implies that the clustered value is exactly equal to the actual hourly value, implying that data should be closely centered around the diagonal for k =2800 to be an appropriate number of clusters.

Figure I.1: Fit of hourly data with $\bar{k}$=2800.

(a) Inelastic electricity demand for DK-west (GWh).

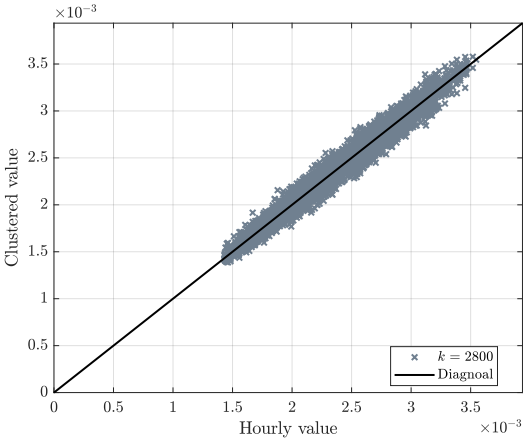

(b) Inelastic electricity demand for DK-East (GWh).

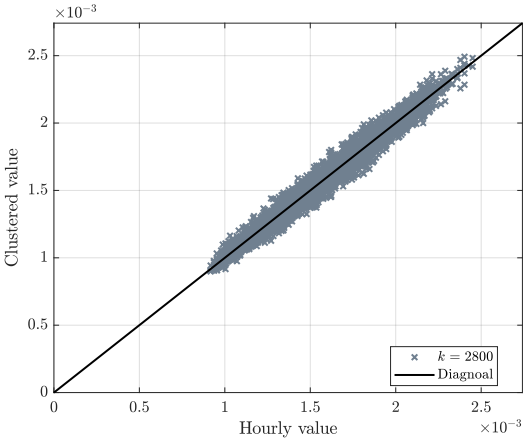

(c) Inelastic heat demand for DK (GWh).

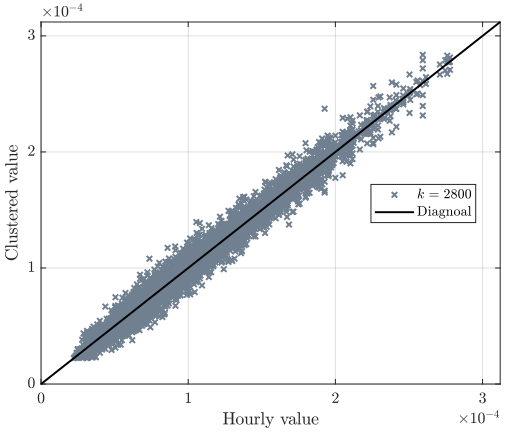

(d) Industrial power generation in DK (GWh).

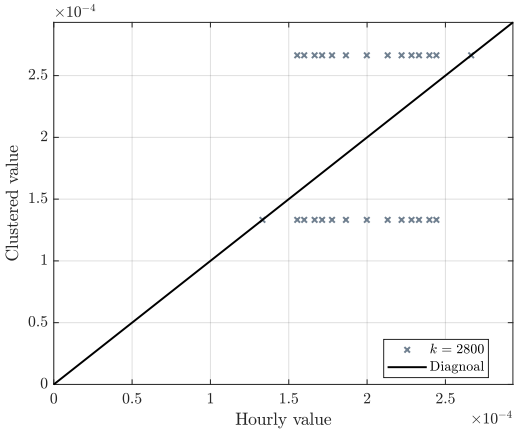

Note: The diagrams should be read from left to right, i.e. points on the same horizontal line defines a cluster. The diagonal defines the point where the clustered exogenous data is equal to the hourly data, implying that observations closely centered around the diagonal indicates an accurate cluster.

continues on the next page...

Figure I.1: The determination of the maximum number of clusters, $\bar{k}$.

(e) Residual load for NO (GWh).

(f) Residual load for SE (GWh).

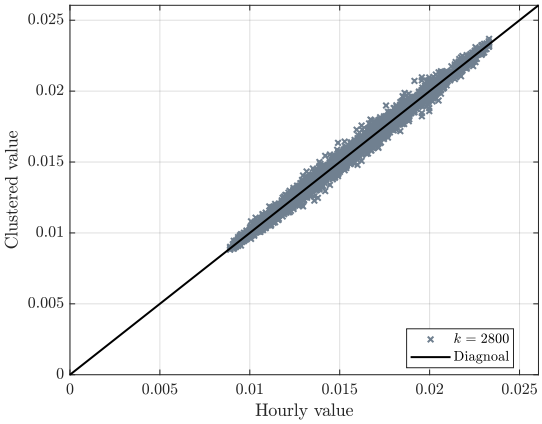

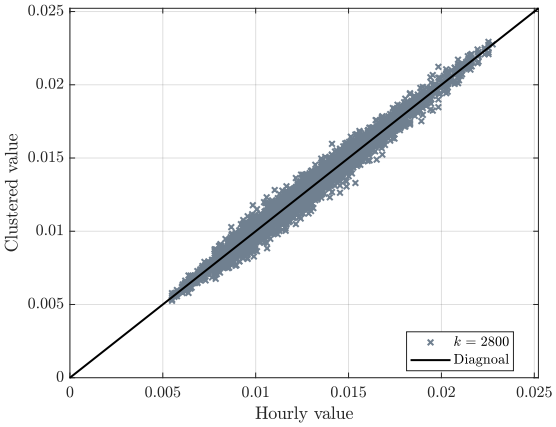

(g) Residual load for FI (GWh).

(h) Residual load for DE (GWh).

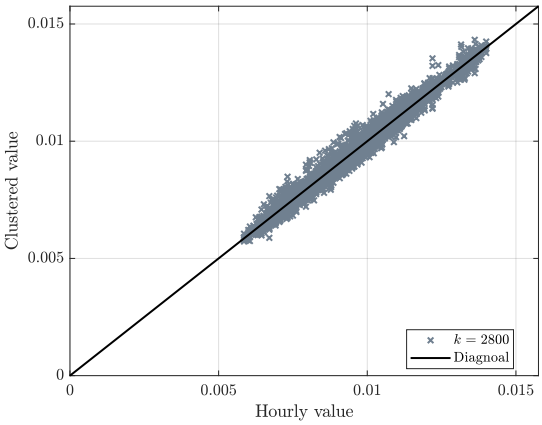

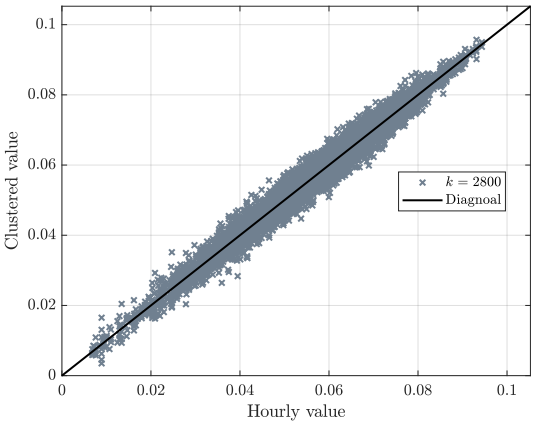

(i) Residual load for NL (GWh).

(j) Residual load for GB (GWh).

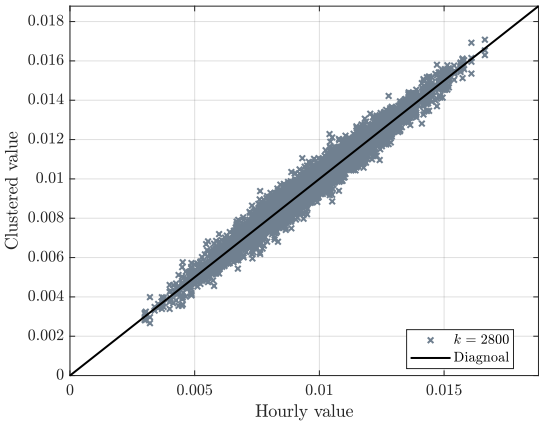

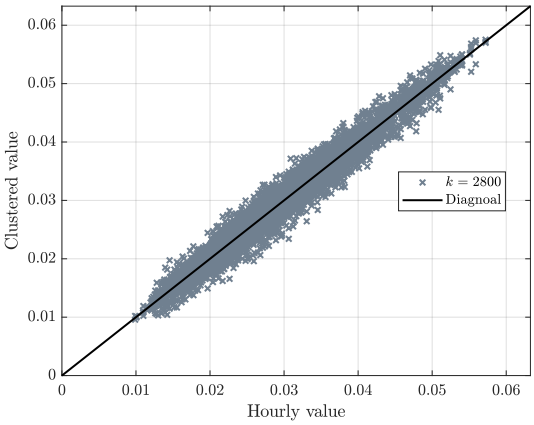

Note: The diagrams should be read from left to right, i.e. points on the same horizontal line defines a cluster. The diagonal defines the point where the clustered exogenous data is equal to the hourly data, implying that observations closely centered around the diagonal indicates an accurate cluster.

continues on the next page...

Figure I.1: The determination of the maximum number of clusters, $\bar{k}$.

(k) Productivity of wind power in DK-West (GWh).

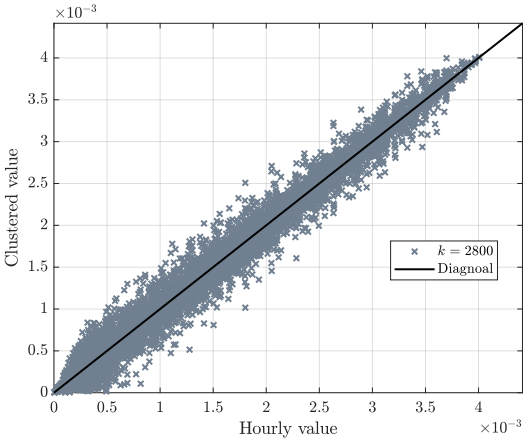

(l) Productivity of wind power in DK-East (GWh).

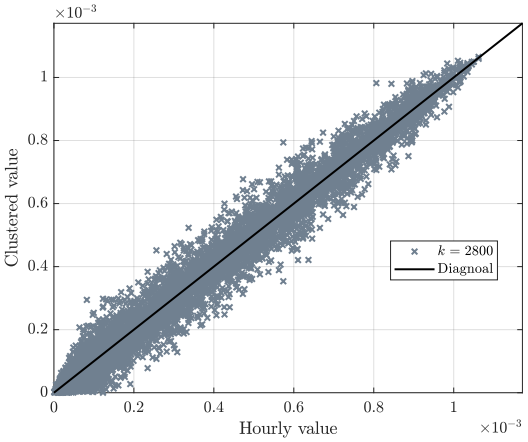

(m) Productivity of solar power in DK-West (GWh).

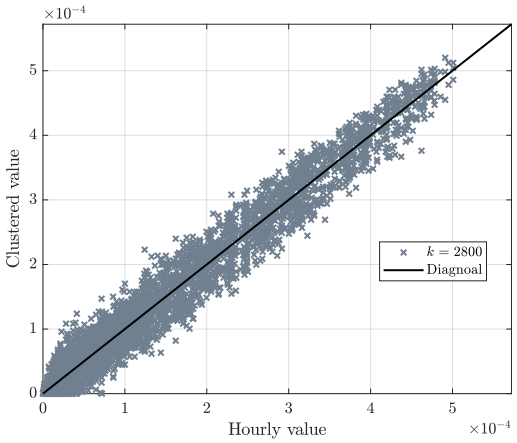

(n) Productivity of solar power in DK-East (GWh).

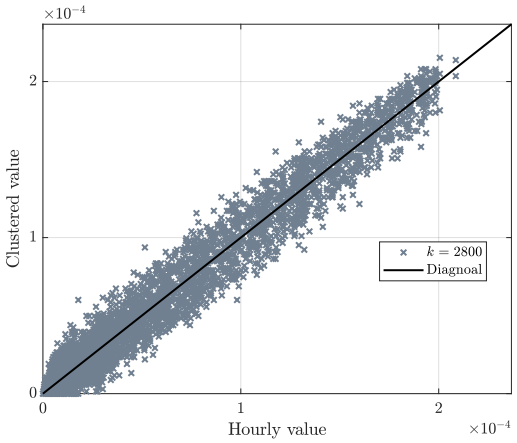

(o) Productivity of solar heat in DK-West (GWh).

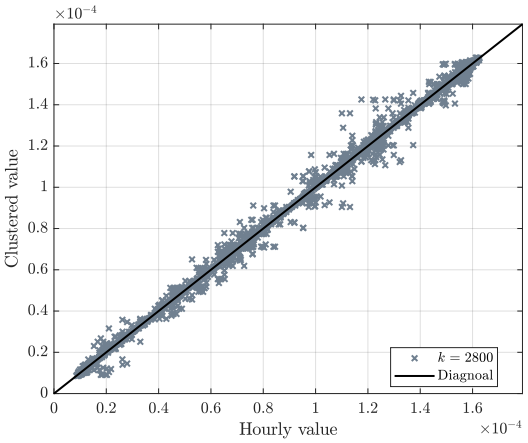

(p) Productivity of solar heat in DK-East (GWh).

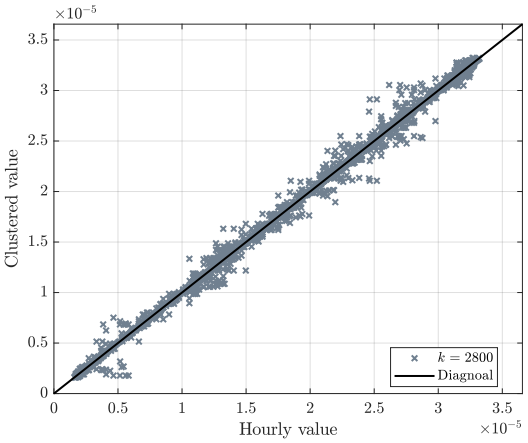

Note: The diagrams should be read from left to right, i.e. points on the same horizontal line defines a cluster. The diagonal defines the point where the clustered exogenous data is equal to the hourly data, implying that observations closely centered around the diagonal indicates an accurate cluster.

continues on the next page...

Figure I.1: The determination of the maximum number of clusters, $\bar{k}$.

(q) Hydro power water inflow for DE (GWh).

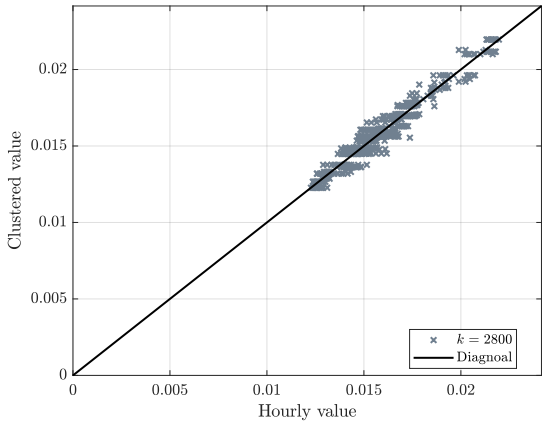

(r) Hydro power water inflow for all but DE (GWh).

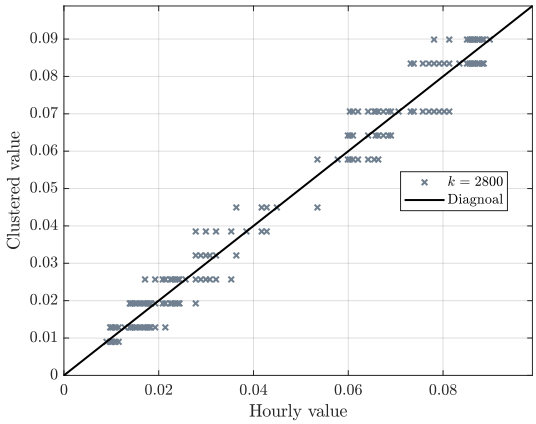

Note: The diagrams should be read from left to right, i.e. points on the same horizontal line defines a cluster. The diagonal defines the point where the clustered exogenous data is equal to the hourly data, implying that observations closely centered around the diagonal indicates an accurate cluster.

J Smoothing out kinks in piece-wise linear functions

Consider the piece-wise linear function with a single kink:

$$f(x) = \begin{cases} a_1 + b_1 x, & x \leq k \\ a_2 + b_2 x, & x > k \end{cases},$$

where the linear function is continuous in $x = k$ such that

$$a_1 - a_2 = (b_2 - b_1)k.$$

To smooth out the function we use two piece-wise linear functions on the form

$$g_1(x) = \alpha_1 + \frac{\beta_1}{2}\left(x - |x - \gamma_1|\right)$$
$$g_2(x) = \alpha_2 + \frac{\beta_2}{2}\left(x + |x - \gamma_2|\right),$$

where $\gamma_1, \gamma_2 \geq 0$. The functions g_1, g_2 can also be formulated as the linearly kinked functions:

$$g_1(x) = \begin{cases} \alpha_1 - \frac{\beta_1}{2}\gamma_1 + \beta_1 x, & x \leq \gamma_1 \\ \alpha_1 + \frac{\beta_1}{2}\gamma_1, & x \geq \gamma_1 \end{cases}$$
$$g_2(x) = \begin{cases} \alpha_2 + \frac{\beta_2}{2}\gamma_2, & x \leq \gamma_2 \\ \alpha_2 - \frac{\beta_2}{2}\gamma_2 + \beta_2 x, & x \geq \gamma_2 \end{cases}$$

For the g functions to be used as a basis for the f function, we thus need $\gamma_1 = \gamma_2 = \gamma = k$ Summing over g_j functions then yield:

$$g(x) \equiv g_1(x) + g_2(x) = \begin{cases} \alpha_1 + \alpha_2 + \gamma\frac{\beta_2 - \beta_1}{2} + \beta_1 x, & x \leq \gamma \\ \alpha_1 + \alpha_2 + \gamma\frac{\beta_1 - \beta_2}{2} + \beta_2 x, & x > \gamma \end{cases}$$

Thus to fit the slopes of the linear function f we need $\beta_1 = b_1$ and $\beta_2 = b_2$. Imposing this and setting $\alpha_2 = 0$ for simplicity we get

$$\alpha_1 = a_1 + k\frac{b_1 - b_2}{2}.$$

We can approximate the absolute value functions using

$$|x| \approx \sqrt{x^2 + \epsilon^2},$$

where $\epsilon > 0$ is an error term. The resulting approximation is illustrated in figure J.1 below. As ϵ is lowered towards zero, we can get arbitrarily close to the piece-wise linear function (solid line).

Figure J.1: Varying ϵ in smoothing piece-wise linear function

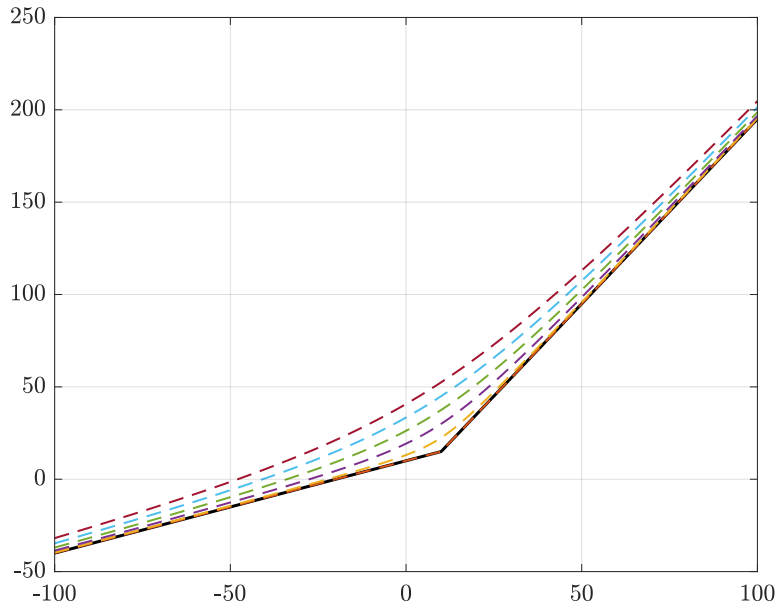

The figure shows how varying the error term ϵ improves the approximation. Here $\epsilon \in \{0, 10, 20, 30, 40, 50\}$.

K A potential fix of the aggregation of storage firms

In this appendix we consider the state-transition-contingent aggregation scheme. For convenience we here restate the system of equations characterizing the behavior in one state k_i:

$$\begin{aligned}
E_{k_i|k_j} &= \underline{\mathrm{E}} + \left(Y_{k_i} - \underline{E}\right) \Phi\left(\frac{p_{k_i} - c - a\theta_{k_i|k_j}}{\sigma}\right) + \left(\bar{E} - Y_{k_i}\right) \Phi\left(\frac{p_{k_i} - c - \theta_{k_i|k_j}}{\sigma}\right) \\
\theta_{k_i|k_j} &= \beta\theta_{k_j} + \underline{\eta}_{k_i|k_j} - \bar{\eta}_{k_i|k_j} \\
S_{k_i|k_j} &= S_{k_i-1} + f\left(Y_{k_i} - E_{k_i|k_j}\right) \\
\bar{\eta}_{k_i|k_j} &= \left(S^{max}_{k_i|k_j} - \bar{S}\right) \nabla S^{max}_{k_i|k_j} \\
\underline{\eta}_{k_i|k_j} &= -S^{min}_{k_i|k_j} \nabla S^{min}_{k_i|k_j}.
\end{aligned}$$

The state variable and continuation values were defined as weighted averages:

$$\begin{aligned}
S_{k_i-1} &\equiv P_{-1,(0,k_i)} S_0 + P_{-1,(k_1,k_i)} S_{k_1|k_i} + \ \ldots \ + P_{-1,(k_k|k_i)} S_{k_k|k_i} \\
\theta_{k_i} &\equiv P_{k_i|k_1} \theta_{k_i|k_1} + P_{k_i|k_2} + \ \ldots \ + P_{k_i|k_k} \theta_{k_i|k_k}.
\end{aligned}$$

Recall that the probabilities $P_{-1,(k_j|k_i)}$ were backward looking. Thus $P_{-1,(k_j|k_i)}$ denoted the probability that in state k_i, the previous state was k_j. The probabilities $P_{k_i|k_j}$ were forward looking, thus denoting the probability that to transition to state k_j from state k_i. As mentioned in section 9.3.4 the biggest problem with this aggregation approach, is that the variation in the state variable (S) is too dampened.

To figure out why this might be the case, consider the definition of the state variable in S_{k_i-1}. Apply the law of motion for $S_{k_i|k_i}$ and rearrange to get:

$$S_{k_i-1} = \frac{1}{1 - P_{-1,(k_i|k_i)}} \left[P_{-1,(k_i|k_i)} f\left(Y_{k_i} - E_{k_i|k_j}\right) + \sum_{j \neq i} P_{-1,(k_j|k_i)} S_{k_j|k_i} \right]$$

Furthermore, substitute for all other $S_{k_j|k_i}$ using the law of motion and rewrite as:

$$S_{k_i-1} = \frac{1}{1 - P_{-1,(k_i|k_i)}} \left[\sum_{j} P_{-1,(k_j|k_i)} f\left(Y_{k_j} - E_{k_j|k_i}\right) \right] + \frac{1}{1 - P_{-1,(k_i|k_i)}} \left[\sum_{j \neq i} P_{-1,(k_j|k_i)} S_{k_j-1} \right],$$

or alternatively simply:

$$S_{k_i-1} = \sum_{j} \alpha_{j,k_i} f\left(Y_{k_j} - E_{k_j|k_i}\right) + \sum_{j \neq i} \alpha_{j,k_i} S_{k_j-1}, \qquad \text{where} \ \ \alpha_{j,k_i} \equiv \frac{P_{-1,(k_j|k_i)}}{1 - P_{-1,(k_i|k_i)}}.$$

From this we note the following:

- S_{k_i-1} is based on a linear combination of other states (S_{k_j-1}), with **weights summing to 1:**

$$\sum_{j \neq i} \alpha_{j,k_i} = 1.$$

- The weights on the storage decisions ($Y_{k_j} - E_{k_j|k_i}$) sums to at least one:

$$\sum_{j} \alpha_{j,k_i} = 1 + \alpha_{i,k_i} \geq 1.$$

- The term α_{i,k_i} that determines the weight on storage decisions, is actually the **the ratio of hours where state k_i transitions into itself to hours where it does not.** In particular let n_{k_i} denote the total number of hours in state k_i and $n_{k_i|k_i}$ the number of hours where state k_i transitions into itself. We then have:

$$\alpha_{i,k_i} = \frac{n_{k_i|k_i}/n_{k_i}}{1 - n_{k_i|k_i}/n_{k_i}} = \frac{n_{k_i|k_i}}{n_{k_i} - n_{k_i|k_i}}.$$

Now, recall that the storage decision variable ($Y_{k_i} - E_{k_j|k_i}$) was scaled according to realistic hourly levels. Thus when the state variable S_{k_i-1} is defined the weights in α_{j,k_i} would then ideally scale the storage terms ($Y_{k_i} - E_{k_j|k_i}$) up, to reflect the number of hours (n_{k_i}) included in the state k_i. In other words, we require that

$$\sum_{j} \alpha_{j,k_i} = n_{k_i}.$$

Using the expressions above for the α_{j,k_i} weights, note that **this is only the case iff $\mathbf{n_{k_i|k_i} = n_{k_i} - 1}$**. Once again in other words: The aggregation method **only** scales the storage decisions ($Y_{k_i} - E_{k_j|k_i}$) appropriately when the state represents **purely seasonal variation**, where the state k_i transitions into itself all hours except for one. Furthermore, the weights on the storage decisions are otherwise unambiguously **too low**, thus implying that the aggregation method **dampens fluctuations in the state variable**, when the states represent other than purely seasonal variation.

To fix the problem include a constant χ_i in the law of motions:

$$S_{k_i|k_j} = S_{k_i-1} + \chi_i f\left(Y_{k_i} - E_{k_i|k_j}\right). \tag{105}$$

Going through the same steps as outlined in above, the level of stored energy (state variable) is then given by

$$S_{k_i-1} = \sum_{j} \chi_j \alpha_{j,k_i} f\left(Y_{k_j} - E_{k_j|k_i}\right) + \sum_{j \neq i} \alpha_{j,k_i} S_{k_j-1}.$$

For the aggregation to imply that the weights on $f(Y-E)$ sums to n_k, we then need

$$\sum_j \chi_j \alpha_{j,k_i} = n_{k_i}.$$

This is a system of linear equations that identifies $k-1$ of the χ_j terms.